On-line Economic Dispatch of Distributed Generation Using Artificial Neural Networks

M. Arumuga Babu[1(✉)], R. Mahalakshmi[2], S. Kannan[3], M. Karuppasamypandiyan[4], and A. Bhuvanesh[5]

[1] Department of EEE, Tejaa Shakthi Institute of Technology for Women, Coimbatore, India
arumuga1978@gmail.com
[2] Department of EEE, Sri Krishna College of Technology, Coimbatore, India
[3] Department of EEE, Ramco Institute of Technology, Rajapalayam, India
[4] Department of EEE, University College of Engineering, BIT Campus, Trichy, India
[5] Department of EEE, Mepco Schlenk Engineering College, Sivakasi, India

Abstract. In recent years, distributed generators (DG) are most widely installed in distribution system to meet the increasing demand and especially to reduce the losses. According to demand, dispatch of generator should be modified for economic operation. The Economic Dispatch (ED) of DGs are usually solved by conventional methods such as Lambda iteration method, Dynamic Programming etc., or any optimization technique such as Genetic algorithm (GA), Evolutionary Programming (EP) etc., This off-line methods of solving ED problem require comparatively large computation time and are not suitable for on-line applications. Therefore, it is important to estimate Real Power dispatch values within a short period. This paper presents an On-line ED of various non-renewable DGs for various demands using Artificial Neural Networks namely Back Propagation Neural Network (BPNN) and Radial Basis Function Neural Network (RBFNN). The input pattern for Neural Networks (NN) is demand and output is corresponding optimal real power dispatch. The input and output patterns for NN is obtained using evolutionary programming method. In this work two diesel engines and two fuel cells are used as DG. This case study has been illustrated in a distribution system having two types of four numbers of DGs. The test result shows that the proposed method is better for real time ED.

Keywords: Back propagation neural network · Distributed generators · Economic dispatch · Evolutionary programming · Radial basis function neural network

1 Introduction

According to the definition of CIGRE, Distributed Generation (DG) is defined as the generating plant with a capacity of less than 100 MW, usually connected to the distribution networks that are neither centrally planned nor dispatched [1]. One of the drawbacks of using non-renewable DG in distribution system is its fuel cost. Hence, to reduce this fuel cost the DGs should be optimally dispatched.

B.K. Panigrahi et al. (Eds.): SEMCCO 2014, LNCS 8947, pp. 275–283, 2015.
DOI: 10.1007/978-3-319-20294-5_24

Economic dispatch (ED) is one of the most important optimization problems in power system operation and planning. ED economically dispatch the generators according to demand while satisfying physical and operational constraints. Classical methods such as Lambda iteration, Base point Participation factor, Gradient method, Newton's method and Lagrange multiplier method can solve ED problem under the assumption that the incremental cost curves of the generating units are monotonically increasing piecewise-linear functions. However, in reality, the cost curves of generating units are non-convex. Classical based techniques fail to address these types of problems satisfactorily and lead to sub optimal solutions producing huge revenue loss over time. Dynamic programming (DP) can solve ED problem with inherently nonlinear and discontinuous cost curves. But it suffers from the curse of dimensionality or local optimality [2].

ED problems are also solved by many optimization algorithms namely Genetic algorithm (GA) [3, 4], Evolutionary Programming (EP) [5], Particle Swarm Optimization (PSO) [6], Artificial Immune system (AIS) [7], Differential Evolution Algorithm (DE) [8] Biogeography-based optimization (BBO) [9], Simulated Annealing (SA) [10] etc., The main drawbacks of these optimization algorithms are time consuming because for every demand the programs needs to be run to get optimal result. Hence, it is not suitable for on-line application.

This paper presents an online ED of four non-renewable DGs using Neural Network (NN). Two Types of NN has been developed for On-Line Estimation of ED namely Back Propagation Neural Network (BPNN) and Radial Basis Neural Network (RBFNN). The case study has been implemented on a four DGs test system.

2 Problem Formulation

The ED of DGs may be formulated as non-linear optimization problem. Two types of DGs are considered here. They are diesel engines and two fuel stacks. The objective function in a diesel engine consists of the fuel cost function similar to the cost function used for conventional generating plants. The operating cost of fuel cell system takes the fuel costs and includes the efficiency of fuel cell. The constraints include power generation capacity limits.

The objective function is:

$$minF_T = F_{diesel} + F_{fuelcell} \tag{1}$$

where, F_{diesel} is Fuel cost of diesel generator, $F_{Fuel\text{-}cell}$ is Fuel cost Fuel-cell

Subject to,

$$P_D = \sum_{i=1}^{n} P_{Gi} \tag{2}$$

$$P_G^{min} \leq P_G \leq P_G^{max} \tag{3}$$

where, P_D is Demand, P_G is Real power generation of DGs,n is number of DG's and P_G^{min}, P_G^{max} is Minimum and maximum capacity of DGs.

2.1 Diesel Generator

The objective function in a diesel engine consists of the fuel cost function similar to the cost function used for conventional thermal generating plants.

$$F_{diesel} = \sum_{i=1}^{n} \left(a_i * P_{diesel,i}^2 + b_i * P_{diesel,i} + c_i \right) \tag{4}$$

where F_{diesel} is the diesel generator fuel cost; n is the number of diesel generator; $P_{diesel,i}$ is the diesel generation output in kW of unit i. a_i, b_i, c_i are fuel cost coefficient of i^{th} generator.

2.2 Fuel Cell Plant

The operating cost of fuel cell system takes the fuel costs and includes the efficiency of fuel cell. When fuel is transferred into power, the cost function considers the efficiency of fuel cell. The generation cost of fuel cell is as follows:

$$F_{fuelcell} = \sum_{i=1}^{n} b_i \left(\frac{P_{FC,i}}{n_{FC,i}} \right) \tag{5}$$

where $F_{fuelcell}$ is the fuel cell generation cost; b_i is the natural gas cost in \$/kg; $P_{FC,i}$ is fuel cell generation of the ith plant; $n_{FC,i}$ is fuel cell efficiency of unit i.

3 Review of Neural Networks

In this work BPA based ANN and RBF based ANN is used to solve the present problem.

3.1 BPA Based ANN

A multilayer feed forward network trained by back propagation is the most popular and versatile form of neural network for pattern mapping or function approximation problem. The structure of a BPA based multilayer feed forward network is shown in Fig. 1.

The ANN utilized here contains three layers. These are input, hidden, and output layers. During the training phase, the training data is fed into the input layer. The data is propagated to the hidden layer and then to the output layer. This is called the forward pass of the Back Propagation Algorithm. In the forward pass, each node in hidden layer gets input from all the nodes of input layer, which are multiplied with appropriate weights and then summed. The output of the hidden node is the non- linear transformation of the resulting sum. Similarly each node in output layer gets input from all the nodes of hidden layer, which are multiplied with appropriate weights and then summed. The output of this node is the non-linear transformation of the resulting sum.

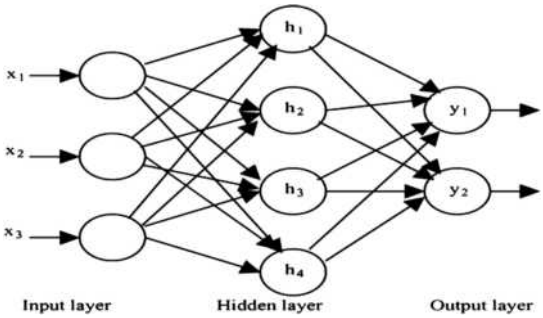

Fig. 1. Structure of BPA based neural network

3.2 RBF Based ANN

RBF networks are feed-forward networks trained using a supervised training algorithm. They are typically configured with a single hidden layer of units whose activation function is selected from a class of functions called basis functions.

Radial Basis Function Neural Network is the three layers feed forward neural network. Figure 2 shows the schematic diagram of a RBF neural network. In RBFNN the input neurons are directly fed to input layer. Then, the output of the input layer is fed to hidden layer without adding any weight. The transfer function of hidden nodes is same as that of multivariate Gaussian density function,

$$\emptyset_j(x) = \exp\left(-\frac{x - u_j^2}{2\sigma_j^2}\right) \tag{6}$$

Where x is the input vector u_j,σ_j are the center and the spread of the corresponding Gaussian function. $\| \cdot \|$ denotes the Euclidean distance between x and u_j. Then, the connections in the second layer is weighted and the output nodes are linear summation units [11].

The value of the k_{th} output node y_k is given by,

$$y_k(x) = \sum_{j=1}^{h} w_{kj}\emptyset_j(x) + w_{k0} \tag{7}$$

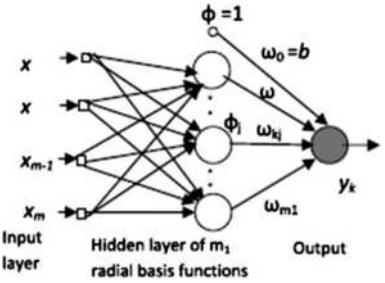

Fig. 2. Structure of RBF neural network

where w_{kj} is the connection weight between the k_{th} output node and j_{th} hidden node and w_{k0} is the bias term.

The training algorithm for RBF neural network is summarized as below.

- Determine the unit centres u_j by the K-means clustering algorithm.
- Determine the unit width σ_j using a heuristic approach that ensures the smoothness and continuity of the fitted function. The width of any hidden node is taken as the maximum Euclidean distance between the identified centres.
- Compute weights of the second layer connections are determined by linear regression using a least-squares objective function.

4 Development of Neural Network for on-Line Power Dispatch of DGs

Many optimization techniques are proposed to solve ED problem [3–10]. However, these methods are needed to solve every time when the system load changes so these methods are not suitable for the on-line power dispatch.

4.1 Training Data Development

The generation of the appropriate training data is an important step in the development of ANN models. For the ANN to accurately predict the output, the training data should represent the complete range of operating conditions of the system under consideration. For model development, a large number of training data is generated through off-line power system simulation. The schematic diagram of proposed approach is given in Fig. 3.

The procedure for generating training data to develop the neural network is as follows:

- First, a range of situations is generated by randomly varying the real power demand between 100 kW to 950 kW.

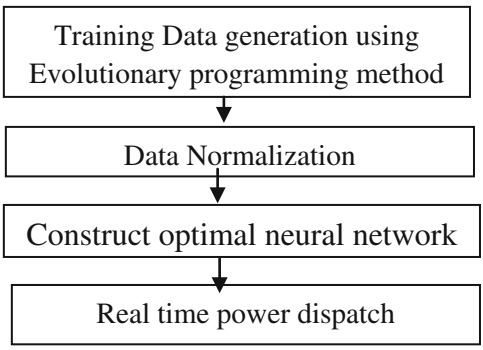

Fig. 3. Schematic diagram of the proposed approach

- For each demand compute real power dispatch of DGs using evolutionary algorithm.

4.2 Data Normalization

During training of the neural network, higher valued input variables may tend to suppress the influence of smaller ones. Also, if the raw data is directly applied to the network, there is a risk of the simulated neurons reaching the saturated conditions. If the neurons get saturated, then the changes in the input value will produce a very small change or no change in the output value. This affects the network training to a great extent. To avoid this, the raw data is normalized before the actual application to the neural network. One way to normalize the data x is by using the expression.

$$x_n = \frac{(x - x_{min})}{(x_{max} - x_{min})} + starting\ value \tag{8}$$

Where x_n is the normalized value, x_{min} and x_{max} are the minimum and maximum values of the variable.

4.3 Network Development

The input after normalization is presented to the ANN networks for training. After training, the networks are evaluated through a different set of input–output data. Once the networks are trained and tested, they are ready for estimating the real power dispatch of DGs.

5 Simulation Results

The proposed NN is implemented on four DGs system under various power demands. Two diesels and two fuel cells are used as DGs. The fuel cost coefficient, generation capacity for diesel, fuel cell and fuel cell efficiency is presented in Table 1. The demand is varied between 100 kW to 950 kW. The simulation studies were carried out by developing program on MATLAB 13.

In the ANN model a sum of 250 input-output pairs are generated in which 200 used for training and 50 used for testing. Based on evolutionary algorithm for each demand the optimum real power dispatch of DGs is obtained. The parameters used for evolutionary programming are population size 200; maximum iteration 100; beta = 0.025.

Table 2 shows the real power dispatch values of four types of DGs obtained using evolutionary programming, BP neural network and RBF neural network.

Figures 4 and 5 shows the testing patterns error for four DGs obtained using BP neural network and RBF neural network respectively.

Figures 6 and 7 shows the Training performance of BP neural network and RBF neural network respectively.

The parameters settings and performance of proposed neural network is presented in Table 3.

Table 1. Parameters of DGs

DG type	Fuel cost coefficient for diesel/natural gas cost for fuel cell			Generation capacity (kW)		Cell efficiency
	c($/hr)	b($/kWh)/($/Kg)	a($/(kW)^2 h)	P_{min}	P_{max}	
Diesel1	0.4333	0.2333	0.0074	25	400	——
Diesel2	0.2731	0.1453	0.0042	15	350	——
Fuel cell1	0	0.05	0	0	100	90 %
Fuel cell2	0	0.05	0	0	150	95 %

Table 2. Dispatch for different load levels in test system

Methods	Demand (kW)	Dispatch of DGs (kW)			
		$P_{Diesel1}$	$P_{Diesel2}$	$P_{Fuel\ Cell1}$	$P_{Fuel\ Cell2}$
EP	810.9502	212.8403	348.4443	99.9234	149.7422
BPNN		212.5039	349.4207	99.9524	149.7422
RBFNN		212.9961	347.3780	99.3582	149.1423
EP	914.5509	317.3113	347.5691	99.9182	149.9298
BPNN		315.1947	349.4319	99.9595	149.7411
RBFNN		316.6144	348.5779	99.9176	149.7411
EP	727.4762	168.2298	309.2145	99.9453	149.8229
BPNN		167.4437	310.0856	99.9801	149.9667
RBFNN		168.5832	309.9683	99.9127	149.5437

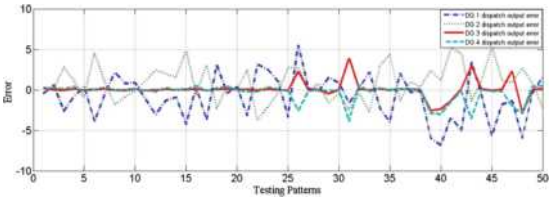

Fig. 4. Error plot for testing patterns of BPNN

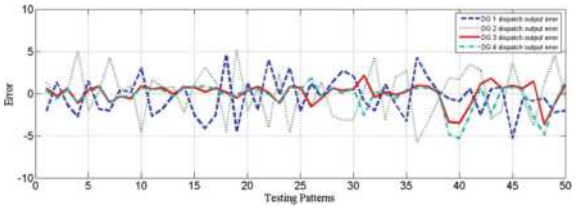

Fig. 5. Error plot for testing patterns of RBFNN

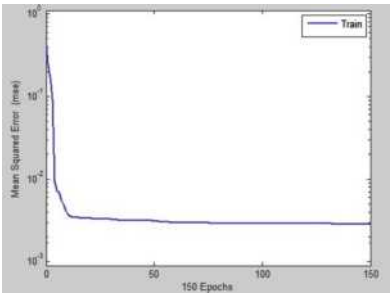

Fig. 6. Training performance of BPNN

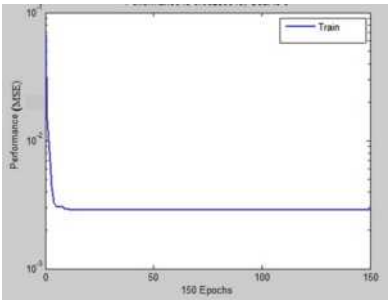

Fig. 7. Training performance of RBFNN

Table 3. Performance of the network

Neural network type	No. of hidden neurons	No. of inputs	No. of outputs	Training time (s)	Training error (mse)	Testing time (s)	Testing error (mse)
BPNN	6	1	4	69	0.00170	0.0936	0.0641
RBFNN	——	1	4	1.62	0.00028	0.046	0.0021

The time taken by the EP for calculating dispatch of DGs for 200 different loading condition is approximately 3854 s. This time may reduce to 69 s when BPNN is chosen. Further the time may reduce to 1.62 s when RBFNN is chosen also from Table 3 it is inferred that the RBFNN testing error is comparatively lower than BP neural network error. Hence, RBFNN is more suitable for on-line ED of DGs.

6 Conclusion

This paper has presented an ANN-based estimation of Real power dispatch of non-renewable DGs for on-line applications. Computer simulation was carried out on the 4 DGs System. Test results show that the proposed BPA based approach and RBF based approach provides accurate estimation of real power dispatch of DGs. In

comparison with BPNN, the RBFNN accurately predict power dispatch of DGs. Hence RBFNN is more suitable for on line ED of DGs in distribution system.

References

1. CIGRE: Impact of increasing contribution of dispersed generation on the power system. Working Group 37.23, (1999)
2. Basu, M., Chowdhury, A.: Cuckoo search algorithm for economic dispatch. Energy **60**, 99–108 (2013)
3. Walter, D.C., Sheble, G.B.: Genetic algorithm solution of economic dispatch with Valve point loading. IEEE Trans. Power Syst. **8**, 1325–1332 (1993)
4. Cheng, P.H., Chang, H.C.: Large scale economic dispatch by genetic algorithm. IEEE Trans. Power Syst. **10**(4), 1919–1926 (1995)
5. Yang, H.T., Yang, P.C., Huang, C.L.: Evolutionary programming based economic dispatch for units with non-smooth fuel cost functions. IEEE Trans. Power Syst. **11**, 112–118 (1996)
6. Gaing, Z.-L.: Particle swarm optimization to solving the economic dispatch considering the generator constraints. IEEE Trans. Power Syst. **18**(3), 1187–1195 (2003)
7. Panigrahi, B.K., Yadav, S.R., Agrawal, S., Tiwari, M.K.: A clonal algorithm to solve economic load dispatch. Electr. Power Syst. Res. **77**(10), 1381–1389 (2007)
8. Wang, S.K., Chiou, J.P., Liu, C.W.: Non-smooth/non-convex economic dispatch by a novel hybrid differential evolution algorithm. IET Gener. Transm. Distrib. **1**(5), 793–803 (2007)
9. Bhattacharya, A., Chattopadhyay, P.K.: Biogeography-based optimization for different economic load dispatch problems. IEEE Trans. Power Syst. **25**(2), 1064–1077 (2010)
10. Wong, K.P., Fung, C.C.: Simulated annealing based economic dispatch algorithm. IEE Proc. Gener. Transmission and Distribution **140**(6), 509–515 (1993)
11. Devaraj, D., Yegnanrayana, B., Ramar, K.: Radial basis function networks for fast contingency ranking. Electr. Power Energy Systems **24**, 387–395 (2002)

Multi-objective Generation Scheduling Using Modified Non-dominated Sorting Genetic Algorithm- II

S. Dhanalakshmi[1(✉)], S. Kannan[2], S. Baskar[3], and K. Mahadevan[4]

[1] Velammal College of Engineering and Technology, Viraganoor, Madurai, India
dhanaml26@gmail.com
[2] Ramco Institute of Technology, Rajapalayam, India
kannaneeeps@gmail.com
[3] Thiagarajar College of Engineering, Madurai, Tamilnadu, India
sbeee@tce.edu
[4] PSNA College of Engineering and Technology, Dindugal, India
mahadevand@rediffmail.com

Abstract. This paper presents a Modified Non-dominated Sorting Genetic Algorithm-II (MNSGA-II) solution to Multi-objective Generation Scheduling (MOGS) problem. The MOGS problem involves the decisions with regards to the unit start-up, shut down times and the assignment of the load demands to the committed generating units, considering conflicting objectives such as minimization of system operational cost and minimization of emission release. Through an intelligent encoding scheme, hard constraints such as minimum up/down time constraints are automatically satisfied. For maintaining good diversity in the performance of NSGA-II, the concepts of Dynamic Crowding Distance (DCD) is implemented in NSGA-II algorithm and given the name as MNSGA-II. In order to prove the capability of the proposed approach 10 units, 24-hour test system is considered. The performance of the MNSGA-II are compared with NSGA-II and validated with reference Pareto front generated by conventional weighted sum method using Real Coded Genetic Algorithm (RGA). Numerical results demonstrate the ability of the proposed approach, to generate well distributed pareto front solutions for MOGS problem.

Keywords: Dynamic crowding distance · Emission · Generation scheduling · Multi-objective optimization · Non-dominated sorting genetic Algorithm-II · Real coded genetic algorithm unit commitment

1 Introduction

Generation Scheduling (GS) is used to schedule the generators, in a power system, such that the total system production cost over the given time period is minimized while meeting various plant and system constraints such as the loading levels, the amount of spinning reserve for each unit and satisfying minimum up-time and down-time constraints. GS problem is a nonlinear, mixed integer combinatorial optimization

B.K. Panigrahi et al. (Eds.): SEMCCO 2014, LNCS 8947, pp. 456–470, 2015.
DOI: 10.1007/978-3-319-20294-5_40

problem. The global optimal solution can be obtained by complete enumeration, which is not practicable to large power systems due to its excessive computation time [1, pp. 131–160].

A number of methods have been used previously for solving the above problem and each method has its own difficulties. The various traditional methods used for this problem are Priority List based method, Branch and Bound, Dynamic Programming and Lagrangian Relaxation [2, 3]. In the Priority List method an exhaustive enumeration of all unit combinations are performed at each load level. Hence, it is hard to handle when the dimension of the problem is huge, whereas in the case of Branch-and-Bound method, finding the optimal solution is time consuming, because it can only be obtained by successive elimination of a set of inappropriate solutions [4]. Based on the "Principle of Optimality", Dynamic Programming was suggested for GS problem. But the main drawback of this was that it could not take into account the coupling time constraints and also time dependent start-up costs [5]. Lagrangian Relaxation method is superior to Dynamic Programming due to its higher solution quality and faster computational time [6] but there is no guarantee in getting an optimal solution. In addition, it is very difficult to handle the minimum up and down time constraints unless some heuristic method was used.

Recently, Evolutionary Algorithms(EAs) are having widespread application because of its two important aspects like very simple, function independent and they are not limited by the properties of the function such as continuity, existence of derivates, unimodality etc. Genetic Algorithm (GA) [7–10], Evolutionary Programming (EP) [11], Simulated Annealing (SA) [12], Tabu Search (TS) [13], Fuzzy Logic/expert systems [14–16], and Artificial Neural Networks (ANN) [17] were applied to solve this problem. But the results obtained by these methods required a considerable amount of computational time especially for a large system size. Hence recently, the traditional methods are integrated with these methods to solve this problem more effectively. These hybrid methods are claimed to accommodate more complicated constraints and also claimed to have better quality solutions even though the system under consideration is very large [18–20].

Due to the increasing environmental pollution caused by the fossil-fuelled electric power plants, the U.S. Clean Air Act amendments of 1990 have forced the utilities to reduce the emissions from such power plants [21]. Hence, it is essential to consider the emission as another objective and GS problem becomes Multi-objective Generation Scheduling (MOGS), which is a multi-objective optimization problem (MOOP) due to conflicting nature of operating cost and emission release.

In general, for solving MOOP, Weighted sum method provides a set of Pareto-optimal solutions by varying the weights, which requires multiple runs [22]. Further, the main disadvantage of this method is that it can't be used to find good distribution of pareto-solutions, for non-convex problems [23]. To overcome this, the ε-constraint method of Multi-objective optimization was used. It is based on reformulating the MOOP by keeping one of the most preferred objectives and restricting the rest of the objectives with some user-specified value ε [24]. These values are adjusted to generate the entire Pareto optimal solution. It is obvious that the solution will depends upon the chosen ε value and this method will consume more time. Currently, the ability of Evolutionary Multi-objective Algorithms (EMOAs) to find Pareto-optimal

solutions is an attractive tool to solve these type of problems with multiple and conflicting objectives [25]. Evolutionary multi-objective search using Multi-Objective Genetic Algorithm towards preferred regions of the pareto front has been discussed for power system generation scheduling problem [26, 27].

Among these algorithms, NSGA-II algorithm is very popular and used to solve various power system multi-objective optimization problems, but still NSGA-II algorithm suffers in maintaining diversity among the solutions in the Pareto front. Hence in addition to NSGA-II, this paper makes use of diversity maintenance strategy which is based on Dynamic Crowding Distance (DCD) [27].

The objective of this paper is to solve the MOGS problem as a true multi-objective optimization problem and by using NSGA-II algorithm with DCD. To validate the performance of NSGA-II and MNSGA-II, conventional weighted sum method using RGA is used. In addition, in order to deal hard constraints of MOGS problem effectively intelligent coding [28, 29] is employed in this paper.

The organization of this paper is as follows. Section 2 addresses the MOGS problem formulation. Section 3 deals with basic introduction of MNSGA-II. The MNSGA-II implementation to the MOGS problem and intelligent coding scheme are described in Sect. 4. Section 5 provides test results and finally Sect. 6 concludes.

2 Multi-objective Generation Scheduling (MOGS)

The objective of MOGS problem is to minimize the operating cost and emission release over the scheduled time period, subjected to generator operational and spinning reserve constraints. MOGS problem is formulated as follows:

2.1 Objectives

2.1.1 Operating Cost

The total operating cost can be mathematically represented as in Eq. (1).

$$f_1 = \sum_{i=1}^{N} \sum_{t=1}^{T} \left[F_i(P_i^t) + ST_{i,t}(1 - U_{i,t-1}) \right] U_{i,t} + (1 - U_{i,t})\, SD_{i,t} \quad \$/hr \tag{1}$$

where, $F_i(P_i^t)$ is represented as,

$$F_i(P_i^t) = \sum_{i=1}^{N} a_i + b_i P_i + c_i P_i^2 \tag{2}$$

where, N is the number of generators, T is the number of time periods, a_i,b_i and c_i are fuel cost coefficients of the ith generator; and P_i^t is the real power output of the ith generator at tth hour and $U_{i,t}$ is the ith unit status at tth hour.

2.1.2 Emission

The total emission of atmospheric pollutants, caused by the operation of fossil-fueled thermal power generation can be expressed in terms of (mg/Nm^3) as

$$f_2 = \sum_{i=1}^{N} \sum_{t=1}^{T} (\alpha_i + \beta_i P_i + \gamma_i P_i^2) \tag{3}$$

2.2 Constraints

2.2.1 Generation Capacity Constraint

For stable operation, real power outputs of each generator must be restricted by lower and upper limits as follows:

$$P_{i,\min}\ U_{i,t} \ \leq \ P_{i,t} \ \leq \ P_{i,\max}\ U_{i,t} \tag{4}$$

2.2.2 Power Balance Constraint

By neglecting losses, the total electric power generation must cover the total power demand $P^t{}_{demand.}$ Hence,

$$\sum_{i=1}^{N} P_{i,t}\, U_{i,t} \ = \ P^t_{demand} \tag{5}$$

2.2.3 Spinning Reserve Constraint

$$P^t_{demand} \ + \ R_t \ = \ \sum_{i=1}^{N} P_{i,\max}\ U_{i,t} \tag{6}$$

2.2.4 Minimum up/Down Time Constraints

Minimum Up time

$$U_{i\,,t} = \ 1\,; \ \ \sum_{j=ts}^{t-1} U_{i,j} < MUT_i \ , \ \ for\, i = 1, \ldots\ldots N, \ \ t = t_s + 1, \ldots\ldots T \tag{7}$$

Minimum Down time

$$U_{i\,,t} = \ 0\,; \ \ \sum_{j=td}^{t-1} (1 - U_{i,j}) < MDT_i \ , \ \ for\, i = 1, \ldots\ldots N, \ \ t = t_d + 1, \ldots\ldots T \tag{8}$$

3 Modified Non-dominated Sorting Genetic Algorithm – II (MNSGA – II)

3.1 Introduction

Before describing the non-dominated sorting genetic algorithm-II (NSGA-II), it is necessary to discuss some terminologies related to it. They are termed as non-dominated sorting, crowding distance, elitism and crowded-tournament operator. The first step of an NSGA-II is to sort the population according to non-domination levels. In order to find solutions of the first non-dominated front in a population, each solution can be compared with every other solution in the population, to find if it is dominated. To find the individuals in the next non-dominated front, the first front solutions are discarded temporarily and the same procedure is repeated until all population members are classified.

To get an estimate of the density of solutions surrounding a particular solution in the population, an average distance of the two solutions on either side of the solution along each of the objectives is calculated. This quantity serves as an estimate of the perimeter of the cuboids formed by using the nearest neighbors as the vertices. This is termed as crowding distance. The overall crowding distance value is calculated as the sum of individual distance values corresponding to each objective. Each objective function is normalized before calculating the crowding distance. In NSGA-II once, the non-dominated sorting is over, the new population is filled by solutions of different non-dominated fronts, one at a time. First the best non-dominated front is filled and continues with solutions of the second non-dominated front and so on. All fronts which could not be accommodated are simply deleted. One important thing to be noted is, when the last allowed front is being considered, there may exists more solutions in the last front than the remaining slots in the new population. The crowded-tournament operator guides the selection process at the various stages of the algorithm toward a uniformly spread-out pareto-optimal front. Every population has two attributes: non-domination rank and crowding distance. Between two different populations with differing ranks, the population with better rank is preferred. If both populations belong to the same front, then the population with larger crowding distance is preferred.

3.2 MNSGA – II

In MOEAs, the horizontal diversity of Pareto-front is very important. The horizontal diversity is often realized by removing excess individuals in the non-dominated set (NDS) when the number of non-dominated solutions exceeds population size. NSGA-II uses Crowding Distance (CD) measure as given in (9) to remove excess individuals. The individuals having lower value of CD are preferred over individuals with higher value of CD in removal process.

$$CD_i = \frac{1}{r}\sum_{k=1}^{r} \left| f_{i+1}^{k} - f_{i-1}^{k} \right| \tag{9}$$

where, r is the number of objectives, f_{i+1}^k is the k^{th} objective of the $i+1^{th}$ individual and f_{i-1}^k is the k^{th} objective of the $i-1^{th}$ individual after sorting the population according to crowding distance. The major drawback of crowding distance is lack of uniform diversity in obtained non-dominated solutions as illustrated in Fig. 1.

In Fig. 1, if normal crowding distance method is adopted then the individuals C, D, and E are deleted from NDS, since they have small cd values. Because of that, some parts of paretofront are too crowded and some parts are with sparseness. Also, cd of B is small, because one side of the rectangle is short, while another side is long. However, the cd of F is large because the length of one side almost equal to another side. If one individual must be removed between the individuals B and F, because of small cd value, individual B will be removed and F will be retained in NDS. But, in order to get good horizontal diversity the individual B should be maintained, because the individual B helps to maintain uniform spread. To overcome this problem, dynamic crowding distance (DCD) method is recently suggested [28, 29].

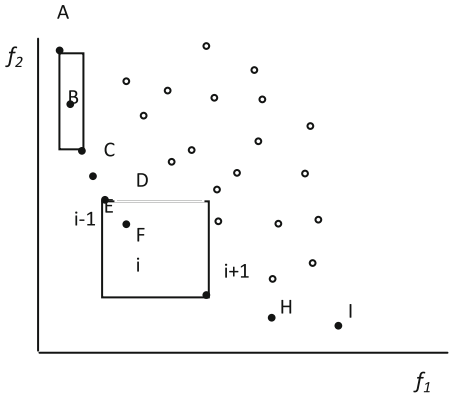

Fig. 1. Crowding distance of individuals

In this approach, one individual with lowest DCD value every time is removed and recalculates DCD for the remaining individuals. The individuals DCD are calculated as follows:

$$DCD_i = \frac{CD_i}{\log\left(\frac{1}{V_i}\right)} \tag{10}$$

Where CD_i is calculated by Eq. (9), V_i is based on Eq. (11),

$$V_i = \frac{1}{r}\sum_{k=1}^{r}\left(\left|f_{i+1}^k - f_{i-1}^k\right| - CD_i\right)^2 \tag{11}$$

V_i is the variance of CDs of individuals which are neighbors of the i^{th} individual. V_i can give information about the difference variations of CD in different objectives. In Fig. 1, the individual B has larger value of V_i than the individual F and DCD of B is larger than F. Therefore, the individuals similar to B in the NDS will have more chance to retain.

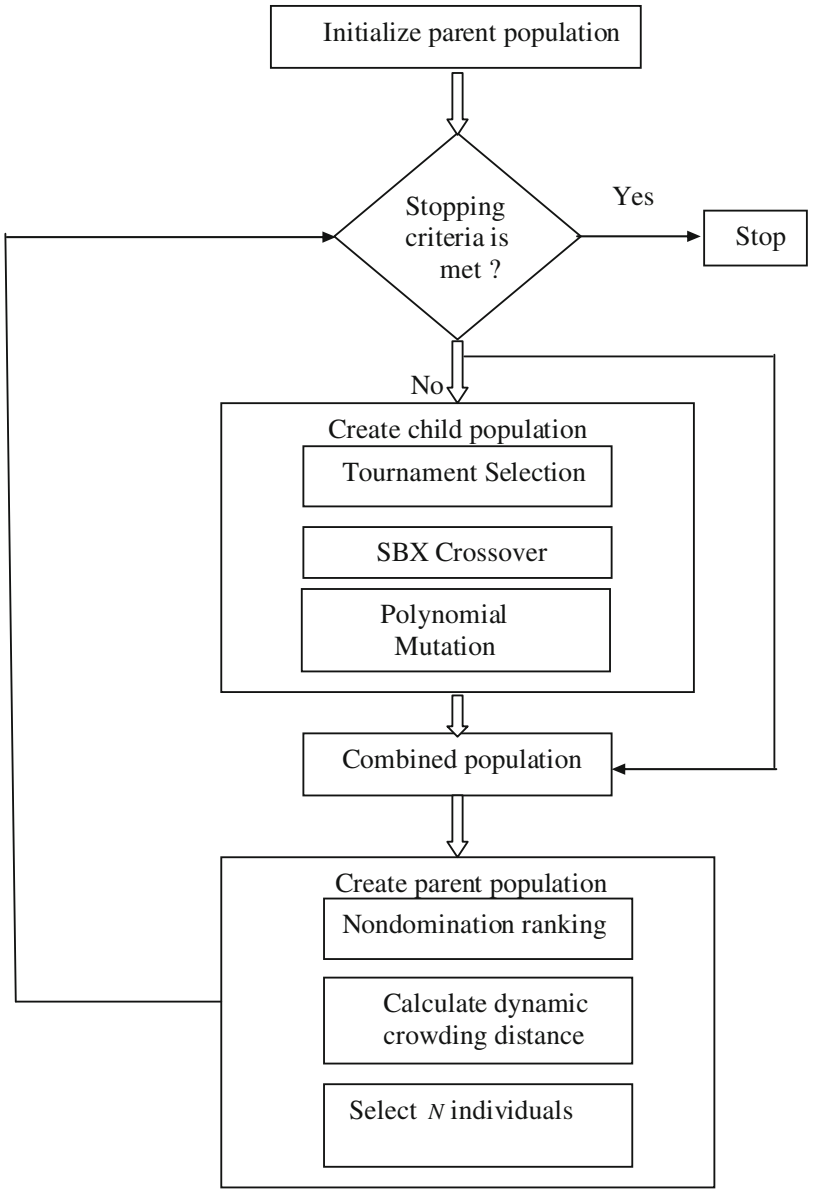

Fig. 2. Computational flow of MNSGA_II

3.3 Computational Flow

The computational flow chart of MNSGA_II is shown in Fig. 2.

4 Implementation of MOGS Problem

In the case of NSGA-II and MNSGA-II the population is generated using real numbers. In fitness function calculation, this real number vector is first rounded to the nearest integer number and then converted to a binary vector of 10 bits. Using intelligent coding scheme [30, 31] this binary vector is converted to a UC schedule without up/down constraint violations.

4.1 Penalty Parameter-Less Constraint-Handling Scheme

In this paper, a constraint-handling method which does not require any penalty parameter is used for handling other than minimum up/down time constraints. In this scheme, all feasible solutions have zero constraint violation and all infeasible solutions are evaluated according to their constraint violation alone. In penalty parameter-less scheme, the fitness function is calculated using (12) [32].

$$F(x) = \begin{Bmatrix} f(x) & \text{if } g_j(x) \geq 0 \ \forall \ j = 1, 2, \ldots\ldots\ldots m \\ f_{\max} + \sum_{j=1}^{m} (g_j(x)) & \text{otherwise} \end{Bmatrix} \tag{12}$$

The advantage of this scheme when compared with the usual penalty parameter based scheme are the tedious process of choosing a suitable penalty parameter can be avoided and no need to evaluate the objective function value for constraint violation, which reduces the computation time. Thus, intelligent coding and penalty parameter-less constraint handling schemes are applied to the MOGS problem to effectively handle the hard and soft constraints.

5 Test Results

The implementation of NSGA-II and MNSGA-II algorithms are carried out using MATLAB Version 7.4 on a Pentium dual core processor desktop computer operating at 2 GHz with 1 GB RAM. The population size is selected as 120. Crossover probability (P_c) and mutation probability (P_m) are fixed at 0.9 and 0.1 respectively. Crossover index (η_c) and mutation index (η_m) are selected as 4 and 18 respectively. The maximum numbers of iterations is fixed at 500 and maximum function evaluations are fixed at 100000. The effectiveness of the algorithm has been tested on a 10 unit 24 h test system. To determine the optimal dispatch for a UC schedule, Quadratic Programming technique is used [33].

5.1 Test System Description

The 10 unit test systems operating cost and emission release function are used in this paper to demonstrate the performance of the proposed method. The demand of the system was divided into 24 intervals. The detailed fuel cost coefficients, emission coefficients, the lower power limits/upper power limits and minimum up/down time are taken from [26].

5.2 Generation of Reference Pareto Front

To compare the performance of MNSGA-II and NSGA-II multiple run generated reference pareto-front is used which is obtained using Real Coded Genetic Algorithm (RGA) with weighted sum approach [23]. The MOGS problem is treated as single objective optimization problem by linear combination of normalized objectives as follows.

$$\text{Minimize } C = w f_{1\_\text{norm}} + (1 - w) f_{2\_\text{norm}} \tag{13}$$

where, C is the combined objective function, f_{1_norm} and f_{2_norm} are the normalized objectives of f_1 and f_2. To generate 25 non-dominated solutions the algorithm is applied 25 times with varying weighting (w) factors as a uniform random number varying between 0 and 1.

5.3 Results and Discussion

The NSGA-II and MNSGA-II are applied to the MOGS problem with and without intelligent coding. Without intelligent coding, NSGA-II and MNSGA-II algorithms are not able to produce even feasible solutions. Whereas with intelligent coding, the NSGA-II and MNSGA-II algorithms have been applied ten times with different initial population, to show the effectiveness of the algorithm. The best results obtained in 10 trails are reported in Tables 1 to 4. From the Tables 1, 2, 3 and 4, it is clear that, all the hard constraints like minimum up/down time and demand constraint are satisfied.

Table 1 gives the hourly dispatch (U1-U10) for best total operating cost and the corresponding total emission release using NSGA-II. From Table 1, it is observed that the best total operating cost is 778470 $/hr and the corresponding total emission release is 874750 mg/Nm^3, using NSGA-II. Similarly Table 2 represents the best total emission release is 700010 mg/Nm^3, and the corresponding total operating cost is 810040 $/hr using NSGA-II.

Table 3 gives the hourly dispatch (U1-U10) for best total operating cost and the corresponding total emission release using MNSGA-II. From Table 3, it is observed that the best total operating cost is 764240 $/hr and the corresponding total emission release is 783240 mg/Nm^3, using MNSGA-II. Similarly Table 4 represents the best total emission release is 585830 mg/Nm^3, and the corresponding total operating cost is 789870 $/hr using MNSGA-II.

Table 1. Hourly dispatch, best total operating cost ($) and corresponding total emission release (mg/Nm^3) using NSGA-II

Hour	Hourly dispatch (MW)										Best total operating cost ($)	Corresponding total emission release (mg/Nm^3)
	U1	U2	U3	U4	U5	U6	U7	U8	U9	U10		
1	54	72	90	108	135	172.13	445.15	94.72	288	0	**778470**	**874750**
2	54	72	90	108	135	158	403.10	63.91	288	0		
3	54	72	90	108	135	146.14	367.81	38.05	288	0		
4	54	72	90	108	135	143.06	358.62	31.32	288	0		
5	52	72	90	108	135	0	435.99	88.01	288	0		
6	54	72	90	108	135	0	445.32	94.85	288	26.84		
7	0	72	90	108	135	0	468	134.10	288	76.90		
8	54	72	90	108	135	0	445	94.85	288	26.84		
9	54	72	90	108	0	0	468	125.32	288	65.68		
10	54	0	90	108	0	0	468	135	288	99		
11	54	0	90	108	0	0	468	124.44	288	64.56		
12	54	0	90	108	0	0	468	117.85	288	56.15		
13	54	72	90	108	0	0	435.94	87.98	288	18.08		
14	54	72	90	108	0	0	429.94	83.58	288	12.48		
15	54	72	90	108	0	0	424.69	79.73	288	7.57		
16	54	72	90	108	0	0	450.93	0	288	32.07		
17	54	72	90	108	0	0	435.93	0	288	18.07		
18	54	72	90	108	0	0	420.94	0	288	4.06		
19	54	72	90	108	0	0	381	0	288	0		
20	54	72	90	108	0	0	366	0	288	0		
21	54	0	90	108	0	0	377.70	45.30	288	0		
22	54	72	90	108	0	0	370.20	39.80	288	0		
23	54	72	90	108	0	0	404.25	64.75	288	0		
24	54	72	90	108	135	0	468	135	288	109		

Table 2. Hourly dispatch, best total emission release (mg/Nm^3) and corresponding total operating cost ($) using NSGA-II

Hour	Hourly dispatch (MW)										Best total emission release (mg/Nm^3)	Corresponding total operating cost ($)
	U1	U2	U3	U4	U5	U6	U7	U8	U9	U10		
1	54	0	90	0	0	244	468	135	288	180	**700010**	**810040**
2	54	0	90	0	0	208.68	468	135	288	128.32		
3	54	0	90	0	0	189.82	468	133.31	288	75.87		
4	54	0	90	0	0	186.63	468	126.36	288	67.01		
5	54	0	90	0	0	185.12	468	123.07	288	62.81		
6	54	0	0	108	0	189.32	468	132.21	288	74.47		
7	0	0	0	108	0	218.21	468	135	288	154.79		
8	0	0	0	108	0	202.86	468	135	288	112.14		
9	0	0	0	108	0	191.49	468	135	288	80.51		
10	0	0	90	108	0	0	468	135	288	153		
11	0	72	90	108	0	0	468	116.53	288	54.47		
12	54	72	90	108	0	0	446.44	95.67	288	27.89		
13	54	72	90	108	0	0	435.94	87.98	288	18.08		
14	54	0	90	108	0	0	456.94	103.36	288	37.69		
15	54	0	90	108	0	0	451.69	99.52	288	32.79		
16	0	0	90	108	0	0	468	0	288	141		
17	0	0	90	108	0	0	468	0	288	112		
18	0	0	90	108	0	0	468	0	288	83		
19	0	0	90	108	0	0	422.82	78.36	288	5.82		
20	0	0	0	108	0	0	450.94	98.97	288	32.09		
21	0	0	0	108	0	0	460.81	106.19	288	0		
22	0	0	90	108	0	0	442.92	93.08	288	0		
23	54	0	90	108	0	0	445.80	95.20	288	0		
24	54	0	90	108	0	203.13	468	135	288	112.87		

Table 3. Hourly dispatch, best total operating cost ($) and corresponding total emission release (mg/Nm^3) using MNSGA-II

Hour	Hourly dispatch (MW)										Best total operating cost ($)	Corresponding total emission release (mg/Nm^3)
	U1	**U2**	**U3**	**U4**	**U5**	**U6**	**U7**	**U8**	**U9**	**U10**		
1	54	72	90	108	135	172.13	445.15	94.72	288	0	**764240**	**783240**
2	54	72	90	108	135	158	403.10	63.91	288	0		
3	54	72	90	108	135	146.14	367.81	38.05	288	0		
4	54	72	90	108	135	143.06	358.62	31.32	288	0		
5	0	72	90	108	135	150.36	380.38	47.26	288	0		
6	54	72	90	108	135	159.48	407.52	0	288	0		
7	54	72	90	108	135	174.07	450.93	0	288	0		
8	54	72	90	108	135	159.48	407.52	0	288	0		
9	54	72	90	108	135	148.67	375.33	0	288	0		
10	54	72	90	108	135	141.38	353.62	0	288	0		
11	54	72	90	108	135	131.86	325.31	0	280.83	0		
12	54	72	90	108	135	198..90	0	135	288	101.1		
13	54	0	90	108	135	210.53	0	135	288	133.47		
14	54	72	90	108	135	188.48	0	130.38	288	72.14		
15	54	72	90	108	135	186.13	0	125.26	288	65.61		
16	0	72	90	108	135	190.32	0	134.41	288	77.27		
17	0	72	90	108	135	185.46	0	123.80	288	63.74		
18	0	72	90	108	135	180.59	0	113.19	288	50.22		
19	0	72	90	108	135	182.55	0	117.45	288	0		
20	54	72	90	0	0	0	407.13	66.87	288	0		
21	54	72	90	0	0	0	459	0	288	0		
22	54	72	90	108	0	0	410	0	288	0		
23	54	72	90	108	0	0	443.69	0	288	25.31		
24	54	72	90	108	0	219.79	468	0	288	159.21		

Table 4. Hourly dispatch, total best emission release (mg/Nm^3) and corresponding total operating cost ($) using MNSGA-II

Hour	Hourly dispatch (MW)										Total best emission release (mg/Nm^3)	Corresponding total operating cost ($)
	U1	**U2**	**U3**	**U4**	**U5**	**U6**	**U7**	**U8**	**U9**	**U10**		
1	54	0	90	108	135	177.20	460.24	105.78	288	40.78	**585830**	**789870**
2	54	0	90	108	135	180.12	467.98	0	288	48.90		
3	54	0	90	108	135	169.17	436.36	0	288	18.47		
4	54	0	0	108	135	179.69	467.61	0	288	47.70		
5	0	0	0	108	135	191.49	468	0	288	80.51		
6	0	0	0	108	135	202.86	468	0	288	112.14		
7	0	0	0	108	135	238	468	135	288	0		
8	0	0	0	108	135	187.26	468	127.74	288	0		
9	0	0	90	108	0	187.89	468	129.11	288	0		
10	0	0	90	108	0	179.27	466.42	110.31	288	0		
11	0	0	90	108	0	171.96	444.67	94.37	288	0		
12	0	72	90	108	135	213.18	0	135	288	140.82		
13	0	72	90	108	135	205.77	0	135	288	120.23		
14	0	72	90	108	135	201.54	0	135	288	108.46		
15	0	0	90	108	135	216.88	0	135	288	151.12		
16	54	0	90	108	135	194.93	0	135	288	90.07		
17	54	0	90	108	135	188.48	0	130.38	288	72.14		
18	54	0	90	108	135	183.61	0	119.77	288	58.61		
19	0	0	90	108	0	217.94	0	135	288	154.06		
20	0	0	90	0	0	0	468	132	288	0		
21	0	0	90	0	0	0	468	117	288	0		
22	0	0	90	108	0	0	442.92	93.08	288	0		
23	0	0	90	108	0	0	468	127	288	0		
24	54	0	90	108	0	203.13	468	135	288	112.87		

NSGA-II and MNSGA-II produces the pareto-optimal solutions in a single simulation run. Figure 3 illustrates the best pareto front obtained using NSGA-II and MNSGA-II. The comparison with respect to reference Pareto front is also presented in the same figure. When compared to NSGA-II, the pareto front obtained in MNSGA-II is much better in terms of non-domination level. Also the solution obtained using NSGA-II and MNSGA-II are well distributed, whereas solution obtained by RGA are poorly distributed and is having less number of non-dominated solutions

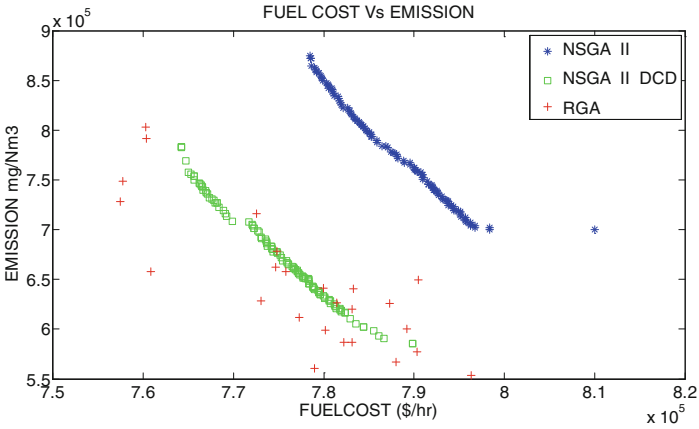

Fig. 3. Pareto optimal solutions for the 10 unit 24 h test system using NSGA-II, MNSGA-II and RGA

6 Conclusion

Multi-objective generation scheduling problem is considered with objectives of minimization of total operating cost and total emission release using modified NSGA-II algorithm. Intelligent coding scheme is employed to effectively satisfy minimum up/down time constraints. To demonstrate the effectiveness of MNSGA-II and intelligent coding scheme, 10 units 24-hour test system is taken. The reference Pareto front is generated using weighted sum method with RGA. The results obtained shows that the MNSGA-II is an effective tool for handling MOGS problem to generate a pareto front in a single simulation with the best computational time. Results also show that, pareto front obtained using MNSGA-II is well distributed with more number of non-dominated solutions as compared to the obtained pareto front by reference and the NSGA-II.

References

1. Wood, A.J., Wollenberg, B.F.: Power Generation, Operation and Control, 2nd edn. Wiley, New York (1996)
2. Yamin, H.Y.: Review on methods of generation scheduling in electric power systems. J. Electr. Power Syst. Res. **69**, 227–248 (2004)
3. Padhy, N.P.: Unit commitment – a bibliographical survey. IEEE Trans. Power Syst. **19**, 1196–1205 (2004)
4. Lee, F.N.: Short-term unit commitment – a new method. IEEE Trans. Power Syst. **3**, 691–698 (1988)
5. Pang, C.K., Sheble, G.B., Albuyeh, F.: Evaluation of dynamic programming based methods and multiple area representation for thermal unit commitment. IEEE Trans. Power Apparatus syst. **100**, 1212–1218 (1981)
6. Virmani, S., Imhof, K., Mukherjee, S.: Implementation of lagrangian based unit commitment problem. IEEE Trans. Power Syst. **10**, 772–777 (1995)
7. Kazarlis, S.A., Bakirtzis, A.G., Petridis, J.: A genetic algorithm solution to the unit commitment problem. IEEE Trans. Power Syst. **11**, 83–92 (1996)
8. Orero, S.O., Irving, M.R.: A genetic algorithm for generation scheduling in power systems. Int. J. Electr. power Energy syst. **18**, 19–26 (1996)
9. Swarup, K.S., Yamashiro, S.: Unit commitment solution methodology using genetic algorithm. IEEE Trans. Power Syst. **17**, 87–91 (2002)
10. Dasgupta, D., Mcgregor, D.R.: Thermal unit commitment using genetic algorithms. IEE Proc. Gen Trans. Dist. **141**, 459–465 (1994)
11. Juste, K.A., Kita, H., Tanaka, E., et al.: An evolutionary programming solution to the unit commitment problem. IEEE Trans. Power Syst. **14**, 1452–1459 (1999)
12. Mantawy, A.H., Abdel-Magid, Y.L., Selim, S.Z.: A simulated annealing algorithm for unit commitment. IEEE Trans. Power Syst. **13**, 197–204 (1998)
13. Mantawy, A.H., Abdel-Magid, Y.L., Selim, S.Z.: Unit commitment by tabu search. Proc. Inst. Elect. Eng. Gen. Trans. Dist. **145**, 56–64 (1998)
14. Saneifard, S., Prasad, N.R., Smolleck, H.: A fuzzy logic approach to unit commitment. IEEE Trans. Power Syst. **12**, 988–995 (1997)
15. Ouyang, Z., Shahidehpour, S.M.: Heuristic muti-area unit commitment with economic dispatch. IEE Proc. **138**, 242–252 (1991)
16. Tong, S.K., Shahidehpour, S.M., Ouyang, Z.: A heuristic short-term unit commitment. IEEE Trans. Power Syst. **6**, 1210–1216 (1991)
17. Wang, C., Shahidehpour, S.M.: Effects of ramp-rate limits on unit commitment and economic dispatch. IEEE Trans. Power Syst. **8**, 1341–1350 (1993)
18. Ongsakul, W., Petcharaks, N.: Unit commitment by enhanced adaptive lagrangian relaxation. IEEE Tran. Power Syst. **19**, 620–628 (2004)
19. Cheng, C.P., Liu, C.W., Liu, C.C.: Unit commitment by lagrangian relaxation and genetic algorithms. IEEE Trans. power Syst. **15**, 707–714 (2002)
20. Mahadevan, K., Kannan, P.S.: Lagrangian relaxation based particle swarm optimization for unit commitment problem. J. Power Energy Syst. **27**(4), 320–329 (2007)
21. Bharathi, R., Kumar, M.J., Sunitha, D., Premalatha, S.: Optimization of combined economic and emission dispatch problem – a comparative study. In: Proceedings of Eighth International Power Engineering Conference, pp. 134–139 (2007)
22. Dhillon, J.S., Parti, S.C., Kothari, D.P.: Stochastic economic emission dispatch. Electr. Power Syst. Res. **26**, 197 (1993)

23. Deb, K.: Optimization using evolutionary algorithms, 2nd edn, pp. 171–280. Wiley, New York (2001)
24. Yokoyama, R., Bae, S.H., Morita, T., Sasaki, H.: Generation dispatch based on probability security criteria. IEEE Trans. Power Syst. **3**, 317–324 (1988)
25. Abido, M.A.: Evolutionary algorithms for electric power dispatch problem. IEEE Trans. Evol. Comput. **10**(3), 315–329 (2006). doi:10.1109/tevc.2005.857073
26. Zio, E., Baraldi, P., Pedroni, N.: Optimal power system generation scheduling by multi-objective genetic algorithms with preferences. Reliab. Eng. Syst. Saf. **94**, 432–444 (2009)
27. Li, Y.F., Pedroni, N., Zio, E.: A memetic evolutionary multi-objective optimization method for environmental power unit commitment. IEEE Trans. Power Syst. **28**(3), 2660–2669 (2013)
28. Luo, B., Zheng, J., Xie, J., Wu, J.: Dynamic crowding distance - A new diversity maintenance strategy for MOEAs. In: 4th International Conference on Natural Computation (ICNC 2008), vol. 1, pp. 580–585 (2008)
29. Dhanalakshmi, S., Kannan, S., Mahadevan, K., Baskar, S.: Application of modified NSGA-II algorithm to combined economic and emission dispatch problem. Int. J. Electr. Power Energy Syst. **33**(4), 992–1002 (2011)
30. Baskar, S., Subbaraj, P., Chidambaram, P.: Application of genetic algorithms to unit commitment problem. IE(I) J. **81**, 195–201 (2001)
31. Dhanalakshmi, S., Kannan, S., Baskar, S., Mahadevan, K.: Intelligent genetic algorithm for generation scheduling under deregulated environment. In: Panigrahi, B.K., Suganthan, P.N., Das, S., Satapathy, S.C. (eds.) SEMCCO 2011, Part I. LNCS, vol. 7076, pp. 282–289. Springer, Heidelberg (2011)
32. Manoharan, P.S., Kannan, P.S., Baskar, S., Iruthayarajan, M.W.: Penalty parameter-less constraint handling scheme based evolutionary algorithm solutions to economic dispatch. IET Gener. Transm. Distrib. **2**, 478–490 (2008)
33. Danaraj, R.M.S., Gajendran, F.: Quadratic programming solution to emission and economic dispatch problems. IE (I) J. **86**, 129–132 (2005)

Indian Road Traffic Surveillance System using Blob Tracking for ATIS Applications

Balaji Ganesh Rajagopal, Appavu alias Balamurugan Subramanian, and Midhun Kumar Ayyalraj

Abstract— **Intelligent Transportation System is an Emerging area to solve multiple transportation problems. Several forms of inputs are needed in order to solve ITS problems. Advanced Traveler Information System (ATIS) is a core and important ITS area of this modern era. This involves travel time forecasting, efficient road map analysis and cost based path selection, Detection of the vehicle in dynamic conditions and Traffic congestion state forecasting. This Article designs and provides an algorithm for traffic data generation which can be used for the above said ATIS application. By inputting the real world traffic situation in the form of video sequences, the algorithm determines the Traffic density in terms of congestion, number of vehicles in a given path which can be fed for various ATIS applications. The Algorithm deduces the key frame from the video sequences and follows the Blob detection, Identification and Tracking using connected components algorithm to determine the correlation between the vehicles moving in the real road scene.**

Keywords **– Traffic Transportation, Traffic Density estimation, Blob Identification and Tracking, Relative Velocity of vehicles, Correlation between vehicles.**

I. INTRODUCTION

INTELLIGENT Transportation System is an Emerging Area to Solve multiple transportation Issues. Advanced Travelers Information System is a core area of ITS which gives amenities to the traveler by providing valuable information which can be used by the traveler for path selection, travel time forecasting and time management.

Traffic flow monitoring and traffic analysis based on computer vision techniques, and especially traffic analysis and monitoring in a real-time mode raise precious and complicated demands to computer algorithms and technological solutions. Most convincing applications are vehicle tracking, and the crucial issue is initiating a track automatically. Traffic analysis then leads to reports of speed violations, traffic congestions, accidents, or illegal behavior of road users. Various approaches to these tasks were suggested by many scientists and researchers [1,3]

Balaji Ganesh Rajagopal, Assistant Professor in the Department of Computer Science and Engineering, Ramco Institute of Technology, Rajapalayam-626117, Tamilnadu, India (phone: +918220037222; e-mail:balajiganeshr@ gmail.com).

Dr.Appavu alias Balamurugan Subramanian, Professor and Head, Department of Information Technology, K.L.N. College of Information Technology, Pottapalayam 630611, Tamilnadu, India. (e-mail: app_s@yahoo.com)

Midhun Kumar Ayyalraj, Assistant Professor, Department of Information Technology, K.L.N. College of Information Technology, Pottapalayam 630611, Tamilnadu, India. (e-mail:midhuntce@gmail.com)

One of the main aspects was to modify these algorithms to fit to real-time road monitoring processes, and as a consequence the prototype of system for traffic analysis was developed. Technically this system is based on stationary video cameras as well as computers connected to wide area network.[2,4]

The application is utilizing image-processing and pattern recognition methods designed and modified to the needs and constraints of road traffic analysis. These are combined together gives functional capabilities of the system to monitor the road, to initiate automated vehicle tracking, to measure the speed. [6]

Image processing and object/pattern recognition of moving objects, chosen for the system, lead to complex mathematical, algorithmic and programming problems. Many articles have considered particular questions related to scene modeling, object geometry accounting, image contours processing. There is a lack of information on methods and algorithms used in digital monitoring technology, perhaps for commercial reasons. [7]

In the cell transmission model, a very simple model and yet it is able to recover most of the phenomena observed in real traffic. There are many other traffic flow models suggested in the literature that also reproduce traffic flow, in some cases with more precision than the cell transmission model. However, one of the challenges for real time on-ramp metering control consists on having calibrated traffic flow models. [3]

Grid method is the most common method in road density analysis. However, the determination of grid size, position and orientation is rather arbitrary. It also fails to provide information within grids, and may bring obstacles to road selection process, since grid boundaries may ‘split’ the roads into several parts and ultimately give rise to the loss of information about connectivity. [5]

Fractal geometry method is devised by introducing self-similar fractal concepts. This method splits the whole study area into self-similar grids iteratively and the algorithm stops when the features within grids are homogeneous. It has the setback that the initial grid size exerts too much influence on computed road density, and the information lost at larger grid may not be recovered. Mesh density based on sub-region avoids several of the aforementioned setbacks. However, it neglects geographical characteristics of road networks and may not reflect information about the area each road is serving and its relative importance. [5]

The problem of road monitoring as it is chosen in our research is presented as a sequence of independent processing steps intended to solve tasks logically connected to each other.

These steps are in hand of the following order of algorithmic processing: video stream input to computer (personal computer or specialized one), its conversion to a sequence of single frames, Key Frame Selection, Blob Identification, Blob Coloring, Blob Tracking, Analysis of relative velocities of the Blobs.

This paper mainly describes about the relative velocities of the moving blobs by utilizing the individual blobs velocity and draws the Probability Density Function (PDF) which then determines the density of the road surface.

The paper is organized as follows. Section 2 explains the Selection of Key frames from the input Video Sequence. Section 3 explains the extraction of Blobs. Section 4 outlines the blob spatial moment and the correlation among the blobs which includes centroid extraction. Section 5 discusses the experimental results and Section 6 presents the conclusion of proposed algorithm.

II. KEY FRAME SELECTION

A. Overview

For every video input to be processed, key frame selection is the initial step which selects the frames that best describes the important change detected in the input video. Here we propose a method to select the key frame based on color histogramming technique.

B. Color Histogramming

This technique detects the peak change in the RGB values of the pixel in each frame. The Frame's RGB values are appropriately sampled in the 64 bin space which derives the key frame. By sorting each frame against the RGB Pixel value, the frame which most deviates from the rest of the frames is obtained. In The Color Histogramming technique the Mean R,G,B Value of each frame is calculated which then sorted and the deviation of R,G,B Mean value with other frames is listed out as shown in Fig.1. The Frames with the highest deviation and lowest deviation are considered as key frames.

Our Experimental results show that this technique is cost effective in-terms of run time memory requirements. This approach also reduces the constraints on the input requirements when compared to other techniques like edge histogram and wavelets and distance descriptor matching. The Method of Color Histogramming is easy to implement and cost effective in terms of both Space and Time complexity. Around 100 sets of video are applied over this algorithm to test the accuracy of the results. Color Histogramming can be applied to a large volume of data since it uses n-bin technique to group the pixels by which pre-processing is done at an earlier stage to avoid keeping unwanted information through all phases of the algorithm.

Image Number	Red Mean Value	Green Mean Value	Blue Mean Value
img10.jpg	92.3166666	118.041025	109.735353
img11.jpg	92.3166666	118.041025	109.735353
img12.jpg	92.2833333	118.046153	109.711111
img14.jpg	92.2833333	118.046153	109.711111
img15.jpg	92.2385416	117.970256	109.670707
img16.jpg	92.2385416	117.970256	109.670707
img9.jpg	92.1916666	117.873846	109.586868
img8.jpg	92.1552083	117.869743	109.489898
img7.jpg	92.155208	117.869743	109.489898
img17.jpg	92.064583	117.710769	109.413131
img18.jpg	92.064583	117.710769	109.413131
img43.jpg	92.079166	117.817435	109.333333
img44.jpg	92.079166	117.817435	109.333333
img45.jpg	92.1	117.810256	109.370707
img47.jpg	92.1	117.810256	109.370707

Table.1. Showing the Color Histogram values for the individual frames which are sorted based on the Deviation Descriptor.

Figure.1. Showing the Best 2 Frames which are more deviated from each other based on the Color Histogram Value

III. BLOB DETECTION AND TRACKING

A. Overview

Here we propose an algorithm to detect each and every moving vehicle designated as blobs. A blob is defined to be a filled square and any square that can be reached from that square by moving horizontally or vertically. A blob is a connected region that can be found out by traversing through the pixels of the image.

B. Blob Detection

Here we designed and experimented with a kernel which can be moved over the image to find out all the connected components. A Connected component refers to an object which has coherency of features when compared to the rest of the objects. The kernel shown in Fig 2 is moved over the image to find the connected components. For position S in the kernel Neighbouring pixels A, B, C & D are checked for the least label value. The pixel with minimal Label value is added to the list of connected pixels. Similarly many groups of connected pixels are grouped.

A	**B**	**C**
D	**S**	

Figure.2. Blob Detection Kernel used to analyze the neighbourhood pixels for connected component S:Source Pixel, A,B,C,D:Neighbourhood Pixel

Algorithm

1. Read the Image Array
2. Initialize labelTable, xMinTable, xMaxTable, yMinTable, yMaxTable, massTable to 0

   Initialize labelBuffer to the no. of pixels in the image
3. For Each Pixel S the nearest pixels are verified

   A B C

   D S
4. Assign Labels for each Pixel and enter it into labelTable
5. Iterate through pixels looking for connected regions.
6. Find the neighbouring pixel with the least labelValue
7. If the found neighbour is a foreground pixel

   a. Set S Pixel Label value to min and assign the least labelValue to the pixel

   b. Update min & max X, Y values on the found neighbour into labelTable

   c. Increment the massTable value
8. If the found neighbour is not a foreground pixel

   a. Enter the min & max X, Y values into the xMinTable, xMaxTable, yMinTable, yMaxTable

   b. Increment the label value
9. Repeat Steps 3 to 8 for all pixels
10. Rearrange the labelValue of the each labelBuffer starting from 0
11. Assign color value to each labelValue (Blob)

The algorithm uses Five Tables (xMin, yMin, xMax, yMax, MassTable) to identify the nearest and least neighborhood pixel. The kernel is made to pass through the entire array set of images. For each neighbor pixel, the labels are assigned and it is compared with the rest of the neighbours.

If the found neighbor posses Label value less than the current pixel's Label value, then the neighbor pixel is designated as the new pixel and its x,y position in the array are entered into the corresponding tables.

To ensure the reliability of Blob Detection Algorithm, during the free flow traffic in which the vehicles can be passed through with greater velocity and to identify the missed vehicles between the two key frames, a Middle frame approach is suggested. This approach compares the no. of blobs with an intermediate frame that lies exactly in the middle of the two key frames. The frame is taken into account, so that a moving object with higher velocity gets out in between the key frames and can be neglected in the further processing.

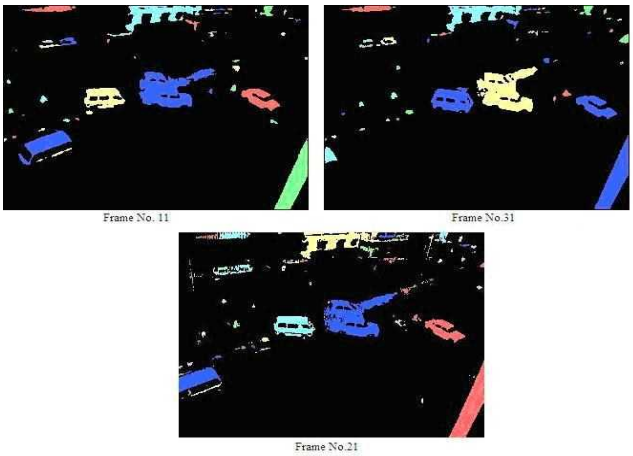

Figure.3. Result of Blob Detection Algorithm which Detects the Moving Foreground Pixels & Colours the Blobs (Key Frame1, Key Frame2, Middle Frame)

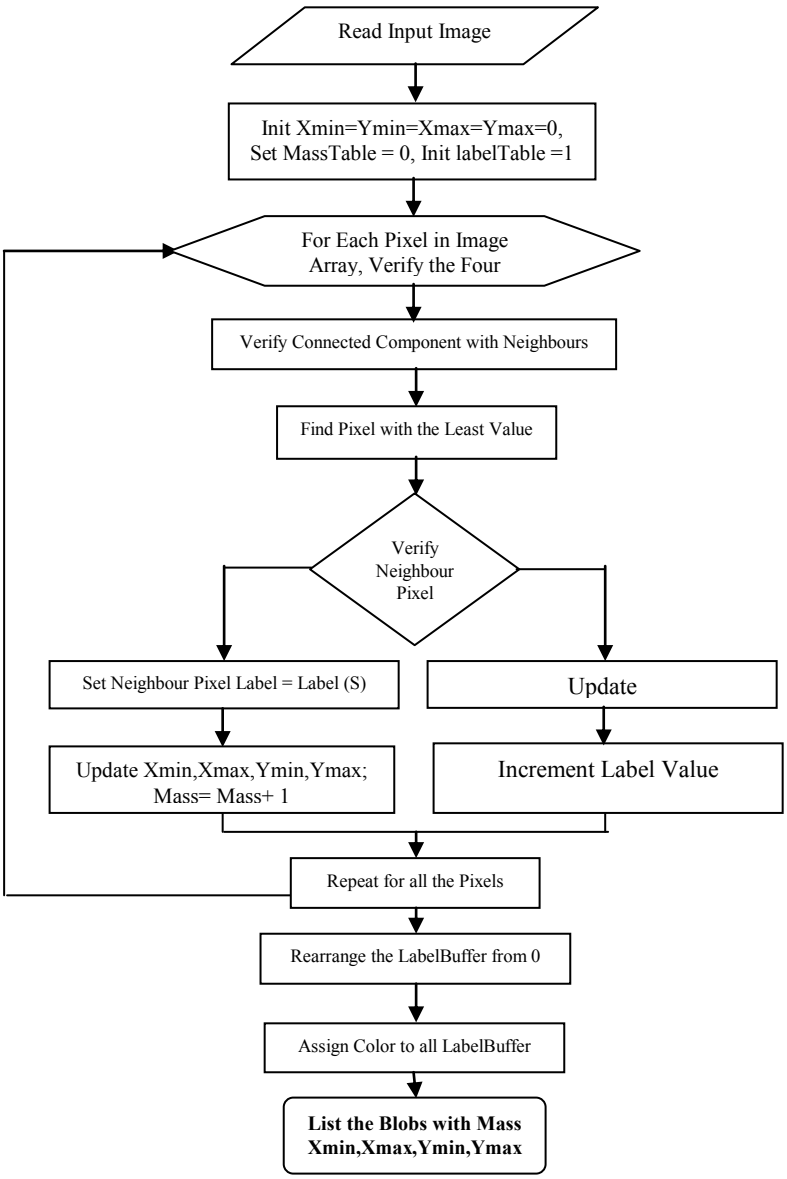

Figure. 4. Flow Chart Depicting Blob Detection Algorithm based on Connected Pixel Region.

C. Blob Filtering

In this Section, the identified Blobs are labelled from 1 to n Numbers. Each blob's X and Y position is calculated and the mass of each blob is calculated. The massTable in the above algorithm provides the value of each blob's spatial mass which can be calculated.

The blobs listed based on the algorithm in the previous section consists of all the blobs in the input frames. Blob filtering is carried out to filter out the stationary blobs which are basically the background pixels in the input frames. Three sets of conditions are applied over the blob list to find out the blobs which contain only the vehicles which are correlated between the two frames.

Blobs which are stationary over a set of frames and Blobs that are having mass less than the specified threshold, where the threshold is calculated based on trial and error basis.

Blobs whose change is very low, this is carried out to avoid erroneous blobs because of the internal movement of the camera and lightning conditions

The Blobs are Filtered using (1) and are sorted out. The filtered Blobs need to be tracked to find out the spatial movement of the blobs and their correlation between the frames. The correlation between the frames is found out to conclude whether the blobs have their movement independent or depend on some other blobs. This is found out by comparing the blobs that are having equal mass between the frames. The final list of blobs is analysed for their spatial movement. A rectangle is drawn over the blobs to track it across the frame.

$$\text{Bi}=\begin{cases}\mathbf{b_i} \; where & ((\mu(b_i)>th1)\,\&\& \\ & ((\delta(b_{i,f_a}(x),b_{i,f_b}(x))>th2)\,\&\& \\ & (\delta(b_{i,f_a}(y),b_{i,f_b}(y))>th2))\end{cases} \quad (1)$$

Where, μ =Mass of the Blob, f_a =Frame 1, f_b = Frame 2, δ =Difference in the position of the object between frame 1 and frame 2, Number of Blobs Detected (i) = 0 to n, th1, th2 = Threshold. B_i is the list of blobs from the set b_i which satisfies the threshold condition.

Figure 5 Blob Filtering Constraints Applied over the list of Blobs and Convex Hull Marked over Similar Moving Blobs

D. Blob Tracking

These moving blobs represent the vehicle motion in the images. It has asserted that the convex hull surrounding a vehicle in an image is a good approximation of the projection of a vehicle in the image. In the Blob Filtering, we exclude the blobs whose mass is less than 100 pixels. To characterize the moving blobs, we calculate the convex hull and calculate the centroid for the blobs. The area of each blob is calculated and is indexed by the vertical location of its centroid in the image. This area is an indicator of blob size relative to its location in the image.

Having located a vehicle in one image, the vehicle is tracked across images by enforcing co- linearity of the centroid of the convex hulls. The Figure 6 presents a representation of three convex hulls with centroid (x1, y1), (x2, y2), and (x3, y3).

E. Velocity Estimation

Figure.6. Moving Blobs Identified between Frame 1 and Frame 2 by applying Equation (1)

For a set of Two Blobs, Calculate the velocity of the blobs by fixing a reference point and calculate the displacement. Calculate the time difference between the frames and hence calculate the velocity of the individual blobs.

A point in the previous frame, p , will be associates with a point in the current frame based on the minimum Euclidean distance, However, in order to determine the Minimum distance, all the distance between reference point p and all other points c1 , c 2 ...c n must be established

$$E_d=\sqrt{(P_x-x_{cb})^2+(P_y-y_{cb})^2} \quad ;\forall b\in B \quad (2)$$

For every blob $b\in B_i$ in the image, the bounding box and centroid, λ = (x_{cb}, y_{cb}) are extracted where x_{cb} and y_{cb} denotes the points connecting the diagonal of the convex hull marked over the blob. Centroid is computed by calculating the blob's spatial moment and is given in (3) and (4). This centroid will be used for tracking object.

$$u_{pq}=\sum_{x_b=0}^{m-1}\sum_{y_b=0}^{n-1}{x_b}^p\,{y_b}^q:(x_b,y_b)\in b,\forall b\in B \quad (3)$$

$$x_{cb}=\frac{u_{10}}{u_{00}},y_{cb}=\frac{u_{01}}{u_{00}} \quad (4)$$

The ratio between the pixels and length in meters can then be defined by assuming that the ratio of world to pixel space is given as $\frac{\omega}{\zeta}$, which is calculated by determining the

Systems DPI with relative to the input image.

Further, we can derive the velocity in actual world unit using is given in (5) as

$$v_\tau = \frac{(\lambda_n - \lambda_{n-1})\frac{\omega}{\zeta}}{\tau_n - \tau_{n-1}} ms^{-1} \quad (5)$$

F. Speed-Flow-Density Relationship

Speed, flow, and density are all related to each other. The relationships between speed and density are not difficult to observe in the real world, while the effects of speed and density on flow are not quite as apparent.

Under uninterrupted flow conditions, speed, density, and flow are all related by the following equation:

$$q=k*v \quad (6)$$

Where q = Flow (vehicles/hour)
v = Speed (miles/hour, kilometers/hour)
k = Density (vehicles/mile, vehicles/kilometer)

Because flow is the product of speed and density, the flow is equal to zero when one or both of these terms is zero. It is also possible to deduce that the flow is maximized at some critical combination of speed and density.

Under Interrupted Flow Conditions, the Vehicle Speed, Density and Flow are related using a Gaussian PDF. The velocity of vehicles follows a normal distribution, the resulting PDF for the differential velocity v of two vehicles a and b is given by:

$$f_V(v) = \frac{1}{\sqrt{2\Pi}\sqrt{\sigma_a^2 + \sigma_b^2}} e^{-\frac{1}{2}\frac{(v-(v_a - v_b))^2}{\sigma_a^2 + \sigma_b^2}} \quad (7)$$

IV. Experimental Results

Experimental results of the proposed vehicle speed estimation are presented to demonstrate the real-time velocity estimation of random vehicles. The algorithm is implemented using Java Advanced Imaging Package, Java Media Framework and executes on a 2.6 GHz Pentium Intel dual core with 4 GB ram memory and 500 GB hard disk. The experiment was set up to monitor the speed of vehicles moving along the selected road lane. The real-world scene was recorded in 6 seconds.

The Proposed Method is tested over a range of videos taken at different scenarios like Bad Light, Rainy(or) Snow Days, Interrupted Traffic scene at Urban road side, Uninterrupted Traffic Scene at National Highways, Video Taken at Tunnels.

The Results of the various video scenario at various part of the Algorithm is given in Table.2.

Video Scenario	No. of Input Videos (120)	Frame Selection *	Blob Detection *	Blob Tracking*
At Bad Light	38	91.8	95.4	89.7
At Rain (or) Snow Days	20	95.67	91.43	90.25
Interrupted Traffic	22	98.4	99.32	97.646
Uninterrupted Traffic	27	99.21	99.98	98.89
At Tunnels	13	98.12	97	89.91

(* Accuracy in Percentage)

Table.2. Accuracy of the Piece-wise Algorithms under various dynamic video streams taken at different conditions

Since the key frame selection algorithm is used, the system is said to be in the state of intrinsic ie., the total input should be available before the start of the process.

The overall performance of the Algorithm with 2 sets of Input data at various locations and conditions are shown in Table.3 and Illustrated in Graph.1

Video Scenario	No. of Input Videos (120)	Accuracy of the Results (%)
At Bad Light	38	92.3
At Rain (or) Snow Days	20	92.45
Interrupted Traffic	22	98.45533
Uninterrupted Traffic	27	99.36
At Tunnels	13	95.01

Table.3. The Accuracy of the Overall System at various Dynamic Conditions.

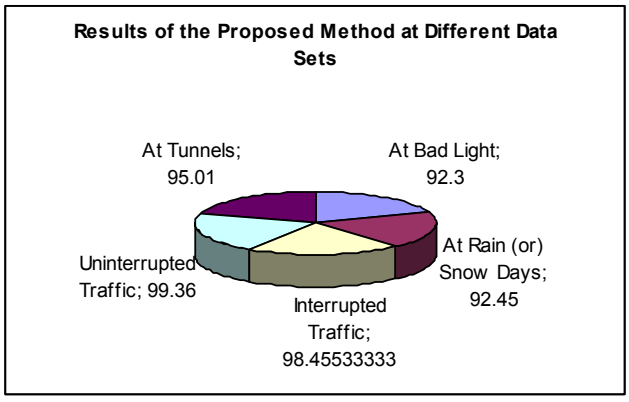

Graph 1. The Distribution of the System's Performance over Different Data Sets.

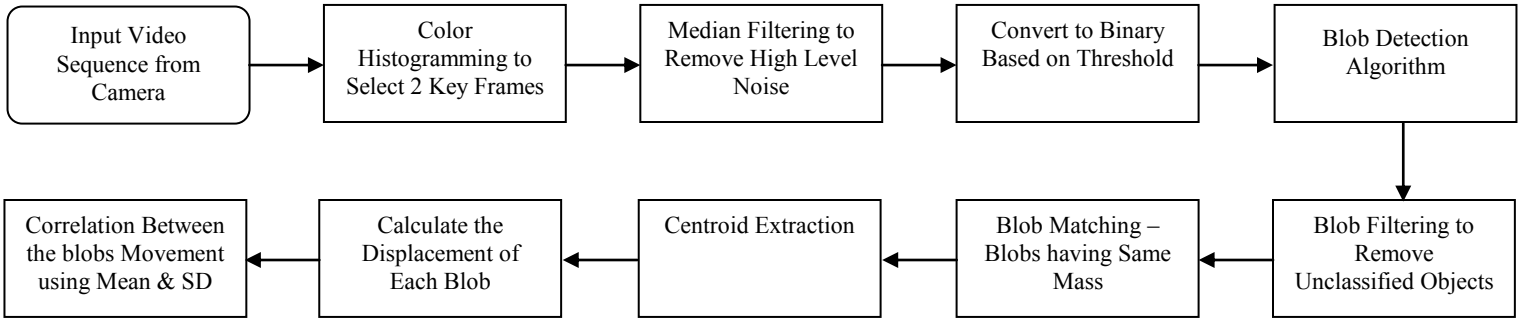

Figure.7. Overall Architecture of the System

Methods	Advantages (+), Short Comings(-)	
Lane Masking & Contour Extraction	+	Easy to Implement, Quick Results
	-	Applicable Only to Uninterrupted Traffic Situations on Highways with Lanes
Cell Transmission Model	+	Very Simple Model, Traffic is simulated based on Kinetic Theory
	-	Less Precision, Cant able to deduce traffic at high densities
Grid Method	+	Widely used Model, Earlier Conclusions
	-	Grid Size and Number of Grids within the picture are hard to apply
Point Based Method	+	Individual Analysis of Vehicles is Easy.
	-	Hard to implement at Interrupted Traffic Flow Junctions
Proposed Method	+	Easy to Implement, Good flow of Logic from Top to Bottom, Readapted to Different Density – Flow Correlation.
	-	Long Mathematical Steps, High Time Bound, Constraints in Input Video

Table.4. Shows the Comparative Study of Various Road Traffic Density Analysis Methods.

V. CONCLUSION

The Proposed Solution for the Analysis of the Traffic Situation is efficient and produces approximated results on all the video sequence. This Method deduces, whether the road traffic is congested or free flow. As this algorithm also detects the number of blobs in the given traffic scene, which makes further analysis of the road traffic. The method describes the step by step process in the analysis and so, there are several midterm results like key frame selection, Blob Detection in the proposed solution which can be useful in all video surveillance systems.

Traffic Situation, the proposed method plays a vital role for future enhancements The outputs of this system, can be a mandatory input for all kind of Advanced Traveler Information Systems and also for various domains of ITS applications.

The proposed solution is based on some input constrain including illumination effect of the video frames and camera angle. Future research work may be directed towards accounting the illumination changes as the object moves across the frame. The process can be extended to capture the video sequence in multiple lanes with the use of revolving camera instead of multiple stationary cameras.

REFERENCES

[1] Tomas Rodriguez, Narciso Garcia, "An adaptive, real-time, traffic monitoring system", Springer-Verlag 2010, Machine Vision and Applications (2010), 555–576

[2] Cheng-You Cui · Ji-Sun Shin · Fumihiro Shoji, Hee-Hyol Lee," Traffic signal control based on a predicted traffic jam distribution", IEEE transactions on Artificial Life Robotics (2009) 134–137

[3] Oscar Rosas-Jaimes , Luis Alvarez-Icaza," Vehicle density and velocity estimation on highways for on-ramp metering control", Springer - Nonlinear Dynamics (2007) 49:555–566

[4] E. Atkociunas, R. Blake , A. Juozapavicius , M. Kazimianec," Image Processing in Road Traffic Analysis", Nonlinear Analysis: Modelling and Control, 2005, Vol. 10, No. 4, 315–332.

[5] LIU Xingjian, AI Tinghua, LIU Yaolin," Road Density Analysis Based on Skeleton Partitioning for Road Generalization", Geo-spatial Information Science 12(2): Volume 12, Issue 2 June 2009, 110-116

[6] H. A. Rahim, R. B. Ahmad, A. S. M. Zain, U. U. Sheikh," An Adapted Point Based Tracking for Vehicle Speed Estimation in Linear Spacing", International Conference on Computer and Communication Engineering (ICCCE 2010), 11-13 May 2010, Kuala Lumpur, Malaysia

[7] Robert Nagel, "The Effect of Vehicular Distance Distributions and Mobility on VANET Communications", 2010 IEEE Intelligent Vehicles Symposium University of California, San Diego, CA, USA, June 21-24, 2010

Detecting Contrast Enhancement based Image forgeries by Parallel Approach

Ms.S.T Suryakanthi Sornalatha
Department of Computer science and Engineering
Mepco Schlenk Engineering College
Sivakasi,India
stsuryacse@gmail.com

Ms.S.Devi Mahalakshmi
Department of Computer science and Engineering
Mepco Schlenk Engineering College
Sivakasi,India
sdevi@mepcoeng.ac.in

Ms. Dr.K.Vijayalakshmi
Department of Computer science and Engineering
Ramco Institute of Technology
Rajapalayam,India

***Abstract*— Contrast and brightness of digital images can be adjusted by contrast enhancement. Mostly digital images are stored in Jpeg format in real application like Internet and Mobile phones. In order to reduce the size digital images are compressed with high, middle and low quality factor. Move and paste type of images are created by malicious person, in which contrast of one source image is enhanced to match the other source image. Detecting global contrast enhancement on previously Jpeg compressed images can identified using global contrast enhancement detection algorithm. Zero height gab bins of histogram used to identify the global contrast enhancement. Zero height gap bins/peaks are used to identify the composite images created by contrast enhancement. Contrast enhancement technique aimed at detecting image tampering has grown in different applications area such as law enforcement, surveillance. Composite detection algorithm and global contrast enhancement detection algorithms are presented here. In order to increase the image processing task parallel approach is used.**

Keywords **–** Contrast enhancement, Parallel approach, Zero height gab bins/peaks, Jpeg Compression.

I.INTRODUCTION

Now a days digital image editing skills becomes very popular and digital image manipulation becomes convenient and easy.Malevolent user may perform innocent manipulation to tinker the digital images.Information delivered in images might become no longer believable.In the application such as surveillance and news recording, it is necessary to certify the integrity and originality of images.

Primary goal of digital image forensics is the identification of image regions which was undergone some form of alteration[19-21]. Digital forensics techniques used to detect the image tinkering operations such as alteration, deletion etc.

Low contrast image quality globally improved when using global contrast enhancement. The enhanced output image, produced by this enhancement is free from noise and ringing artifacts. It may have more exposure on some part of the image and less exposure on some other part of the image when high contrast gain occurs.

The enhanced output image may lack in local details. Using local contrast enhancement, the local details of an image can be better defined. However, local contrast enhancement may produce the output image with noise when too much contrast gain occurs. Besides these, it may be poor in global contrast. For some images, applying the local contrast enhancement along with global contrast enhancement is much better than that of global contrast enhancement alone or local contrast enhancement alone.

Previous works deal with image manipulation detection with classifier based approaches and specific image manipulations. Each manipulation leaves distinct fingerprints on images, so it is feasible to test the enforced manipulation. Manipulation specific detection techniques used to recover the image processing history. Prior works focus on 2 different type of image alterations. 1. Non content changing operation includes resampling [4], contrast enhancement [7,8,9,12,13], compression [5], sharpening filtering [6], median filtering [10,11]. 2. Content changing operations includes splicing and composition[17,18]. Contrast enhancement including statistical intrinsic fingerprints[7,16], Gamma correction[8], reverse engineering of double Jpeg compressed images[9], noise features[15].

Prior contrast enhancement forensics algorithms works well under the assumption that the gray level histogram of original image shows a smooth contour. But digital images are stored in Jpeg format compressed with medium or low quality factor in real applications such as internet. Quality factor (Q=50) medium, less than 50 (<50) referred as low quality. Low quality Jpeg compression causes unsmoothness and generates thick peak bins in gray level histogram. In that case, prior works fail to detect the contrast enhancement in previously Jpeg compressed images. To solve such a problem Detection of global contrast enhancement algorithm is proposed.

An important application is to find the move and paste type of image forgeries. Composite images are created by 2 source images, in which contrast of one source image is enhanced to match the other source image. Single source and both source enhanced images are identified using the concept of zero height gab bins and peaks. Then composition region is located using difference between the similarity measures in different image blocks of regions.

This paper organized as follows. In Section II previous works on global contrast enhancement detection algorithm. In section III proposed global contrast enhancement detection algorithm has been discussed. In section IV proposed composite detection algorithm by parallel approach has been discussed. Result and discussions are presented in section V and conclusion is drawn in section VI.

II.PREVIOUS WORK

Stamm and Liu [3] proposed a contrast enhancement detection algorithm as follows.

Get the normalized histogram of image h(x).

Modified histogram g(l) is obtained by performing the element wise multiplication between h(l) and a "'pinch off" p(l) function so that

$$g(l) = p(l)\, h(l) \quad \text{where}$$

$$p(l) = \begin{cases} \frac{1}{2} - \frac{1}{2}\cos\left(\frac{\pi l}{N_p}\right) & l \le N_p \\ \frac{1}{2} + \frac{1}{2}\cos\left(\frac{\pi(l-255+N_p)}{N_p}\right) & l \ge 255 - N_p \\ 1 & else \end{cases}$$

where N_p is the width of the region over which p(l) decays from 1 to 0. The pinch off function is designed to both remove impulsive histogram components which may occur due to saturation effects as well as to minimize the frequency domain effects of multiplying h(l) by p(l), which behaves similar to a windowing function. Calculate E, a normalized measure of the energy in the high frequency components of the pixel value histogram, from g(l) according to the formula

$$E = \frac{1}{N}\sum_k |\mathcal{B}(k)G(k)|$$

where N is the total number of pixels in the image, $G(k)$ is the DCT of g(l), and $\mathcal{B}(l)$ is a weighting function which takes values between 0 and 1. The purpose of $\mathcal{B}(l)$ is to deemphasize low frequency regions of $G(k)$ is to deemphasize low frequency regions of where nonzero values do not necessarily correspond to contrast enhancement artifacts.

$$\mathcal{B}(k) = \begin{cases} 1, & c \le k \\ 0 & else \end{cases}$$

where c is the entry of the 256 point DFT corresponding to a desired cut off frequency. $\mathcal{B}(k)$ is zero for all values greater than k = 256 because symmetry properties inherent in the DFT of real valued signals make it unnecessary to measure these values. After E has been calculated, the decision rule δ_{ce} is used to classify an image as unaltered or contrast enhanced, such that

$$\delta_{ce} = \begin{cases} image\ is\ not\ contrast\ enhanced, & E < \delta_{ce} \\ image\ is\ contrast\ enhanced, & E \ge \delta_{ce} \end{cases}$$

Detection depends upon the presence or absence of an intrinsic fingerprint introduced into an image's histogram by a pixel value mapping. The intrinsic fingerprints of contrast enhancement operations add energy to the high frequency components of an image's pixel value histogram. It fails to detect contrast enhancement in the previously low quality JPEG-compressed images.

III. GLOBAL CONTRAST ENCHANCEMENT DETECTION

From the study of peak/gap artifacts from contrast enhancement [1], the zero height gap bins are absent in compressed images since there is absence of a distinct pixel value mapping applied to all pixels. A pixel value mapping relationship exists in flat regions, but not in other regions. Therefore, the zero-height gap feature can be used for detecting global contrast enhancement in both uncompressed and compressed images.

Algorithm:

1) Normalized gray level histogram of image is denoted by nh(x) where x = 1,2,….256.

2) Bin k is called as zero height gab bin if it satisfies

$$\begin{cases} nh(k) = 0 \\ \min\{nh(k-1), nh(k+1)\} > \mathrm{r} \\ \frac{1}{2\omega+1}\sum_{x=k-\omega}^{x=k+\omega} nh(x) > \mathrm{r} \end{cases}$$

first sub equation says that the current bin is null. The second sub-equation keeps two neighboring bins larger than the threshold τ. In the third sub equation the average of neighboring (2w1 + 1) bins are taken which should be larger than τ. Here w1 = 2 and τ = 0.00001. This algorithm focus on the detection of isolated zero-height gap bins which are rarely occurs in the middle of histograms.

3) Count the number of zero-height gap bins, denoted by N

4) If N is larger than the decision threshold, contrast enhancement is detected, else not.

Figure 1 shows the (a) raw image, (b) compressed image with quality factor 10 and (c) contrast enhanced compressed image with quality factor 10. Figure 2 shows the corresponding normalized histogram for images in figure 1.

IV. PROPOSED COMPOSITE DETECTION ALGORITHM

In this section, composite contrast enhanced image detection algorithm is proposed. Figure 3 shows the block diagram of composition detection algorithm.

A. Detection of Gap and Peak bins

Initially test image is divided into non overlapping blocks. The position of detected gab bins labelled as $[V_{gp}{}^{i}(0), V_{gp}{}^{i}(1) \ldots V_{gp}{}^{i}(k), \ldots , V_{gp}{}^{i}(255)]$ where $V_{gp}^{i}(k) = 1$ if the bins at k is a gap; $V_{gp}^{i}(k) = 0$ otherwise.Peak bins which behave as impulse noise can be locate by median filtering and labelled as

$$[V_{pk}{}^{i}(0), V_{pk}{}^{i}(1) \ldots V_{pk}{}^{i}(k), \ldots , V_{pk}{}^{i}(255)]$$

where $V_{pk}^{i}(k) = 1$ refers to peak ; $V_{pk}^{i}(k) = 0$ otherwise.
i = 1,2…N_b; N_b – Number of divided blocks.

Fig.1 (a) Raw image; (b) Compressed Raw image with quality factor Q=10; (c) Contrast enhanced compressed image

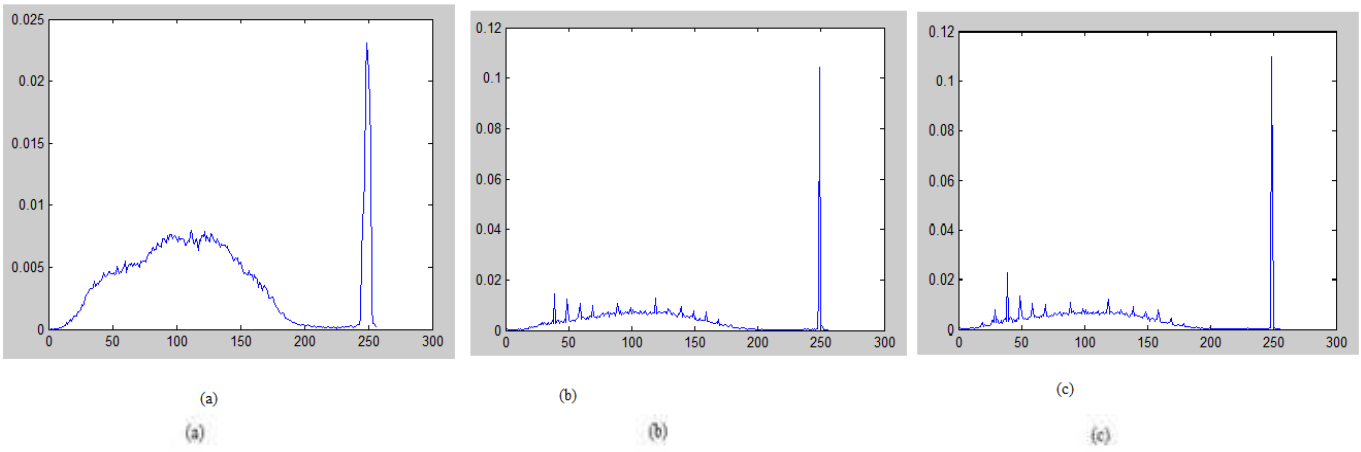

Fig.2 Normalized histogram of (a) Raw image; (b) Compressed Raw image with quality factor Q=10; (c) Contrast enhanced compressed image

To decrease detection errors, the extracted peak/gap positions are corrected by co-existing peak/gap positions.

$$C_{gp} = \sum_{i=1}^{N_b} \frac{V_{gp}^i}{N_b}$$

The detected co-existing gap positions as labelled as

$$V_{gp} = [V_{gp}(0),\ V_{gp}(1) \ldots\ V_{gp}(k), \ldots, V_{gp}(255)]\ .$$

$V_{gp}(k) = 1$ if $C_{gp}(k)$ is larger than the threshold, $V_{gp}(k) = 0$ otherwise. The corrected gap position vector, generated as

$$V_{gpc}^i = V_{gp}^i \odot V_{gp}$$

Similarly, the corrected peak position vector can also be calculated.

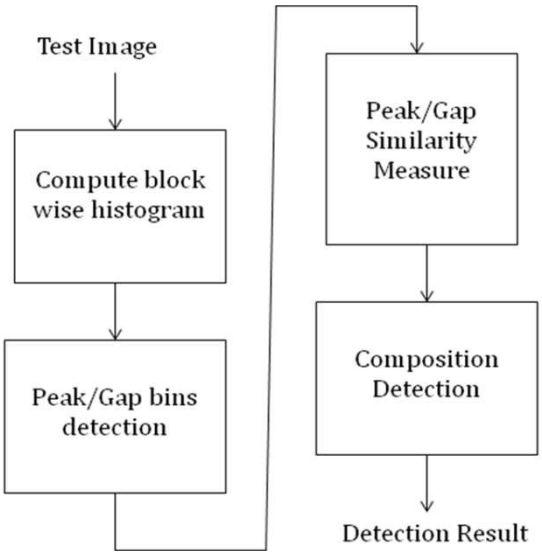

Fig.3 Block diagram of composite image detection.

B. Gab based similarity measure

To distinguish two source regions, calculate reference position vector. The reference gap position vector for located source region can be set as

$$V_{gpr} = {V_{gpc}}^k \text{ where}$$

$$k = {}^{\arg\ max}_{i\{1,2\ldots N_b\}} (|V_{gpc}^i|)$$

Effective Detection Range $\Omega_{gpr} = \Omega_k$. Similarity between V_{gpc}^i and V_{gpr} , denoted by Sm_g^i and calculated by

$$\frac{\sum_{k\in\Omega_i \cap \Omega_{gpr}} V_{gpc}^i(k).V_{gpr}(k)}{\sum_{k\in\Omega_i \cap \Omega_{gpr}} V_{gpc}^i(k).V_{gpr}(k)+\overline{V}_{gpc}^i(k).V_{gpr}(k)+V_{gpc}^i(k).\overline{V}_{gpr}(k)}$$

C. Peak based similarity measure

The reference peak position vector calculated by

$$V_{pkr}(k) = l\left(\sum_{n\in N_R} V_{pkc}^n(k) > 0\right)$$

Where k = 1,2...255 and

$$N_R = \{i | Sm_g^i > t_g\}$$

t_g is a threshold taken as 0.7. $\Omega_{pr} = U_{n\in N_R}\Omega_n$ .Similarity between V_{pkc}^i and V_{pkr}, denoted by Sm_p^i and calculated by

$$\frac{\sum_{k\in\Omega_i \cap \Omega_{pkr}} V_{pkc}^i(k).V_{pkr}(k)}{\sum_{k\in\Omega_i \cap \Omega_{pkr}} V_{pkc}^i(k).V_{pkr}(k)+\overline{V}_{pkc}^i(k).V_{pkr}(k)+V_{pkc}^i(k).\overline{V}_{pkr}(k)}$$

D. Fusion

Fusion value for each block denoted by m^i and calculated by

If $Sm_g^i \neq -1$ and $Sm_p^i \neq -1$ then

$$Sm^i = (Sm_g^i + Sm_p^i)/2$$

Otherwise

$$Sm^i = max(Sm_g^i, Sm_p^i)$$

for all blocks $m^i > t$ then it is identified as single source enhanced image. Otherwise m^i values classified as 2 sets. (i.e) $Sm^i \geq t$ in one set and $Sm^i < t$ in another set. It is identified as both source enhanced image. Figure 4(c) shows the detection result of this algorithm.

E. Parallel approach

Parallel processing improves the performance of the system by speeding up the execution[2]. Composition detection algorithm repeated for each block of image. So each block of image is processed in parallel manner. It increases the performance of image processing task.

V. RESULT

A. Test Data

Dataset 1:

Uncompressed Colour Image Database (UCID) [14]. It has 1338 uncompressed images.

Dataset 2:

CASIA1 Tampered Image Detection Evaluation Database. It has 921 spliced color images.

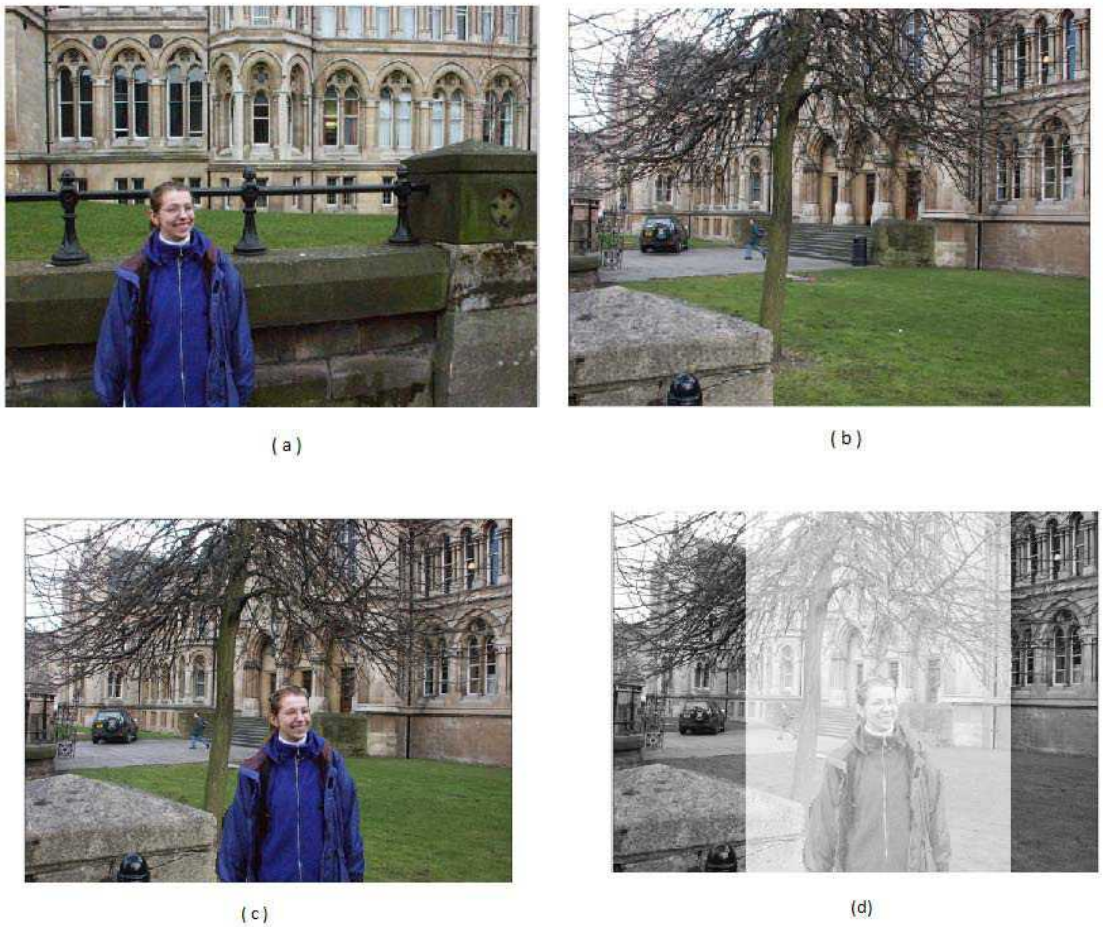

Fig. 4 (a) and (b) Source images;(c) Composite image created by contrast enhancement (d) Detection Result

B. Experimental Discussion

Proposed global contrast enhancement detection algorithm, works well for previously Jpeg compressed images with medium and low quality factor. It means that image enhancement techniques are applied after the Jpeg compression strategy. Prior works for composition detection fails to identify which type of manipulation was enforced. But proposed composite detection method identifies the manipulation using the similarity Sm^i values.

Splicing attack more or less similar to move-and- paste attack. Both techniques modifies the certain region of image. But move-and-paste attack uses portion of the original image as its source image. i.e the source and destination of the modified image originated from the same image. This algorithm also identifies the splicing attack. The future work is to identify the forgeries in double Jpeg compressed images

Dataset	UCID images	CASIA1 Spliced images
	True Positive Rate	True Positive Rate
Proposed Composite image detection	85%	80%
ExistingMethod Stamm and Liu [3	55%	75%

VI. CONCLUSION

In this paper, two contrast enhancements based algorithms have been proposed. These algorithms based on histogram bins and peaks analysis. Parallel approach used to increases the performance of the system. Zero height gap bins, similarity

measures are exploited as identifying features. Composition detection algorithm works well for previously Jpeg compressed images. In future this work extended to images undergone to post processing.

ACKNOWLEDGMENT

The authors would like to thank the Institutes for providing the databases. They also thank the anonymous reviewers and associate editor for their comments that greatly improved the manuscript.

REFERENCES

[1] Gang Cao, Yao Zhao, Rongrong Ni and Xuelong Li,"Contrast Enhancement-Based Forensics in Digital Images",IEEE Trans. Information forensics and security, vol. 9, No. 3 April 2013

[2] Eric Olmedo, Jorge de la Calleja, Antonio Benitez, and Ma. Auxilio Medina,"Point to point processing of digital images using parallel computing",IJCSI International Journal of Computer Science Issues, Vol. 9, Issue 3, No 3, May 2012

[3] M. C. Stamm and K. J. R. Liu, "Forensic detection of image manipulation using statistical intrinsic fingerprints," IEEE Trans. Inf. Forensics Security, vol. 5, no. 3, pp. 492–506, Sep. 2010.

[4] A. C. Popescu and H. Farid, "Exposing digital forgeries by detecting traces of resampling," *IEEE Trans. Signal Process.*, vol. 53, no. 2, pp. 758–767, Feb. 2005

[5] T. Bianchi and A. Piva, "Detection of non-aligned double JPEG compression based on integer periodicity maps," IEEE Trans. Inf. Forensics Security, vol. 7, no. 2, pp. 842–848, Apr. 2012.

[6] G. Cao, Y. Zhao, R. Ni, and A. C. Kot, "Unsharp masking sharpening detection via overshoot artifacts analysis," IEEE Signal Process. Lett., vol. 18, no. 10, pp. 603–606, Oct. 2011.

[7] M. C. Stamm and K. J. R. Liu, "Forensic estimation and reconstruction of a contrast enhancement mapping," in Proc. IEEE Int. Conf. Acoust., Speech Signal, Dallas, TX, USA, Mar. 2010, pp. 1698–1701.

[8] G. Cao, Y. Zhao, and R. Ni, "Forensic estimation of gamma correction in digital images," in Proc. 17th IEEE Int. Conf. Image Process., Hong Kong, 2010, pp. 2097–2100.

[9] P. Ferrara, T. Bianchiy, A. De Rosaz, and A. Piva, "Reverse engineering of double compressed images in the presence of contrast enhancement," in Proc. IEEE Workshop Multimedia Signal Process., Pula, Croatia, Sep./Oct. 2013, pp. 141–146.

[10] M. Kirchner and J. Fridrich, "On detection of median filtering in digital images," in Proc. SPIE, Electronic Imaging, Media Forensics and Security II, vol. 7541, San Jose, CA, USA, Jan. 2010, pp. 1–12.

[11] C. Chen, J. Ni, and J. Huang, "Blind detection of median filtering in digital images: A difference domain based approach," IEEE Trans. Image Process., vol. 22, no. 12, pp. 4699–4710, Dec. 2013.

[12] T. Arici, S. Dikbas, and Y. Altunbasak, "A histogram modification framework and its application for image contrast enhancement," IEEE Trans. Image Process., vol. 18, no. 9, pp. 1921–1935, Sep. 2009.

[13] S. Battiato, A. Bosco, A. Castorina, and G. Messina, "Automatic image enhancement by content dependent exposure correction," EURASIP J. Appl. Signal Process., vol. 12, pp. 1849–1860, Jan. 2004.

[14] G. Schaefer and M. Stich, "UCID—An uncompressed colour image database," in Proc. SPIE, Storage and Retrieval Methods and Applications for Multimedia, vol. 5307, San Jose, CA, USA, 2004, pp. 472–480.

[15] Fan, H. Cao, and A. C. Kot, "Estimating EXIF parameters based on noise features for image manipulation detection," IEEE Trans. Inf.Forensics Security, vol. 8, no. 4, pp. 608–618, Apr. 2013.

[16] A. Swaminathan, M. Wu, and K. J. R. Liu, "Digital image forensics via intrinsic fingerprints," IEEE Trans. Inf. Forensics Security, vol. 3, no. 1, pp. 101–117, Mar. 2008.

[17] D. Mahajan, R. Ramamoorthi, and B. Curless, "A theory of frequency domain invariants: Spherical harmonic identities for BRDF/lighting transfer and image consistency," IEEE Trans. Pattern Anal. Mach. Intell., vol. 30, no. 2, pp. 197–213, Feb. 2008.

[18] J. O'Brien and H. Farid, "Exposing photo manipulation with inconsistent reflections," ACM Trans. Graph., vol. 31, no. 1, pp. 1–11, 2012.

[19] H. Farid, "Image forgery detection," *IEEE Signal Process. Mag.*, vol. 26, no. 2, pp. 16–25, Mar. 2009.

[20] B. Mahdian and S. Saic, "A bibliography on blind methods for identifying image forgery," *Image Commun.*, vol. 25, no. 6, pp. 389–399, Jul. 2010.

[21] S. Bayram, I. Avcubas, B. Sankur, and N. Memon, "Image manipulation detection," *J. Electron. Imag.*, vol. 15, no. 4, pp. 04110201–04110217, 2006.

SECURITY PROBLEMS OF STORING BIG DATA IN CLOUD

Mrs.M.Swarna Sudha AP, Mrs.B.Vijayalakshmi AP, Ms.P.M.G.Jegathambal AP

Department of Computer Science and Engineering

Ramco Institute of Technology, Rajapalayam.

Abstract:With the advancement in technology, industry, e-commerce and research a large amount of complex and pervasive digital data is being generated which is increasing at an exponential rate and often termed as big data. Big Data concern large-volume, complex, growing data sets with multiple, autonomous sources. Traditional Data Storage systems are not able to handle Big Data and also analysing the Big Data becomes a challenge and thus it cannot be handled by traditional analytic tools. Cloud computing plays a very vital role in protecting data, applications and the related infrastructure with the help of policies, technologies, controls, and big data tools. Cloud Computing can resolve the problem of handling, storage and analysing the Big Data as it distributes the big data within the cloudlets. Currently, storing the data safely and efficiently on Cloud is one of the biggest challenges in Cloud computing. There is always a potential risk to the security of Big Data storage in Cloud Computing. These security and privacy issues have been addressed in this paper.

1.INTRODUCTION

A growing number of companies are using the technology of big data to store and analyse peta bytes of data including web logs, click stream data and social media content to gain better insights about their customers and their business. Security and privacy issues are magnified by velocity, volume and variety of big data, such as large scale cloud infrastructures, diversity of data sources and formats, streaming nature of data acquisition and high volume inter-cloud migration. The use of large scale cloud infrastructures, with a diversity of software platforms, spread across large networks of computers, also increases the attack surface of the entire system.

Big data refers to high volume, high velocity, and/or high variety information assets that require new forms of processing to enable enhanced decision making, insight discovery and process optimization. Due to its high volume and complexity, it becomes difficult to process big data using on-hand database management tools or traditional data processing applications. An effective option is to store big data in the cloud, as the cloud has capabilities of storing big data and processing high volume of user access requests in an efficient way. When hosting big data into the cloud, the data security becomes a major concern as cloud servers cannot be fully trusted by data owners. Traditional security mechanisms are not adequate for this scenario.

1.1. Big Data

Big data is commonly unstructured and require more real-time analysis. It represents the progress of the human cognitive processes, usually includes data sets with sizes beyond the ability of current technology, method and theory to capture, manage, and process the data within a tolerable elapsed time. Big data has typical characteristics of five ‘V’s, volume, variety, velocity, veracity and value. Big data sets come from many areas, including meteorology, complex physics simulations, genomics, biological study, gene analysis and environmental research.

Big data technologies describe a new generation of technologies and architectures, designed to economically extract value from very large volumes of a wide variety of data, by enabling high-velocity capture, discovery, and/or analysis. In particular, big data can be further categorized into big data science and big data frameworks. Big data science is ``the study of techniques covering the acquisition, conditioning, and evaluation of big data," whereas big data frameworks are ``software libraries along with their associated algorithms that enable distributed processing and analysis of big data problems across clusters of computer units". An instantiation of one or more big data frameworks is known as big data infrastructure.

Owing to the uniqueness of big-data, designing a scalable big-data system faces a series of technical challenges, including:

i) First, due to the variety of disparate data sources and the sheer volume, it is difficult to collect and integrate data with scalability from distributed locations. For instance, more than 175 million tweets containing text, image, video, social relationship are generated by millions of accounts distributed globally.

ii)Second, big data systems need to store and manage the gathered massive and heterogeneous datasets, while provide function and performance guarantee, in terms of fast retrieval, scalability, and privacy protection. For example, Facebook needs to store, access, and analyze over 30 pertabytes of user generate data.

iii) Third, big data analytics must effectively mine massive datasets at different levels in real time or near real time - including modelling, visualization, prediction, and optimization - such that inherent promises can be revealed to improve decision making and acquire further advantages.

1.2. Cloud Computing

Cloud Computing, the long dreamed vision of computing as a utility, enables convenient and on-demand network access to a centralized pool of configurable computing resources that can be rapidly deployed with great efficiency and minimal management overhead. Cloud model is composed of the following essential characteristics such as on-demand self-service, ubiquitous network access, location independent resource pooling, rapid resource elasticity, usage based pricing, outsourcing, etc. Cloud computing improves organizations performance by utilizing minimum resources and management support, with a shared network, valuable resources, bandwidth, software's and hardware's in a cost effective manner and limited service provider dealings. Basically it's a concept of providing virtualized resources to the consumers.

The service models of cloud models are as follows:

1.Cloud Software as a Service (SaaS)—Use provider's applications over a network.

2.Cloud Platform as a Service (PaaS)—Deploy customer-created applications to a cloud.

3.Cloud Infrastructure as a Service (IaaS)—Rent processing, storage, network capacity, and other fundamental computing resources.

The deployment models, which can be either internally or externally implemented in a cloud model are as follows:

- Private cloud—Enterprise owned or leased
- Community cloud—Shared infrastructure for specific community
- Public cloud—Sold to the public, mega-scale infrastructure
- Hybrid cloud—Composition of two or more clouds

There are several major cloud computing providers including Amazon, Google, Salesforce, Yahoo, Microsoft and others that are providing cloud computing services. Cloud computing providers provide a variety of services to the customers and these services include e-mails, storage, software-as-a-services, infrastructure-as-a-services etc.

2. BIG DATA PROCESSING ON CLOUD

The technique to process big data has become a fundamental and critical challenge for modern society. Cloud is a pay-as-you-go business model by offering IT services using economies of scale. Cloud computing is the use of computing resources (hardware and software) that are delivered as a service over a network (typically the Internet). Cloud computing provides an ideal platform for big data storage, dissemination and interpreting with its massive computation power. In many today's real world applications, such as social networks, complex network monitoring, the scientific analysis of protein interactions and wireless sensor networks self monitoring, it is unavoidable to encounter the problem of dealing with big data and big data streams on cloud.

Amazon EC2 infrastructure as a service is a typical cloud based distributed system for big data processing. Amazon S3 supports distributed storage. MapReduce is adopted as a programming model for big data processing over cloud computing. The extension of the traditional Hadoop framework to develop a novel framework named Incoop by incorporating several techniques like task partition and memorization-aware schedule.

Attribute-Based Encryption (ABE) has emerged as a promising technique to ensure the end-to-end data security in cloud storage system. It allows data owners to define access policies and encrypt the data under the policies, such that only users whose attributes satisfying these access policies can decrypt the data. When more and more organizations and enterprises outsource data into the cloud, the policy updating becomes a significant issue as data access policies may be changed dynamically and frequently by data owners.

2.1. Hadoop Framework

Hadoop is designed to process large amounts of data, regardless of its structure. In fact, Hadoop has long been the mainstay of the big data movement. Apache Hadoop is an open-source software framework that supports massive data storage and processing. Instead of relying on expensive, proprietary hardware to store and process data, Hadoop enables distributed processing of large amounts of data on large clusters of commodity servers. Hadoop has many advantages, and the following features make Hadoop particularly suitable for big data management and analysis:

***Scalability*:** Hadoop allows hardware infrastructure to be scaled up and down with no need to change data formats.

***Cost Efficiency*:** Hadoop brings massively parallel computation to commodity servers, leading to a sizeable decrease in cost per terabyte of storage, which makes massively parallel computation affordable for the ever-growing volume of big data.
Flexibility: Hadoop is free of schema and able to absorb any type of data from any number of sources. Moreover, different types of data from multiple sources can be aggregated in Hadoop for further analysis.
***Fault tolerance*:** Missing data and computation failures are common in big data analytics. Hadoop can recover the data and computation failures caused by node breakdown or network congestion.

2.2. HDFS
The Hadoop Distributed File System permits individual servers in a cluster to fail without aborting the computation process by ensuring data is replicated with redundancy across the cluster. There are no restrictions on the data that HDFS stores - it can be unstructured and schema-less. Hadoop HDFS and HBase are responsible for data storage. HDFS is a distributed file system developed to run on commodity hardware that references the GFS design. HDFS is the primary data storage substrate of Hadoop applications. An HDFS cluster consists of a single *Name Node* that manage the file system metadata, and collections of *Data Nodes* that store the actual data. A file is split into one or more blocks, and these blocks are stored in a set of Data Nodes. Each block has several replications distributed in different Data Nodes to prevent missing data. Apache HBase is a column-oriented store modeled after Google's Big table. Thus, Apache HBase provides Big table-like capabilities above on top of HDFS. HBase can serve both as the input and the output for Map Reduce jobs run in Hadoop and may be accessed through Java API, REST, Avor or Thrift APIs.

2.3. Map Reduce
The core of Hadoop is the Map Reduce framework, which was created at Google in response to the problem of creating web search indexes. MapReduce distributes a computation over multiple nodes, thus solving the problem of data that is too large to fit onto a single machine. Combining this technique with Linux servers presents a cost-effective alternative to massive computing arrays. Hadoop MapReduce is the computation core for massive data analysis. The MapReduce framework consists of a single master *JobTracker* and one slave *TaskTracker* per cluster node. The master is responsible for scheduling jobs for the slaves, monitoring them and re-executing the failed tasks. The slaves execute the tasks as directed by the master. It can sort a petabyte of data in only a few hours. The parallelism also provides some possibility of recovering from partial failure of servers or storage during the operation.

2.4. Big data advantages
In Big data, the software packages provide a rich set of tools and options where an individual could map the entire data landscape across the company, thus allowing the individual to analyse the threats he/she faces internally. This is considered as one of the main advantages as big data keeps the data safe. With this an individual can be able to detect the potentially sensitive information that is not protected in an appropriate manner and makes sure it is stored according to the regulatory requirements. There are some common characteristics of big data, such as
a) Big data integrates both structured and unstructured data.
b) Addresses speed and scalability, mobility and security, flexibility and stability.
c) In big data the realization time to information is critical to extract value from various data sources, including mobile devices, radio frequency identification, the web and a growing list of automated sensory technologies.
All the organizations and business would benefit from speed, capacity, and scalability of cloud storage. Moreover, end users can visualize the data and companies can find new business opportunities. Another notable advantage with big-data is, data analytics, which allow the individual to personalize the content or look and feel of the website in real time so that it suits the each customer entering the website. Big Data provides the opportunity to consolidate and analyse logs automatically from multiple sources rather than in isolation. This could provide insight that individual logs cannot, and potentially enhance intrusion detection systems (IDS) and intrusion prevention systems (IPS) through continual adjustment and effectively learning “good” and “bad” behaviours.

2.5. The risks associated with Big Data technologies:

- Big Data implementations typically include open source code, with the potential for unrecognised back doors and default credentials.
- The attack surface of the nodes in a cluster may not have been reviewed and servers adequately hardened.
- User authentication and access to data from multiple locations may not be sufficiently controlled.
- Regulatory requirements may not be fulfilled, with access to logs and audit trails problematic.

- There is significant opportunity for malicious data input and inadequate data validation.

2.6. Security issues

Cloud computing comes with numerous security issues because it encompasses many technologies including networks, databases, operating systems, virtualization, resource scheduling, transaction management, load balancing, concurrency control and memory management. Hence, security issues of these systems and technologies are applicable to cloud computing. For example, it is very important for the network which interconnects the systems in a cloud to be secure. Also, virtualization paradigm in cloud computing results in several security concerns. Data security not only involves the encryption of the data, but also ensures that appropriate policies are enforced for data sharing. In addition, resource allocation and memory management algorithms also have to be secure. The big data issues are most acutely felt in certain industries, such as telecoms, web marketing and advertising, retail and financial services, and certain government activities. The data explosion is going to make life difficult in many industries, and the companies will gain considerable advantage which is capable to adapt well and gain the ability to analyze such data explosions over those other companies. Finally, data mining techniques can be used in the malware detection in clouds.

3. THREATS AND ITS COUNTERMEASURES

The following seven major threats are analysed in cloud computing.

3.1. Abuse and Nefarious Use of Cloud Computing

IaaS providers offer their customers the illusion of unlimited compute, network, and storage capacity — often coupled with a 'frictionless' registration process where anyone with a valid credit card can register and immediately begin using cloud services. Some providers even offer free limited trial periods. By abusing the relative anonymity behind these registration and usage models, spammers, malicious code authors, and other criminals have been able to conduct their activities with relative impunity. PaaS providers have traditionally suffered most from this kind of attacks. Future areas of concern include password and key cracking, DDOS, launching dynamic attack points, hosting malicious data, botnet command and control, building rainbow tables, and CAPTCHA solving farms.

Remediation

- Stricter initial registration and validation processes.
- Enhanced credit card fraud monitoring and coordination.
- Comprehensive introspection of customer network traffic.

3.2. Insecure Application Programming Interfaces

Cloud Computing providers expose a set of software interfaces or APIs that customers use to manage and interact with cloud services From authentication and access control to encryption and activity monitoring, these interfaces must be designed to protect against both accidental and malicious attempts to circumvent policy.

Remediation

- Ensure strong authentication and access controls are implemented in concert with encrypted transmission.
- Understand the dependency chain associated with the API.

3.3. Malicious Insiders

The threat of a malicious insider is well-known to most organizations. This threat is amplified for consumers of cloud services by the convergence of IT services and customers under a single management domain, combined with a general lack of transparency into provider process and procedure.

Remediation

- Enforce strict supply chain management and conduct a comprehensive supplier assessment.
- Require transparency into overall information security and management practices, as well as compliance reporting.

3.4. Shared Technology Vulnerabilities

IaaS vendors deliver their services in a scalable way by sharing infrastructure. To address this gap, a virtualization hypervisor mediates access between guest operating systems and the physical compute resources.

Remediation

- Implement security best practices for installation/configuration.
- Monitor environment for unauthorized changes/activity.
- Promote strong authentication and access control for administrative access and operations.
- Enforce service level agreements for patching and vulnerability remediation.
- Conduct vulnerability scanning and configuration audits.

3.5.Data Loss/Leakage

There are many ways to compromise data. Deletion or alteration of records without a backup of the original content is an obvious example. Unlinking a record from a larger context may render it unrecoverable, as can storage on unreliable media. Loss of an encoding key may result in effective destruction. Finally, unauthorized parties must be prevented from gaining access to sensitive data.

Remediation

- Implement strong API access control.
- Encrypt and protect integrity of data in transit.
- Analyses data protection at both design and run time.
- Implement strong key generation, storage and management, and destruction practices.
- Contractually demand providers wipe persistent media before it is released into the pool.
- Contractually specify provider backup and retention strategies.

3.6. Account, Service & Traffic Hijacking

Attack methods such as phishing, fraud, and exploitation of software vulnerabilities still achieve results. Credentials and passwords are often reused, which amplifies the impact of such attacks. If an attacker gains access to your credentials, they can eavesdrop on your activities and transactions, manipulate data, return falsified information, and redirect your clients to illegitimate sites.

Remediation

- Prohibit the sharing of account credentials between users and services.
- Leverage strong two-factor authentication techniques where possible.
- Employ proactive monitoring to detect unauthorized activity.
- Understand cloud provider security policies and SLAs.

3.7. Unknown Risk Profile

Versions of software, code updates, security practices, vulnerability profiles, intrusion attempts, and security design, are all important factors for estimating your company's security posture. Information about who is sharing your infrastructure may be pertinent, in addition to network intrusion logs, redirection attempts and/or successes, and other logs.

Remediation

- Disclosure of applicable logs and data.
- Partial/full disclosure of infrastructure details (*e.g.*, patch levels, firewalls, etc.).
- Monitoring and alerting on necessary information.

4. CONCLUSION

In this paper, we have highlighted the security and privacy problems that need to be addressed to make Big Data processing and computing infrastructure more secure. Common elements specific to Big Data arise from the use of multiple infrastructure tiers (both storage and computing) for processing Big Data; the use of new compute infrastructures such as NoSQL databases (for fast throughput necessitated by Big Data volumes) that have not been thoroughly vetted for security issues; the non-scalability of encryption for large data sets; the non-scalability of real-time monitoring techniques that might be practical for smaller volumes of data; the heterogeneity of devices that produce the data; and the confusion surrounding the diverse legal and policy restrictions that lead to ad hoc approaches for ensuring security and privacy.

REFERENCES

[1] Ren, Yulong, and Wen Tang. "A Service Integrity Assurance Framework For Cloud Computing Based On Mapreduce" Proceedings of IEEE CCIS2012. Hangzhou: 2012, pp 240 – 244, Oct. 30 2012-Nov. 1 2012

[2] N, Gonzalez, Miers C, Redigolo F, Carvalho T, Simplicio M, de Sousa G.T, and Pourzandi M. "A Quantitative Analysis of Current Security Concerns and Solutions for Cloud Computing.". Athens: 2011. pp 231 – 238, Nov. 29 2011- Dec. 1 2011

[3] Hao, Chen, and Ying Qiao. "Research of Cloud Computing based on the Hadoop platform."Chengdu, China: 2011, pp. 181 – 184, 21-23 Oct 2011.

[4] Lu, Huang, Ting-tin Hu, and Hai-shan Chen. "Research on Hadoop Cloud Computing Model and its Applications." Hangzhou, China: 2012, pp. 59 – 63, 21-24 Oct. 2012.

[5] Wie, Jiang , Ravi V.T, and Agrawal G. "A Map-Reduce System with an Alternate API for Multi-core Environments." Melbourne, VIC: 2010, pp. 84-93, 17-20 May. 2010.

[6] A, Katal, Wazid M, and Goudar R.H. "Big data: Issues, challenges, tools and Good practices."Noida: 2013, pp. 404 – 409, 8-10 Aug. 2013.

[7] Cloud Security Alliance Security Guidance http://www.cloudsecurityalliance.org/guidance

[8] Top Threats to Cloud Computing http://www.cloudsecurityalliance.org/topthreats.html

RAMCO INSTITUTE OF TECHNOLOGY

(Approved by AICTE, New Delhi and Affiliated to Anna University, Chennai)
North Venganallur Village, Rajapalayam - 626 117, Tamil Nadu.

National Conference on Innovations in Engineering, Science & Technology

6th & 7th March, 2015

CERTIFICATE

This is to certify that Dr./Mr./Ms. .....K...Ragavan..... of ...Ramco....Institute....of.... .....Technology..... presented a paper entitled ...Comparative.....Analysis.....of..... .....SVM.....and.....BPA.....for.....wheel chair.....Detection..... National Conference on Innovations in Engineering , Science and Technology - NCIEST , organised by Ramco Institute of Technology , Rajapalayam during 6th & 7th March, 2015.

J. Rajakarunakaran

Dr.S.Rajakarunakaran
Organizing Secretary - NCIEST

Dr.R.V.Mahendra Gowda
Principal

RAMCO INSTITUTE OF TECHNOLOGY

(Approved by AICTE, New Delhi and Affiliated to Anna University, Chennai)
North Venganallur Village, Rajapalayam - 626 117, Tamil Nadu.

National Conference on Innovations in Engineering, Science & Technology

6th & 7th March, 2015

CERTIFICATE

This is to certify that Dr./Mr./Ms. K. Ragavan of Ramco Institute of Technology presented a paper entitled Design of Hilbert - Pair of Wavelets

National Conference on Innovations in Engineering , Science and Technology - NCIEST, organised by Ramco Institute of Technology ,Rajapalayam during 6th & 7th March, 2015.

J. Rajakarunakaran

Dr.S.Rajakarunakaran
Organizing Secretary - NCIEST

Dr.R.V.Mahendra Gowda
Principal

PERFORMANCE COMPARISON OF EQUALIZERS FOR WIRELESS COMMUNICATION SYSTEM

Mydhili S.K. and A.Rajeswari
Department of Electronics and Communication Engineering,
SVS College Of Engineering, Coimbatore-642 109.
Professor & Head, Department of Electronics and Communication Engineering,
Coimbatore Institute of Technology, Coimbatore.
E-mail: s_k_mydhili@yahoo.com

One of the important techniques, which can combat and exploit the frequency-selectivity of the wireless channel in providing high data rate wireless systems, lie in the hand of equalization. The wireless systems that is evolved in the last few decades necessitates in the design and analysis of equalization techniques. The current trend as well as the future generation of wireless systems is supposed to possess very high spectral efficiency, presence of rapidly time varying channels due to high mobility and the availability of partial or no channel state information at the transmitter and/or receiver which prescribes MIMO systems. When the data is transmitted at high bit rates, over mobile radio channels, the channel impulse response can extend over many symbol periods, which lead to Inter-symbol interference (ISI). This paper analyses the performances of equalization techniques by considering 2 transmit and 2 receive antenna (2×2 MIMO) over a flat fading Rayleigh multipath channel and provides a bit error rate analysis of the same.

A DEFENSE TECHNIQUES BASED ON SI MODEL FOR CERTAIN ATTACKS IN IEEE802.15.4 BASED WSN

S.Periyanayagi Department of ECE,
Ramco Institute of Technology, Rajapalayam, Tamil Nadu
V.Sumathy, Department of ECE,
Government College of Technology, Coimbatore, Tamil Nadu,
Email: periplsp@gmail.com,Sumi_gct2001@yahoo.co.in

Security is the first and foremost concern in many networking scenarios which replaces the performance rapidly. The aspects of wireless sensor network security are described by challenges, requirements, defense techniques and possible attacks. The main aim of the paper is is to provide a general overview of sensor networking security and highlight the need for efficient defense techniques able to withstand various attacks that target their confidentiality, functionality and availability. A defense technique based on swarm intelligence for certain attacks like jamming attack and denial of sleep attack has been proposed to detect these vulnerabilities for IEEE802.15.4 based WSN. Simulation results reveal the effectiveness of the proposed system.

Matrix Converter Based Solar Photo Voltaic System for Reactive Power Compensation using Sinusoidal Pulse Width Modulation

K.Muneesh Raja
PG Scholar, Department of EEE
Kalasalingam University
Krishnankoil-626126, India
Muneeshraja.raja@gmail.com

K.Vijayakumar
Research Scholar, Department of EEE
Kalasalingam University
Krishnankoil-626126, India
Kumark86@gmail.com

S.Kannan
Professor, Department of EEE
Ramco Institute of Technology
Rajapalayam-626117, India
kannaneeeps@gmail.com

***Abstract*—Reactive power is a subject of great concern for the operation of Alternating Current (AC) power systems. It has always been a challenge to obtain the balance between a minimum amount of reactive power flow to maximize capacity for active power flow and a sufficient amount of reactive power flow to maintain a proper system voltage profile. This work mainly deals with the compensation of reactive power by using Solar Photovoltaic Power System. Single-phase matrix converter is used for developing AC voltage. Single-phase matrix converter can be used as a Rectifier and as an Inverter. The same system could be used for real power exchange utilizing free energy (Solar) thus minimizing the utility power supply. Bidirectional energy flow is possible with matrix converter for battery charging. Use of matrix converter improves the quality of output voltage with reduced Total Harmonic Distortion. Sinusoidal Pulse Width Modulation (SPWM) is used for generating pulses to the matrix converter. Digital control of proposed real and reactive power compensation improves the overall efficiency of the system and reliability.**

Keywords-Matrix Converter, Solar Photo Voltaic, Reactive Power Compensation, SPWM

I. INTRODUCTION

Sun is the major source for solar energy and it is available throughout the year. Reactive power compensation using solar energy is an interesting task. If the reactive power was compensated, the quality of power is improved, and the power factor is maintained almost at unity. Solar PV panel receives the solar radiation from the Sun and is converted into electrical power. This output power has minimum voltage of 24V and varying. This output voltage was given to the boost converter to obtain a constant voltage of 48V. The output of boost converter is then given to the matrix converter. Here the matrix converter acts as an inverter and the DC voltage is converted into AC. The output of matrix converter is given to a step-up transformer to match the converter voltage with line voltage for reactive power compensation. Normally utility supplies power to the load. The power comprises both real and reactive power components. Our aim is to compensate the reactive power and maintain the reactive power of utility side to minimum, nearly zero. Using of matrix converter improves the quality of output voltage and reduces the THD and controlled bidirectional power flow is possible. This is used for real power transfer to the grid and for charging the battery from the grid when there is sufficient output from solar.

II. SOLAR PANEL

The model is established using basic circuit equations of the photovoltaic (PV) solar cells together with the effects of solar irradiation and temperature changes. This model was developed in MATLAB Simulink [1]. PV array is formed with series and parallel combination of PV solar cells. The output of PV cell voltage is the function of photocurrent that is mainly determined by load current depending on the solar irradiation [2].

$$V_c = \frac{AkT_c}{e}\ln\left(\frac{I_{ph}+I_0-I_c}{I_0}\right) - I_a R_a \qquad (1)$$

where the symbols are defined as follows:

e: Electron charge (1.602×10^{-19}C).
k: Boltzmann constant ($1.3810^{-23} \times$ J/°K).
I_c: Cell output current, A.
I_{ph}: Photocurrent, function of irradiation level and junction temperature (5A).
I_0: Reverse saturation current of diode (0.0002A).
R_s: Series resistance of cell (0.001 Ω).
T_c: Reference cell, operating temperature (20°C).
V_c: Cell output voltage, V.

Figure 1 shows the Simulink model of solar panel. The panel was developed to produce the output of 250 Watts.

978-1-4799-3975-6/14/$31.00 ©2014 IEEE

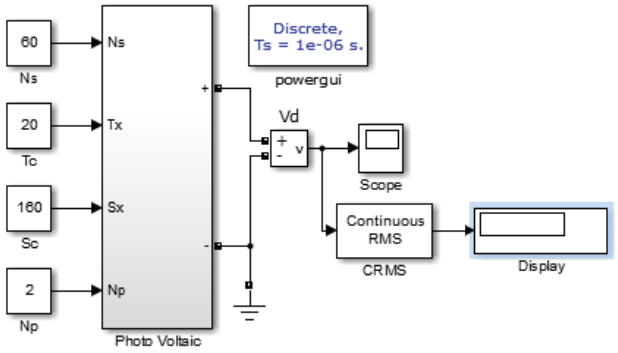

Fig. 1 Simulink model of solar panel

A. *Characteristic curves*

Figure 2 shows the I-V characteristics and Figure 3 shows the P-V characteristics of the solar panel.

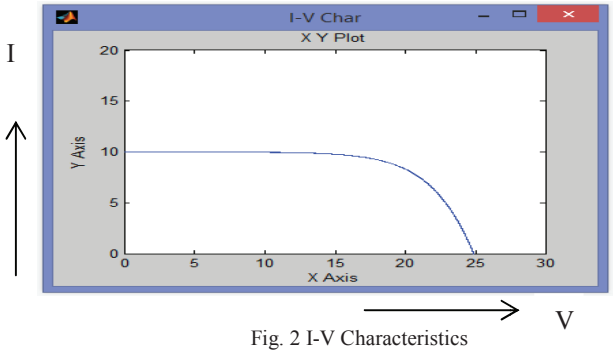

Fig. 2 I-V Characteristics

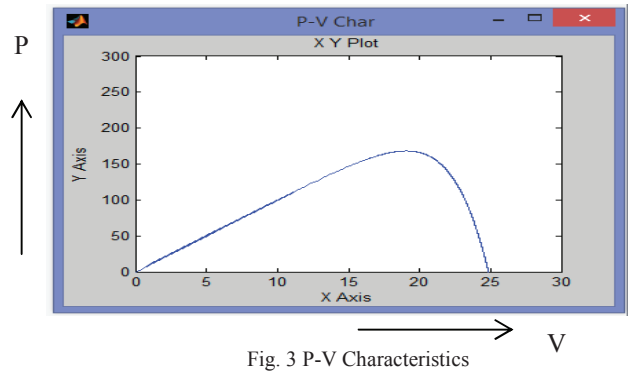

Fig. 3 P-V Characteristics

III. DC-DC BOOST CONVERTER

DC-DC boost converter is a converter, which produces output greater than the input. The range of output voltage is depending upon the firing angle (α), and the input voltage. Equation (2), (3) and (4) is used to express the output voltage and filter design of the boost converter [3]. In this work the boost converter was designed to produce the output of 50 V and 5 A. The boost converter can be used for battery charging also [4]. Figure 4 shows the Simulink model of the boost converter.

$$V_0 = \frac{V_s}{(1-\alpha)} \quad (2)$$

$$L = \frac{R*\alpha(1-\alpha)^2}{2f_s} \quad (3)$$

$$C = \frac{V_0*\alpha}{f_{s*}\Delta V_0*R} \quad (4)$$

V_0 – Output voltage
V_s – Input voltage
α – Firing angle
f_s – Switching frequency
R – The equivalent load

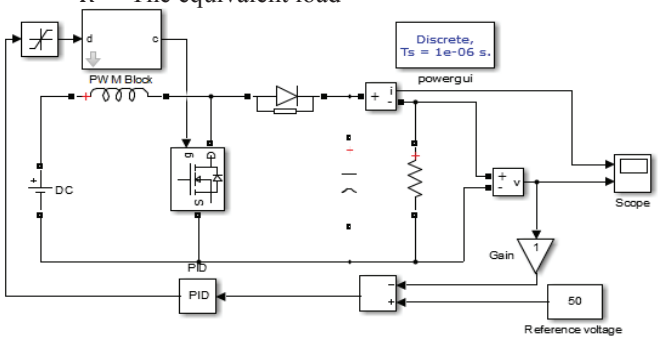

Fig. 4 DC-DC boost converter

IV. MATRIX CONVERTER

Matrix converter comprises of bidirectional switches for each leg. A single-phase matrix converter has four bidirectional switches coupled with anti-parallel diodes. Using this, the matrix converter can be used as a rectifier, inverter and Cycloconverter [5], [6]. Use of matrix converter improves the quality of output voltage with reduced THD. The controlled reverse power flow is also possible using matrix converter. The matrix converter acts as an inverter. Figure 5 shows the Simulink model of single-phase matrix converter operating as inverter.

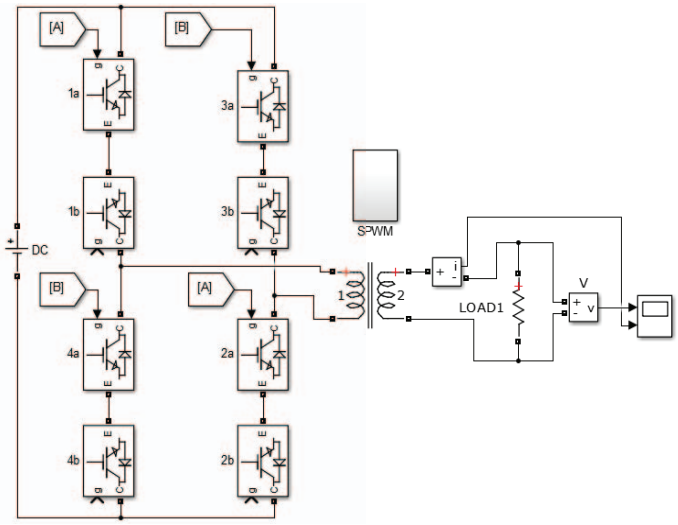

Fig.5 Simulink model of Matrixconverter

A. Sinusoidal Pulse Width Modulation (SPWM)

The matrix converter requires pulses to operate. For this, a Pulse Width Modulation technique is required. In this paper, SPWM technique is proposed. In SPWM the sine wave will be taken as reference and high frequency triangular wave as reference signal as shown in figure 6. Based on the reference signal the pulses are produced and the output was driven [7], [8].

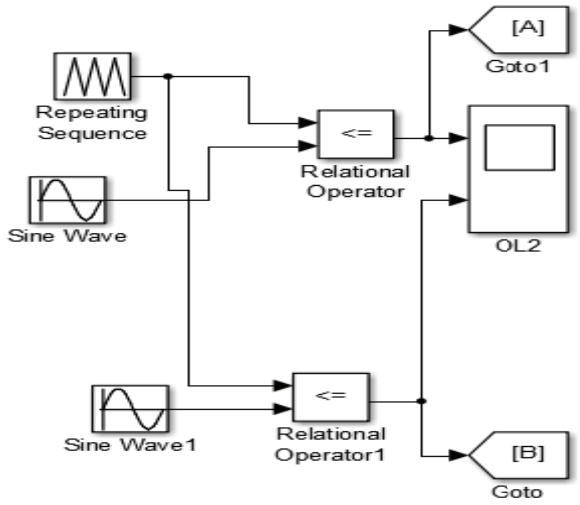

Fig. 6 Simulink model of SPWM

V. Reactive Power

The work producing power measured in watts (W), or kilowatts (kW) is considered to be the real power. Real power produces the mechanical output of a motor. Reactive power is not used to do work but it is needed to operate equipment and is measured in Volt-Amperes-reactive (VAr) or kiloVAr (kVAr). If the load is pure resistive, then doesn't need to bother about the reactive power. However, nowadays most of the loads are not purely resistive. It may be inductive or capacitive in nature. For this type of loads, reactive power compensation is required.

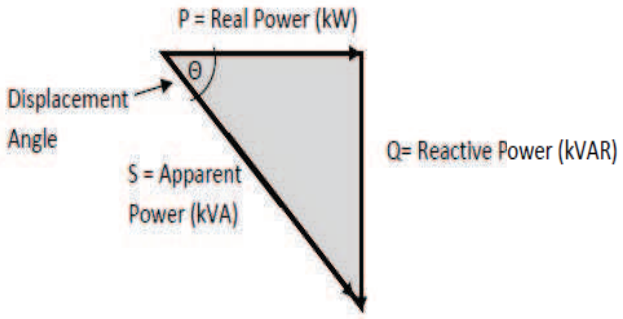

Fig. 7 Power triangle

$$S = P+jQ \qquad (5)$$

From the power triangle, it is clearly known that compensation of reactive power decreases, as the apparent power equals the real power. Thus, the total consumption of power is also reduced. It reduces the payment of the bill [9].

VI. Simulation Results

Figure 8 shows the output voltage waveform of solar panel.

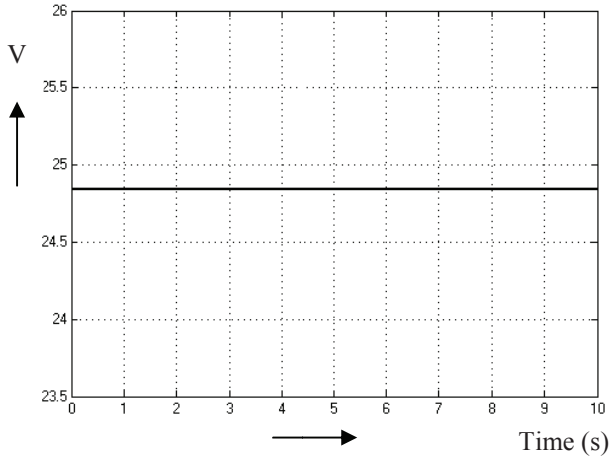

Fig. 8 Output voltage of Solar panel

Figure 9 shows the output voltage and current waveform of the boost converter.

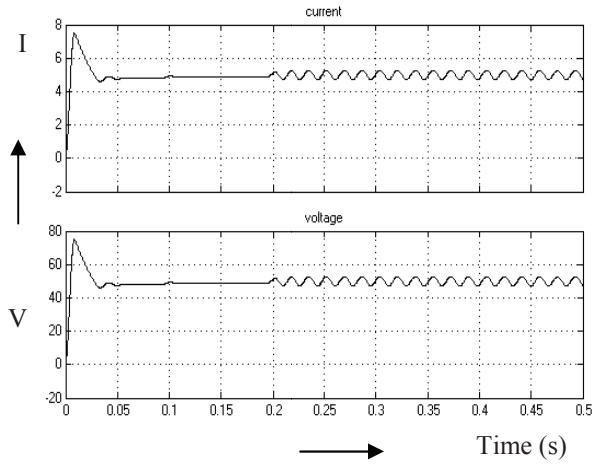

Fig. 9 Output of boost converter

The output which is driven from solar panel is given to the boost converter as input. The boost converter produces the output of 50 Volts DC. This output is given to the matrix converter to convert into AC. The output of the matrix converter is further modified and connected with grid for reactive power compensation.

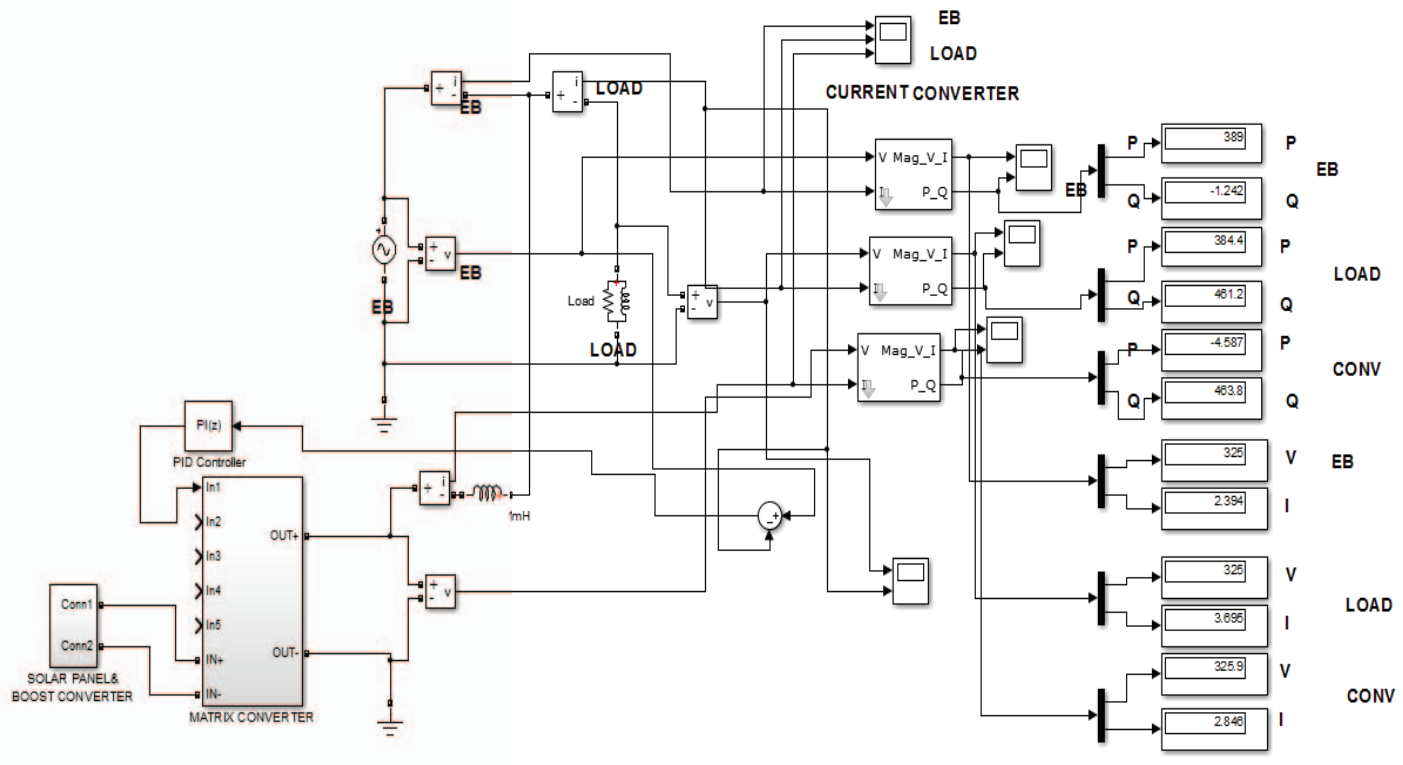

Fig. 10 Simulink model of the proposed work

This model applicable as reactive power compensator is shown in figure 10. Figure 11 shows the output of the matrix converter as standalone solar photovoltaic inverter.

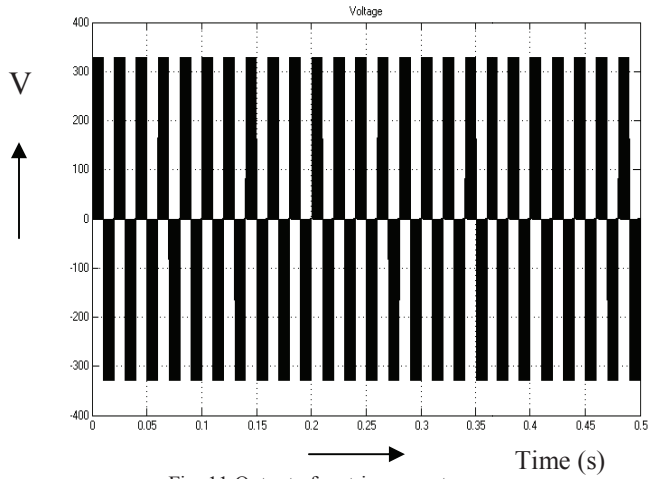

Fig. 11 Output of matrix converter

Figure 12 shows the voltage and current waveform of the utility side before compensation. Here the current waveform was lagging with the voltage. This results in lagging power factor.

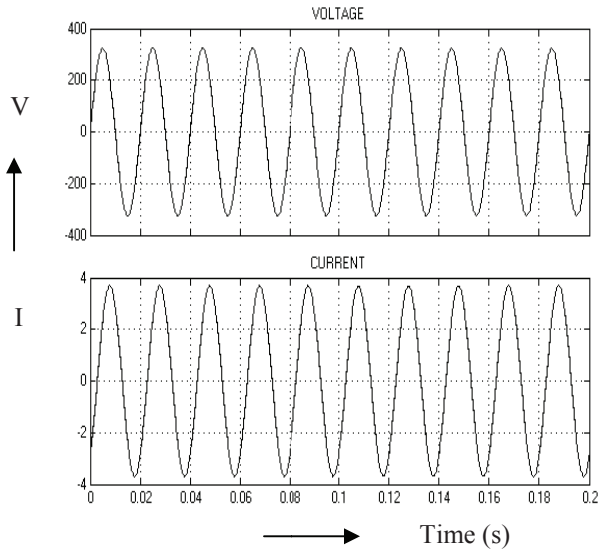

Fig. 12 Utility power before compensation

Figure 13 shows the voltage and current waveform of the utility side after reactive power compensation. Here the waveform of voltage and current are in phase with each other, which shows the power factor of the system is unity.

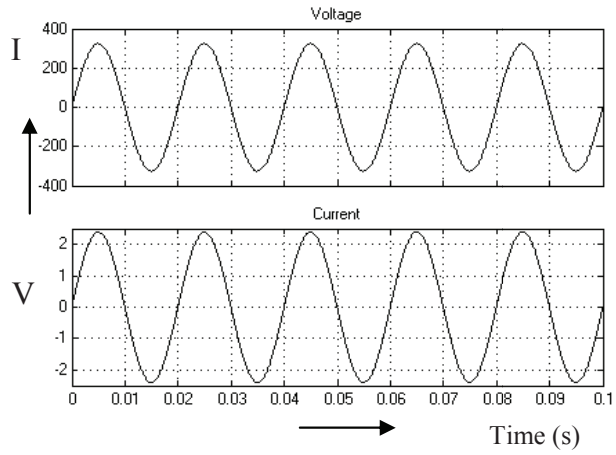

Fig. 13 Utility power after compensation

Figure 14 shows the current waveforms of utility side, load side, and converter side after compensation. Here the changes on the load current will be compensated by the converter and the current of the utility current remains in phase with the utility voltage.

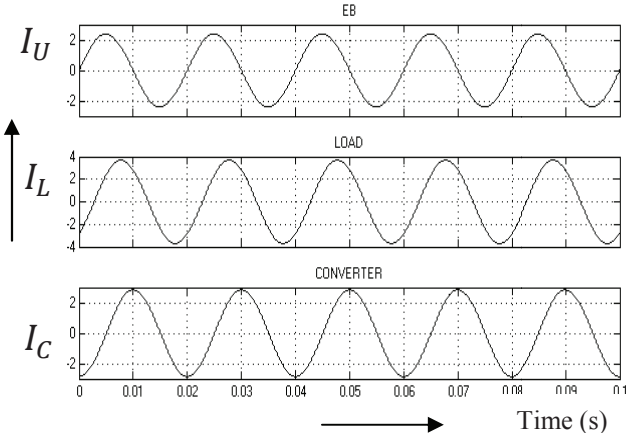

Fig. 14 Current waveform after compensation

Tables I and II show the parameters of real power, reactive power, voltage and current on the source side, load side and converter side. Table I shows the values before compensation and Table II shows the values after compensation.

TABLE I. PARAMETERS BEFORE COMPENSATION

	Source side	Load side	Converter side
Real power	385 W	385 W	0 W
Reactive power	461.2 VAr	461.2 VAr	0 Var
Voltage	325 V	325 V	325 V
Current	3.695 A	3.695 A	0 A

TABLE II. PARAMETERSAFTER COMPENSATION

	Source side	Load side	Converter side
Real power	389 W	385 W	-4 W
Reactive power	-1.2VAr	461.2 VAr	463.4Var
Voltage	325 V	325 V	325.9 V
Current	2.394 A	3.695 A	2.846 A

VII. CONCLUSION

This paper presents a simulation model for the matrix converter based solar photovoltaic system for reactive power compensation in MATLAB-Simulink. The proposed model is a solution for reactive power compensation using solar energy. The model also has a capability of real power transfer, which is received from solar panel.

ACKNOWLEDGMENT

The authors are grateful to the Management and the Head of the institution of Kalasalingam University and Ramco Institute of Technology, for giving all necessary support and providing facilities for making this research paper a successful one.

REFERENCES

[1] Zhang Housheng and Zhao Yanlei, "Research on a Novel Digital Photovoltaic Array Simulator", International Conference on Intelligent Computation Technology and Automation, 2010, 1077-1080.

[2] Mohammad Seifi, Azura Bt. Che Soh, Noor Izzrib. Abd. Wahab, and Mohd Khair B. Hassan, "A Comparative Study of PV Models in MATLAB/SIMULINK", World Academy of Science, Engineering and Technology, 2013, 108-113.

[3] K.H. Edelmoser and F. A. Himmelstoss,"Bi-directional DC-to-DC Converter for Solar Battery Backup Applications", 35th Annual IEEE Power Electronics Specialists Conference,Aachen, Germany, 2004, 2070-2074.

[4] K. Ogura, T. Nishida, E. Hiraki and M. Nakaoka,"Time-sharing Boost Chopper Cascaded Dual Mode Single-phase Sine wave Inverter for Solar Photovoltaic Power Generation System", 35th Annual IEEE Power Electronics Specialists Conference, Aachen, Germany, 2004, 4763-4767.

[5] K.Vijayakumar, R. Sundar Raj and S.Kannan, "Realization of Matrix Converter as revolutionized Power Electronic Converter employing Sinusoidal Pulse Width Modulation", IEEE International Conference on Computational Intelligence and Computing Research, 2013, 1-5.

[6] K.Vijayakumar, R. Sundar Raj and S.Kannan, "Application of Sinusoidal Pulse Width Modulation Based Matrix Converter as Revolutionized Power Electronic Converter," Power Electronics and Renewable energy systems, Lecture Notes in Electricel Engineering, Vol. 326, 2014, 9-17.

[7] Ajay Kumar Gola and Vineeta Agarwal,"Implementation of an Efficient Algorithm for a Single Phase Matrix Converter", Journal of Power Electronics, vol. 9, no. 2, March 2009, 198-206.

[8] G.N. Surya and Subroto Dutt, "A Simplified Switch Modulation Strategy for Matrix Converter", International Journal of Engineering and Innovative Technology (IJEIT),vol.1, Issue 3, March 2012, 160-165.

[9] Narain G. Hingorani, "Understanding FACTS Concepts and Technology of Flexible AC Transmission System", Hingorani Power Electronics, Los Altos Hills, CA.

PET IMAGE RECONSTRUCTION USING ANN-EM METHOD

[1]P.Iniyatharasi
Department of ECE
Kalasalingam University
Virudhunagar, Tamil Nadu, India
shalniyapari@gmail.com

[2]Dr.M.Pallikonda Rajasekaran
Professor and Head of the Department of ECE
Kalasalingam University
Virudhunagar, India
mpraja80@gmail.com

[3]Mr.T.Arun Prasath
Department of ICE
Kalasalingam University
Virudhunagar, Tamil Nadu, India
arun.aklu@gmail.com

[4]Dr.S.Kannan
Professor and Head of the Department of EEE,
RamcoInstitute of Technology,
Virudhunagar, Tamil Nadu, India
kannaneeeps@gmail.com

Abstract—**Imaging is a broad field which covers all aspects of the analysis, modification, compression, visualization, and generation of images. There are at least two major areas in imaging science in which applied mathematics has a strong impact: image processing, and image reconstruction. In image processing the input is a (digital) image such as a photograph, while in image reconstruction the input is a set of data. Image processing techniques treat an image and apply numerical algorithms to either improve the given image or to extract different features of it. Image reconstruction refers to the technique used to create an image of the interior of a body (or region) non-invasively, from data collected on its boundary.Current imaging problems deal with the image quality and the computational tools used to create the image. The performance of ANN-EM algorithm is compared with the simultaneous version of co-ordinate descent algorithm (CD) and de-noising algorithm. Algorithms are compared in terms of prediction and parameters like Peak Signal to Noise Ratio (PSNR), Mean Square Error (MSE) and Root Mean Square Error (RMSE) and Elapsed time for the algorithms. The results shows that ANN-EM based algorithm provides better reconstructed time compared to other two techniques.**

Keywords—ANN-EM algorithm, Co-ordinate descent algorithm,De-noising algorithm, PSNR, MSE, RMSE, Reconstruction time

I. INTRODUCTION

Image reconstruction methods plays vital roleto many of the new applications of medical imaging. In this paper we start with coverage of a number of common ideas that occur in a wide area of problems, including reconstructing images from non-uniformly sampled data, reconstructed image from projection data, reconstruction from under sampled data, and automatically focusing images. There are at least two major areas in imaging science in which applied mathematics has a strong impact: image processing, and image reconstruction. In image processing the input is a (digital) image such as a photograph, while in image reconstruction the input is a set of data. Image processing techniques treat an image and apply numerical algorithms to either improve the given image or to extract different features of it.

The use of the positron emission tomography (PET) camera is to rotate around the patient in order to take the pictures of the patient of from different angles. These "pictures" acquired from the nuclear medicine camera are called projections. These projections are put together to obtain a patient's image is called image reconstruction. There are two types of algorithm are used in image reconstruction they are analytical and iterative algorithms. An algorithm is a mathematical procedure which is implemented on a computer. In medical imaging, image reconstruction is performed in a system with reconstruction algorithms. These measurements are reconstructed into cross-sectional images. Tomography image reconstruction formsan individual image of a patient body in medicalimaging applications.

EM (Expectation Maximization) is considered as an important approach for Image Reconstruction which can be used as an impulse an iterative solver that finds an optimal solution possible algorithms are: ART, EM. EM won't be requiring the computation of gradients and it is also constant.The EM algorithm is used to locate the maximum likelihood parameters of a geometric model in some of the cases where the equations cannot beable to solvein a straight line. Naturally these models involve hidden variables in addition to unidentified parameters and identified data observations. That is, whichever there are mislaid values among the data, or the replica can be formulated more simply by assuming the reality of additional unnoticed data points. In geometric models with hidden variables, this usually is not potential. Instead, the result is classically a set of interlocking equations where the solution to the factorsinvolves the rate of the suppressed variables and vice-versa, howeveralternating

[978-1-4799-6438-3/15/$31.00 ©2015 IEEE]

one set of equations into the other creates an impenetrable equation.

Radial Basis Functions emerged as analternate of artificial neural network in 80's. This is efficient for potential functions, clustering, functional approximation, spline interpolation and mixture models. RBF's are fixed in a two dissimilar types of layer neural network, where each concealed unit implements a radial activated function. The output units implement a weighted sum of concealed unit results. The input is hooked on RBF network which is nonlinear when the result is linear. They have excellent approximation capabilities. Due to their nonlinear approximation properties, RBF networks are able to model difficultplanning, which view neural networks can only bemold by means of multiple mediator layers.

In sequence to use a Radial Basis Function Network there is a need to denote the concealed unit activation function, the amount of processing units, a norm for modeling a given assignment and atraining algorithm reused for calculating the factors of the network. RBF weights can be calculated which called network is training. Inorder to fit the network results to the particular inputs. After training the algorithm, the RBF network can be used with data where its own information is similar to that of the training set.

II. RELATED WORKS

ISWLS shows similar performance to WLSduring the first iterations but it has better noise manipulation.Finally, ordered subsets ISWLS (OS-ISWLS), the OS version ofISWLS, shows its best performance between the first six–nine iterations.Its behaviour seems to be a compromise between OS-ISRAand OS-WLS[1].Dynamic MR Image reconstruction method from partial (k,t)-space measurements is introduced that recovers and inherently separates the information in the dynamic scene. The reconstruction model is based on a low-rank plus sparse decomposition prior, that can be related to robust principal component analysis[2].

Algebraic reconstruction method simultaneous ART (SART), three–dimensional (3-D) object from its projections.The algebraic methods have, many advantages over the more popular Filtered Back projection approaches and have also recently been shown to perform well for 3-D cone-beam reconstruction[3].Vocal tract parameters and glottal excitations are characterized using Line Spectral Pairs (LSP) and pitch residual respectively.To evaluate the comparative performance of RBF and state of the art GMM based voice conversion system[4]. The kinestatic charge detector (KCD) combined with the multilevel scheme algebraic reconstruction technique (MLS-ART) for X-ray computer tomography (CT) reconstruction.

The KCD provides excellent detective quantum efficiency and contrast resolution[5].The spatially variant detector response can reduce spatial resolution in PET. In iterative reconstruction methods, the detector can be modelled into the system response matrix (SRM). Unfortunately, the SRM for current PET scanners is very large. Here evaluating PET reconstruction using generalized natural pixel functions. With these pixel functions, the SRM becomes block-circulant for a ring-PET scanner, because of this there is substantially reducing the number of non-redundant elements in the SRM[6].Unpenalized and penalized weighted least-squares (WLS) reconstruction methods for positron emission tomography (PET), where the weights are based on the covariance of a model error and depend on the unknown parameters[7].

Space-alternating generalized EM (SAGE) algorithms for image reconstruction, which update the parameters sequentially using a sequence of complete-data space.Here they introduce new hidden-data spaces that are less informative than the conventional complete-data space for Poisson data and that yield significant improvements in convergence rate[8]. A method for Bayesian reconstruction which relies on updates of single pixel values, rather than the entire image, at each iteration. The technique is similar to Gauss-Seidel (GS) iteration for the solution of differential equations on grids[9].There are two types of iterative reconstruction algorithms, namely, the maximum likelihood with expectation maximization (ML-EM) and the weighted least squares with conjugate gradient (WLS-CG) algorithms. Both algorithms are effective in compensating for the non uniform attenuation distribution in the thorax region and the spatially variant detector response function of the imaging system.A neural network based image compression method is presented[10].

Comprehensive approach for sclera image quality measure, which includes quality filter and quantitative quality assessment unit, feature evaluation unit, and score fusion unit. The results show that the combination score is highly correlated with the sclera recognition accuracy and can be used to improve and predict the performance of sclera recognition systems[11]. Magnetic Resonance Imaging (MRI) image reconstruction, based on the frequency domain Super-Resolution (SR) algorithm, is presented. Images can be obtained from sets of irregularly located frequency domain samples are combined into the high resolution MRI image. The SR reconstruction replaces the usually applied direct averaging of low-resolution images[12]. A filter design method, compatible with SUPER algorithm, was investigated and tested on MR images. After coils sensitivities estimation, the data from the phased array elements was finally combined using this modified SUPER algorithm[13].

Neural networks offer the potential for providing a novel solution to the problem of data compression by its ability to generate internal data representationneurons which are intended to abstract and model some of the functionality of the human nervous system in an attempt to partially capture some of its computational strengths[14].The method of reconstruction from SPECT data is proposed, which is build on the EM approach to maximum likelihood reconstruction from emission tomography data. This method can be illustrated by an application to data from brain scans[15].They

[978-1-4799-6438-3/15/$31.00 ©2015 IEEE]

use highly overlapping views, geometric data, and semanticsurface classification in order to boost existing 2D algorithms. A 3D model is computed from the overlapping views, and the model is segmented into semantic labels using height information, colour qualities of the images[16].

III. MATERIALS AND METHODOLOGY

A)WLS-CD (Weighted Least Square-Coordinate Descent)

In multivariable minimization, coordinate descent methods minimize the objective by solving a sequence of scalar minimization sub problems. Each and every sub problem improves the estimation of the solution by correcting these solutions along a selected coordinate with all other coordinates fixed. Coordinate descent is impressive because of its simple: scalar minimization is much easier than multivariable minimization. Coordinate descent is efficient when the sub problems can be solved quickly. For some applications, the sub problem solutions can be expressed in closed form. It can be expressed as,

$$\min_{u\in R^n} E(u) = |u|_1+\lambda\|A_u\text{-}f\|^2 \quad (1)$$

Where $f\in R^m$and A is an m×n matrix with m<n (the matrix is wide).

The ICD-WLS algorithm the Poisson data can be outlined as follows.

$$\overline{Yi} = \sum_j p_{ij}x_{ij}(1) + r_i \quad (2)$$

Where x_{ij} be a starting positive image vector. Than can set it via the FBP reconstructed image.

For *j*= 1. . .*n* updating each pixel:

$$x_j^{(K+1)} = x_j^{(k)} \sqrt{\frac{1}{\sum_{i=1}^m pij} \sum_{i=1}^m \frac{p_{ij}\, y_i^2}{\bar{y}_i^2}} \quad (3)$$

Assume an objective image be discredited into n pixels with emission rates x = [x1 . . . xj . . . x_n] T. Assume that the emission source is verified by m detectors (i = 1 . . . m). According to the assumption of the experimental photon counts which are independent to the Poisson random variables greater than the region of interest.

$$\overline{Yi} = \sum_j N_{ij} + R_i \approx poisson\left\{\sum_j p_{ij}x_j + r_i\right\} \quad (4)$$

Wherey_i indicates the i^{th} detector recording emissions, which contain the photon counts emitted by all the pixels and the information of emissions brought by background actions. $\{R_i\}$ are also independent Poisson variables: R_i∼Poisson $\{r_i\}$.Background rates $\{r_i\}$ are assumed to be known. N_{ij} is the real numbers of photons emitted from the jth pixel and corrected by the i^{th}detector discard. The system matrix element P_{ij} denotes the probability of an emission from pixel j is stored at detector tube i. x_j is the accepted value of pixel j.

To concern iterative coordinate descent openlytowards the WLS, we mayattempt to modernize$x_j$by comparing the partial derivative to nil. This method of WLS consists of swapping the logarithm of the prior mass on X by adifferent cost function at the n + 1^{th}renew. The whole data space of the typical WLS algorithm for thisdifficulty is to locate the unobservable random variables.

According to the SAGE algorithm, it has been established in CD-WLS. It utilizes a sequence of small total-data spaces namely, "concealed" data spaces. Here, theychoose a most obvious and easyconcealed data space which consists of those photons emitted from a particular pixel. To minimize the new objective function in each "concealed" data space, then calculated the partial derivate for each given pixel x_j.

$$x_j^{(k+1)} = x_j^k \sqrt{\frac{1}{\sum_{i=1}^m p_{ij}} \sum_{i=1}^m \frac{p_{ij}\, y_i^2}{\left(\sum_{j=1}^n p_{ij}x_j^k\right)^2}} \quad .$$

$$x_j = \sqrt{\frac{x_j^2}{\sum_{i=1}^m p_{ij}} \sum_{i=1}^m \frac{p_{ij}\, y_i^2}{\left(\sum_{j=1}^m p_{ij}\, x_j\right)^2}} \quad (5)$$

(6)

The ROF (Rudin-Osher-Fatemi) form for image de-noising is the following,

$$u = \arg\min \int_\Omega |\nabla_u|\, dx + \lambda \left\|u-g\right\|^2 \quad (7)$$

Where the blur image is g and λ >0 is a parameter.Unlike the ordinary weighted least square algorithm, the coordinate descent-weighted least square algorithm is to decrease each WLS objective function using iterative coordinate descent in a series of the small

[978-1-4799-6438-3/15/$31.00 ©2015 IEEE]

"concealed" data spaces. Even though the CD-WLS algorithm is applied by sequential pixel renew of the image, with each renew the present pixel is chosen to decrease the WLS price function, then the use of "concealed"data spaces makes CD-WLS algorithm congregate faster than the ordinary WLSalgorithm. A novel algorithm, named as FCD-WLS was the combination of the Fuzzy segmented based CD algorithm with the WLS algorithm (FCD-WLS) is proposed for PET image reconstruction.Simulations using both synthetic data and images corroborated the analytical findings and validated the effectiveness of the proposed schemes[18].

B) DE-NOISING ALGORITHM

A different de-noising approach based on non-local estimation appeared in recent times, where pixels of the exact image which is estimated from regions that are found similar to the region middle at the estimated pixel. These methods, unlike the transform-based single,initiate a very few artifacts in the approximate but often more smooth image details. Based on adetailed adaptive weighting scheme, the standard based de-noising appears to be the most top of them and achieves results aggressive to the ones produced by the most top transform-based techniques.

The idea of employing related data patches from a different locality is popular in the video processing field under the term of "block-matching", where this is used to recover the coding effectiveness by developing the similarity among blocks which follow the movement of objects in successive frames. Conventionally block-matching has found unbeaten application in combination with transform-based techniques. Such applications include video compression (MPEG standards) and video de-noising, where noise of the image is attenuated in 3D DCT domain.

We propose a method called de-noising which can be applied to the given original image and that is based on valuable filtering in 3D transform domain which can be combined by sliding window transform that could be processed with block-matching. We agree to the block-matching model for a single noisy image; s the method of image blocks in a sliding manner, we explore for blocks that exhibit resemblance to the presently-processed one. Efficient noise attenuation is done by approaching a contraction operator on the transform coefficients. These results improvedin de-noising performance and effective detail maintenance in the limited estimates of the matched blocks.

The pre-processing of the block in a given input image is processed in the initial stage then the final estimate that are obtained from the previous stage is the weighted average of all overlapping local block-estimates. By doing pre-processing step we come across a problem called over completeness to overlap. We can avoid the previous problem by blocking artifacts and the further improvement in the estimation ability is done.

The OS algorithm plays an important role to accelerate PETimage reconstruction. OS can be applied into any algorithm,which involved a sum over projection[17].

C) ANN-EM (Artificial Neural Network- Expectation Maximization)

RBF Networks can have severalnumbers of concealed levels and outputs with linear or non linear creation. Though, RBF Networks are commonlyrelated with structural designs with only one concealed levels without weights and with an output levels with linear creation. Such structural design is worked because it permits the division of the training in two pointsthat is the radial units factors are resolute the weights of the output levels. In generalit can be calculated simply The majorityof ordinary RBF is the Gaussian function, which is specified by $\Phi_j(d_j(x))$-$e^{-dj(x)}$. Neurons with Gaussian RBF present a very discriminatoryreaction, withelevatedcreation for modelsecure to the radial unit core and extremely small creation for distant models.A Reconstruction constraint was added to the networks as a post training step.A gradient descent optimization on the RBF parameters can be able toachieve according to the formulae below:

$$\frac{\partial E}{\partial \sigma_j} = \sum_n \sum_k \{y_k(x^n) - t_k^n\} w_{ij} \exp\left(-\frac{\left\|x^n - \mu_j\right\|^2}{2\sigma_j^2}\right) \frac{\left\|x^n - \mu_j\right\|^2}{\sigma_j^3} \quad (8)$$

$$\frac{\partial E}{\partial \sigma_j} = \sum_n \sum_k \{y_k(x^n) - t_k^n\} w_{ij} \exp\left(-\frac{\left\|x^n - \mu_j\right\|^2}{2\sigma_j^2}\right) \frac{(x_i^n - \mu_{ji})}{\sigma_j^2} \quad (9)$$

As a result of resources of training, the neural network forms the essential function of a certain mapping. Sequentially to form such a mapping we have to discover the network weights and topology. There are two types of training algorithms: supervised and unsupervised. RBF networks are used in supervised applications. In anorganized application, we are presented with a set of data samples called training set formatching network outputs are known.

In this case the network factors are found such that they decrease a price function of the training set. In unproven training the output assignment is not obtainable for the particular set. A huge variety of training algorithms has been experienced for training RBF networks. In the primary approaches, to every data model was dispensed a source function. This resultshowed to be exclusive in conditions of memory storage and theamount of factors. On the additional hand, accurate fit to the training facts may cause terrible generalization. New approaches choose randomly or supposed well-known the concealed unit weights and evaluate the output weights by solving a method of equations whose results is known in the training set.

The radial basis function midpoints are equallydispersed in the information space. The function which is modeled can be obtained by interpolation. Less basis functions then given data examples are used. A least squares

[978-1-4799-6438-3/15/$31.00 ©2015 IEEE]

result that decreases the exclamationmistake is projected. An adaptive training algorithm for decreasing a given price function is a gradient descend algorithm. Back propagation alters iteratively the network weights creating an allocate for the derivatives of the price function with value to those weights. Expectation-maximization algorithm using a gradient descent algorithm move toward the input-output distributions is employed in this paper.

Back propagation algorithm couldinvolvenumerous iterations and that can get caught into local minima of the price function. For a least output variance, the training charge is identical to the contrary of the wholeamount of data samples related to that concealedunit, therefore the midpointbe in contacts to the conventionalprimary order geometricassessment.correspondingly, next order geometricassessment can be engaged for the covariance matrix. The output weights are calculated in a second stage with means of Least Mean Square assessment. Outliers and data overlapping could cause bias in the factorassessment. Algorithms using robust statistics as Median RBF and Alpha-trimmed Mean RBF have been employed for hidden unit estimation. A set of generator functions is proposed in for hidden unit activation function selection. Stochastic selection has been considered in for the radial basis functions. RBF network topology isresolute by the amount of concealed units. A range of procedures have been worked for calculating a proper network topology.

IV. RESULTS AND DISCUSSION

The quality of reconstructed image can be measured by many parameters. The most commonly used image quality parameters are Mean Square error (MSE), peak signal to noise ratio error (PSNR), Root Mean Square error (RMSE) and Normalized Absolute Error (NAE). If the PSNR value is large, then the reconstructed image quality will also increase.

A) Mean Square Error (MSE)

MSE is one of the important image quality parameter to find the better quality of reconstructed image.MSE can be given as

$$\text{MSE}=\frac{1}{\text{MN}}\sum_{x=1}^{M}\sum_{y=1}^{N}[f(x,y)-f'(x,y)]^2 \quad (10)$$

Where f(x, y) is the original image, f'(x, y) is compressed image and M, N are the dimensions of the images.

B) Peak Signal to Noise Ratio (PSNR)

It is ratio between size of the input image to the square of Mean Square Error (MSE). If PSNR is high then the quality of compressed image is also increased.

$$\text{PSNR}=10\ log_{10}[\frac{MXN}{MSE^2}] \quad (11)$$

Where M×N is the size of an input image.

C) Root Mean Square Error (RMSE)

RMSE is just the square root value for Mean Square Error (MSE). Thus by finding this parameter, we can able to minimize the error in reconstructed image.

$$\text{RMSE}=[\frac{1}{\text{MN}}\sum_{x=1}^{M}\sum_{y=1}^{N}[f(x,y)-f'(x,y)]^2]^{1/2} \quad (12)$$

Where f(x, y) is the original image, f'(x, y) is compressed image and M, N are the dimensions of the images.

D) Reconstruction time

The reconstructed time gives the value of elapsed time in seconds from the process of input image to reconstructed image

The simulation results for images for all the three algorithms are shown below. The images with better reconstruction performance with the better MSE and high PSNR are included in the following figures.

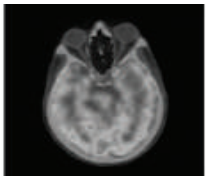

Fig 1: Input Image

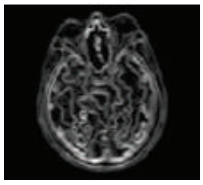

Fig 2: Reconstructed image using ANN-EM

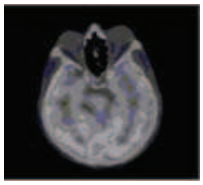

Fig 3: Reconstructed image using CD algorithm

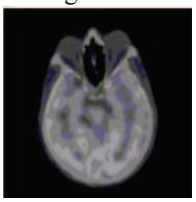

Fig 4: Reconstructed image using De-noising algorithm

Fig (1-4) signifies the input image and reconstructed image of three algorithms i.e. ANN-EM, CD and De-noising Algorithm.

[978-1-4799-6438-3/15/$31.00 ©2015 IEEE]

Table I: Image quality parameters using three different algorithms

From the table it's clear that ANN-EM algorithm is having better reconstruction time by comparing to other two algorithms.

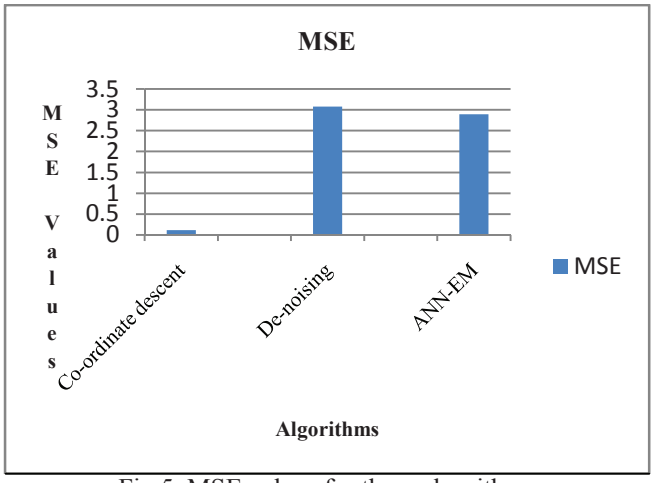

Fig 5. MSE values for three algorithms

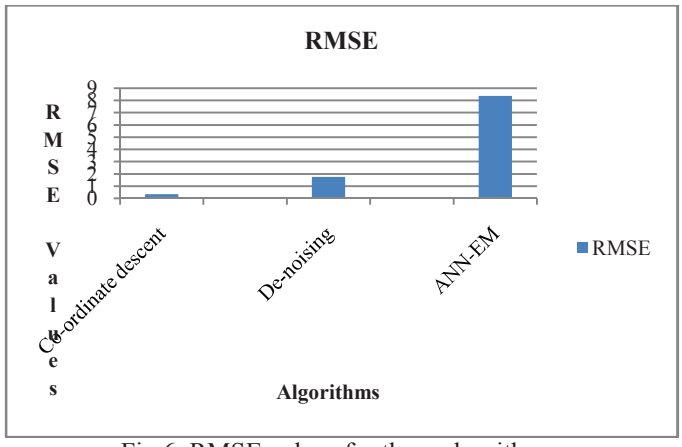

Fig 6. RMSE values for three algorithms

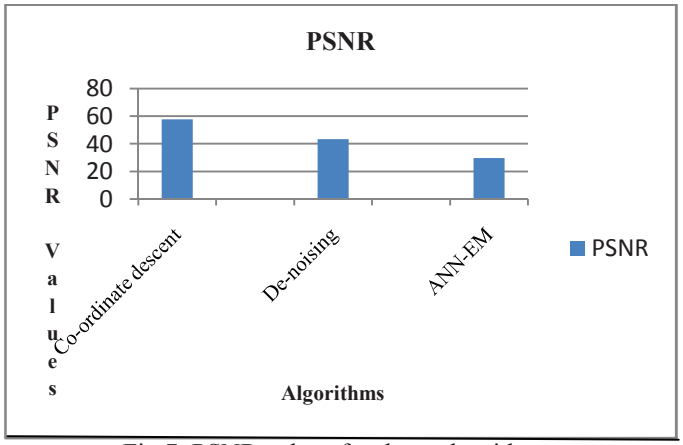

Fig 7. PSNR values for three algorithms

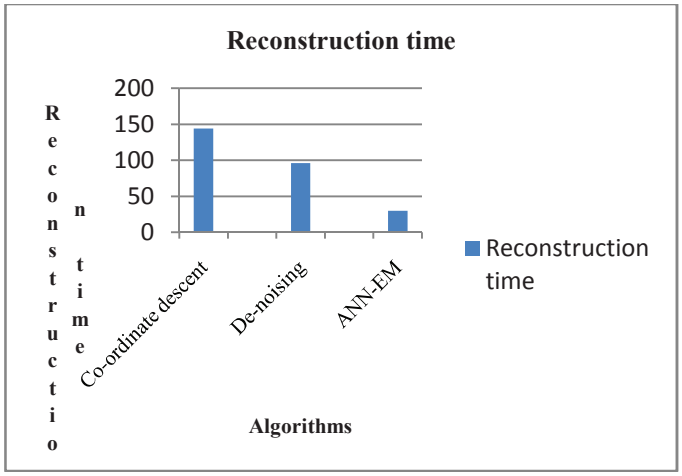

Fig 8. Reconstructed time values for three algorithms

The above figures (Fig. 5 to 8) shows the comparison of image quality parameters such as MSE, RMSE and Reconstructed time by using ANN-EM, Co-ordinate Descent, and De-Noising algorithm. All the input images given here are 256×256 image size. The parameters of the reconstructed

Algorithms/ Parameters	MSE	RMSE	PSNR	Reconstruction time
ANN-EM	2.8951	8.3819	29.6639	2.1996
Co-ordinate descent	0.1117	0.3343	57.6490	144.111805
De-noising	3.0760	1.7539	43.2510	95.972113

image are depicted using different formulae. By calculating MSE and PSNR values of the reconstructed image we can able to predict the quality ofreconstructed image. Here, by

[978-1-4799-6438-3/15/$31.00 ©2015 IEEE]

comparing three different algorithms we can conclude that the CD coding has better MSE and PSNR.

CONCLUSION

In this paper we presented a comparison of reconstruction techniques based on Co-ordinate Descent (CD), De-noising and ANN-EM coding for scan testing to reduce test data volume. Reconstructed images for different input images are obtained by these three algorithms. Image quality parameters are calculated for the reconstructed image and comparison chart is provided for Mean Square Error (MSE) and Peak Signal to Noise Ratio (PSNR), Root Mean Square Value (RMSE) and reconstructed time. By comparing the performance parameters of reconstructed image for these three algorithms, we conclude that ANN-EM coding is efficient technique for image reconstruction by calculating elapsed time for the reconstructed image. We review and discuss about the algorithms for reconstruction of image namely, WLS (Weighted Least Square), De-noising and ANN-EM Techniques.

ACKNOWLEDGMENT

We thank the Department of Electronics and Communication Engineering of Kalasalingam University, (Kalasalingam Academy of Research and Education), Tamil Nadu, India for permitting to use the computational facilities available in Centre for Research in Signal Processing and VLSI Design which was setup with the support of the Department of Science and Technology (DST), New Delhi under FIST Program in 2013.

REFERENCE

[1] Karali .E, Pavlopoulos .S, Lambropoulou .S, and Koutsouris .D," ISWLS: Novel Algorithm for Image Reconstruction in PET",IEEE Trans on information technology in biomedicine, Vol. 15,No. 3,pp. 381-386, 2011

[2] Benjamin Trémoulhéac, NikolaosDikaios, David Atkinson, and Simon R. "DynamicMR Image Reconstruction–Separation From Undersampled (k,t)-Space via Low-Rank Plus Sparse Prior". IEEE Trans On Medical Imaging,Vol. 33,No. 8,pp. 1689-1701, 2014

[3] Yu Chen, Member,StefaanVandenberghe, Steven Staelens, Jan Verhaeghe, and Stephen J. Glick. "PET Reconstruction Using GeneralizedNatural Pixels and a Monte Carlo Generated System Matrix", IEEE Trans on Nuclear Science Symposium Conference Record. Vol. 14,No. 441,pp. 3458-3462, 2006

[4] Nirmal J.H, SuparvaPatnaik , and MukeshA.Zaveri." Line Spectral Pairs Based Voice Conversion using Radial Basis Function" ACEEE International journal on Signal & Image Processing,Vol. 4,No. 2,pp. 26-33, 2013

[5] Klaus Mueller and RoniYagel, "Rapid 3-D Cone-Beam Reconstruction with theSimultaneous Algebraic Reconstruction Technique (SART) Using 2-D Texture Mapping Hardware", IEEE Trans on medical imaging,Vol. 19,No. 12,pp. 1227-1237, 2000.

[6] Huaiqun Guan, WaleedGaber .M, Frank A.DiBianca, and Yunping Zhu "CT Reconstruction by Using the MLS-ART Technique andthe KCD Imaging System—I: Low-Energy X-Ray Studies", IEEE Trans on medical imaging,Vol. 18,No. 4,pp. 355-358, 1999

[7] John M. M. Anderson, Mair B. A, MuraliRao, and Chen-Hsien Wu. "Weighted Least Squares Reconstruction Methods for Positron Emission Tomography", IEEE Trans on medical imaging, Vol. 16,No. 2,pp. 3380-3384, 1997

[8] Jeffrey A. Fessler, "Penalized Weighted Least-Squares Image Reconstruction for Positron Emission Tomography", IEEE Trans on Medical Imaging, Vol. 13,No. 2,pp. 290-300, 1994

[9] Ken Sauer, Charles Bouman"ALocal Update Strategy for Iterative Reconstruction from Projections", IEEE Trans on signal processing,Vol. 41,No. 2,pp. 534-548, 1993

[10] Benjamin M. W.Tsui, XiDeZhao, Eric C. Frey, and Grant T. Gullberg," Comparison Between ML-EM and WLS-CG Algorithms for SPECT Image Reconstruction", IEEE Trans on nuclear science,Vol. 38,No. 6,pp. 1766-1772, 1991

[11] Zhou, Zhi, Eliza Y. Du, Luke Thomas .N, and Edward J. Delp."A comprehensive approach for sclera image quality measure." International Journal of Biometrics ,Vol. 5,No. 2,pp. 181-198, 2013

[12]Malczewski, Krzysztof, and RyszardStasinski, "High resolution MRI image reconstruction from a propeller data set of samples."International Journal of Functional Informatics and PersonalisedMedicine,Vol. 1,No. 3,pp. 311-320, 2008

[13] Giovannetti, Giulio, Vittorio Viti,VincenzoPositano,MariaFilomenaSantarelli,LuigiLandini,AntonioBenassi . "Coil sensitivity map-based filter for phased-array image reconstruction in Magnetic Resonance Imaging." International Journal of Biomedical Engineering and TechnologyVol. 1,No. 1,pp. 4-17, 2007

[14] Siva NagiReddy.k, Dr..Vikram B.R, L.KoteswaraRao, Sudheer Reddy B."Image Compression and Reconstruction Using a New Approach by Artificial Neural Network" International Journal of Image Processing,Vol. 6,No. 2,pp. 68-85, 2012

[15] Peter J. Green."Bayesian Reconstructions From Emission Tomography Data Using a Modified EM Algorithm",IEEE Transon medical imaging, Vol. 9,No. 1,pp. 84-93, 1990

[16]Weinshall D, Golbert A."Object Detection in Multi-view 3D Reconstruction Using Semantic and Geometric Context"ISPRS Annals of the Photogrammetry onRemote Sensing and Spatial Information Sciences,Vol. 3,No. 3,pp. 97-102, 2013

[17]Hongqing Zhu, HuazhongShu, Jian Zhou and LiminLuo."A Weighted Least Squares PET ImageReconstruction Method Using Iterative Coordinate Descent Algorithms",IEEE conference paper,Vol. 7.No. 4,pp.3380-3382

[18] Ioannis D. Schizas, Member, IEEE, and Georgios B. Giannakis,"Covariance Eigenvector Sparsity for Compression and Denoising,IEEE Transactions on signal processing, Vol. 60, No. 5,2012

[978-1-4799-6438-3/15/$31.00 ©2015 IEEE]

EXPERIMENTAL SETUP FOR REACTIVE POWER COMPENSATION

V. Suresh Kumar[1], J. Kohila[2], S.Ponnayirasundaravel[3], S.Kannan[4]

[1] *M. Tech Student, Power Electronics & Drives, Dept. of EEE, Kalasalingam University.*

[2]*Assistant Professor, Dept. of EEE, Kalasalingam University.*

[3]*Assistant Professor, Dept. of EEE, Kalasalingam University.*

[4] *Professor, Dept. of EEE, Ramco Institute of Technology.*

Abstract- This paper mainly deals with the experimental setup for reactive power compensation using two AC sources. Two isolation transformers, step down transformer, auto transformer, Power Harmonic Analyzer (PHA), Digital multi-meter and two tube-light loads are used in the experimental setup. The Reactive power consumed by the load is due to more inductive nature of loads. Compensating the reactive power in a system is a challenging task nowadays. Even though many means of reactive power compensations are dealt with earlier, this paper presents a very simple way of VAr compensation. But there are few experimental setup to analyze this task. This paper mainly focuses about the reactive power compensation for two tube-light loads with a simple experimental setup.

Keywords- auto transformer, Experimental setup, Fluorescent Lamp Load, Isolation Transformer, Reactive power.

I. INTRODUCTION

In our day to day life we are using so many inductive and power electronics loads, due to these loads the reactive power consumption of the load get increased, which in turn decreases the availability of active power at the transformer side [1]. So we have to avoid the drawing of reactive power from the mains supply, by locally injecting reactive power to the load at the customer end by some external VAr sources. By relieving the street distribution transformer from supplying the reactive power demanded by the tube-light loads, that transformer is empowered to deliver the real power alone to its maximum VA capacity. That is a 100 kVA distribution transformer can be made to deliver 100kW with local VAr compensation by consumer end. If the compensator itself consumes more active power for its own operation then it will lead to more electricity consumption cost. So, have to concentrate on both the reactive power injected and active power absorbed by the compensator. In this experimental, the reactive power is compensated for the inductive load of two tube-lights by using one isolation and step down transformers. By maintain the voltage variations for the main source and external source we achieved the reactive power compensation. The reactive power from the compensator to the tube-lights can be made to flow just by maintaining the RMS value of the external source (compensating transformer) by manually adjusting the autotransformer just greater than (say 230.1 Vrms) the voltage of the main source as shown in Figure 1.

The difference between these two voltages depends on the VAr required by the load. That is, if the VAr demand is more at the consumer load then the RMS voltage value of external source must be increased further from 230.1 Vrms.

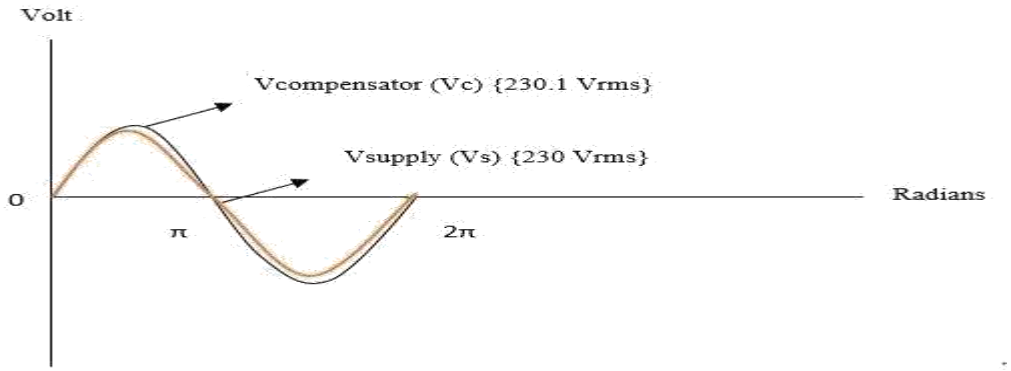

Figure 1: Voltage Waveform of supply and compensator

II. REACTIVE POWER

Figure 2 shows the power triangle for a single tube-light. The active power consumed by one tube light is P= 55 W, the reactive power essentially required by the tube-light to provide a platform to actively convert the real power into useful work (here the useful work is light output) within load is Q= 66VAr and the total power (called as apparent power), the vector sum of P+ jQ, is S=86VA.

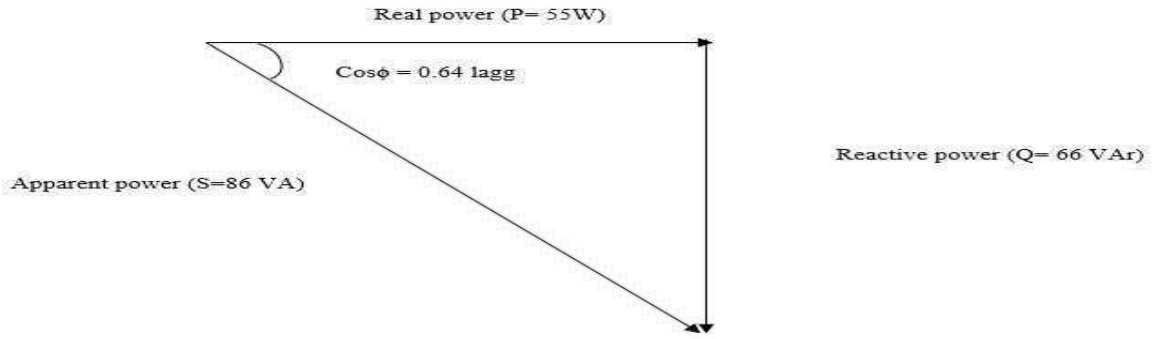

Figure 2: Power Triangle for single tube light of 55 Watts of Real/Active power (theoretical assumption)

Reactive power (VAr, Q) is the essential component for the majority of power consumed by the consumer loads, without which the real power (Watt, P) cannot be utilized within the load arrangement for the work (Heat or Mechanical) being done. Drawing excess of reactive power from the utility, reduces the availability of real power at the utility side [2]. The real power must be drawn from the utility (street distribution transformer in this case) side only and reactive power (for the maximum extent) must not be drawn from the utility for the maximum real power transfer from the utility. Normally power electronics and inductive loads will consume more reactive power from the utility. In electrical quantity reactive power Q is defined as follows:

$$\mathbf{Q = V*I*\sin\phi}$$

Where,

Q= reactive power, delivered by utility (Ideally Q = zero)

V= voltage of utility.

I= current of utility.

Sinϕ= sine of the angle difference between utility voltage and utility current.

III. BASIC CONSTRUCTION OF EXPERIMENTAL SETUP

The basic construction of experimental setup consists of five main parts:

A. Isolation Transformer (230V:230V)/2A
B. Step down transformer (230V:12V)/2A
C. Auto transformer (230V:270V)/4A
D. Power and Harmonic Analyzer (440V/100A), 3 phase 4 wire instrument
E. Load (2*(55W/86VA/66VAr/ P.F = 0.5 lag Fluorescent Lamp))

A. Isolation Transformer:

Isolation transformer is normally 1:1 (230V:230V) transformer which is used for transfer of electrical power from AC source to the load, at the same time it isolates the sensitive loads from power utility and give protection to the sensitive loads. Here we are using 230V/230V isolation transformer for supplying two tube-light loads. The neutral and phase of the load are isolated from the main's side neutral and phase in order to establish the proper injection of reactive current (I sinϕ) demanded by the tube-lights. In between the primary and secondary windings of isolation transformer, there is a capacitive coupling and there is a copper foil shield to reduce the coupling noise. It blocks DC and allows AC.

B. Step-down Transformer:

Step-down transformer has more number of turns in the primary winding side and has less number of turns in the secondary side. The main operation is to reduce the 230V voltage of utility to 12V at its secondary. Normally the primary is made of up small gauge wires and secondary is made up of large gauge wires, to increase the current at secondary. The step-down transformers can act as step-up transformer by connecting it in opposite manner and vice-versa. The dot polarity test is needed when it is connected to a single phase AC source. Here the 230V/12V transformer is connected in series with the secondary of isolation transformer-2 (the compensator here).

C. Auto Transformer:

Auto transformer is the single winding transformers with multiple taps and a riding carbon brush the varying O/P voltage can be obtained i.e) step-up or step-down based on the position of carbon brush. The main advantages of this transformer is low leakage reactance, low losses and low excitation current. The main disadvantage is that, there is no electrical isolation between input and output. Here single phase 230V/4A auto transformer is used for the experimental setup.

D. Power and Harmonic Analyzer:

Power and Harmonic Analyzer is a hand-held digital measuring instrument and it is interfaced with system. It is a mains cum battery operated - portable instrument. This measuring equipment can be able to measure single phase and three phase voltages, currents, active power, reactive power, power factor, apparent power, angle difference between voltage and current, harmonics up to 99^{th} order, vector diagrams, graphs of waveforms, etc in a single setup with the user-friendly keys. The main advantage of this equipment is that, it can record all the data and waveforms in this kit and transfer to a Personal Computer. Here, using it for monitoring the actual instantaneous active power and reactive power consumed by the load and the compensation is done by the isolation transformer-2 (a VAr source here).

E. Load:

The load may be an inductive, capacitive or power electronic load. The pure resistive load does not consume any reactive power, since a resistor load does not store any energy instead of it dissipates the real power. Here using single phase load is used i.e) two tube-lights with inductive choke (not electronic choke). This inductive load consumes more reactive power and observes poor lagging power factor P.F=0.5 [3]. So to increase the power factor, going to compensate that reactive power by using the compensator (isolation transformer-2 and the step-down transformer (Vc).

IV. EXPERIMENTAL SETUP CIRCUIT DIAGRAM

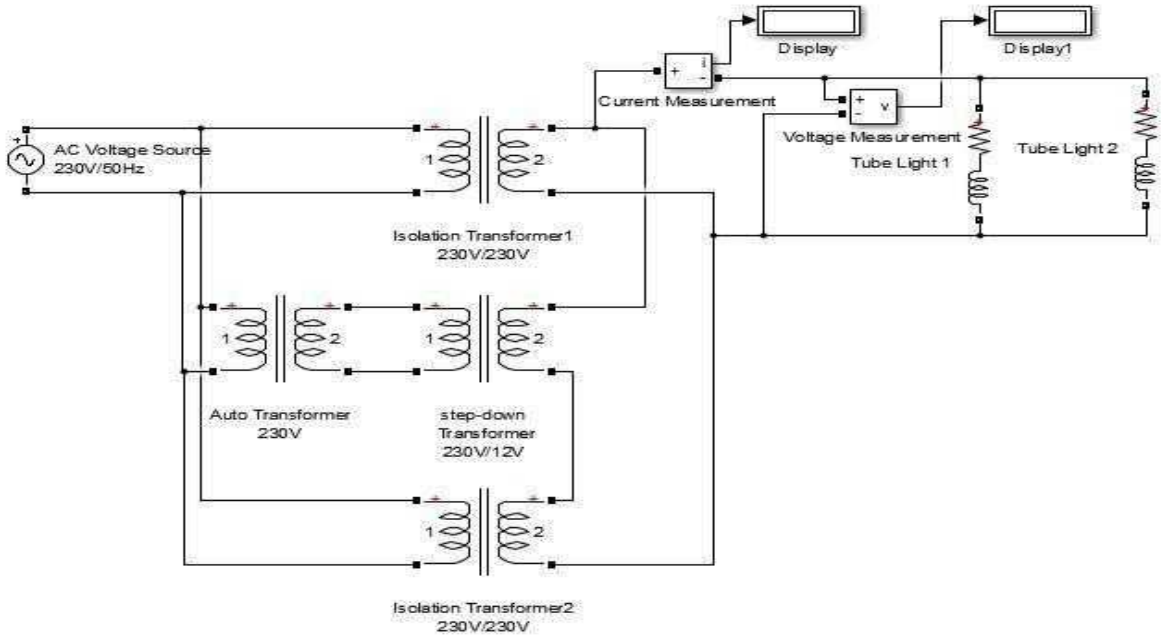

Figure 3: Experimental setup circuit diagram

Figure 3 shows the real time circuit connection diagram for the reactive power compensation experimental setup. The whole setup is used to act as a single capacitor connected in parallel to compensate

reactive power. In this, the single phase 230V utility is supplying power to the load via isolation transformer-

1(230V/230V). The same single phase source is connected to another isolation transformer-2 which is connected in parallel (shunt) to the grid with the series connection to secondary of a step-down transformer (230V/12V) to establish a dominating peak voltage (Vpeak) with respect to mains utility voltage), which in together compensates the reactive power needed by the inductive loads with the manual variable voltage of AC applied to the primary of the step-down transformer via auto transformer. By maintaining the voltage difference between the main (Vs) and the compensating parallel transformer-2 (Vc), the reactive power is injected (Vc>Vs) [4].

V. EXPERIMENTAL SETUP

Figure 4 shows the experimental setup of the reactive power compensation kit, which includes all the devices as mentioned above in the construction.

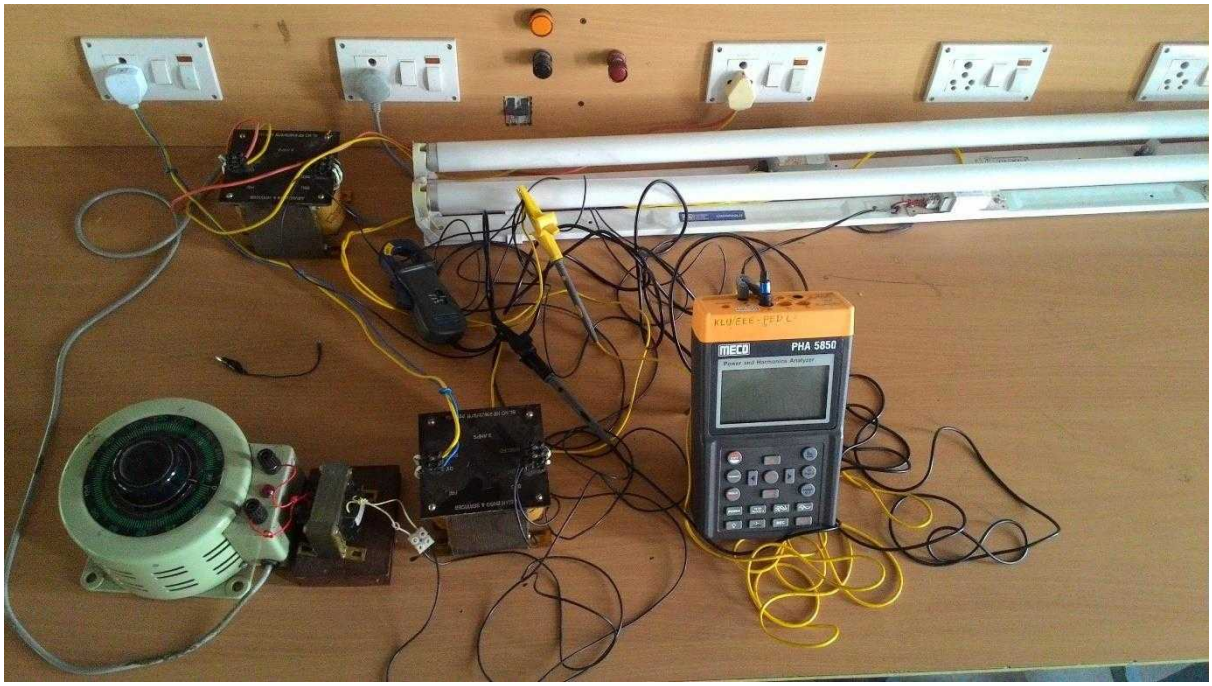

Figure 4: Experimental setup

The experimental setup is configured based on the circuit diagram. The monitoring equipments used are Power and Harmonic Analyzer and digital multi-meters for AC voltage and current measurement.

VI. RESULTS

The results obtained from the experimental setup using Power and Harmonic Analyzer and digital multi- meter are shown in Table 1:

Table 1: Main transformer reading before and after compensation for the two tube-light loads

MAIN TRANSFORMER READING	**BEFORE COMPENSATION**	**AFTER COMPENSATION**
voltage	246 V	248 V
current	1.0 A	500 mA
Real power	123 W	80 W (ideally 123W)
Reactive power	220 VAr	95 VAr (ideally 0VAr)
Power factor	0.5	0.64 (ideally more than 0.95)

VII. Conclusion

This paper presents a new methodology for the reactive power compensation using two AC sources with a simple experimental setup. The overall performance was satisfactory, but the existing injection transformer setup injecting real power also, due to the phase displacement between the two sources and due to different inductance of Transformers. So, this setup provides both real and reactive power transfer. The future aim is equivalent to demonstrate the same setup in three phase transformers and in three phase inverter kit.

VIII. Appendix

Single phase AC voltage source: 230V/50Hz, Isolation transformer 1: 230V/230V, Isolation transformer 2: 230V/230V, Load: 2 Fluorescent lamps, Step-down transformer: 230V/12V, Auto-transformer: 230V, Approximate inductance value of the load: 2.5H

Measuring devices: Digital multi-meter, Power and Harmonic Analyzer

IX. References

1) C.Sankaran, “Power Quality”, CRC Press LLC, 2002.

2) N.G.Hingorani and L.Gyugyi, “Understanding FACTS: Concepts and Technology of Flexible AC Transmission Systems”. New York: Institute of Electrical and Electronics Engineers, 2000.

3) Arindam Ghosh, Gerard Ledwich, “Power Quality Enhancement Using Custom Power Devices”, Kluwer academic Publishers, 2002.

4) K.R.Padiyar, “Facts Controllers in Power Transmission and Distribution”, New Age International (P) Ltd., Publishers, 2007.

A PRODUCTION COST MODEL FOR REACTIVE POWER IN ELECTRICITY MARKET

D.Danalakshmi[1], S.Kannan[2]

[1]*Research Scholar, Kalasalingam University, Krishnankoil, Tamil Nadu, India*

[2]*Department of EEE, Ramco Institute of Technology, Rajapalayam, Tamil Nadu, India*

Abstract - In a restructured power market, supply of reactive power is an essential ancillary service provided by an Independent System Operator taking into account the voltage stability and reliability of the power system. The generators are the main producer of reactive power. The production cost of generator reactive power should be consideredfor reactive power pricing. In this paper, the production cost of real and reactive power was considered in the objective function of the optimal power flow problem.Different methods were presented to obtain the reactive power cost equation of the generator. The triangular method is based on generator power factor to allocate the cost for reactive power service. Real power based method and apparent power based method depends on the opportunity cost of the generator for reactive power cost allocation. These methods are illustrated with IEEE-14 bus power systems to show its validity andpracticability.

Keywords:Opportunity cost, optimal power flow, Reactive power cost functions, Restructuring.

I. INTRODUCTION

In a restructured power system, one of the most important issues of Independent System Operator (ISO) is to maintain the reactive power. Steady supply of reactive power improves the stability and reliability of the power system. Inadequate reactive power in the system leads to voltage collapses and has been a major cause of blackout across the world, e.g. United states and Canada in the year 2004 [1]. In a restructured electricity market, the ISO aims to utilize the available reactive power resources efficiently. It is essential to determine the price payment to market participants for providing the reactive power service in the system.

In deregulated power system, the reactive power service is separated from the real power services and is considered as one of the activity of system operator. The cost of reactive power service is recovered based on various methods in deregulated power system. In some power system, cost of reactive power is included in active power price. In some system, the power factor is used for calculation of cost of reactive power service[2]. In reactive power pricing based on load power factor, the generators have to produce necessary power at a specified range of power factor. If the power factor deviate the specified range, the reactive power has to be priced. In a pool type competitive electricity market, ISO constitutes the appropriate payment mechanism and market structure for reactive power services so that the reactive power producers are encouraged to participate in the electricity market.

Many researches have been carried out for pricing of reactive power service. Practical restructured power systems adopt different pricing strategies for reactive power. Dona and Paredes have proposed a reactive power pricing technique using decoupled OPF with an objective of minimization of operational cost as well as the

transmission losses [3]. Chu and Chen have proposed the reactive power cost allocation using modified Y-bus

matrix [4]. Rider and Paucar have introduced a reactive power pricing method which is solved by Interior point method [5]. Chung et al. have presented a reactive power pricing method in which the reactive power production cost by generators and capacitors are minimized in the objective function [6]. Deksnys and Staniulis have introduced a method for reactive power cost equation of generators, synchronous condenser and static reactive power sources [7].

Allocation of generator production cost and generator transmission cost using reactive power flow tracing method are determined in [8]. An electricity tracing method is used to charge the reactive power provider for the actual amount of transmission line loading and loads [9]. Ashutosh et al have proposed the application of power flow tracing method for reactive power pricing [10]. In this paper, we have compared the three methods for framing the reactive power cost equation and calculated the production cost of reactive power service in a power market.

The rest of the paper is organized as follows: Section II explains the methods for reactive power production cost model of the generator. Section III describes the formulation of OPF problem and Section IV analyses the results and compared the reactive power production cost allocation in IEEE 14 bus system. Finally Section V provides the conclusion.

II. REACTIVE POWER COST MODEL OF THE GENERATOR

The reactive power produced by a synchronous generator is composed of two cost components. They are explicit cost and the implicit cost [11]. Explicit cost is the investment costs and operating cost. Implicit cost refers to the opportunity cost which depends on the reduction in its active power generation. The following methods have been considered to evaluate the cost of generator reactive power.

A. Triangular method

The cost calculation of generator reactive power is based on the active power cost equation. The reactive power equation for the generators follows the same quadratic structure as active power using the power triangle relationship [2]. The reactive power cost function is represented as

$$C(Q) = a'Q^2 + b'Q + c' \tag{1}$$

where a', b', c' are cost coefficients which are derived from the active power cost coefficient (a_p, b_p and c_p) and generator power factor ($\cos\theta$). They are calculated as follows from power triangle relationship.

$$\left[a' = a_p \sin^2\theta,\ b' = b_p \sin\theta \text{ and } c' = c_p\right]$$

B. Maximum Apparent power based Opportunity cost method

Synchronous generators are rated in maximum MVA at specified voltage and power factor. The generator real power output is usually limited by the capability of its prime mover. The generator reactive power output is limited by armature current, field current and end region heating limit [12].The mutual relationship between real and reactive power output of synchronous generator are represented by capability curve as shown in Fig.1.

Let $V_t$is the generator terminal voltage

$I_a$is the steady state armature current.

$P_g$and Q_g are real and reactive power generation from the synchronous generator.

E_f is the excitation voltage and

X_s is the synchronous reactance of the generator.

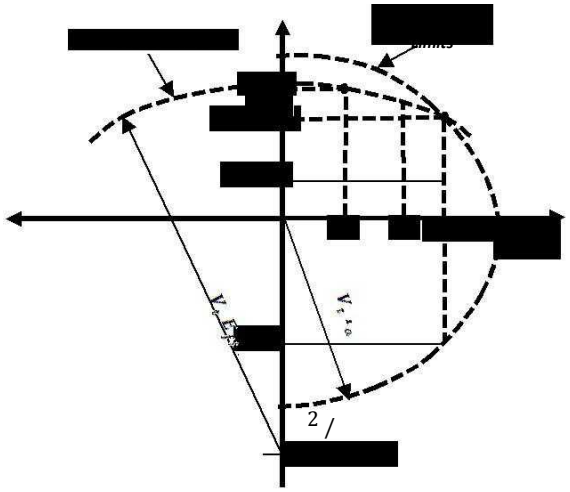

Fig. 1. Capability curve of synchronous generator

The production cost of generator reactive power is called opportunity cost. The production of reactive power reduces the active power output of the generator and may leads to financial loss to the generator. Opportunity cost can be approximately evaluated as [8]:

$$C_{qgi}(Q_{Gi}) = \left[C_{pgi} (S_{Gi,\max}) - C_{pgi} \sqrt{S^2_{Gi,\max} - Q^2_{Gi}} \right] K_{Gi} \quad (2)$$

where $C_{qgi}$is the reactive power production cost of the *i*-thgenerator, C_{pgi} is the active power production cost of the *i*-th generator, P_{Gi} and Q_{Gi} are the real and reactive power of generator i, $S_{Gi,max}$is the apparent power of generator, K_{Gi} is the profit rate of the active power, which is usually chosen between 0.05~0.1. In this paper, K_{Gi}= 0.1.

C. Maximum real power based opportunity cost method

If the generator is operating at its maximum active power P_{max} and there is no reactive power. In such situation S equals P_{max}. To generate reactive power from the generator, it is required to reduce the real power. Suppose the generator needs to produce the reactive power Q_A which has been operating at its maximum power, it is required to reduce the real power from P_{max} to P_A as shown in Fig. 1. Hence the generator reactive power production results in reduction of real power [2].

$$P_A = \sqrt{\max^2 - Q_A^2} \quad (3)$$

$$\Delta P = P_{\max} - P_A \quad (4)$$

The opportunity cost of Q_A depends on the profit of $\Delta P = P_{\max} - P_A$. Hence the generator production cost of reactive power Q_A while the generator operating point is moved from P_{max} to P_A is as follows

$$Cost(Q_A) = Cost(\Delta P) \tag{5}$$

$$Cost(Q_A) = Cost(P_{\max}) - Cost(P_A) \tag{6}$$

$$Cost(Q_A) = Cost(P_{\max}) - Cost(P_{\max} - \Delta P) \tag{7}$$

Usingthe equations 3, 4 and 7, the cost value of reactive power is calculated for different values of $Q_A$with respect to P_A. The cost expression for reactive power is calculated by fitting a curve into a quadratic polynomial form as below

$$Cost(Q) = a'Q^2 + b'Q + c' \tag{8}$$

This reactive power cost equation is simple and can provide results for reactive power pricing.

III. Optimal Power Flow (OPF) problem formulation

The real and reactive power production cost of the generator is obtained by solving the OPF. The OPF problem is defined as minimizing the system objective function, i.e. summation of quadratic cost functions of active and reactive power cost of the system [2]. The OPF problem formulation is:

Objective function

$$\sum_{i \in g} C_{pgi}(P_{gi}) + C_{qgi}(Q_{gi}) \tag{9}$$

where g is the number of generators; $C_{pgi}(P_{gi})$ is the active power cost function of the *i*-th generator; $C_{qgi}(Q_{gi})$ is the reactive power cost function of the *i*-th generator respectively.

The constraints considered in this OPF problem are the set of equality and inequality constraints. The equality constraints are standard power flow equations and inequality constraints are the generation, voltage and line flowlimits of the system, as shown below:

Load flow equations:

$$P_{gi} - P_{di} - \sum_{j \in N} \left|V_i^{\bullet}\right| \left|V_j^{\bullet}\right| \left|Y_{ij}\right| \cos(\theta_{ij} + \delta_j - \delta_i) = 0 \tag{10}$$

$$Q_{gi} - Q_{di} + \sum_{j \in N} \left|V_i^{\bullet}\right| \left|V_j^{\bullet}\right| \left|Y_{ij}\right| \sin(\theta_{ij} + \delta_j - \delta_i) = 0 \tag{11}$$

where *N i*s the number of buses in the system; P_{gi} and Q_{gi} are the active and reactive power generation in *i*-th bus, respectively; P_{di} and $Q_{di}$are the active and reactive power demand in *i*-th bus, respectively; $Y_{ij} = Y_{ij} \angle \theta_{ij}$ is the element in the bus admittance matrix between bus i and j; $V_i^{\bullet} = V_i \angle \delta_i$ and $V_j^{\bullet} = V_j \angle \delta_j$ are the bus voltage at bus i and j, respectively.

Active and Reactive power generation limits:

$$P_{gi,\min} \le P_{gi} \le P_{gi,\max}$$

$$Q_{gi,\min} \le Q_{gi} \le Q_{gi,\max}$$

$$\leq Q_{gi,\max} \quad (12)$$

(13)

$$P_{gi}^2 + Q_{gi}^2 \le S_{gi,\max}^2 \tag{14}$$

where $P_{gi,\ min}$ and $P_{gi,\ max}$ are the minimum and maximum value of the active power generation at *i*-th bus; $Q_{gi,\ min}$ and $Q_{gi,\ max}$ are the minimum and maximum value of the reactive power generation at *i*-th bus; $S_{gi,max}$is the maximum apparent power at *i*-th bus, respectively.

Bus voltage limits:

$$V_{i,\min} \le |V_i| \le V_{i,\max} \tag{15}$$

where $V_{i,\ min}$ and $V_{i,\ max}$ are the minimum and maximum value of the voltage limit at *i*-th bus, respectively.

Transmission line limits:

$$S_l \le S_l^{\max}; l \in N_l \tag{16}$$

where S_l is line loading and $S_l^{\max}$ is maximum loading limit of *l*-th line and N_l is the total number of transmission line.

The optimization problem takes the form

$$\min_x \quad f(x) \tag{17}$$

Subject to

$$g(x) = 0$$
$$h(x) \le 0$$

The optimization problem is solved using MATPOWER [13]. The optimization vector x consist of voltage magnitude, voltage angle and the vector of generator real and reactive power respectively.

IV. Results and Discussion

To investigate validity of the methods, it has been applied to IEEE 14 bus system. The system has 5 generators and 20 transmission lines. Table I and Table II shows the generator characteristics and load characteristics with non capacitive load respectively. The base of generator apparent power is 100MVA. The voltage limit is $0.9\ p.u \le |V_i| \le 1.05\ p.u$ and swing bus voltage is $V_i = 1.05\ p.u$ *and* $\delta_i = 0$ .The generator power factor are taken as 0.97 and generator 3 with power factor of 0.85.

TABLE I

GENERATOR CHARACTERISTICS

Generator No.	Bus no.	P_{max}(MW)	P_{min}(MW)	Q_{max}(MVAr)	Q_{min}(MVAr)	Real Power coefficient		
						a_p	b_p	c_p
1	1	332	50	100	-100	0.0430	20	0
2	2	140	10	50	-50	0.25	20	0
3	3	100	12	100	-60	0.01	40	0
4	6	100	10	30	-30	0.01	40	0
5	8	100	10	30	-30	0.01	40	0

Three different cases have been analyzed. In the first case, the reactive power cost equations are framed using triangular method. In the second case, the reactive production cost equation are framed using apparent power based opportunity cost method and in the third case, the maximum real power based opportunity cost approach is used to frame the reactive power production cost equations of the IEEE-14 bus system. Table III shows the comparison of results for these three cases.

TABLE II

LOAD CHARACTERISTICS

Bus No	Active power(MW)	Reactive power (MVAr)
2	21.7	12.7
3	94.2	19.0
4	47.8	3.9
5	7.6	1.6
6	11.2	7.5
9	29.5	16.6
10	9.0	5.8
11	3.5	1.8
12	6.1	1.6
13	13.5	5.8
14	14.9	5.0

TABLE III

ANALYSIS OF RESULTS IN IEEE 14 BUS SYSTEM

	Bus. No	P_g (MW)	Q_g (MVAr)	Generator Actual real power production cost ($/h)	Generator actual reactive power production cost ($/h)	Total cost ($/h)
Case 1 (Triangular method)	1	33.2331	10.0177	712.2	42.3316	12656.33
	2	140.0	28.0272	7700	147.5069	
	3	53.1197	10.0167	2153	216.2728	
	6	13.2143	14.3828	530.3	112.9067	
	8	23.3083	13.2509	937.8	104.0155	
Case 2 (Apparent power based opportunity cost method)	1	33.2331	10.0216	712.2	20.4754	12282.12
	2	140	29.6654	7700	81.3318	
	3	53.1396	10.0170	2153.8	40.1682	
	6	10.1046	12.8339	405.2	51.5005	
	8	26.3773	13.7873	1062.1	55.3392	
Case 3 (Real power based opportunity cost method)	1	33.2331	10.0782	712.2	70.7204	12534.39
	2	140	7.9637	7700	20.7357	
	3	52.8162	10.0675	2140.5	133.9180	
	6	10.0171	30.0	401.7	186.4606	

	8	26.9906	20.0211	1086.9	81.2575	

From Table III, the following observations are made:

- The active power production cost at the generator bus changes slightly when the objective function changes.
- For each test case, the reactive power production cost fluctuates significantly at the generator buses.
- The active power production cost is much higher than the reactive power production cost at various generator buses.
- When the reactive power production cost is included in the objective function, the total production cost of the generator is increased.
- The total reactive power generation cost in triangular method is greater than that of apparent power based opportunity cost method and real power based opportunity cost method. This will encourage and motivate the reactive power provider to invest and provide reactive power service to keep the power system in a secure manner. On the other hand, in deregulated power markets where the reactive power is priced low, based on apparent power and real power based opportunity cost method. This will make less motivation among the reactive power suppliers to support for the reactive power service. Thus the modeling of reactive power production cost equation using triangular method seems to provide good pricing of reactive power. This will encourage the reactive power provider for their active participation to provide reactive power for enhancement of stable and reliable operation of power system.

V. CONCLUSION

In this paper, both active and reactive power production costs of the generators are considered in the objective function of the OPF problem. Three different methods are employed to obtain the reactive power cost equation for the generator. The IEEE 14 bus system is used to verify the validity of the method. Results confirm that the reactive power cost obtained through triangular method is higher than the cost obtained through real power based cost method and apparent power based method. Finally, based on motivating the generators to provide reactive power service and also providing good production cost for real and reactive power, the triangular method yields better production cost for generator real and reactive power.

ACKNOWLEDGMENT

The authors gratefully acknowledge the management of Kalasalingam University, Krishnankoil and Ramco Institute of Technology, Rajapalayam, Tamil Nadu, India for their constant support and encouragement during this research.

REFERENCES

[1] US-Canada Power System Outage Task Force,"Blackout in the United States and Canada: Causes and Recommendations," Issued in April 2004. Available: http://www.iwar.org.uk/cip/resources/blackout-03/ch1-3.pdf

[2] S. Hasanpour · R. Ghazi · M. H. Javidi, "A new approach for cost allocation and reactive power pricing in a deregulated environment" *Electrical Engineering*, vol. 91, issue.1, pp 27-34, Springer-Verlag 2009.

[3] Dona V.M. andParedes A.N., "Reactive power pricing in competitive electric markets using the transmission losses function," *Power Tech conference,* IEEE porto, vol.1,pp 1–6, 10-13 September, 2001.

[4] Chu. W and Chen. B, "Allocating the costs of reactive power purchased in an ancillary services market by modified Y-bus matrix method," *IEEE Transaction on Power System*, vol.19, issue. 1, pp.174-179,February 2004.

[5] Rider M.J. and Paucar V.L.,"Application of a nonlinear reactive power pricing model for competitive electric markets," *IEE Proc. Generation Transmission Distribution*,vol. 151,issue.3, pp.407-415,May2004.

[6] Chung CY, Chung TS, Yu CW and Lin XJ, "Cost-based reactive power pricing with voltage security consideration in restructured power systems," *Electric Power System Research*,vol. 70, issue.2, pp.85-92, July 2004.

[7] Deksnys R andStaniulis R,"Pricing of reactive power services," *Oil Shale Estonian Academy Publisher*, vol. 24, pp.363-376,2007.

[8] Dai ,Y., Liu, X. D., Ni,Y.X., Wen, F.S., Han, Z.X., Shen, C.M. Felix F. Wu, " A cost allocation method for reactive power service based on power flow tracing," *Electric power system research*,vol.64, issue.1, pp. 59-65, Jan. 2003.

[9] Mala De, Swapan and Goswami, K, "Reactive power cost allocation by power tracing based method", *Energy Conversion and Management*, vol. 64, pp. 43-51, December 2012.

[10] AshutoshTiwari and Ajjarapu. V, "Reactive Power Cost Allocation Based on Modified Power Flow Tracing Methodology," Power Engineering Society General meeting IEEE 2007, E-ISBN: 1-4244-1298-6, pp.1-7, June 2007.

[11] John Lamont , W., and Jian Fu, "Cost Analysis of Reactive Power Support," *IEEE Transactions on Power Systems*,vol.14, issue.3, pp. 890-898, August 1999.

[12] Bhattacharya, K., and Jin Zhong, "Reactive power as an ancillary service", *IEEE Transaction on Power Systems*, vol.16, issue.2, pp. 294-300, May 2001.

[13] Zimmerman.R and Gan.D. MATPOWER 4.0, A MATLAB power system simulation package, Cornell University, Available from: http://www.pserc.cornell.edu /matpower. Feb. 2011.

REACTIVE POWER COMPENSATION USING STATCOM FOR SINGLE PHASE DISTRIBUTION SYSTEM

M.Gerald Geafori Titus[1], S.Rajendran[2], S.Ponnayirasundaravel[3], S.Kannan[4]

[1] *M. Tech Student, Power Electronics & Drives, Dept. of EEE, Kalasalingam University.*

[2] *Assistant Professor, Dept. of EEE, Kalasalingam University.*

[3] *Assistant Professor, Dept. of EEE, Kalasalingam University.*

[4] *Professor, Dept. of EEE, Ramco Institute of Technology.*

Abstract - This paper presents a STATCOM based reactive power compensation control using MATLAB/SIMULINK. Whenever the reactive power compensation take place at the distribution side for the different load condition, STATCOM plays a major role to support the reactive power compensation in generation and transmission system. With the PI controller a reference voltage is generate with the sinusoidal PWM pulse was produced to reduce the reactive power loss. The DC capacitor is used to maintain the constant energy at the input of the STATCOM .The STATCOM also reduces the harmonics present in the grid side. STATCOM is used to improve the power factor, Reactive power loss can be completely minimized. The voltage variation in the transmission line is also minimized with the help of STATCOM.

Keywords: Control design, PI controller, STATCOM (sine PWM)

I. INTRODUCTION

In Alternating Current transmission and distribution system the quantity reactive power is a great concern which determines the quality of power. The total power in AC network is calculated as the algebraic sum of real and reactive power. From this the compensation of reactive power improves the power quality. In older days the reactive power was compensated by using reactors and capacitors. For various loads multiple numbers of reactors and/or capacitors were required. This type of compensation was complicated when non-linear loads are applied and also leads to higher cost and maintenance. In this work the reactive power compensation for non-linear load was proposed by using STATCOM[1]. In this system single DC link capacitor is used for compensation. The capacitor will acts as an input for an inverter. By varying the pulse width of the inverter the compensation was achieved. STATCOM is one of the FACTS family device which recently used for reactive power compensation. In STATCOM only one capacitor and reactor are used for reactive power compensation. Normally the reactor acts as a filter for the inverter and the capacitor acts as the input for the inverter. STATCOM is operated as a shunt connected static VAr compensator based on voltage source converter whose capacitive and inductive output current can be controlled in synchronization with the grid. Here the closed loop control of STATCOM is achieved by using PI controller. STATCOM is to be able to exchange reactive power with the ac power network (i.e., to a value high enough for the STATCOM to be able to produce ac voltage at the value required). The voltage across the capacitor is maintained at the required value by continually adjusting the magnitude and polarity of the active component of the current at the ac side of the STATCOM. When the DC voltage across the capacitor needs to be increased, the STATCOM adjusts the magnitude and polarity of the active component of the current flowing through its ac

side so that active power is drawn from the ac power system and converted to dc power in order to charge the capacitor[2].

.

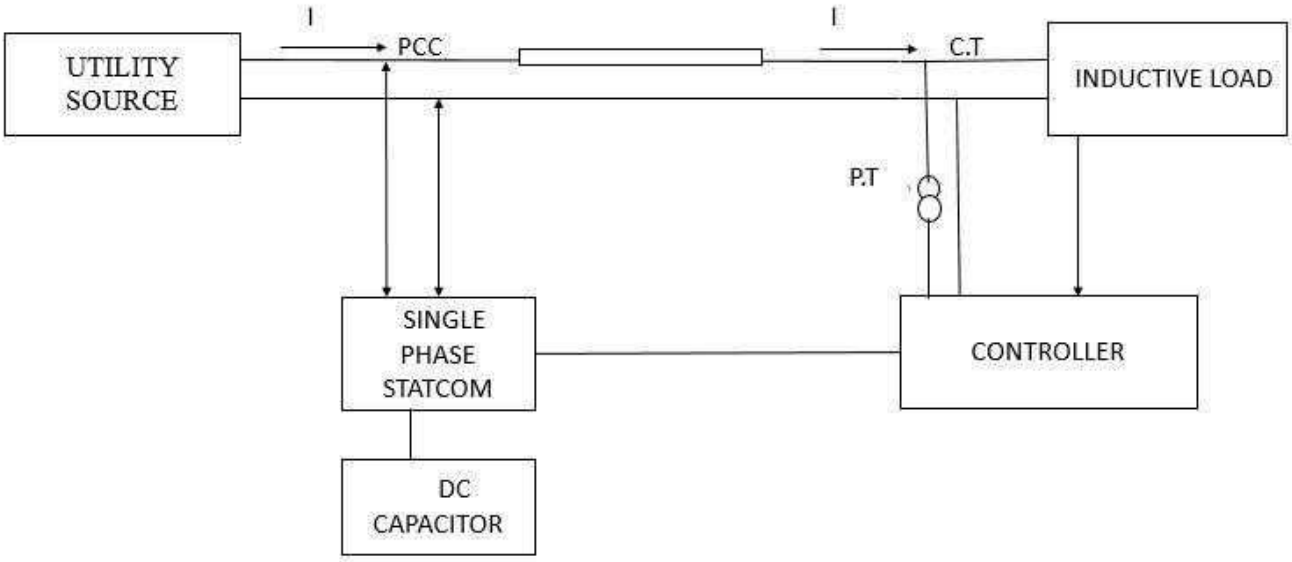

Figure 1: Block Diagram of STATCOM

II. REACTIVE POWER

The work producing power, measured in watts (W), or kilowatts (kW) is considered to be the real power. Real power produces the mechanical output of a motor. Reactive power is not used to do work but it is needed to operate apparatus and is measured in Volt-Amperes-reactive (VAr) or (kVAr). If the load is pure resistive, then it doesn"t need any reactive power. However, most of the loads are not purely resistive. They may be moreover inductive or capacitive in nature. For this type of loads, reactive power compensation is required.

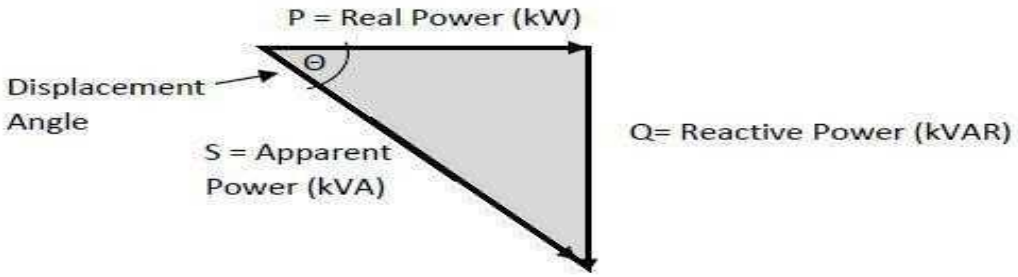

Fig. 2 Power triangle

From the power triangle, it is clearly known that consumption of reactive power decreases, as the apparent power equals the real power. Thus, the total consumption of apparent power by the load is also reduced. It reduces the payment of the bill in HT service connection (two part Tarrif).

A. Voltage Source Converter (VSC)

A voltage-source converter is a power electronic appliance, which generates a sinusoidal voltage with any essential magnitude, frequency and phase angle. Voltage source converters are widely used in adjustable speed drives, but can also be used to mitigate voltage sags. The VSC is used either to totally change the voltage or to add the missing voltage in the transmission line. The „missing voltage" is the difference between the nominal voltage and the actual voltage. The converter is generally based on various kind of energy storage, which will supply the converter with a D.C voltage. The solid state electronics base converter is then switched to get the preferred output voltage. Generally the VSC is utilized for voltage sag/swell mitigation, but also used for power quality issues like flicker and harmonics that are produced in network ac system [3].

A STATCOM is a device that compensates the reactive power and provide and the voltage support to an ac system. Due to the advance of technique of power electronics devices, VSC-based converters have been progressively used in STATCOM system[4]. The normal VSC-based STATCOM consists of a voltage source converter, linked to an energy storage device (DC capacitor) on one side and maintain AC power system on the other-hand, and a control system based on the conventional method with scheme controller.

III. PROPOSED SIMULATION RESULTS

Figure 3. shows the simulation model of single phase load for 1000 w

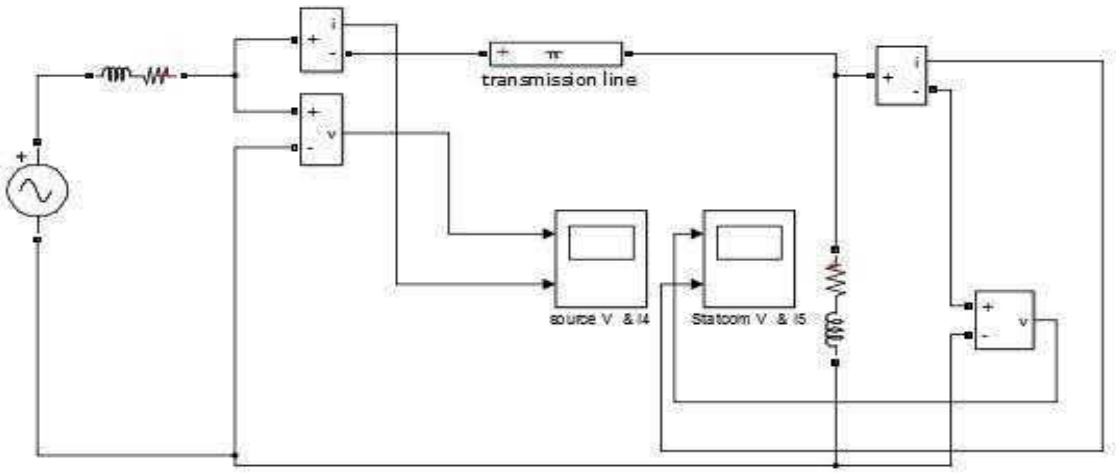

Figure 3 Single phase load system before compensation

Fig.4 shows the output voltage and current waveform for source side before compensation

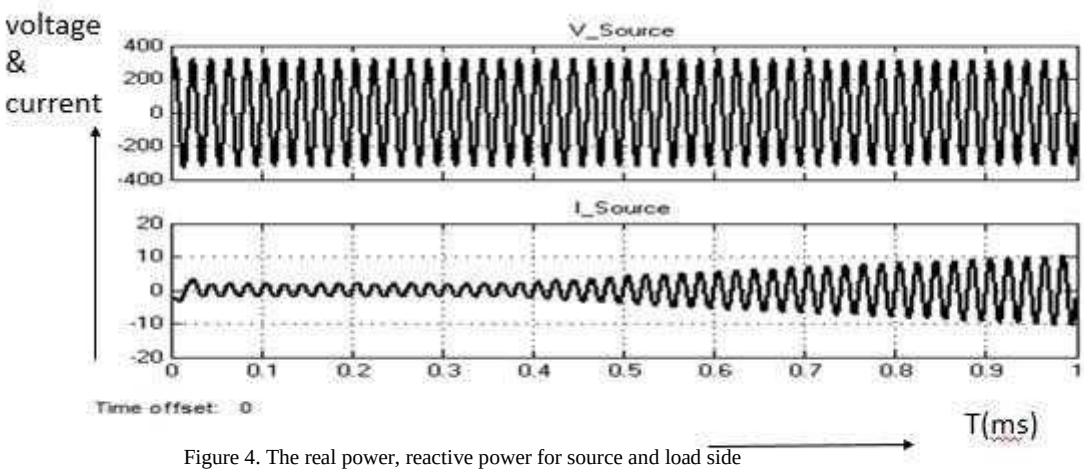

Figure 4. The real power, reactive power for source and load side

Figure 5 shows the real power, reactive power for source side and load side before compensation

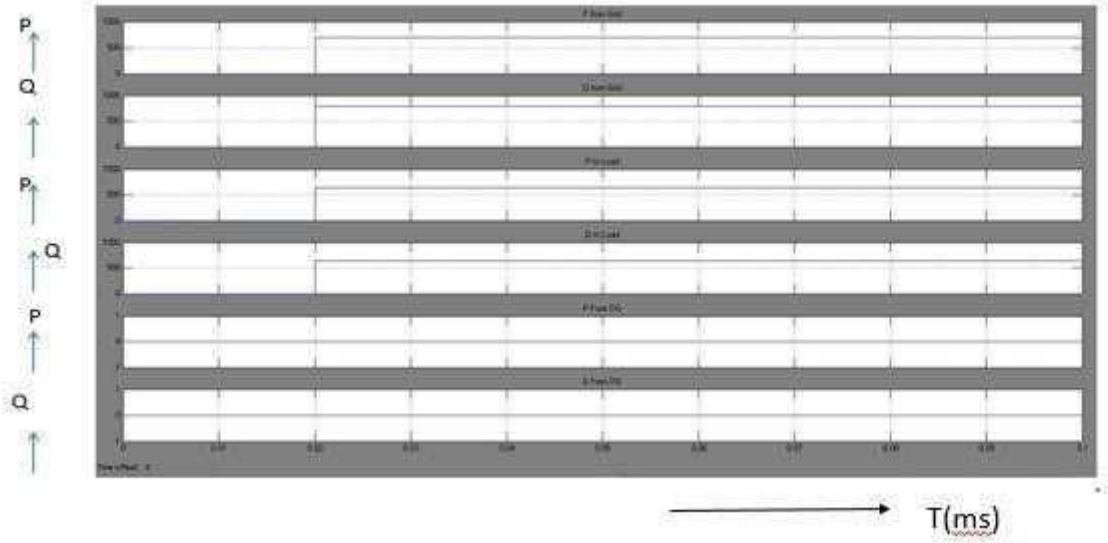

Fig 5. Real and reactive power for source side before compensation

From the source the power is delivered to load through transmission line at that condition reactive power compensated for the 1000 W load. Power quality is decreased due to the more inductive load usage in the distribution system

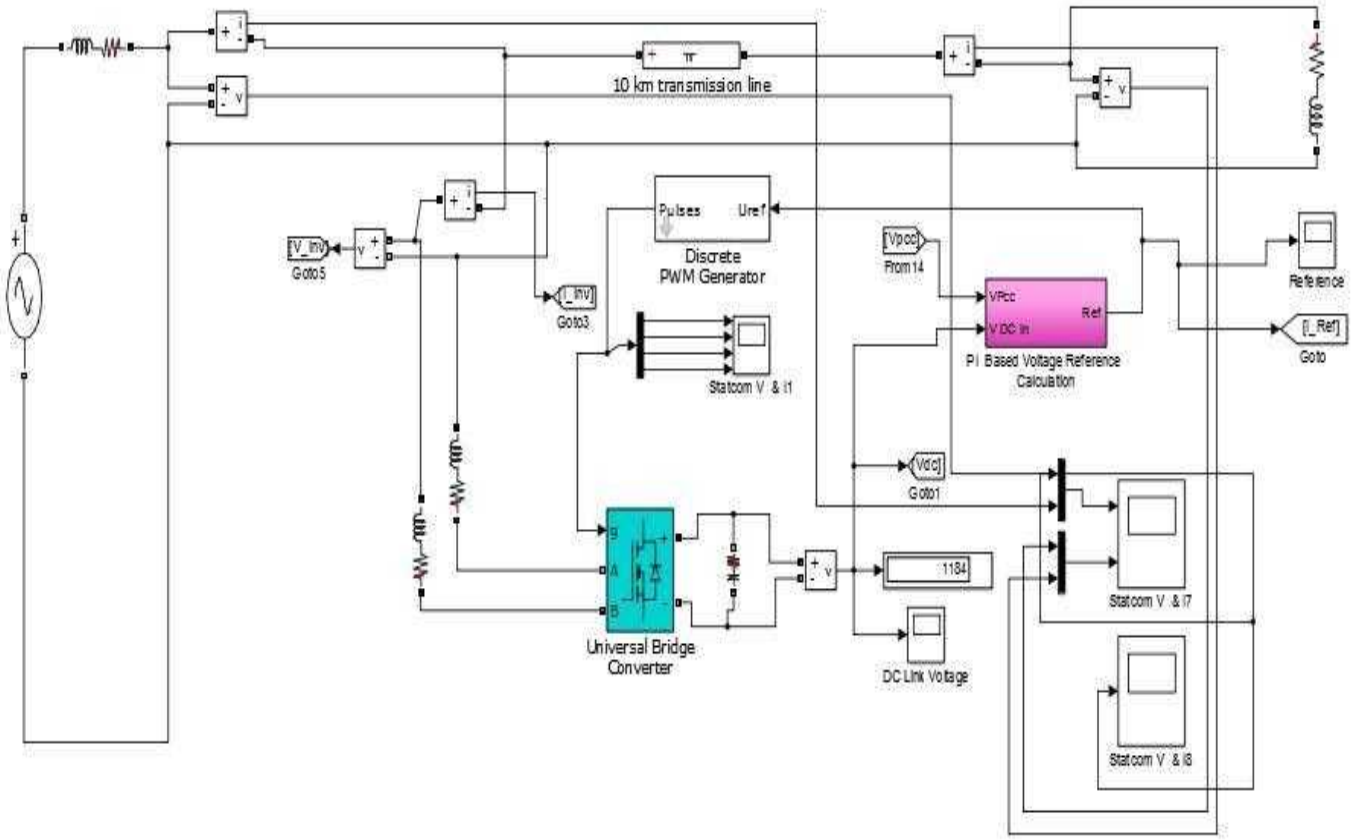

Fig 6.Simulationmodel of proposed work

When utility source is injecting the power to the load then the reactive power demand takes place in the distribution system due to the inductive nature of load[5]. By measuring the reference voltage by PI controller, and by minimizing the error, the conduction pulse width of inverter switches are controlled for reactive power injection in the line by the STATCOM. The Power factor is maintained as unity at the generation side of the distribution system. So the utility does not need to take care of or deliver the reactive power to the load"s VAr demand. STATCOM injects the required reactive power to the distribution system to improve the power factor, voltage stability.

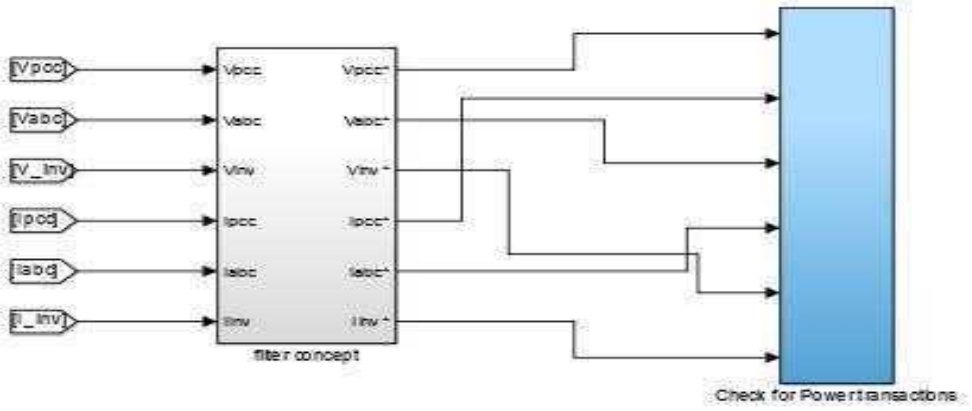

Fig 7 The source side and load side, STATOM side real power, reactive power and power factor values

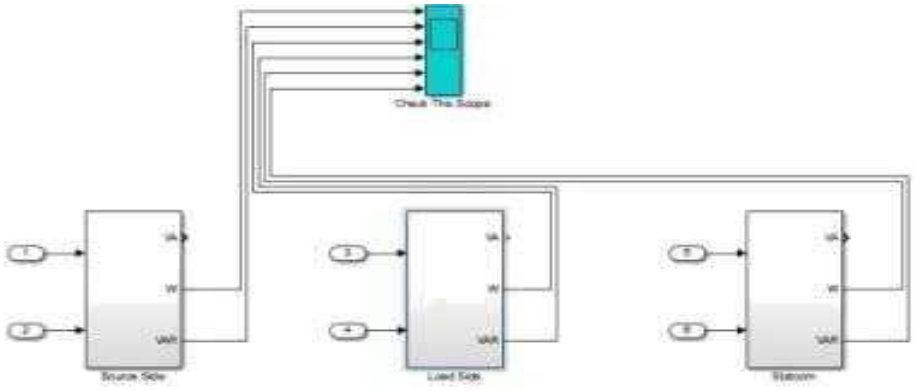

Figure 8 shows the PI control with error comparator

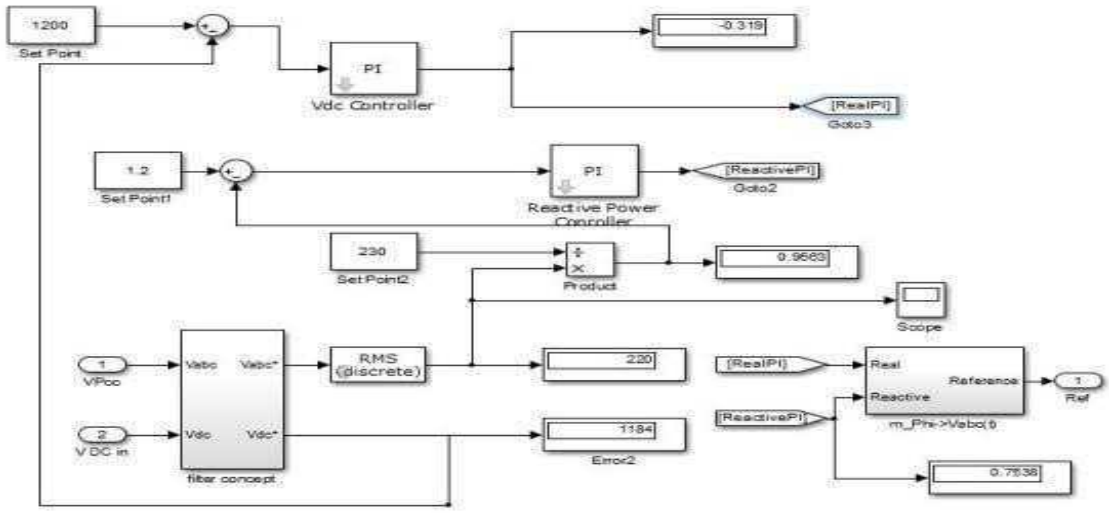

Fig 8.Pi measurement for STATCOM after compensation

Figure 9 Shows the output voltage &current waveform for source and load side

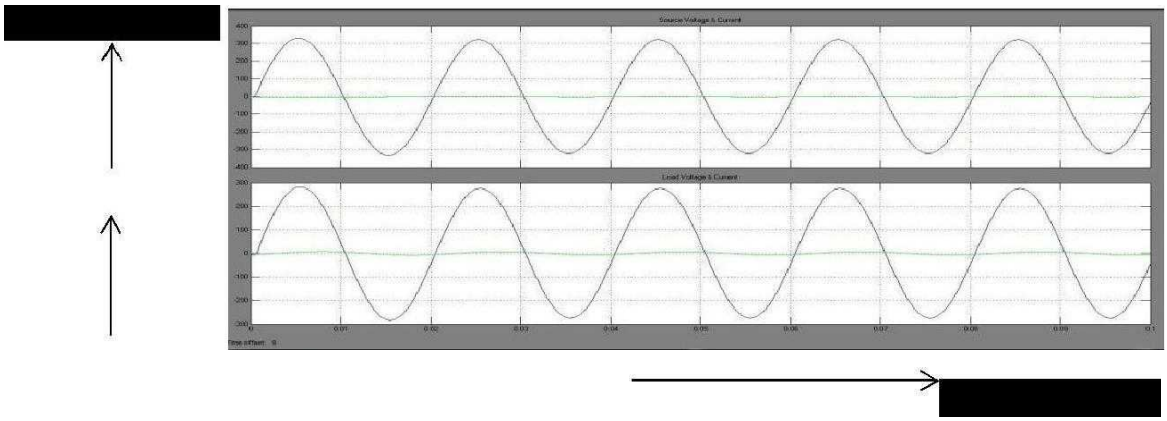

Fig 9. Shows the voltage and current waveform of the utility side after reactive power compensation. Here the waveform of voltage and current are in phase with each other, which shows the power factor of the system is unity.

Figur10. waveform after compensation

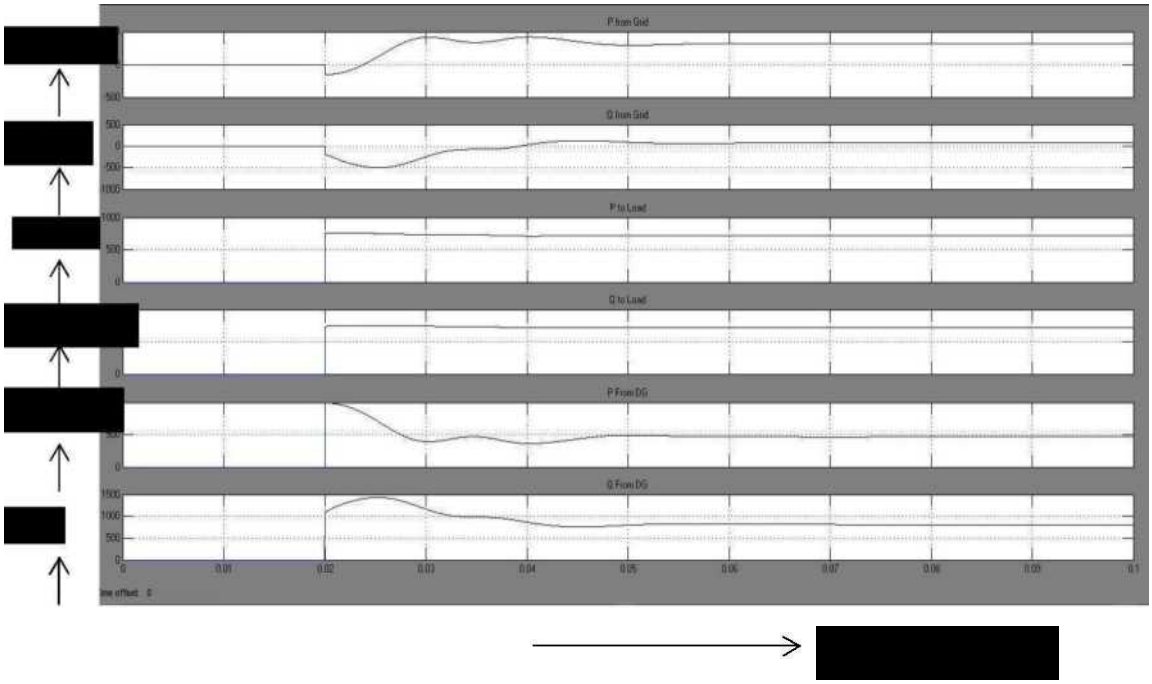

Fig 10. output waveform for the real power and reactive power for the source side ,load side and the STATCOM after compensation

Power is delivered from source side to load side in the transmission line. At that condition inverter which is consuming the real power from the transmission line and inject the reactive power to the distribution system with the system[6]. STATCOM is injecting the reactive power for the load of 1000W.

IV.CONTROLLER

The main aim is to retain the constant voltage magnitude at the point where the sensitive/critical loads are connected, in a distribution system under the system disturbances. The control system measures the RMS voltage at the load point. The VSC switching strategy is based on a sinusoidal PWM technique which offers simplicity and good response to the ac system. Since custom power device is used for low-power application the high switching frequencies can be used to improve the efficiency of the converter and to reduce the size of the filter at the output of the STATCOM, without significant switching losses. The control condition for the compensator which defines the way the output of the VAr originator has to be varied to increase power flow and to stabilize specific parameter of the Power system[7]. Power system network faces contingencies and dynamic disturbances difficulty.

The controller‟s input is an error signal obtained from a voltage comparator which compares the reference

voltage and RMS value of STATCOM output. The error signal is processed by a PI controller the output is the angle which provides the PWM indicate generation[8]. The active and reactive power exchange with the network simultaneously an error signal obtained by comparing the reference voltage with the RMS voltage measured at the load point. PI controller produces the error signal generate the required angle to make the error to zero, i.e., the load RMS voltage is brought support to the reference voltage. The voltage and reactive power value are compared in PI controller and error signal is calculated and minimised. The signal from controller is given to the hysteresis control to compare the input current and reference current and to adjust the dc voltage to remain as constant[9].

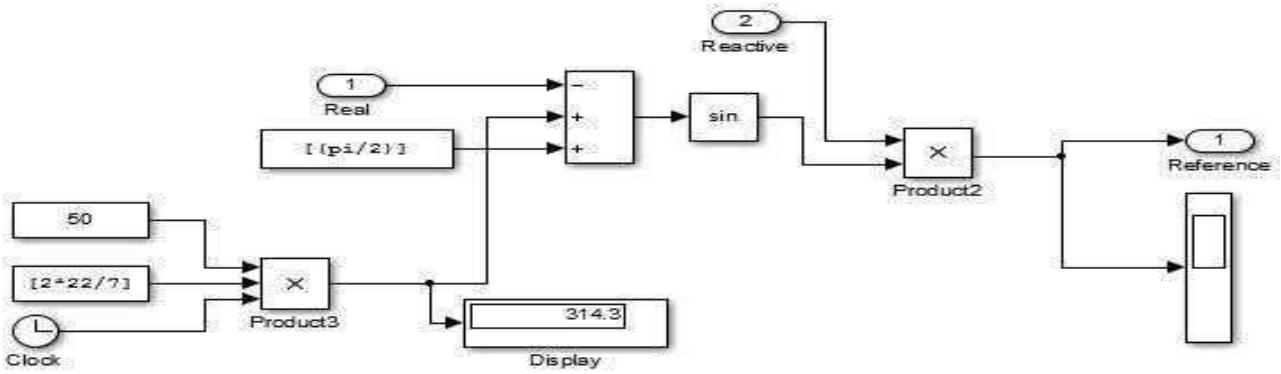

Fig 11 shows the THD analysis before compensation

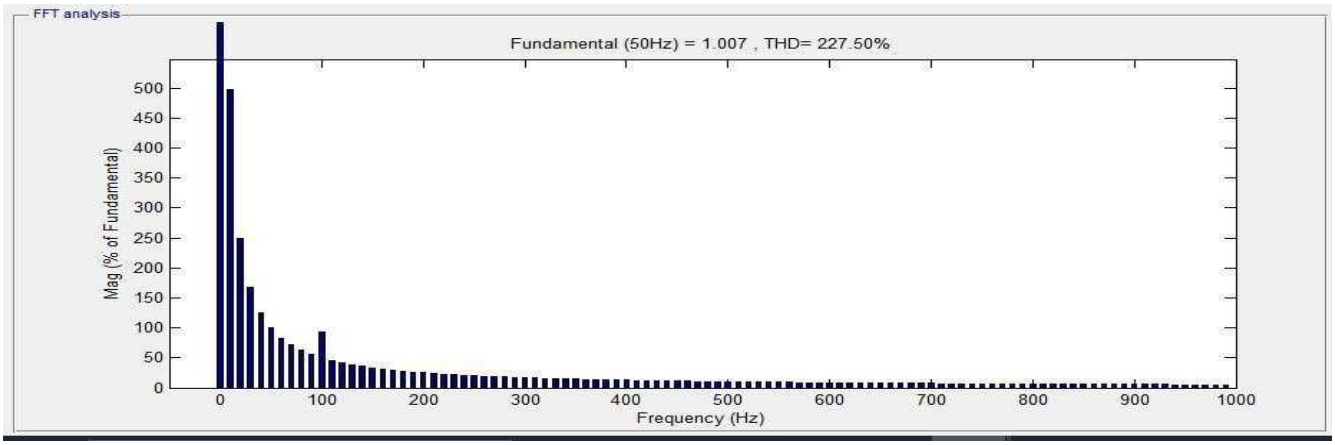

Fig 11 THD analysis before compensating reactive power

Fig 12 shows the THD analysis after compensation the stability of the power which is improved at the distribution system[10]

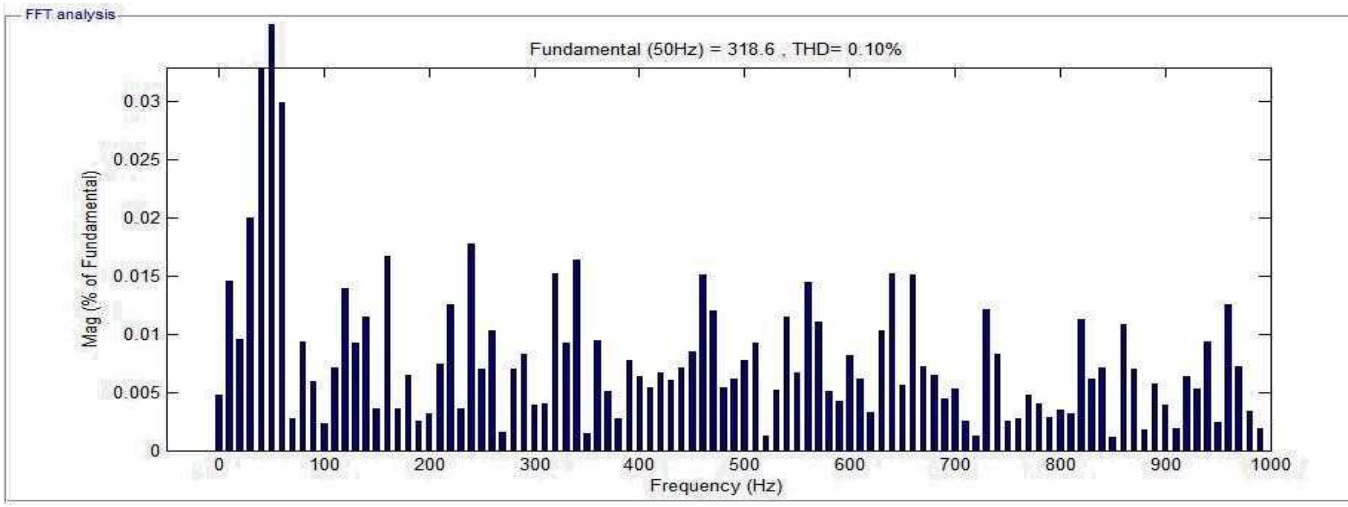

FIG 12 THD measurement after compensating the reactive power

Harmonics	THD
Before compensation	227.50
After compensation	0.10

Tables I and II show the parameters of real power, reactive power, voltage and current on the source side, load side and converter side. Table I shows the values before compensation and Table II shows the values after compensation.

TABLE I.PARAMETER BEFORE COMPENSATION

	Real power (Watts)	**Reactive power(VAr)**	**Power factor**
Source	701.33	791.72	0.6634
Load	639.26	639.26	0.7071

From the above table the real and reactive power consumed by the load was supplied only by the utility. This results in low power factor on the utility side.

TABLE II. PARAMETER AFTER COMPENSATION

	Real power(Watts)	**Reactive power(VAr)**	**Power factor**
Source	1617.53	658.61	0.9978
Load	658.61	668.80	0.707
STATCOM	884.02	719.34	0.7757

From the above table the real and reactive power consumed by the load was supplied by the STATCOM .This results in unity power factor on the utility side.

VI CONCLUSION

In this study the reactive power compensation for single phase distribution system with RL load has been implemented using a single phase shunt connected voltage source converter [VSI]. The VSI is made to act as the STATCOM by maintaining the DC Voltage level across the D.C input side of the VSI. A separate control logic are implemented to draw a mild amount of real power(p) from the grid itself to charge the D.C capacitor, STATCOM as rectifier and separate control strategies are involved to make the STATCOM to work as reactive current source in to and from direction with respect to grid and STATCOM (as reactive power compensator).The shunt connected VSI may also be extended to mitigate harmonics also. The MATLAB-SIMULINK work is done for a capacitor of 1000 WATTS. Here 1000 W RL load has been taken. The reactive power compensated using STATCOM and the power factor which is maintained as unity. The load required 720 VAr reactive power is delivered from STATCOM not from source. Closed loop PI controller has been developed for improving the power factor and compensate the reactive power. So the quality of the input power was improved in the EB side.

ACKNOWLEDGEMENT

The author are grateful to the management and the Head of the institution of Kalasalingam University ,for giving all the necessary support and providing facilities for making this reseach paper a successful

REFERENCES

[1]. Arvindpahade and nitinsaxena "Transient stability improvement by using shunt FACT device (STATCOM) with Reference Voltage Compensation (RVC) control scheme"International Journal of Electrical, electronicsissn No. (Online) : 2277-2626and Computer Engineering 2(1): 7- 12(2013)

[2]. P. S. Sensarma, K. R. Padiyar, V. Ramanarayanan" Analysis and Performance Evaluation of a Distribution STATCOM for Compensating Voltage Fluctuations" IEEE TRANSACTIONS ON POWER DELIVERY, VOL. 16, NO. 2, APRIL 2001

[3]. Dongshen and P. W. Lehn ,Modeling, "Analysis, and Control of a Current Source Inverter-Based STATCOM"" IEEE TRANSACTIONS ON POWER DELIVERY, VOL.17, NO. 1, JANUARY 2002

[4]Yiqiao Liang, C. O. Nwank ,,"A New Type of STATCOM Based on Cascading Voltage-Source Inverters with Phase-Shifted Unipolar SPWM" IEEE TRANSACTIONS ON INDUSTRY APPLICATIONS, VOL. 35, NO. 5, SEPTEMBER/OCTOBER 1999

[5]. Clark Hochgraf , Robert H. Lassete "Statcom Controls for Operation with Unbalanced Voltages**"**IEEE Transactions on Power Delivery, Vol. 13, No. 2, April 1998

[6]. L.T. Moran, P.D. Ziogas, G. Joos, Analysis and design of a threephase synchronous solid-state VAR compensator. IEEE Trans. Indus. Appl. 25(4), 598–608 (1989)

[7]. C. Schauder, H. Mehta, "Vector analysis and control of advanced static VAR compensator". IEEE Proc. Gener. Transm.Distrib. 140(4), 299–306 (1993)

[8]. G. Joos, L.T. Moran, P.D. Ziogas, "Performance analysis of a PWM inverter VAR compensator". IEEE Trans. Power Electr. 6(3), 380–391 (1991)

[9]B.S. Chen, Y.Y. Hsu, A minimal harmonic controller for a STATCOM. IEEE Trans. Indus. Electr. 55(2), 655–664 (2008)

[10]S. Mori, K. Matsuno, M. Takeda and M. Seto, "Development of a Large Static VAR Generator Using Self-Commutated Inverter For Improving Power System Stability,"IEEE Trans. Power Systems, Vol. 8, NO. 1, pp. 371-377 Feb. 1993

ENERGY BASED RELIABILITY INDEX - A TUTORIAL

K. Karthikeyan[1], S. Kannan[2], C. Thangaraj[3]

[1,2]Department of EEE, Ramco Institute of Technology, Rajapalayam
[3]Vice-Chancellor, Vignan University, Andhra Pradesh

Abstract:

It is imperative that, all power system planners must use a scientific method to calculate the reliability of the power system of the present one and the proposed system for the future. In early days, the percentage reserve or the largest unit as the reserve is used as reliability criteria. The Loss of Load Probability (LOLP) is one of the popular reliability index. Energy Not Served (ENS) or the Expected Energy Not Served (EENS) is another probability index, which reflects the probable energy which cannot be served to the customers is a better index for the Power system planners. In this paper, a detailed study of the existing methods and of the Equivalent energy function method (EEF) for calculating Expected Energy Not Served (EENS) is done. The EEF method completes Convolution and de-convolution by employing electric energy directly so that probabilistic modelling is considerably simplified. The EEF method is not only more efficient than any other method available in this topic, but also more flexible in treating assigned energy units. An approximate deconvolution algorithm and a LOLP formula are also explained which enable the carrying out a probabilistic modelling to be even faster. Numerical examples also demonstrated that the algorithm presented in the paper is simple, efficient and more accurate. This paper will be useful for Master students and researchers for understanding and application this method for reliability evaluation.

***Key words*:** Expected energy not served (EENS), Equivalent energy function method (EEFM), Reliability index, Loss of load probability (LOLP) and Loss of load expected (LOLE)

I. INTRODUCTION

At present, power system probabilistic modelling is widely used in utilities. Probabilistic modelling is an important tool to analyse technical and economic properties of a power system. The primary purpose of probabilistic modelling is to simulate the dispatch of generating units and to stimulate the production cost [1]. The basic task of probabilistic modelling is to calculate the electric energy generated by each unit, to get system reliability indices. In generating system reliability analysis, this is measured by, two fundamental indices, i) Probabilistic indices and ii) Energy-based indices [2].

The probabilistic indices are loss of load probability (LOLP) and loss of load expected (LOLE). The energy based indices are loss of energy expected (LOEE) and energy interruption rate (EIR). This LOEE is also called as expected energy not served (EENS).

Utilization of EENS is now increasing, since it reflects the true risk and has more physical significance than LOLP or LOLE. It is now accepted that EENS is more meaningful in both system planning and system operation.

The techniques used for EENS evaluation can be broadly classified as analytical and simulation techniques [3]. In this paper we consider only the analytical techniques since EEF method is analytical in nature.

Probabilistic modelling is usually required to be carried out many times in a power system reliability evaluation. Therefore, it is crucial to develop a probabilistic modelling algorithm which gives sufficiently

precise results within a reasonable computational time. Roy Billinton recursive table method [1] and C.Singh's mean capacity outage table method are such techniques [4].

The method of cumulants [5] is several times faster than the numerical techniques and can easily handle multi block representation of units. But for small systems or those with low forced outage rates, the cumulant method can have limited accuracy [6].

Equivalent load duration curve method, another technique struggles to handle the daily load shapes with flat peak and minimum load [7]. The ELDC is represented by function values at discrete points, on which the convolution and deconvolution formulae are applied the amount of computation is rather high even for a small system.

Another technique based on the moments called segmentation method [8], [9] seriously lacks in producing accurate results and also computational efficiency is very poor.

EEF approach enables us to implement convolution and deconvolution by directly using electric energy, so that probabilistic modelling is considerably simplified [3], [10].

This paper will illustrate that EEF approach is not only more efficient, but also more flexible to treat assigned energy units in probabilistic modelling.

II. EQUIVALENT ENERGY FUNCTION METHOD

In this method, the operations are done on electrical energy rather than load. If we know electric energy consumed in different load level segments and can directly modify it when unit failure effects are taken into consideration, then we will easily carry out a probabilistic modelling. This is the main idea of EEF approach.

A load duration curve can be described by,

$$t = F(x) \tag{1}$$

where x is load level (in MW or per unit), and t is the time interval during which the load is larger than or equal to x. Assume the investigation period is T.

Dividing both side of Eq. (1) by T, we have load duration curve's probability distribution

$$p = \frac{F(x)}{T} = f(x) \tag{2}$$

where p will be considered as the probability at which the load is larger than or equal to x.

A discrete energy function can be defined as follows based on dividing the abscissa into divisions of Δx:

$$E(J) = \int_x^{x+\Delta x} F(x)dx = T \int_x^{x+\Delta x} f(x)dx \tag{3}$$

where,

Δx = greatest common factor of all generating unit capacities.

$J = \langle {}^{x}/_{\Delta x} \rangle + 1$ (4); <> means an integer not greater than x/Δx.

E (J) correspond to the area under a section of the load curve from x to Δx, or the energy that corresponds to this section of load.

If X_{max} is maximum load, then its discrete variable is,

$$N_E = \langle {}^{X_{max}}/_{\Delta x} \rangle + 1 \tag{5}$$

Let the generating unit *i* is having a capacity of c_i and forced outage rate (FOR) of q_i. The Equivalent Load Duration Curve (ELDC) f(x) can be represented as,

$$f^i(x) = p_i f^{(i-1)}(x) + q_i f^{(i-1)}(x - c_i) \tag{6}$$

From equation (3) and (5)

$$E^i(J) = T \int_x^{x+\Delta x} \left[p_i f^{(i-1)}(x) + q_i f^{(i-1)}(x - c_i) \right] dx \tag{7}$$

$$E^i(J) = p_i E^{(i-1)}(J) + q_i E^{(i-1)}(J - K_i) \tag{8}$$

where

$K_i = c_i/\Delta x$; Δx should be selected as a common factor of all unit capacities, so that K_i is always an integer.

The load in the interval (1, J_i) has been shared by proceeding unit *i* generating units when generating unit *i* has been committed. The load energy not served by the systems is,

$$E_{Di} = \sum_{J > J_i} E^i(J) \tag{9}$$

If we consider n generating units, then EENS is given by

$$E_{Dn} = EENS = \sum_{J > J_n} E^n(J) \tag{10}$$

III. CASE STUDY

For step by step illustration of the equivalent energy function method we calculate EENS for a small sample System given in [3]. The test system consists of three identical 40 MW units and their forced outage rate is 0.1; for the load model, we take the hourly load for the period of 8 hours. The load data are given in table 1.

Table 1: Load data for sample system

Hour	1	2	3	4	5	6	7	8
Load (MW)	20	50	80	90	70	80	60	30

Step 1: The load duration curve is plotted as shown in Figure 1.

Step 2: In this example, segment size Δx is chosen as 40 i.e. the maximum common factor of the capacity of all units (or) simply the capacity of the smallest unit 40 MW.

Step 3: Segmenting the load model leads to three levels and their areas i.e. energy within particular segment is calculated. The energy in each segment is 290 MW, 180 MW and 10 MW (from base load to peak load).

Step 4: $J_n = \frac{Total\ Capacity}{\Delta x} = \frac{3 \times 40}{40} = 3$ and $N_E = \langle \frac{X_{max}}{\Delta x} \rangle + 1 = \langle \frac{90}{40} \rangle + 1 = 3$.

Therefore J value varies from 1 to J_n + N_E i.e., 1 to 6.

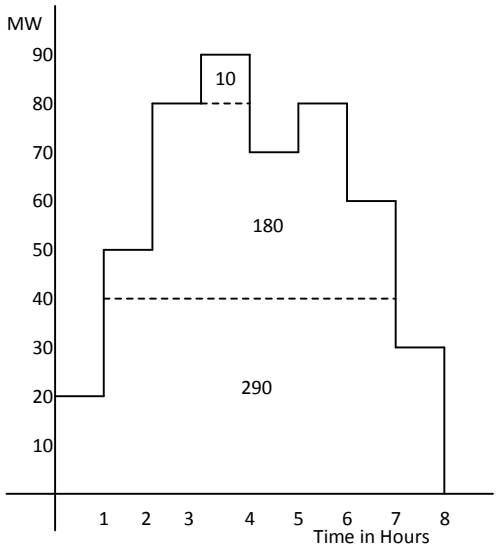

Figure 1. Load Model

Step 5: The Table 2 is formed for 6 J entities and the calculated areas are taken as $E^0(J)$.

Table 2 Unserved Energy Calculation

J	$E^0(J)$	$E^1(J)$	$E^2(J)$	$E^3(J)$
1	290	290	290	290
2	180	191	200.9	209.81
3	10	27	43.4	59.15
4	-	1	3.6	7.58
5	-	-	0.1	0.45
6	-	-	-	0.01

Step 6: The value for the K is calculated as, $K_1 = \frac{c_1}{\Delta x} = \frac{40}{40} = 1$. Similarly K_2 and K_3 also equal to 1.

Step 7: The $E^1(J)$ is calculated based on the equation (8) and it is written as,

$$E^1(J) = p_1 E^{(1-1)}(J) + q_1 E^{(1-1)}(J - K_1)$$
$$E^1(J) = 0.9 \times E^0(J) + 0.1 \times E^0(J - 1)$$

For J = 1

$$E^1(1) = 0.9 \times E^0(1) + 0.1 \times E^0(0)$$
$$E^1(1) = 0.9 \times 290 + 0.1 \times 290$$
$$= 290.$$

It is taken that $E^0(0) = E^0(1)$ for calculation and the result is entered in Table 2. Similarly for other J values also results are calculated and entered in Table 2.

Step 8: Step 7 is repeated for the calculation of $E^2(J)$ and $E^3(J)$ and the results entered in Table 2.

Step 9: As per equation (10)

$$EENS = \sum_{J>3} E^3(J)$$
$$= E^4(J) + E^5(J) + E^6(J)$$
$$= 7.58 + 0.45 + 0.01$$
$$= 8.04 \text{ MWh}$$

CONCLUSION

A detailed study of the equivalent energy function method for calculating the EENS was made. The study shows that the EEF was the most efficient and accurate. It was also quite fast. From the given example we infer that the method can be easily understandable and easily applied to multistate models also. The equivalent energy function method is the most simple and direct method and the computational efficiency is superior to all the other methods. This tutorial will help the young researchers working in the area of Power system planning and Generation Expansion planning.

ACKNOWLEDGEMENT

The authors are grateful to the Management of Ramco Institute of Technology, Rajapalayam and Vignan University, Guntur, Andhrapradesh, for giving all necessary support and providing facilities for making this research paper a successful one.

REFERENCES

1. R. Billinton and R.N. Allan, "Probabilistic assessment of power systems", Invited paper, proceedings of the IEEE, Vol. 88, Feb 2000.
2. R. Billinton and R.N. Allan, "Reliability evaluation of power systems", Longman, London, Plenum Publishers, New York, 1984.
3. Xifan Wang, Jim Mc Donald, "Modern power system planning", McGraw-Hill International Edition-1994.
4. C. Singh et. al, "A concise method for calculating Expected Unserved Energy in generating system reliability analysis", IEEE trans. on power systems, vol. 6, Aug 1991.
5. N.S. Rau, P. Toy, K.F. Schenk, "Expected energy production costs by the method of moments", IEEE Transactions on PAS, Vol. PAS.99, no-5, pp-1908-1917, Sep-Oct 1980.
6. P.S. Nellakanta, M.H. Arsali, "Integrated resource planning using segmentation method based dynamic programming", IEEE trans. on power systems, vol-14. Feb 1999.
7. K.F. Schenk Q. Ahsan, S. Vassus, "Evaluation of production costs of two interconnected electric power systems research", 8 [1984/85] 143-154
8. Duran. H, "A recursive approach to the cumulant method of calculating reliability and production cost", IEEE Transactions on PAS, vol. PAS -104, pp. 82-90, Jan 1987.
9. J. P. Stremel, R. T. Jenkins , R. A. Babb, W. D. Bayless, "Production Costing Using the Cumulant Method of Representing the Equivalent Load Curve", IEEE TRANS, Vol. PAS-99, M 5, 1980.
10. Xifan Wang, "Equivalent energy function approach to power system probabilistic modelling", "IEEE transactions on Power System, vol. 3, No. 3, pp. 823 – 829, August 1988.

PET IMAGE RECONSTRUCTION USING ANN-RBF

[1]P.Shanmugapriya
Department of EEE
Kalasalingam University
Virudhunagar,
Tamilnadu,India
shanpriya3791@gmail.com

[2]Mr.T.Arun Prasath
Department of ICE
Kalasalingam University
Virudhunagar,
Tamilnadu,India
arun.aklu@gmail.com

[3]Dr.M.Pallikonda Rajasekaran
Professor and Head of the
Department of ECE
Kalasalingam University
Virudhunagar,Tamilnadu,India
mpraja80@gmail.com

[4]Dr.S.Kannan
Professor and Head of the
Department of EEE
Ramco Institute of Technology
Virudhunagar,Tamilnadu,India
kannaneeeps@gmail.com

***Abstract*— This paper addresses a non-linear PET image reconstruction using artificial neural network-radial basis function (ANN-RBF). In preceding years, the analytical approach was used to reconstruct the Positron Emission Tomography (PET). This advancement requires a minimization of a convex cost function and accompanied by many problems related to the computational complexity. The poles apart iteration methods are MAP, MLEM and OSEM. It has various compensation compared to predictable approach. This statistical way can provides better and high PSNR along with NAE and RMSE lowest Value in the PET image. An concoction of image quality parameters is regarded to analyze the PET image in this algorithm . The PET image is constructed and simulated in MATLAB /Simulink package.**

***Index Terms* — PET images, Image quality, Image reconstruction, Radial Basis Function (RBF)**

I. INTRODUCTION

Positron emission tomography (PET) is a nuclear medical imaging technique for quantitative measurement of physiologic parameters in vivo based on the detection of small amounts of positron emitter labelled biologic molecules. Proceeding to the scan, the subject is inserted with a trace amount of a harmful compound that consists of an enzyme catalyst attached with an atom with an unstable nucleus. The compound is administered into the vein and socializes in the blood until it is removed by cells that absorb the compound. Henceforth, by selecting the appropriate compound, PET images can have very high quality of being specific. The usage of trace quantities of the compound guarantees that it has no physiological or biochemical changes in the body produced by a drug in therapeutic concentration on the subject. Every destructive nuclide degenerates by the emanation of a positive electron, or positron that increasingly loses energy in the surrounding tissue until it overwhelms with an electron and gives rise to two photons that travel in conflicting ways. This procedure is called Positron Emission Tomography. Image reconstruction is the creation of a two- or three-dimensional image from scattered or incomplete data such as the radiation readings acquired during a medical imaging study. For some imaging techniques, it is necessary to apply a mathematical formula to generate a readable and usable image or to sharpen an image to make it useful. Image reconstruction is the process of getting original image from the projection of object. Restoration quality is analyzed quantitatively in terms of Peak Signal to Noise Ratio (PSNR), Normalized Absolute Error (NAE) and Root Mean Square Error (RMSE).

II. RELATED WORKS

Dynamic positron emission tomography (PET) is a molecular imaging technique that is used to monitor the in vivo spatio-temporal distribution of a radio labeled tracer. Dynamic imaging provides richer information than conventional static PET imaging and has the ability to generate quantitative information about physiological parameters through the identification of kinetic or compartmental models[1]. Image reconstruction in positron emission tomography (PET) uses the collected projection data of the object/patient under examination. Until recently, image reconstruction in commercial clinical PET systems has been performed with analytical reconstruction algorithms based on the filtered back projection method (FBP) [2]. The radial basis function (RBF) neural network architecture is a special type of ANNs that has certain advantages over other network types, including simpler network configurations, faster training procedures, and better approximation capabilities. Surprisingly, not many uses of the RBF architecture have been reported in the literature in solving image classification problems [3]. Accurate system modeling in tomographic image reconstruction has been shown to reduce the spatial variance of resolution and improve quantitative accuracy. System modeling can be improved through analytic calculations, Monte Carlo simulations, and physical measurements. The purpose of this work is to improve clinical fully-3-D reconstruction without substantially increasing computation time [4]. Magnetic Resonance Imaging (MRI) is a noninvasive and nonionizing imaging technique. Offering a variety of contrast mechanisms, it enables excellent visualization of both anatomical structure and physiological function. Owing to these advantages, MRI is one of the major diagnostic imaging modalities A variety of MR techniques therefore aim to reduce the number of data required for accurate reconstruction. [5]. Scatterometer image reconstruction as the inversion of a discrete noisy aperture-

filtered sampling operation. Aperture-filtered sampling is presented and contrasted with conventional and irregular sampling. A reconstruction estimator based on maximum a posteriori (MAP) estimation is proposed to recover the conventional samples from noisy scatterometer measurements[6]. Intravascular photoacoustic (IVPA) imaging is a technique for visualizing atherosclerotic plaques with differential composition. Unlike conventional photoacoustic tomography scanning, where the scanning device rotates around the subject, the scanning aperture in IVPA imaging is enclosed within the imaged object [7]. Reconstruction of a 3-D face model from a single 2-D face image is fundamentally important for face recognition and animation because the 3-D face model is invariant to changes of viewpoint, illumination, background clutter, and occlusions. Given a coupled training set that contains pairs of 2-D faces and the corresponding 3-D faces, we train a novel coupled radial basis function network (C-RBF) to recover the 3-D face model from a single 2-D face image[8]. In positron emission tomography (PET), 3D iterative image reconstruction methods have a huge computational burden. In this paper, we developed a list-mode image reconstruction method using graphics processing units (GPUs). Efficiency of acceleration for GPU implementation largely depends on the method chosen, where a reduced number of conditional statements and a reduced memory size are required[9].It is well known that the interior problem in 2D image reconstruction is not uniquely solvable. Providing additional information about the object may guarantee that a unique solution exists. we use the Poisson likelihood ML-EM algorithm with a mixed region and voxel based image representation to reconstruct from the interior projection data in a single step[10].

III. METHOD

The neural network is an ANN based on radial function which has a function as an alternative of sigmoid functions of the RBF is an activation function. The distance from a center point C which depends only on the RBF function.

$$f(x)=f(|x-c|) \quad ....(1)$$

An artificial neutral network (ANN) is an arrangement and it is based on the natal neural network, such as the brain. The brain has approximately 100 billion neutrons, which can communicate through the electro-chemical signals. The neurons are connected through junctions called synapses. These biologically inspired methods of computing are consider to be the next main advancement in the computing industry. Yet simple living thing brains are capable of functions that are now not viable for computers. Computers do rote possessions well, like keeping ledgers or performing intricate math. But computers have dilemma in recognizing even effortless patterns much less generalizing individuals patterns of the past into events of the future.

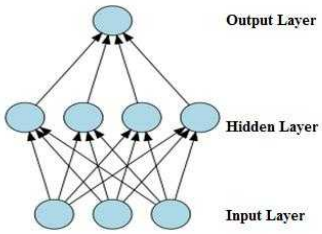

Figure 1: Architechture of ANN-RBF

An artificial neural network is a radial based function network that uses radial basis functions as activation functions. The inputs and neuron parameters gives the output of the network as a linear combination in Radial Basis Function. RBF neural network are used in many application like time series predication and to function estimate. RBF networks have three layers which are input layer, hidden layer and output layer. All the neuron consists of a radial basis function centered on a point with the similar dimensions like the analyst variables. The input layer is prepared of source nodes whose number is identical to the dimension of the input vector . Hidden layer has a erratic number of neurons. The modification from the input space to the hidden layer is nonlinear, while changing to the hidden unit space to the output space is linear.

IV. DEVELOPMENT OF ANN-RBF FOR PET IMAGE RECONSTRUCTION

The different steps that are concerned in the growth of ANN-RBF – based PET image reconstruction are offered below.

A. DATA GENERATION

The improvement in RBF has important steps for accurate training data. This training data analyse the production of RBF and it will characterize the full working system in concern. The RBF has a range of proper input. PET image in image reconstruction comes under system mold, where the pixel values are consider for PET image. The input is given and it is taken out from scanner.

B. DATA NORMALIZATION

Training of the neural network may modify according to their higher valued input variables that contains the influence of smaller ones. Whenever the raw data applied directly to the network, there is a risk of the imaginary neurons attaining the drenched conditions. The changes in the input values will produce a small change or no change in the output value, when the neurons are saturated. This tends to concern the training network to include a great scope. By avoiding the actual application of the neural network, the raw data needs to be normalized.

C. TESTING AND TRAINING

In training and testing, RBF consists of three layers: input layer, hidden layer and output layer. The hidden layer which is tranquil of nonlinear units which are connected directly to all the nodes in the input layer. It has been high sufficient dimension, which serves a different purpose from that in a

multilayer perceptron. Testing has chosen for the proper amount of neurons in hidden layers. A set of input and output vectors are placed in training data.

V. Evaluation Parameters

Discussion of tomographic reconstruction techniques leads to the challenge of determining which method provides the 'best' quality image. Image quality measures the figures of merit used for the estimation of imaging systems. It shows the efficiency of the algorithm and indicates the result.

Peak Signal to Noise Ratio (PSNR) and Mean Square Error (MSE) are used to comparing the squared error between the original image and the reconstructed image. There is an inverse relationship between PSNR and MSE. So a higher PSNR value indicates the higher quality of the image (better). The Peak Signal to noise ratio and mean square error will be calculated as,

$$PSNR = 20 \log (\max N)/\sqrt{MSE} \quad \ldots (2)$$

$$\text{MSE} = \frac{1}{mn}\sum_{i=0}^{m-1}\sum_{j=0}^{n-1}[y(i,j) - \hat{y}(i,j)]^2 \quad \ldots (3)$$

The root mean square error is defined as the root mean square value of the difference between the measured and original image divided by the pixel values.

The NRMSE articulated as a normalized measure of agreement among the reconstructed image ŷ(i,j) and actual image y(i,j). The RMSE and NAE will be calculated by the following equation [5], Normalized Absolute Error (NAE) is a measured from the original image to the decompressed image, with the value of zero as the perfect fit.

$$RMSE = \sqrt{\frac{\sum_{i=1}^{N}(y(i,j) - \hat{y}(i,j))^2}{N}} \quad \ldots (4)$$

$$NAE = \frac{1}{K}\sum_{k=1}^{K}\frac{\sum_{i,j=0}^{N-1} y(i,j) * \hat{y}(i,j)}{\sum_{i,j=0}^{N-1} y(i,j)^2} \quad \ldots (5)$$

The comparison between two digital images can also quantified in terms of the correlation function. These measures the connection between two images, hence they are difference-based measures in balancing.

In above all these equations, y (i,j) is original image; ŷ(i,j) is the reconstructed image.

The time duration required elapsed time in seconds from the process of input image to reconstructed image.

V. Simulation Results

The simulations were achieved using MATLAB-Simulink and verified by using statistical equations. We have chosen PET images in three dimensions for analysis. Figure 2 shows the simulation results using ANN-RBF.

Image quality loss occurs from artefacts depends on background. The functioning of the scanner from the artefacts as well as the context or conditions in which they take place.

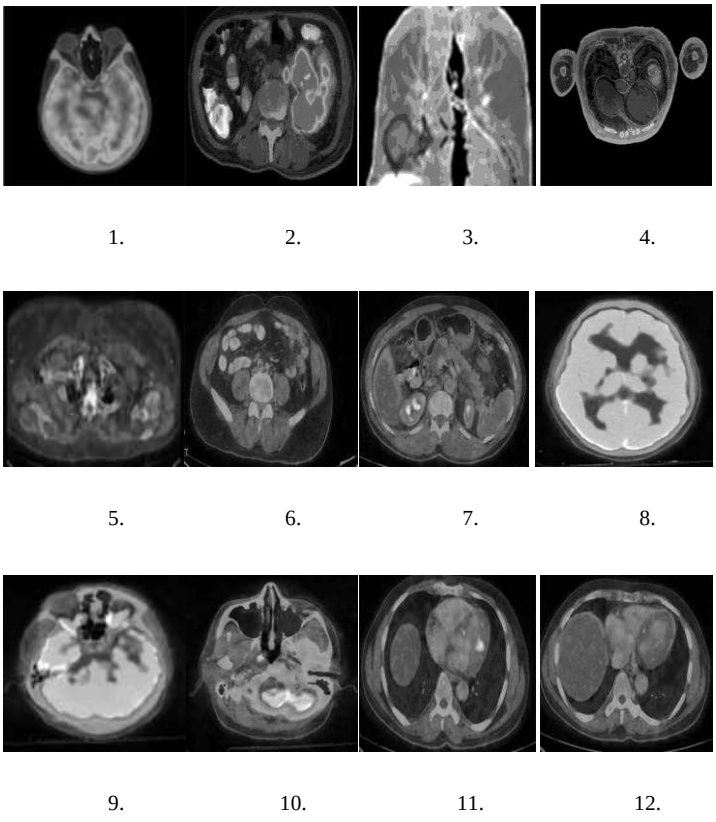

1. 2. 3. 4.

5. 6. 7. 8.

9. 10. 11. 12.

Figure 2: Input PET Images

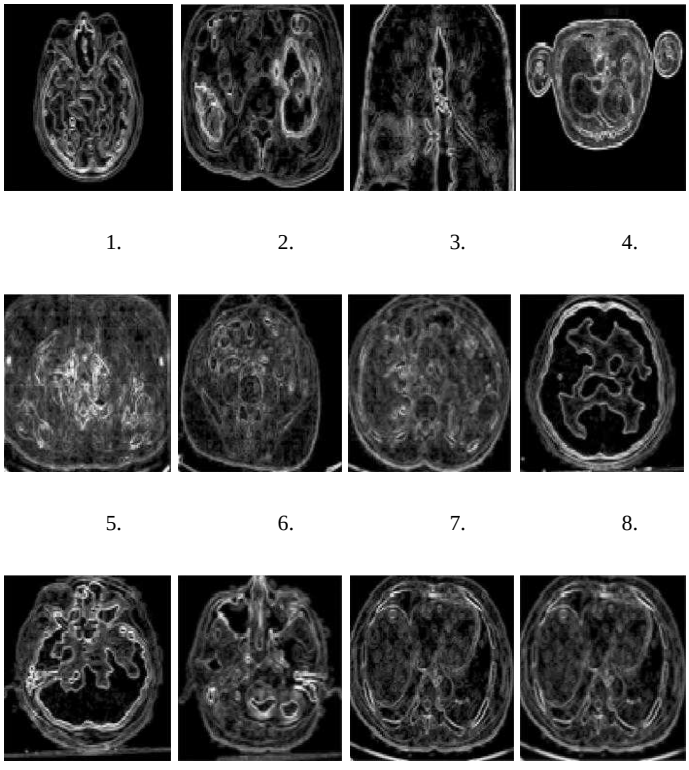

1. 2. 3. 4.

5. 6. 7. 8.

9. 10. 11. 12.

Figure 3: shows the simulation result of ANN-RBF

PET Images	ANN-RBF			Elapsed time for ANN-RBF in seconds
	Image quality parameters			
	PSNR	NAE	RMSE	
1	29.6639	0.2440	8.3819	2.1996
2	52.4465	0.0481	0.6084	2.2620
3	25.5070	0.3576	13.5267	2.0904
4	33.7593	0.1168	5.2309	1.8096
5	31.5942	0.0797	6.7117	2.0124
6	29.3841	0.1870	8.6564	2.0124
7	28.2672	0.1650	9.8442	2.0280
8	26.6253	0.3618	11.8926	2.1840
9	27.3794	0.3038	10.9037	2.2152
10	28.2753	0.2342	9.8350	2.2932
11	27.7353	0.2310	10.4658	2.1840
12	27.8494	0.2104	10.3293	1.8720

Table I: shows the calculated image quality parameter value for ANN-RBF Algorithm

There are 12 PET images. ANN-RBF is used to measure the image quality parameters. They are PSNR, NAE, RMSE. The PSNR has elevated values. The NAE, RMSE

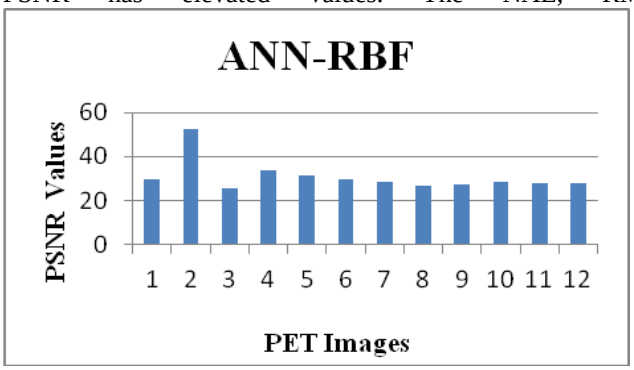

Figure 4: PSNR values for ANN-RBF

Fig 4, shows the calculation of PSNR values by using ANN-RBF. The reconstructed image has better quality in PSNR values.

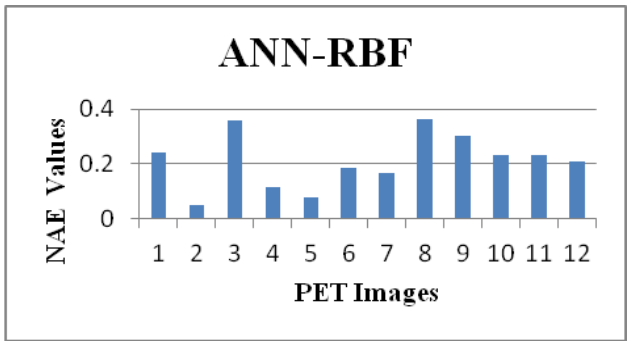

Figure 5: NAE values for ANN-RBF

Fig 5, shows the NAE values calculated by using ANN-RBF. The reconstructed image will give the better image quality in NAE values.

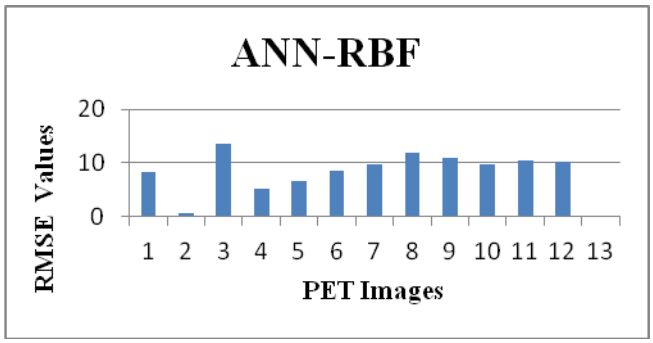

Figure 6: RMSE values for ANN-RBF

Fig 6, shows the RMSE values calculated by using ANN-RBF. The reconstructed image has better image quality in RMSE values for PET images.

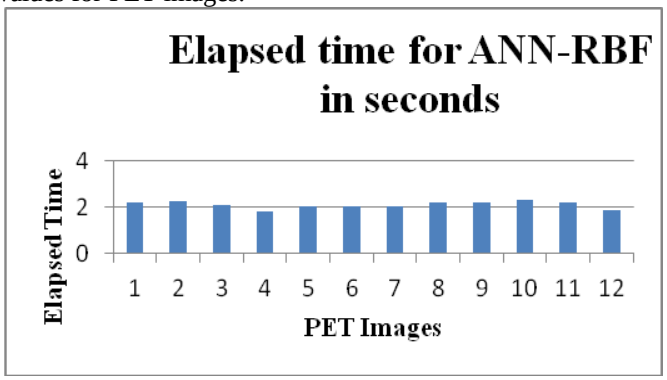

Figure 7: Elapsed time for ANN-RBF

Fig 7, represents the elapsed time for ANN-RBF. It is shown in seconds. Elapsed time for ANN-RBF method is very low when compared with other predictable methods.

VI. CONCLUSION

In this algorithm in order to improve the representation of ANN-RBF algorithm technique was set off in the image reconstruction. The consequent structure sight sees optimally spatial dependencies between image content en route for non-linear image reconstruction. The ANN-RBF based image reconstruction illustrations the auspicious results. The table of results pronounces that the enactment of the ANN-RBF based model is enhanced when paralleled which has less elapsed time. ANN-RBF methods are always a more effective for PET image reconstruction than other conventional methods. The image quality of the resultant images was evaluated using ANN-RBF method.

REFERENCES

[1]. Jeroen Verhaeghe, Dimitri Van De Ville, Member, Ildar Khalidov, Yves D'Asseler, Senior Member, IEEE, Ignace Lemahieu, Member, and Michael Unser," Dynamic PET Reconstruction Using Wavelet Regularization With Adapted Basis Functions", IEEE Trans on Medical Imaging, vol. 27, no. 7, pp. 943-959, 2008

[2]. Karali .E, Pavlopoulos .S, Lambropoulou .S, and Koutsouris .D," ISWLS: Novel Algorithm for Image Reconstruction in PET", IEEE Trans on information technology in biomedicine, Vol. 15,No. 3, pp. 381-386, 2011
[3]. Ilias Maglogiannis, Haralambos Sarimveis, C. T. Kiranoudis, Aristotelis A. Chatziioannou, Nikos Oikonomou, and Vassilis Aidinis," Radial Basis Function Neural Networks Classification for the Recognition of Idiopathic Pulmonary Fibrosis in Microscopic Images", IEEE Trans on Information Technology in Biomedicine, vol. 12, no. 1, pp.42-54, 2008
[4]. Adam M. Alessio, Member, Charles W. Stearns, Senior Member, Shan Tong, Member, Steven G. Ross, Senior Member, Steve Kohlmyer, Alex Ganin, Member and Paul E. Kinahan, Senior Member," Application and Evaluation of a Measured Spatially Variant System Model for PET Image Reconstruction", IEEE Transactions on Medical Imaging, vol. 29, no. 3, pp.938-949, 2010
[5]. Saiprasad Ravishankar and Yoram Bresler," MR Image Reconstruction From Highly
Under sampled k-Space Data by Dictionary Learning", IEEE Transactions on Medical Imaging, vol. 30, no. 5, pp.1028-1041, 2011
[6]. Brent A. Williams, Member, and David G. Long, "Reconstruction From Aperture-Filtered Samples With Application to Scatterometer Image Reconstruction", IEEE Transactions on Geo Science and Remote Sensing, vol. 49, no. 5, pp.1663-1676, 2011
[7]. Yae-lin Sheu, Cheng-Ying Chou, Bao-Yu Hsieh, and Pai-Chi Li," Image Reconstruction in Intravascular Photoacoustic Imaging", IEEE Transactions on Ultrasonics, Ferroelectrics, and Frequency Control, vol. 58, no. 10,pp. 2067-2077, 2011
[8]. Mingli Song, Dacheng Tao, Xiaoqin Huang, Chun Chen, and Jiajun Bu, " Three-Dimensional Face Reconstruction From a Single Image by a Coupled RBF Network", IEEE Transactions on Image Processing, vol. 21, no. 5, pp.2887-2897, 2012
[9]. Shoko Kinouchi, Taiga Yamaya, Eiji Yoshida, Hideaki Tashima, Hiroyuki Kudo, Hideaki Haneishi, and Mikio Suga," GPU-Based PET Image Reconstruction Using an Accurate Geometrical System Model", IEEE Transactions on Nuclear Science, vol. 59, no. 5,pp.1977-1983, 2012
[10]. Jingyan Xu, and Benjamin M. W. Tsui," Interior and Sparse-View Image Reconstruction Using a Mixed Region and Voxel-Based ML-EM Algorithm", IEEE Transactions on Nuclear Science, vol. 59, no. 5, pp. 1997-2007, 2012
[11]. Chao Huang, Kun Wang, Liming Nie, Lihong V. Wang and Mark A. Anastasio," Full-Wave Iterative Image Reconstruction in Photoacoustic Tomography With Acoustically Inhomogeneous Media", IEEE Transactions on Medical Imaging, vol. 32, no. 6, pp. 1097-1110, 2013
[12]. Simon Hawe, Martin Kleinsteuber, and Klaus Diepold," Analysis Operator Learning and its Application to Image Reconstruction", IEEE Transaction on Image Processing, vol. 22, no. 6, pp.20138-2150, 2013
[13]. V. Y. Panin, F. Kehren, H. Rothfuss, D. Hu, and C. Michel, "PET reconstruction with system matrix derived from point source measurements", IEEE Trans. Nucl. Sci., vol. 53, no. , pp. 152-159, 2006.
[14]. T. Yamaya, E. Yoshida, T. Inaniwa, S. Sato, Y. Nakajima, and H.Wakizaka et al., "Development of a small prototype for a proof-of-concept of OpenPET imaging," Phys. Med. Biol., vol. 56, pp. 1123-1137, 2011.
[15]. H. M. Hudson and R. S. Larkin, “Accelerated image reconstruction using ordered subsets of projection data,” IEEE Transaction on Medical Imaging, vol. 13, pp. 601-609, 1994.

Control of Dynamic Voltage Restorer for Injecting Active Power Using Synchronous Reference Frame Theory

J.Kohila
Assistant Professor
Dept. of EEE
Kalasalingam University
Krishnankoil, India
j.kohila@klu.ac.in

S.Kannan
Assistant Professor
Dept. of EEE
Ramco Institute of Technology
Rajapalayam, India
kannaneeeps@gmail.com

V.Suresh Kumar
M.Tech Student
Power Electronics and Drives
Dept. of EEE
Kalasalingam University
Krishnankoil, India
v.sureshkumar6160@gmail.com

***Abstract* - This paper presents a Synchronous Reference Frame Theory(SRF theory) based control strategy for Dynamic Voltage Restorer(DVR) using MATLAB/SIMULINK. The DVR is a normal three phase inverter which converts DC to AC and vice-versa using the dc link capacitor. Whenever utility is distorted by voltage related faults, DVR is active and it protects the load from utility distortions. The control strategy for the DVR plays an important role to make the DVR in active condition whenever distortion occurs. SRF theory is a simple and suitable control strategy for DVR. It acts as the heart of the DVR. This paper also deals with how the DVR is performing under three phase voltage distortion conditions using MATLAB/SIMULINK.**

***Keywords:* DVR, Synchronous Reference Frame Theory, Voltage sag, PLL**

I. INTRODUCTION

Due to some internal or external faults at the distribution side, the voltage level of the utility side becomes poor.The main voltage distortions are voltage sag, voltage swell, unbalanced voltage, voltage harmonics and voltage flickering. This will affect the utility side power quality. So, we can improve the power quality using DVR. DVR uses SRF theory based control for identification and clearance of disturbances. DVR actin stable condition, whenever distortion is not there. DVR injecting voltage through an injection transformer at the Point of common coupling (PCC) [4]. DVR injected voltage compensates the three phase distortions in the utility.

II. DYNAMIC VOLTAGE RESTORER (DVR)

DVR is a normal three phase inverter with 120^0 or 180^0conduction mode. It consists of six pulses, in which three pulses for positive control and the other three pulses for negative control. It comes with a DC link capacitor which stores the energy whenever it is in stable condition. Here the DVR working operation is simulated through professional SIMULINK software called MATLAB/SIMULINK. It provides the exact operation of the device. Here the three phase distortion is created on the utility side to analyse the operation of the DVR. The gate pulses are given by using the sinusoidal pulse width modulation (SPWM). The block diagram for DVR with grid connection is given in Figure 1:

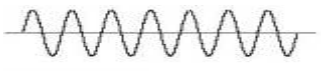

978-1-4799-7075-9/15/$31.00 ©2015 IEEE

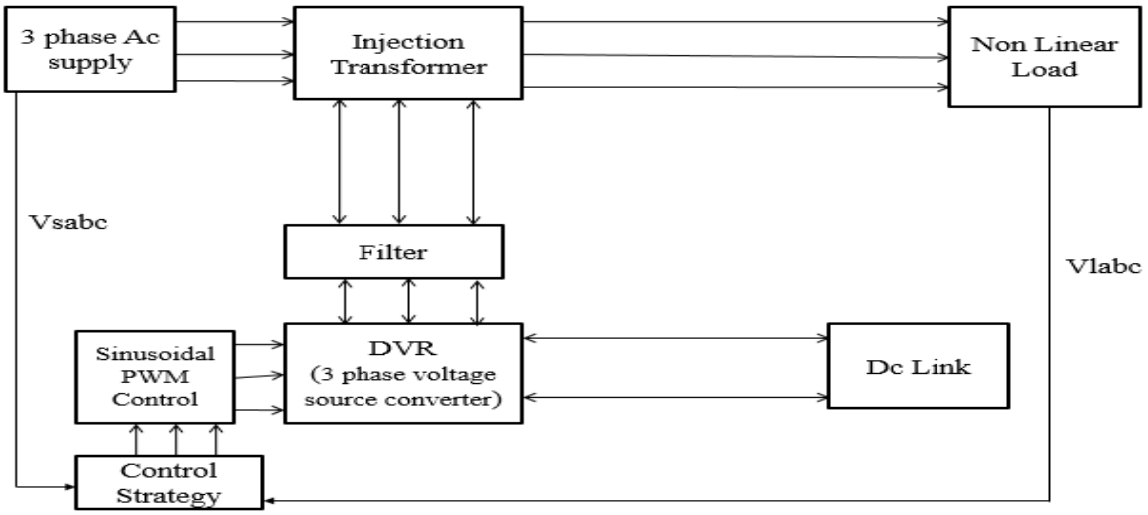

Figure 1: Block Diagram of DVR

III .BASIC STRUCTURE OF DVR

The general model of DVR consists of:

A. Voltage Source Converter (VSC)
B. Sinusoidal Pulse Width Modulation
C. Synchronous Reference Frame Theory
D. DC link
E. A Harmonic filter
F. An Injection/ Booster transformer

A. Voltage Source Converter(VSC)*:*

A VSC is a power electronic converter consists of a dc link storage and Thyristor based switching devices, which can create a sinusoidal voltage for our need. In DVR application, VSC is used to momentarily change the utility voltage or to create the required part of the utility voltage which is missing. There are four main kinds of switching devices they are Gate Turn-Off Thyristor- GTO, Metal Oxide Semiconductor Field Effect Transistor- MOSFET, Insulated Gate Bipolar Transistor- IGBT and Integrated Gate Commutated Thyristor- IGCT. Each type has its own advantages and limitations. The IGCT is a modern compact device with superior performance and reliability that allows constructing VSC with very large power ratings. Because of the highly refined converter design with IGCTs, the DVR can compensate distortions which are beyond the capability of the earlier DVRs using conventional devices. The purpose of storage devices is to give the essential energy to the VSC through the dc link for the generation of injected voltages.

B. Sinusoidal Pulse Width Modulation:

This PWM control is achieved by comparing the Sine Wave (Reference Signal) and Triangular Wave (Carrier Signal) with the help of comparator and to give the positive gate pulses to the upper switches of the inverter and the negative gate pulses are given to the lower switches of the inverter [6] from which the modulation index is calculated using the formula given below:

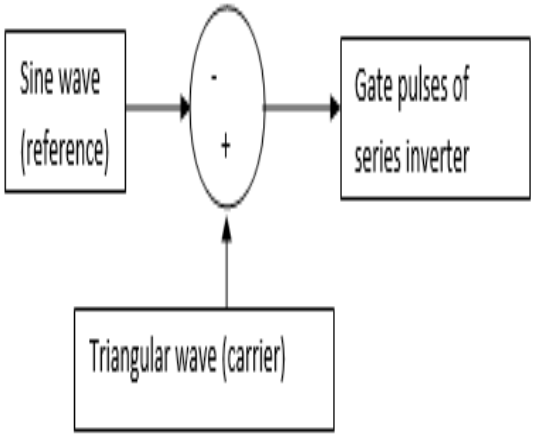

Figure 2: Basic representation of SPWM

$$\textbf{Amplitude Modulation Index} = \frac{\textbf{Peak Magnitude of Reference Signal}}{\textbf{Peak Magnitude of Carrier Signal}}$$

$$\textbf{Frequency Modulation Index} = \frac{\textbf{Peak Magnitude of Carrier Signal}}{\textbf{Peak Magnitude of Reference Signal}}$$

C. Synchronous Reference Frame Theory:

Among the several methods of reference voltage generation, the SRF-based control method is one of the most conventional and the most useful method. SRF method presents excellent features but it requires decisive PLL techniques [1]. This new technique is based on SRF theory using the PLL for phase locking. So, it will work under unbalanced and distorted load conditions. The

proposed SRF control technique uses a-b-c to d-q-0 transformations, filters, and the PLL algorithm shown in Figure 3. The sensing of only the source voltage to realize an SRF theory-based controller operation. Figure 3 describes the block diagram of SRF theory.

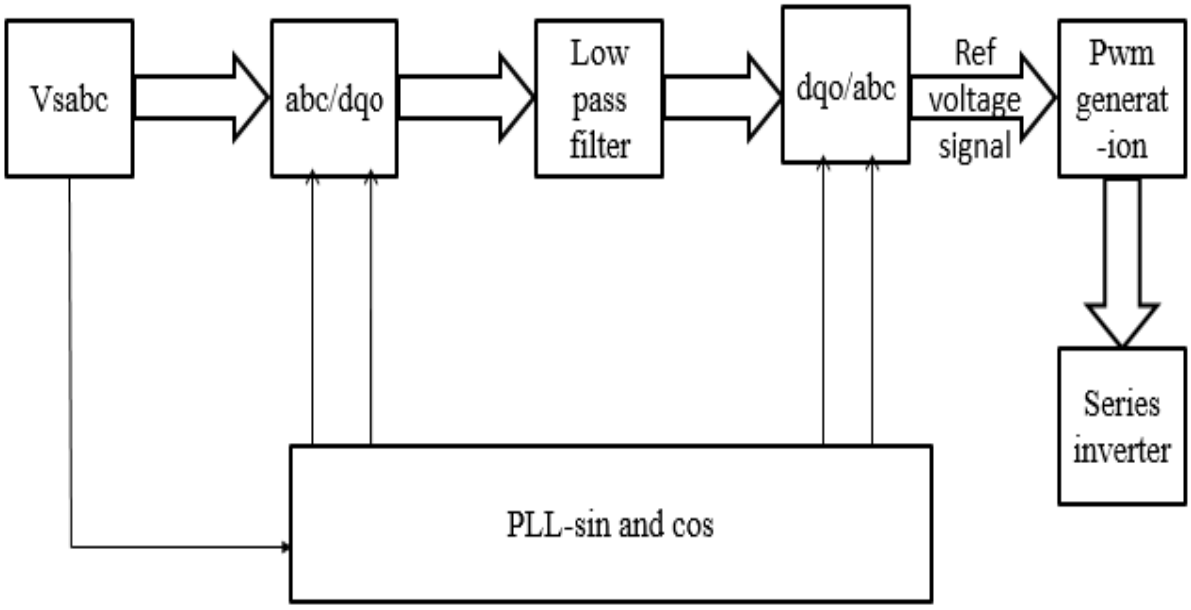

Figure 3:Block diagram of SRF theory

The proposed SRF Theory based DVR control algorithm can be used to resolve the PQ problems linked with utility-voltage harmonics, unbalanced voltages, voltage sag [5] and voltage swell by injecting compensated voltage through injection transformer [2]. In the proposed method, DVR controller determines the reference voltage to be injected by the injection transformer, by relating the positive-sequence component of the utility voltages with load-side line voltages. The utility voltages are transformed into d-q-0 and filtering our required component by using filters and then the inverse transformation is applied to get a-b-c voltages. In addition, the PLL conversion is used for reference voltage calculation [6].

D. DC Link:

The dc link has two main tasks:

- The first task is to charge the dc link source during stable operation.
- The second task is to keep dc link voltage at the nominal range.

E. Harmonic Filter:

The main work of harmonic filter is to keep the harmonic voltage content generated by the VSC within the tolerable level. Two types of filters are available namely active and passive harmonic filters. Active filters are the combination of power electronic components, which requires external power source and passive filters are the combination of electrical components, which does not require any external source [7].

F. Injection/ Booster transformer:

The Injection/Booster transformer is a specifically designed transformer that efforts to limits the coupling noise from the primary side to the secondary side. Its main responsibilities are:

It connects DVR to the distribution side via the High voltage windings and transformers, windings having the ratio of 1:1 and couples the injected compensating voltages created by the voltage source converters to the incoming utility voltage.

In addition to that, Injection/Booster transformer works for the purpose of isolating the load from the utility disturbances.

IV. SIMULINK MODEL OF SYSTEMS

In this section the SIMULINK model of all the systems are presented. Figure 4 shows the SIMULINK model of sinusoidal PWM based three phase inverter.

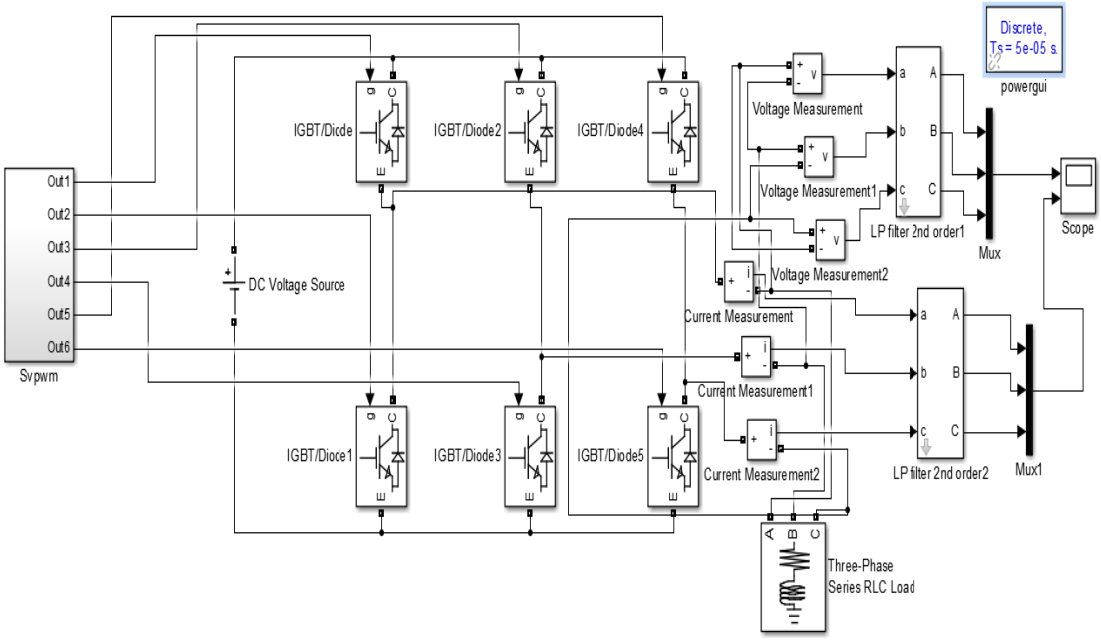

Figure 4: Sinusoidal PWM based 3-phase inverter

Figure 5 shows the MATLAB model of SRF theory which gives control to the PWM technique by generating reference voltage.

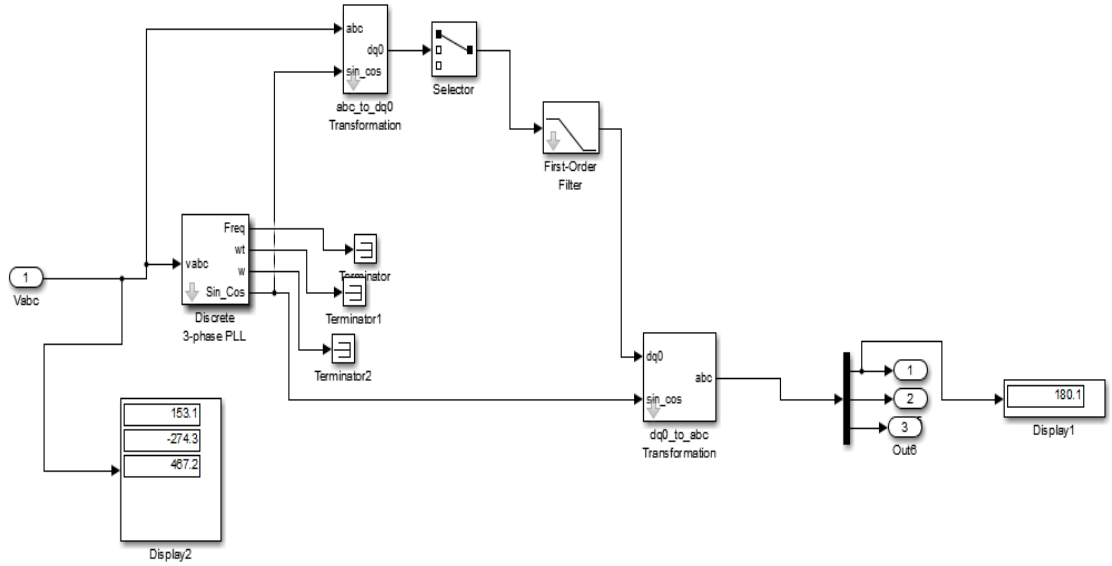

Figure 5: SIMULINK model of SRF theory

The SIMULINK test model of DVR is shown in Figure 6, the test model consists of three phase utility which is supplying 440V, 50 Hz, to the constant load and the DVR is connected in series with the grid line with the help of an injection transformer.

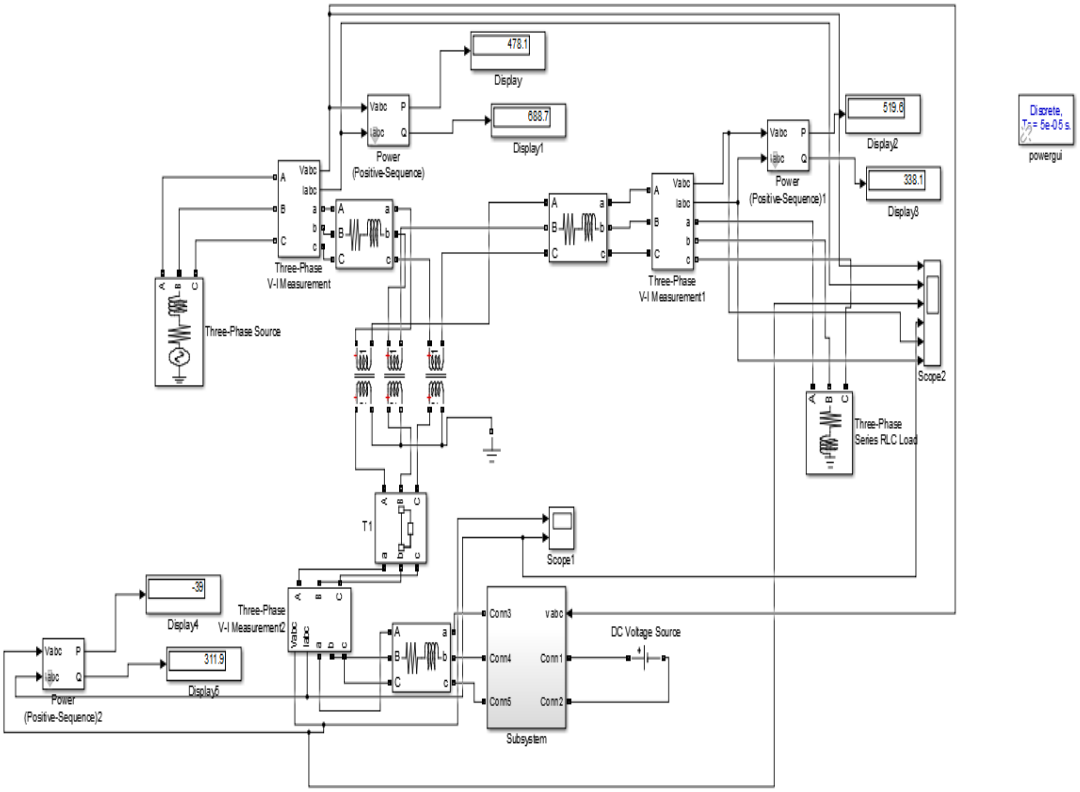

Figure 6: DVR without fault condition

The three phase fault was created on the utility side which makes disturbances on the utility side and analysed how the DVR is performing while utility is under three phase distortion [3].

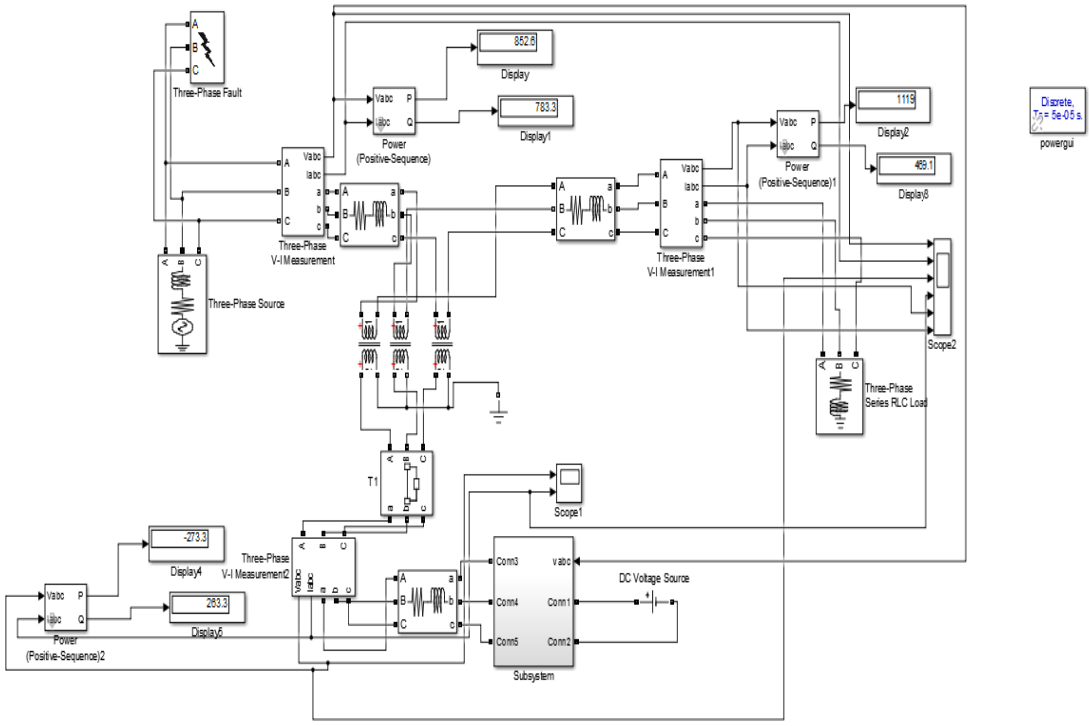

Figure 7: DVR with fault condition

When the system is not under fault it is injecting less active power to support the losses in the line. When the system is under distorted conditions, the DVR is injecting more active power than the system is not in fault to protect the load.

VI. RESULTS

In this section, the results obtained from MATLAB/SIMULINK are presented. Figure 8 shows the output of SPWM inverter. Here the pure sinusoidal wave is obtained by using filters and the voltage and current are in-phase with each other.

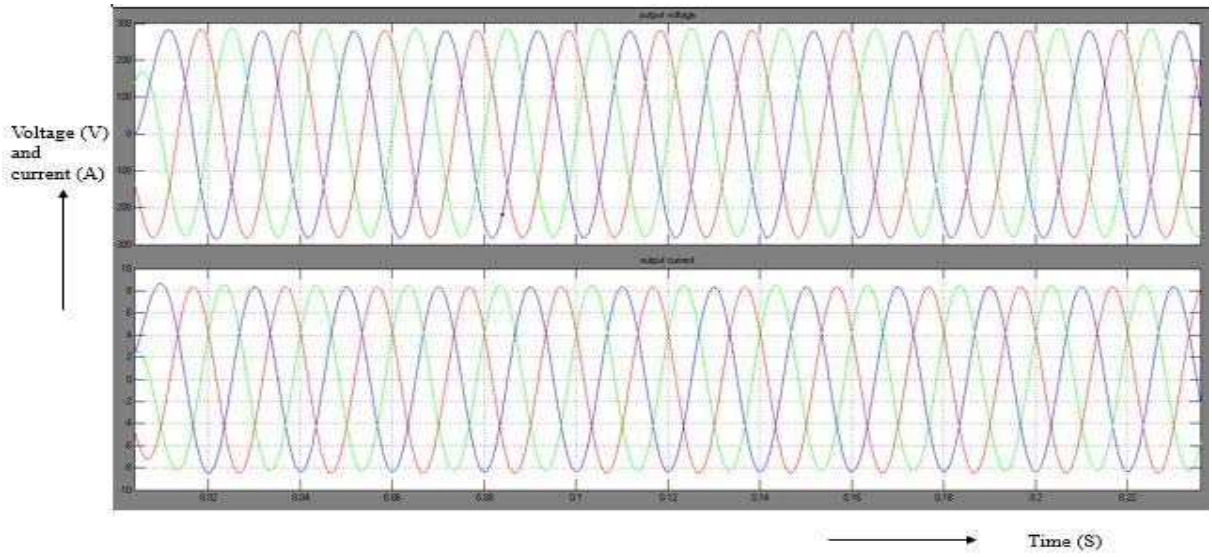

Figure 8: SPWM Output

Tables 1 and 2 represents the active power injected or absorbed by the utility, DVR and load. – sign indicates the injected active power of DVR.

Table 1: P and Q values of system without fault condition

Types	Active Power (P) (Watts)	Reactive Power (Q) (VAr)
Source	478.1	688.7
DVR	-39.0	311.9
Load	519.6	338.1

Table 2: P and Q values of system with fault condition

Types	Active Power (P) (Watts)	Reactive Power (Q) (VAr)
Source	852.6	1119.0
DVR	-273.3	263.3
Load	783.3	469.9

VII. CONCLUSION

In this paper, a new methodology has been developed to control DVR, named SRF theory to inject active power and to eliminate the three phase disturbances in the utility side. The three phase distortions created using the three phase fault block and the performance of DVR was analysed. The sinusoidal PWM technique is used to provide the gate signals for the inverter. The overall performance is satisfactory to protect the load from utility voltage problems.

VIII. APPENDIX

Three phase voltage: 440V, Frequency: 50Hz, RL filter: 0.002 ohms and 1e-3 H, Three phase load: 440V, Frequency: 50 Hz, Switching frequency: 1kHz, Injection transformer ratio- 1:1, DClink voltage source: 440V.

IX. REFERENCES

[1]Mohamadrezapour. V, Bhana sharifiyan. M.B, Feyzi. M.R. Hosseini. S.H, "Design and Simulation of UPQC by Synchronous Reference Frame Theory Considering Loading of Series and Shunt inverters", Journal of Applied Sciences vol. 9 no. 14:2599-2605, 2009, ISSN 1812-5654.

[2] Metin Kesler and Engin Ozdemir, "Synchronous-Reference-Frame-Based Control Method for UPQC under Unbalanced and Distorted Load Conditions", IEEE Transactions on Industrial Electronics, vol. 58, no. 9, Sept. 2011.

[3]Sudharshan Rao Gandimeni and Vijay Kumar. K, "Unified Power Quality Conditioner (UPQC) During Voltage Sag and Swell", International Journal of Emerging Trends in Electrical and Electronics (IJETEE) vo1. 1, Issue. 4, Mar.2013.

[4]C.Sankaran, "Power Quality", CRC Press LLC, 2002.

[5] Hingorani N.G and L.Gyugyi, "Understanding FACTS: Concepts and Technology of Flexible AC Transmission Systems", New York: Institute of Electrical and Electronics Engineers, 2000.

[6] Arindam Ghosh, Gerard Ledwich, "Power Quality Enhancement Using Custom Power Devices", Kluwer Academic Publishers, 2002.

[7] T. Devaraju,V.C.Veera Reddy,M. Vijaya Kumar, "Role of custom power devices in Power Quality Enhancement: A Review", International Journal of Engineering Science and Technology vol. 2, no. 8, 2010, pp.3628-3634.

d-qControl Based Statcom for Reactive Power Compensation

S. Rabik Raja,
PG Scholar, Department of EEE,
Kalasalingam University,
Krishnankoil-626126, India
rabik111992@gmail.com

S.Rajendran,
Assistant Professor, Department of EEE,
Kalasalingam University,
Krishnankoil-626126, India
rsrajendran2008@gmail.com

S.Kannan,
Professor, Department of EEE,
Ramco Institute of Technology,
Rajapalayam-626117, India
kannaneeeps@gmail.com

Abstract: **In AC power system reactive power is one of the major concerns which affect the quality of power. So the compensation of reactive power is essential to improve the power quality. Using various FACTS controllers, the reactive power compensation will be done. In this proposed work the reactive power compensation was done by using static synchronous compensator (STATCOM). A STATCOM is one of the fundamental flexible ac transmission system devices, which can be used for voltage regulation and dynamic voltage control. Many control strategies are available for controlling the behavior of the STATCOM. In this work d-q control based control strategy is used. Using this control strategy the reference voltage and current signals are generated. These reference signals are used to generate pulses for the STATCOM. The generated pulses will dynamically varies depending on the load variation.**

Keywords: FACTS- Flexible AC Transmission System, STATCOM- Static Compensator, d-q control.

1. INTRODUCTION

The term power quality is used in synonymous with supply reliability to indicate the existence of an adequate and secure power supply. Power quality is generally used to express the quality of the voltage. Power Generation, Transmission and Distribution is a difficult process, requiring the working of many components of the power system to maximize the quality of the output. The quality may be reduced by many factors such as Harmonics, reactive power, voltage sag, swell, and transients [1]. Among all, the reactive power is the main component to decrease the quality of the waveform. So we need to compensate the reactive power. Reactive power is required to meet the inductive and capacitive loads. Most of the electrical loads are inductive, hence we need to compensate reactive power. The Reactive power may be compensated in many ways including FACTS controller, fixed capacitors and synchronous condensers etc.[2].

Nowadays, FACTS controllers are used for compensating the reactive power. Here static synchronous compensator (STATCOM) is used to compensate the reactive power. STATCOM has many advantages than other FACTS controllers. The advantages of STATCOM are compensating reactive power, and used for reducing the voltage drops improve the transfer capability of the power in the transmission and distribution lines [3]. The advantages of reactive power compensation are improved power factor, voltage balancing, and improve system stability. So reactive power compensation is needed.The main objective of this paper is to compensate the reactive power by using d-q control method. This method also maintains the voltage at the stability level and the real power also compensated by connecting the same setup in series compensation. The d-q control method is very easy to implement and it gives faster computation.

978-1-4799-7075-9/15/$31.00 ©2015 IEEE

2. REACTVE POWER

Real power is considered to be the work producing power measured in Watts or kilo Watts. Real power produces the mechanical output of a motor. Reactive power is not used to do work but is needed to operate the equipment and is measured in volt-amperes-reactive VAr or kVAr.

From the power triangle shown in Figure 1, the compensation of reactive power decreases the apparent power. Thus, the total consumption of power is also reduced. It reduces the payment of the electricity bill, if kVA is measured.

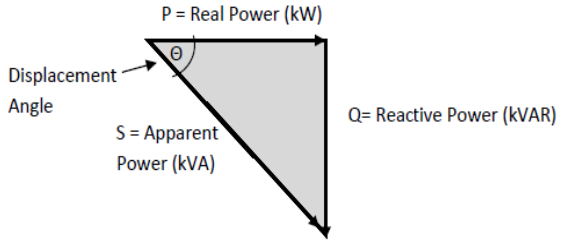

Fig 1. Power triangle

$$S = P + jQ$$

2.1 NEED FOR REACTIVE POWER COMPENSATION

The voltage regulation is increasethe system stability, better utilization of machines connected to the system and to reduce the losses associated with the system and to prevent voltage collapse as well as voltage sag. The impedance of transmission lines and the need for lagging VArby most machines in a generating system results in the consumption of reactive power, thus affecting the stability limits of the system as well as transmission lines [4]. Unnecessary voltage drops lead to increased losses which needs to be supplied by the source and in turn leading to outages in the line due to increased stress on the system to carry this imaginary power.

3. BLOCK DIAGRAM

The block diagram of the proposed work is shown in Figure 2. The three phase source supplies power to the load. This load consume both real and reactive power, due to its inductive nature; not all the loads are purely resistive. It decreases the power quality. So the compensation of reactive power is essential, to improve the power quality. Here STATCOM is used to compensate the reactive power. It is used to control the STATCOM to inject reactive power to the load for compensation. Higher voltage side delivers reactive power to the lower voltage side [5]. Based on this concept the controller operates and produces pulse to the inverter (STATCOM).The controller works on the basics of reference frame theory.

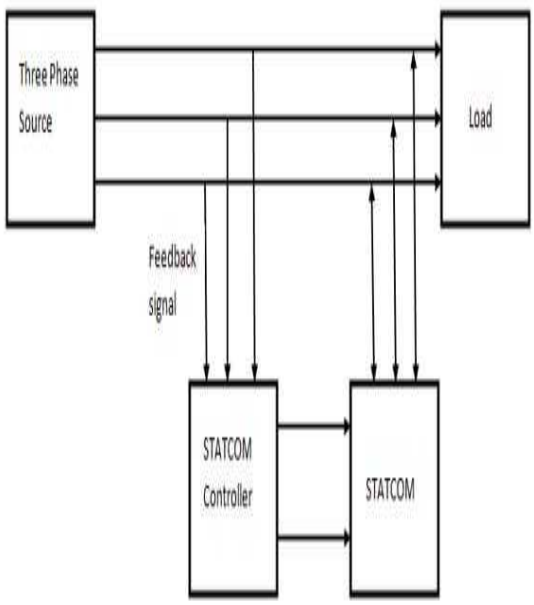

Fig 2. Block Diagram for proposed system

4. SIMULATION OF PROPOSED WORK

The simulation diagram of the proposed work is shown in Figure 3. STATCOM is a normal three phase inverter (bridge inverter) with Controller of d-q control based technique. Programmable voltage source is a pre-programmable source and can be able to supply at specified time. Therefore, we can use programmable voltage source of 440V, 1kVA system as a generator with internal resistance and internal inductance. Here source side voltage and current are measured. Here the load used is a normal linear series RL load.

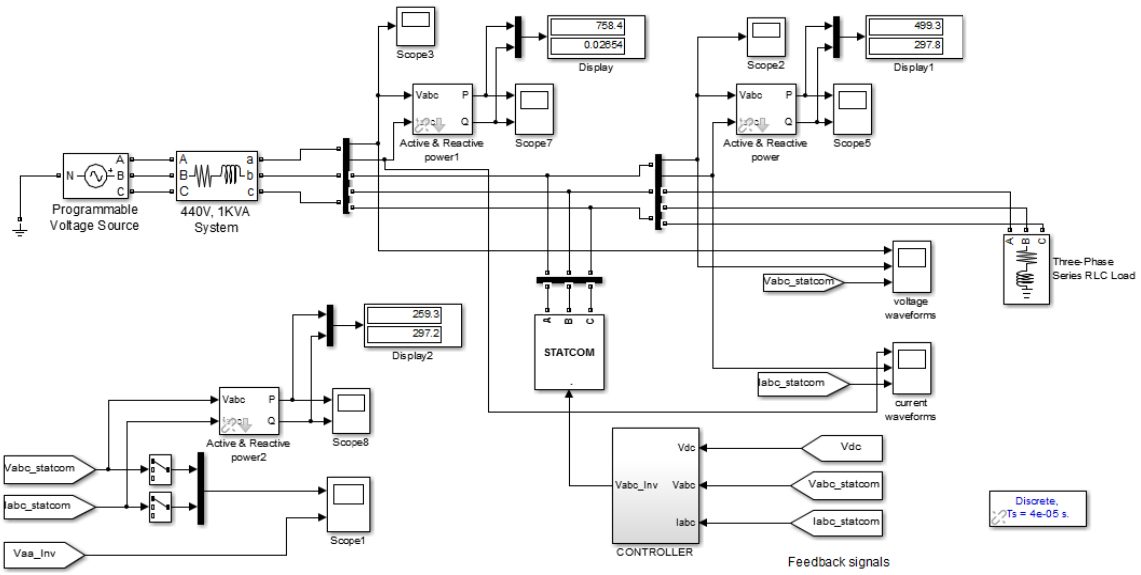

Fig 3. Simulation diagram for d-q control based STATCOM for reactive power compensation

The real and reactive power values for source side, load side and STATCOM side powers are shown in Table 1. The Source side power is the sum of Load side and STATCOM side power.

Table 1. Real and reactive power values

Name	Real Power (Watts)	Reactive Power (Var)
Source Side	758.4	0.02654
Load Side	499.3	297.8
STATCOM Side	259.3	297.2

4.2 STATCOM SIMULATION DIAGRAM

The simulation using the STATCOM is shown in Figure 4. Here bridge inverters are used for converting DC to AC. Two bridges are used, one for positive cycle and another one for negative cycle. An isolation transformer is used before connecting the output of STATCOM to the grid for protection purpose. A DC link capacitor is used to supply the DC power to the STATCOM [6].

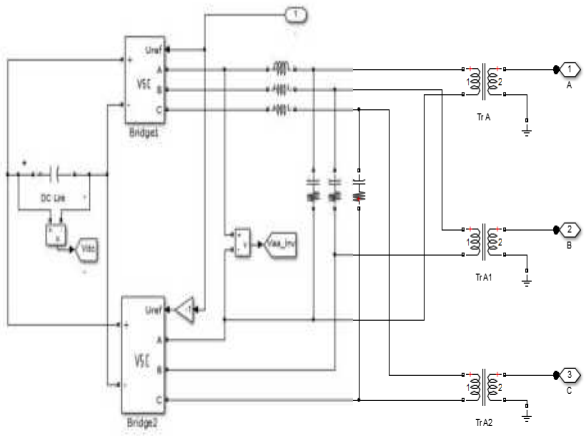

Fig 4. STATCOM Simulation Diagram

4.3 CONTROLLER DIAGRAM

The controller diagram of the STATCOM is shown in Figure 5. Here the fundamental voltage and current signals (a, b, c components) are converted in to direct axis and quadrature axis component (dq0) using reference frame theory. This dq0 component if compared with angles, which is driven from the PLL. From this the reference voltage is generated [7]. This reference voltage is further compared with a carrier signal to create pulses for the STATCOM [8].

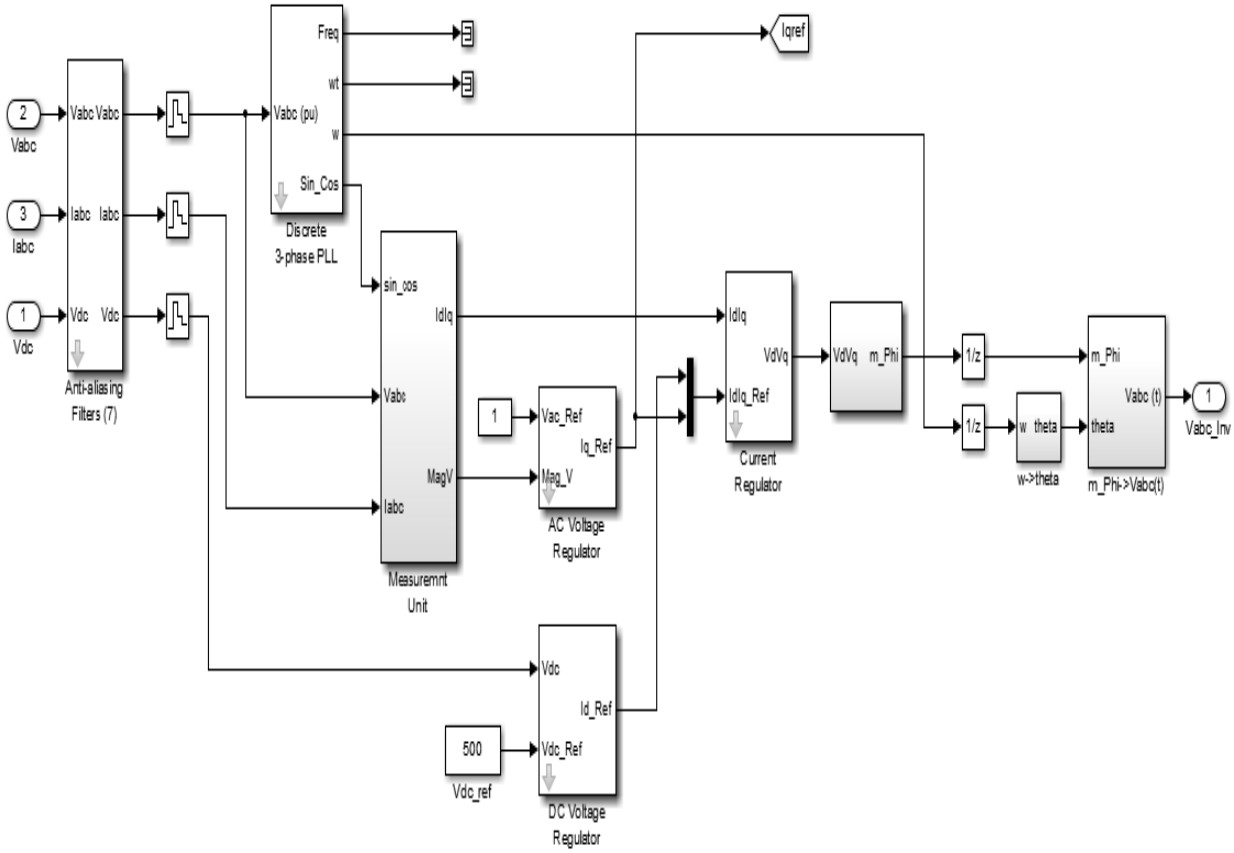

Fig 5.STATCOM Controller

5. RESULTS AND DISCUSSIONS

The simulation results and its output performance are discussed. The output waveforms show the results after carrying out the reactive power compensation by source, load and STATCOM. Voltage stability will be maintained at these output waveforms. Voltage stability consist of both source and load. Here we discussed about the current output waveforms. Finally the reactive power compensation is done using STATCOM and the output waveforms are discussed.

(a)Source Side Waveform

Thesource side output waveform is shown in Figure 6. The waveform consist of real and reactive power of the source. Source side consumed 758.4 Watts real power and 0.02654 VAr reactive power. In this case, it requires less amount of reactive power.

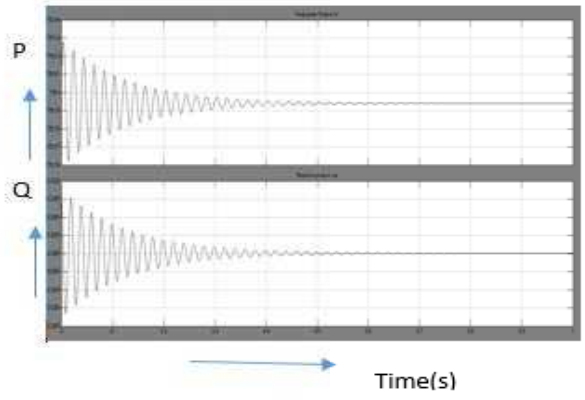

Fig 6.Output waveform for source

(b) Load Side Waveform

The load side output waveform is shown in Figure 7. The waveform consist of real and reactive power of the load. The load consumed 499.3 Watts real power

and 297.8 VAr reactive power. The reactive power injected to the load.

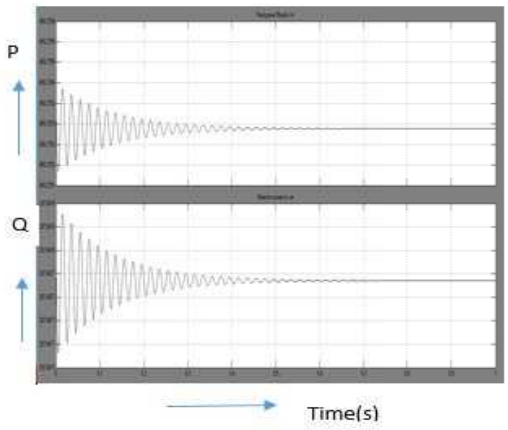

Fig 7. Output waveform for load

(c) STATCOM Side Waveform

The STATCOM side output waveform is shown in Figure 8. The waveform consists of real and reactive power of the load. The STATCOM consumed 259.3 Watts real power and 297.2 VAr reactive power. In simulation, the STATCOM injects reactive power to the load. Reactive power compensation was done by STATCOM.

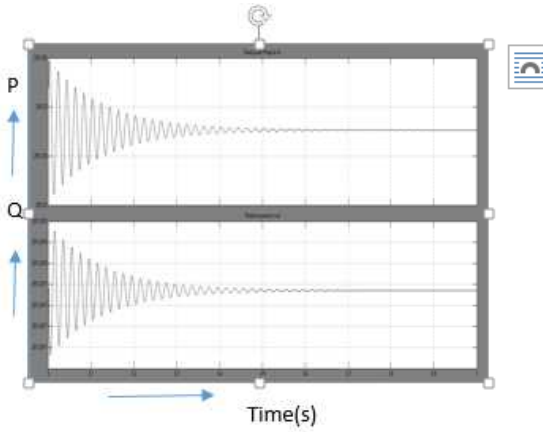

Fig 8. Output waveform for STATCOM

(d) Output Voltage waveform

The output voltage waveform is shown in Figure 9. This waveform consist voltage waveform for source, load and STATCOM. This voltage level is maintained at stable for particular limit. Source side voltage is 440V. Load side voltage is 440V. So the voltage is maintained stable.

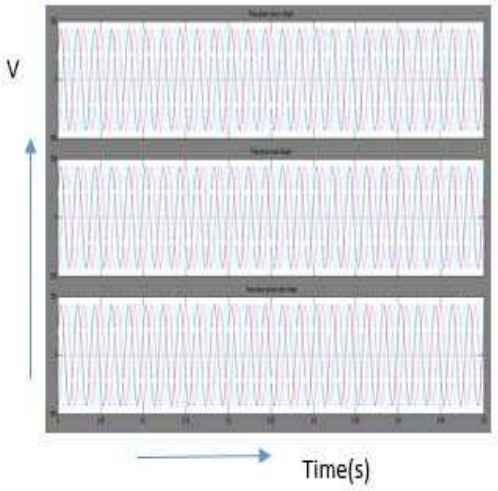

Fig 9.Output waveform for voltage

e) Output Current waveform

The output current waveform is shown in Figure 10. This output waveform consists of source, load and STATCOM current. Source side current value is 5 A. Load side current value is 5 A. STATCOM side current value is 1 A.

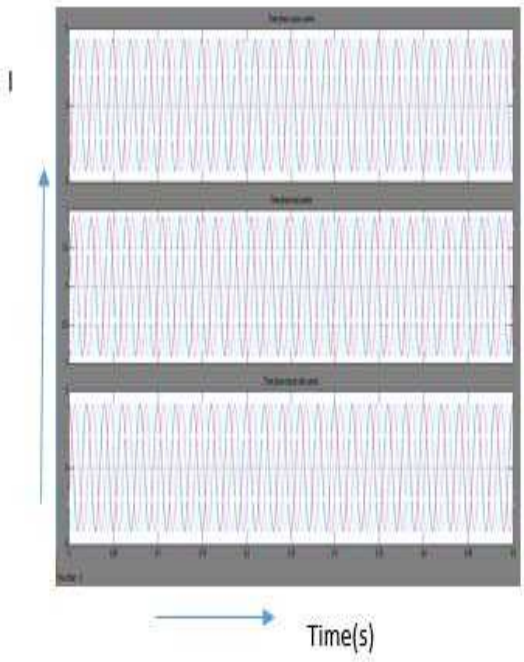

Fig 10. Current output waveform

6. CONCLUSION

This paper introduces a simulation model for d-q control based STATCOM for reactive power compensation to be used in MATLAB Simulink environment. The proposed model is a solution for reactive power compensation using STATCOM. The proposed model has a voltage will be maintained at stable for particular limit. This simulation model clearly shows that the STATCOM can be successfully implemented for the reactive power compensation. The proposed system also maintains the source (Electricity Board) voltage and current in phase with each other after compensation. Thus the power factor of the utility supply is always maintained at a higher value. This results in reduction of payment for electricity and avoids the penalty, for poor power factor.

7. ACKNOWLEDGMENT

The authors are grateful to the Management and the Head of the institution of Kalasalingam University and Ramco Institute of Technology, for giving all necessary support and providing facilities for making this research paper a successful one.

8. REFERENCES

1) A.Arulampalam, M. Barnes, N. Jenkins, and J. Ekanayake, “Power quality and stability improvement of a wind farm using STATCOM sup-ported with hybrid battery energystorage,”Proc. Inst. Elect. Eng., Gen., Transm.,Distrib., vol. 153, pp. 701–710, Nov. 2006.

2) Gerardo Escobar Valderrama, Paolo Mattavelli, and Aleksandar M. Stankovic´, “Reactive Power and Unbalance Compensation Using "STATCOM with Dissipativity-Based Control” IEEE Transactions on Control Systems Technology, VOL. 9, NO. 5, September 2001.

3) PraneshRao, M. L. Crow, and Zhiping Yang, “STATCOM Control for Power System Voltage Control Applications”. IEEE Transactions on Power Delivery, VOL. 15, NO. 4, October 2000.

4) Naveen Goel, R.N. Patel, Member, IEEE, Saji T. Chacko,”Genetically Tuned STATCOM for Voltage Control and Reactive Power Compensation”. International Journal of Computer Theory and Engineering, Vol. 2, No. 3, June, 2010.

5) K. Kobayashi, M. Goto, K. Wu, Y. Yokomizu, and T. Matsumura, “Power system stability improvement by energy storage type STATCOM,” presented at the IEEE Power Tech Conf., Bologna, Italy, 2003.

6) Jain. A, K. Joshi, A. Behal, and N. Mohan, “Voltage regulation with STATCOMs: Modeling, control and results,” IEEE Trans. Power Del., vol. 21, no. 2, pp. 726–735, Apr. 2006.

7) B. S. Chen and Y. Y. Hsu, “An analytical approach to harmonic analysis and controller design of a STATCOM,” IEEE Trans. Power Del., vol. 22, no. 1, pp. 423–432, Jan. 2007.

8) Z. Yang, C. Shen, L. Zhang, M. Crow, and S. Atcitty, “Integration of a STATCOM and battery energy storage,” IEEE Trans. Power Syst., vol. 16, no. 2, pp. 254–260, May 2001.

RAMCO INSTITUTE OF TECHNOLOGY

(Approved by AICTE, New Delhi and Affiliated to Anna University, Chennai)
North Venganallur Village, Rajapalayam - 626 117, Tamil Nadu.

National Conference on Innovations in Engineering, Science & Technology

CERTIFICATE

6th & 7th March, 2015

This is to certify that ~~Dr./Mr./Ms.~~ D. Karthik Prabhu of Ramco Institute of Technology presented a paper entitled Performance Evaluation of Nine-Level modified Cascaded Inverter with different PWM techniques

National Conference on Innovations in Engineering, Science and Technology - NCIEST, organised by Ramco Institute of Technology, Rajapalayam during 6th & 7th March, 2015.

S. Rajakarunakaran

Dr.S.Rajakarunakaran
Organizing Secretary - NCIEST

Dr.R.V.Mahendra Gowda
Principal

Proceedings of the International Conference on "Energy and Sustainability in Engineering Systems 2014" (ICESES2014),Dec 16-18, Coimbatore Institute of Technology, Coimbatore, Tamilnadu, India

Development of Mathematical Model to forecast the Diesel electric Generator performance and exhaust emission

P.Ganesan[1], S.Rajakarunakaran[2], M.Thirugnanasambandam[3], D.Devaraj[4]

1 Senior Research Fellow, Department of Mechanical Engineering, Kalasalingam University, Krishnankoil, Viruthunagar District, Tamilnadu ,India

2 Professor, Department of Mechanical Engineering, Ramco Institute of Technology, Rajapalayam, Virudhunagar District, Tamilnadu, India.

3Assistant Professor,, Department of Mechanical Engineering, Kalasalingam University, Krishnankoil, Viruthunagar District, Tamilnadu ,India

4Senior Professor, Department of Electrical and Electronics Engineering, Kalasalingam University, Krishnankoil, Viruthunagar District, Tamilnadu ,India

E-mail: pganesanmech @gmail.com

Abstract

Rising demand of Diesel electric generators (DG) in the industries causes huge amount of green house gas emissions and air contamination. Hence, it becomes important to forecast the level of emission and flue gas temperature (T_F) and gross efficiency (η) to ensure the nominal emission and effective operation of DGs. The mathematical models are utilized in many complex engineering problems for simulating real-life situations with use of mathematical equations to forecast their future behaviour. In this view, in this study, new mathematical models are suggested for the prediction of CO_2, T_F and η of diesel electric generators (DG). A 180kVA DG is investigated. Data are obtained through number of experiments for 3 phase, 415 volts, DG is operated at different load, speed and torques. The application of newly developed mathematical models showed better results in terms of accuracy and percentage error values. The co-efficient of multiple determination values (R^2) were found to be above 0.99 for all the models. It is found that the Mathematical models are powerful tool for the prediction of emission and performance of DGs.

Keywords: Diesel electric generator; Exhaust emission; performance; Mathematical model; Forecasting.

1. INTRODUCTION

Diesel generator (DG) is a diesel engine coupled to a generator. The DG can generate at nominal power and the surplus energy [1]. As the demand grows for DGs, the amount of release of green house gases (especially CO_2) is also increases and it causes air pollution. With rising concern about global warming and the use of fossil-fuels for power generation, the new concept of renewable distributed generation is getting hold of popularity across the world [2-4]. Therefore it is very important to assess the level emission and performance of DGs for its effective operation and ensure the nominal level of emission. The mathematical models are utilized in many complex engineering problems for simulating real-life situations with use of mathematical equations to forecast their future behaviour [5]. The measurements of exhaust NO, CO, UHC and smoke opacity were correlated against that of key fuel properties and developed emission predictor equations. [6]. It was reported in another study that the mathematical models were developed for the performance and emission parameters of dual fuel diesel engine using hydrogen as secondary fuel to correlate the brake thermal efficiency, UHC, CO and NO by varying engine parameters like load and gaseous fuel. [7].

In this point of view, Mathematical models were aimed for the prediction of CO_2, CO/CO_2 ratio, T_F and η of DG. A 180kVA DG was investigated. The results of the findings are presented in this paper.

2. METHODOLOGY

2.1 Procedure

The procedural steps involved in the development of mathematical are presented below. The description of various stages in this study is presented below:

- Identification of systems/equipment for developing mathematical model. The equipment focused for this study was DGs of different capacities.
- Study of emission characteristics of identified equipment through literature review and preliminary data collection from industries.
- Selection of performance parameters for the identified equipment such as loading conditions, speed, and efficiency etc.,
- Collection of relevant emission related data by conducting experiments in real time using existing model.
- Evaluation of critical performance parameters through detailed data analysis.
- Development of mathematical models and comparison of experimental and predicted data.

2.2 Experimental setup

A 3 phase, 415 volts and Cummins - Powerica DG of 180 kVA was tested. In these DG, the input parameters such as engine rpm, load (Amps), torque were varied and the percentage of carbon-di-oxide from the exhaust gas, the exhaust TF and the η of the DG were measured and noted. The engine rpm was measured using electronic tachometer and other emission parameters such as % CO2, TF and η were measured using a Kane 900 Plus digital hand held flue gas analyzer.

3. RESULTS AND DISCUSSIONS

3.1 Experimentation Vs. Mathematical Model

In this study, new mathematical models were developed for DG of capacity 180 kVA for the calculation of percentage of CO_2, T_F and η . The use of mathematical models is considered to be the reliable and theoretical approach for non-linear problems to predict the accurate results of a particular system. In this study, 200 sets of experimental data were given as input to the development of mathematical model.

The developed mathematical models for 180 kVA DG are presented in equations 1 – 3. It is found that these models have the ability to predict the output parameters with good accuracy. The experimental and mathematically calculated data were compared and the percentage error was estimated. It was determined that the mathematical model results obtained for the percentage of CO_2, T_F and η were within acceptable level. It was obvious from these error values that the percentage errors were within the limits ($\pm 5\%$) [18] and provides better accuracy in the prediction of output parameters using mathematical model.

Also the mathematical models were produced best co-efficient of multiple determination (R^2) values. It is apparent from table 1, that the R^2 values are more than 0.99 and very close to 1, for all the developed mathematical models. It also proved that the mathematical model approach provides quite satisfactory accuracy with reduced percentage error.

$$CO_2 = 0.137\,E_L + (1.3182\times10^{-3})\,N - (4.4455\times10^{-2})\,T \quad (1)$$

$$T_F = (7.728\times10^{-2})\,N - 9.2878\,E_L + 3.9447\,T \quad (2)$$

$$\eta = (4.7392\times10^{-2})\,N - 1.8817\,E_L + 0.6902\,T \quad (3)$$

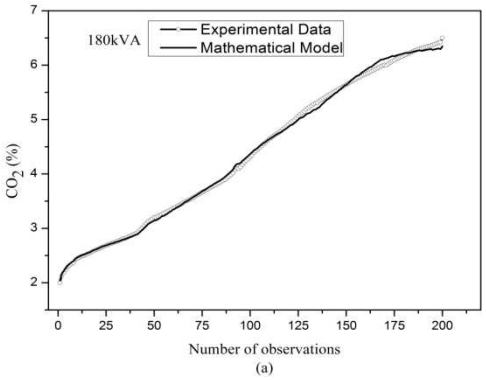

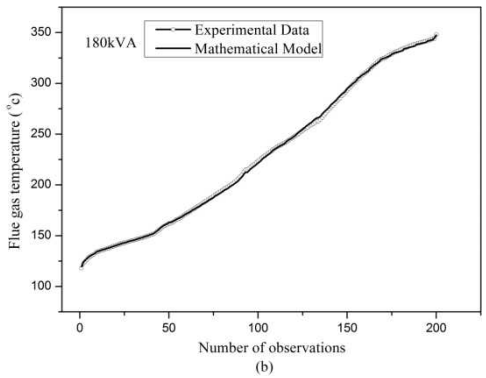

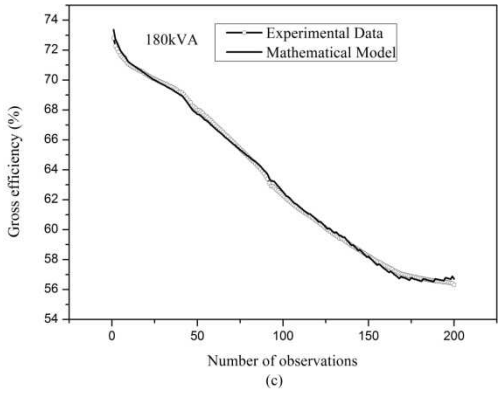

Comparisons of the mathematical model predictions and experimental results of CO_2, T_F and η for 180kVA DG is demonstrated in fig. 1a-c. It is seen that the number of observations are 200. These 200 sets of experimental data are compared with the mathematically calculated data; the key point here is that the curves produced by the experimental results were almost similar with the curves produced by the mathematical models.

Fig. 1: Comparison between experimental and mathematically calculated data for 180kVA DG (a) CO_2 (b) T_F (c) η

Table 1 Co-efficient of multiple determinations (R^2) values of developed mathematical models

Capacity of DG (kVA)	Mathematical model	Co-efficient of multiple determination (R^2)
180	CO_2 (Eqn. 4)	0.9983
	T_F (Eqn. 5)	0.9997
	η (Eqn. 6)	0.9985

4. CONCLUSIONS

Mathematical modelling was used to forecast the CO_2, T_F and η of 180Kva DG. With the use of 200 numbers of experimental observations, new mathematical models were developed. The productions of R^2 values were more than 0.99 and very close to 1, These R^2 values of different mathematical models proved that the mathematical models were suitable for the prediction of CO_2, η and T_F in the DG.

ACKNOWLEDGEMENT

The authors sincerely thank the Department of Science and Technology (DST), New Delhi, Government of India, for its financial grant (No. DST/IS-STAC/CO2-SR-92/11(G)) to carry out this research work under the National Program on Carbon Sequestration Research (NPCSR).

REFERENCES

[1] Kanzumba Kusakana and Herman Jacobus Vermaak, "Hybrid diesel generator/renewable energy system performance modelling", *Renewable Energy*, vol. 67, 2014, pp. 97-102.

[2] N. Jenkins, R. Allan, P.A. Crossley D. Kirschen and G. Strbac, "Embedded generation", IEE Power and Energy Series 31, The IEE, 2000.

[3] L. Kumpulainen and K. Kauhaniemi, "Distributed generation and reclosing coordination", *In: Proc. of Nordic Distribution and Asset Management Conference*, NORDAC, 2004, Espoo, August, 23–24.

[4]L.J. Powell,"An industrial view of utility cogeneration protection requirements", *IEEE Transactions on Industry Applications*, vol. 24, No. 1, 1988, pp.75–81.

[5] Joshua Finn, John Wagner, and Hany Bassily, "Monitoring strategies for a combined cycle electric power generator", *Applied Energy*, vol. 87, 2010,pp. 2621–2627.

[6] Jo- Han Ng, Hoon Kiat Ng and Suyin Gan, " Development of emissions predictor equations for a light - duty diesel engine using biodiesel fuel properties", *Fuel*, vol.95, 2012, pp. 544–552

[7] A.E. Dhole, R.B. Yarasu, D.B. Lata and S.S. Baraskar, "Mathematical modelling for the performance and emission parameters of dual fuel diesel engine using hydrogen as secondary fuel", *Hydrogen Energy*, DOI: 10.1016/j.ijhydene.2014.06.084.

Investigation on the Energy Performance of Industrial Air-Compressors

P.Ganesan[1], S.Rajakarunakaran[2], M.Thirugnanasambandam[3], D.Devaraj[4]

1 Senior Research Fellow, Department of Mechanical Engineering, Kalasalingam University, Krishnankoil, Viruthunagar District, Tamilnadu ,India

2 Professor, Department of Mechanical Engineering, Ramco Institute of Technology, Rajapalayam, Virudhunagar District, Tamilnadu, India.

3Assistant Professor,, Department of Mechanical Engineering, Kalasalingam University, Krishnankoil, Viruthunagar District, Tamilnadu ,India

4Senior Professor, Department of Electrical and Electronics Engineering, Kalasalingam University, Krishnankoil, Viruthunagar District, Tamilnadu ,India

E-mail: pganesanmech @gmail.com

Abstract

Textile industry is one of the energy intensive industries as it employed with lot electrical energy consuming machines like electrical motors, air-compressors, water pumps and lights. Reducing energy consumption and production cost are the primary concerns in these industries. Keeping this in view, an exhaustive energy analysis was carried out in two textile industries focusing on air-compressors. An in-depth analysis was carried out on three air-compressors and the energy and emissions saving potentials are quantified. The outcome of this study showed better results with annual energy saving of 108217.2 kWh and CO2 emission saving of 87.656 tCO_2 / annum.

Keywords: Air-compressor; Textile Industry; Energy Analysis; CO_2 Emission.

1. INTRODUCTION

Industries are the major contributors for the economic escalation of any country. In many of the Asian countries including India, textile industries are vast in numbers in which most of the energy requirements are met through electrical energy followed by the thermal energy. Electrical energy is one of the primary energy sources consumed in cotton textile processing [1]. Next to electrical motors, the air compressor is one which utilizes more energy for the production in textile industry. And significant energy saving potential also exists in industrial air-compressors [2]. Leaks can be a significant source of wasted energy in an industrial compressed air system, sometimes wasting 20–50% of a compressor's output. An unmaintained plant will likely have a leak rate equal to 20% of total compressed air production capacity [3]. Reducing energy consumption through a detailed energy analysis is a cost effective methodology in any energy optimization program [4]. Keeping this in view, an energy performance study has been conducted in two textile industries focusing on air compressors. The energy and emission potentials identified are quantified and presented in this paper.

2. METHODOLOGY

In this section, the procedural steps involved in the study, mathematical models required and collected data are presented.

2.1 Procedural steps

The procedural steps involved in this study are presented in fig.1. The equipment focused for the current study was air- compressor from the two textile industries. Totally three air-compressors were accessed for its performances by collecting the required energy related data from the industries. The data were analysed in detail to identify the energy and indirect emission saving potentials. Then these energy and emission saving

potentials were quantified in terms of electrical energy, bill and CO_2 savings.

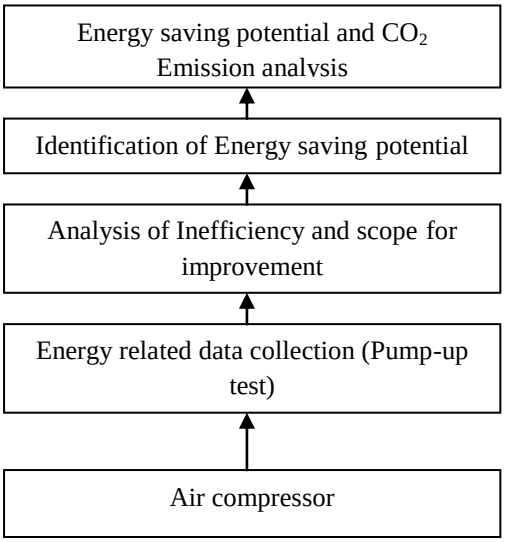

Fig. 1 Procedural steps involved in accessing the energy performance of industrial air-compressors

2.2 Mathematical Model

The mathematical equation required for the assessment of energy performance of air compressors are presented below [3].

Annual energy consumed by the air-compressor was estimated by using following equation

$$AEC = \Sigma[(P_L \times T_L)+(P_{UL} \times T_{UL})] \times h_y \quad (1)$$

Leakage of compressor was estimated by using following equation.

$$CL\ (\%) = (T_L \times 100) / (T_L + T_{UL}) \quad (2)$$

Annual energy saving was estimated by using following equation.

$$AES_{LC} = CFM \times (L_A - L_{UA}) \times (P_L / CFM) \times h_y \quad (3)$$

Actual cfm generated was calculated using the following equation

$$C_{out} = ((P_2-P_1)/P_0) \times (V_{receiver}/ T_R) \quad (4)$$

Annual Bill Saving can be calculated by using following equation.

$$ABS = AES \times INR/KWh \quad (5)$$

CO_2 emission reduction can be estimated by using following equation.

$$E_Y = AES \text{ in } MW.h \times E.F \quad (6)$$

Where, P_L - Power consumed during loading (KWh) ; T_L- Compressor loading time (sec);P_{UL} - Power consumed during unloading (KWh); T_{UL} - Compressor unloading time (sec);hy - annual operating hours; L_A - Actual air leakage (%); L_{UA} - Unavoidable air leakage (%);CFM – cubic feet per minute; P_2 –final pressure; P_1- initial pressure; P_0- atmospheric pressure; T_R –receiver filling time; E.F –Emission factor

2.3. Data Measurements

The industries utilize the air compressors for various pneumatic operations in the facility. The compressed air is generated through screw compressors with the capacities of 139.4, 135.57 and 120 cfm respectively. The capacity test on these three air-compressors was conducted and the data collected are presented in table 2. The instruments utilized for this study is presented in table 1. The Photographs taken during the collection are shown in fig 2.

Table 1 List of instruments with specifications

Name of the instrument	Measurable parameters	Specification range	Accuracy
EXTECH make,3-phase clamp power analyzer with 2000 A, model 382075	Volt, Amps, KW, pf, Hz	Up to 200 A, 2000 A	±1.5% for V and I, ± 2% for KW
Pressure meter (gauges)	Air pressure	0 to 25 (bar)	± 0.03 kPa (0 to 30 kPa)

Table 2 Data collected through capacity test

Description	Values (Air-compressor I, II and III)
Power consumed during loading (kW)	24.13, 25.3 and 21.7
Power consumed during unloading (kW)	6.2, 6 and 4.42
Compressor loading (%)	35.65, 38.77 and 37.96
Compressor unloading (%)	64.35, 61.22 and 61.11
Compressor loading time (sec)	41, 38 and 41
Compressor unloading time (sec)	74, 60 and 66
Receiver volume (m^3)	1.1, 1 and 1
Receiver filling time (sec)	110, 103 and 140 respectively

Fig. 2 Measurement of loading and unloading power in air-compressor

2. RESULTS AND DISCUSSIONS

The performance of the air compressors from the two selected textile industries were checked with the help of capacity test and leakage test. Totally three numbers of air-compressors being used by these industries for their production. It is observed that the compressors were producing 139.4, 135.57 and 120 cfm which are 86.43%, 40.14% and 81.44% of the rated capacity respectively. The total air leakage was found to be 35.65%, 38.77% and 38.32% respectively. As the unavoidable loss should not exceed 10% [5] in an industry, the loss should be reduced by 25.65%, 28.77% and 28.32 respectively. The points where the leakage is taking place could be rectified by tightening the connections or by replacing the damaged parts. Using the equations 1-6, the following parameters were calculated and are presented table 3. It is observed that the annual energy saving of 108217.2 kWh is achieved in these textile industries by utilizing these three air-compressors alone. In turn the indirect CO2 emission saving is estimated at 87.656 tCO2 / annum with no investment and immediate payback.

Table 3Analysis on air compressors (Textile Industry I and II)

Parameters	Values
AEC	105660.1, 55750.8 and 45064.4 kWh
Compressor Leakage	35.65, 38.77 and 38.32% .
AES	51977.3, 30455 and 25784.9 kWh
ABS	INR 865737.6/-
PB	Immediate
EY	87.656 tCO2 / annum

3. CONCLUSIONS

According to the results of this study, the air-compressors are identified as one of the energy intensive equipment in the textile industries and are utilized ineffectively. The capacity test results showed that the air-compressors are producing less cfm than prescribed. The leakage was identified as more than 20% in all the three compressors. Energy and emission saving potentials of the industrial air-compressors are noted as huge with application of proper measures. Further, the study could be extended to other energy intensive equipments to identify the energy and emission saving potentials in the textile industries.

ACKNOWLEDGEMENT

The authors sincerely thank the Department of Science and Technology (DST), New Delhi, Government of India, for its financial grant (No. DST/IS-STAC/CO2-SR-92/11(G)) to carry out this research work under the National Program on Carbon Sequestration Research (NPCSR).

REFERENCES

[1]S.Palamutcu, "Electric energy consumption in the cotton textile processing stages". *International journal of energy*. Vol.35 No.7, 2010, pp. 2945-2952.

[2] R.Saidur, N.A. Rahim and M. Hasanuzzaman, "A review on compressed air energy use and energy savings", *Renewable and Sustainable Energy Reviews*, Vol.14 No.4, 2010, pp. 1135–53.

[3] R. Saidur, M.T. Sambandam, M.Hasanuzzaman, D. Devaraj, S. Rajakarunakaran, and M.D.Islam, "An energy flow analysis in a paper-based industry", *Clean Technology Environment Policy;* Vol.1 No.1, 2010, pp. 462-469.

[4] M.T. Sambandam, D. Devaraj, and S. Rajakarunakaran, "Energy audit - a tool to mitigate energy related CO2 emission in process industries", *International conference on "Climate change and CO_2 management: mitigation, separation and utilization*Anna University, Chennai, 2012, Tamilnadu, India.

[5] Bureau of energy efficiency (BEE)," guide books for energy auditor and manager", Govt. of India,2011,http://www.energymanagertraining.com

Proceedings of the International Conference on
Energy, Environment, Materials and Safety (ICEEMS'14)
December 10-12, 2014, CUSAT, Kochi, India, 1- 6

Analysis of causes and modes of failures of LPG refueling station using fuzzy based FMEA

Rajakarunakaran.S[1], Maniram Kumar.A[2], Arumuga Prabhu.V[3]

[1]*Professor, RAMCO Institute of Technology, Rajapalayam, Tamilnadu*
[2]*Assistant.Professor, Dr.Sivanthi Aditanar College of Engineering, Tiruchendur,*
[3]*Associate Professor, Kalasalingam University, Srivilliputhur,*
Tamilnadu, India.

ABSTRACT

Failure mode effect Analysis (FMEA) is a widely industry recognized method used to recognize the failure modes of a system and their effects or consequences upon it. The failure modes are categorized according to how serious their consequences are, how frequently they occur, and how easily they can be detected. Based on detailed review of the structure and operation modes of the observed LPG refueling system, FMEA identifies the high priority failure modes. Conventionally each risk factor (severity, occurrence and detection) evaluated by experts for failure modes is assumed to have equal importance. However, that may not be the case in reality. Further in our study the fuzzy based FMEA approach revealed a difference in prioritizing failure modes from the traditional methods. These approaches eliminate some of the shortcomings of the traditional approach and sharpen the FMEA tool in identifying the high priority failure modes that should be handled primarily. Thus, the limited resources of businesses can be effectively allocated to eliminate the most severe failure modes.

INTRODUCTION:

Failure mode and effects analysis (FMEA) is anticipated to provide information for risk management decision making. There are significant efforts have been made to overcome the shortcomings of the traditional RPN (Wang et al., 2009). The studies about FMEA considering fuzzy approach use the experts who describe

[1]*Corresponding author. E-mail: srajakarunakaran@yahoo.com*

the risk factors O, S, and D by using the fuzzy linguistic terms. After the assignments of the linguistic terms to the factors, if-then rules were generated taking the linguistic variables as inputs to evaluate the risks. The outputs of the fuzzy inference system were variously named as risk (Chin et al., 2008; Guimaraes & Lapa, 2004), the critically failure mode (Xu et al., 2002), priority for attention (Pillay & Wang, 2003), and fuzzy RPN (Xu et al., 2002) in the fuzzy FMEA studies which consider the fuzzy rule-base approach.

In our paper we proposed a Fuzzy FMEA applied to an auto LPG refueling station. As far as published literatures are concerned, the application of Fuzzy FMEA to an auto LPG refueling station is a fresh task explored in our work .The section 1 gives an introduction of the developments in FMEA. Section 2 proposes the fuzzy FMEA methodology. Section 3 the proposed methodology is applied to an auto LPG refueling station with section 6 presents the conclusion.

FUZZY FMEA

An overall view of the fuzzy logic process is shown in Figure 1, in which there are three major steps to carry out the assessment (i) Fuzzification process uses linguistic variables to convert the three risk factors S, O and D into the fuzzy representations. Using the linguistic variables and their definitions, ranking three risk factors can be made in a scale basis. These inputs are then fuzzified to determine the degree of membership in each input class. (ii) Rule evaluation consists of the expert knowledge about the interactions between various failure modes and effect that is represented in the form of fuzzy if–then rules. (iii) Defuzzification process creates a crisp ranking from the fuzzy RPN to give the prioritization level for the failure modes.

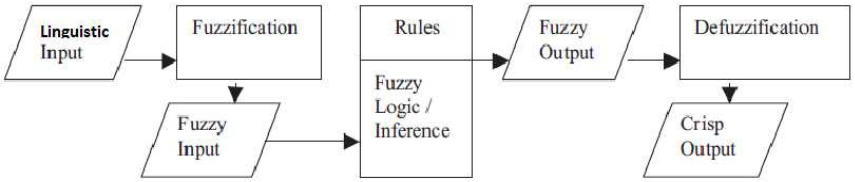

Fig. 1. Fuzzy logic process.

Table 1 list the scales used to measure the three factors. The table shows the five scales and scores of 1–10, to measure the probability of occurrence, severity and the probability of detection. A fuzzy inference approach is considered to represent the assessment information using linguistic terms. To our knowledge, this paper is the first attempt to make the traditional FMEA methodology more applicable for auto LPG refueling station.

Table 1: FMEA scale for occurrence (O), severity (S), not detection (D)

Description	***Occurrence***	***Severity***	***Non detection***	***Score***
Very High	Persistent failures	Hazardous without	Absolute certainity	10

		warning		
	Persistent failures	Hazardous with warning	Probably not detect	9
High	Frequent failures	Very high	Poor chance of detection	8
	Frequent failures	High	Poor chance of detection	7
Medium	Occasional failures	Moderate	May detect	6
	Occasional failures	Low	May detect	5
	Occasional failures	Very low	Good chance to detect	4
Low	Relatively few failures	Minor	Good chance to detect	3
	Relatively few failures	Very minor	Almost certain to detect	2
Almost none	Failure is unlikely	None	Certain to detect	1

CASE STUDY:

The case study of the proposed Fuzzy FMEA is a auto LPG refueling station. Liquefied Petroleum Gas (LPG) is a mixture of light hydrocarbons primarily Butane and propane derived from petroleum, which is gaseous at ambient temperature and atmospheric pressure, is liquefied at ambient temperature with application of moderate pressure. LPG due to its inherent properties is susceptible to fire, explosion and other hazards. Such hazards can have an impact on the property, equipment, plant personnel and public. The Liquefied petroleum gas (LPG) refueling station for which an FMEA was performed has the following key components identified by the experts: Filling Pump, Remote operated valves, High-pressure storage, Dispensing pump, Dispenser, Control system. In order to accommodate within the extent of the paper, the failure modes analysed are restricted to LPG Storage tank, LPG Dispenser and LPG filling process.
The FMEA for LPG refueling station given in the table.2

Table 2 FMEA of LPG refuelling station

No	*Failure Mode*	*Cause*	*Effects*	*Detection*	*Frequency*	*Controls*	*F*	*C*	*D*	*RPN*
LPG Storage tank										
1	Pressure relief malfunction	Mechanical failure	Release of LPG and potential fire explosion	Sensitive verification and Gas detectors	Relatively few failures	Relief valves are vented to a stock No safety hazard	2	6	2	24
2	Over pressure and failure of storage tank	Fill storage on cold day/High temperature environment	Release of LPG and potential fire explosion	Visual gauge inspection	Relatively few failures	Pressure relief valve releases the excess pressure	2	9	2	36
3	Pressure relief device failure	Mechanical failure	Over pressure of the tank	Visual gauge inspection	Relatively few failures	Two relief fixed in the tank	2	9	2	36
4	Piping leak	Mechanical failure /corrosion	Release of LPG and potential fire explosion	Sensitive verification and Gas detectors	Occasional failures	Gas is odorized, Combustible gas detectors	4	8	2	64
5	Storage tank failure	External fire due to large spill of gasoline near the storage	Potential failure of tank due to overheating of metal	Sensitive verification and Gas detectors	Relatively few failures	Gas is odorized Combustible gas detectors	2	9	2	36

		tank								
6	Piping failure	Vehicle impact to dispenser	Potential fire or explosion	Visual inspection and Gas detectors	Relatively few failures	Bollards around dispenser	2	8	3	48
LPG Dispenser										
7	Drive away while connected to dispenser	Human error	Rupture of hose and potential of fire	Visual indication	Occasional failures	Break away coupling	4	6	2	48
8	Hose failure	Mechanical failure	Potential fire	Visual indication	Occasional failures	Hose rated for LPG service	5	5	2	50
9	Leak in connection	O-ring damaged or nozzle damaged	Potential fire	Sensitive verification and Gas detectors	Occasional failures	Dispenser conducts leak check before fill	5	5	2	50
10	Vehicle pressure relief device leaks	Mechanical failure	Potential fire or explosion	Sensitive verification and visual inspection	Relatively few failures	Relief valve on vehicle tank vents	2	6	2	24
11	Nozzles leaks after disconnect	Mechanical failure	Potential fire	Visual indication	Occasional failures	Dispenser valve closes	5	4	2	40
LPG filling process										
12	Vehicle tank isolation valve leaks	Mechanical failure	Potential fire	Sensitive verification and visual inspection	Occasional failures	Checking before loading	2	8	2	32
13	Overfill storage tank	Human error or instrument Failure	LPG release from pressure relief valve with potential fire	Visual indication	Occasional failures	Driver training and established procedures for unloading	5	8	2	80
14	LPG transferring trailer bullet leak	Vehicle impact to truck while unloading damages LPG piping	Potential fire/explosion	Sensitive verification and Gas detectors	Occasional failures	Place barricades before unloading	2	8	2	32
15	Unloading hose connection leaks	Mechanical failure or improper connection	Potential fire	Sensitive verification and Gas detectors	Occasional failures	Check hoses before connecting	4	8	2	64
16	Release from connecting hose	Hose not vented prior to Disconnect human error	Potential fire	Sensitive verification and Gas detectors	Occasional failures	Release vapor via vents before disconnecting	5	4	2	40

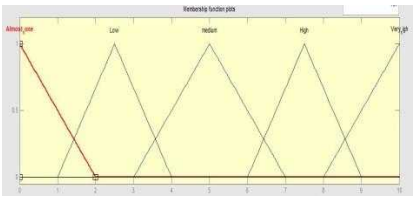

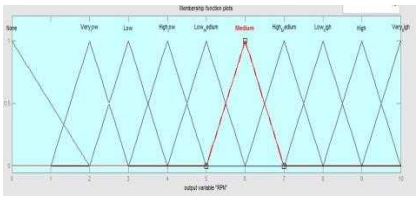

Fig 2:a) Input membership functions (Occurrence, not detection and severity) b) Output membership functions (FRPN)

FUZZIFICATION PROCESS

From the fig 2 a & b, while creating membership functions for input values the 10-level scale is divided into 5 different regions. Being represented by triangular membership functions, these sub-regions respectively are almost none, low, medium, high and very high. For the output variable RPN, the10-level scale is

divided into 10 different parts. These are, respectively, none, very-low, low, high-low, low-medium, medium, high-medium, low-high, high and very high.

RULE EVALUATION:
The occurrence, severity and not detection values of the failures were identified with the help of expert opinions and by using a database of 125 decision rules determined by them specifically. The rules were designed to take into account all possible situations. Examples are given here: "IF occurrence IS almost none AND severity IS almost none AND not detection IS almost none (found) then RPN IS none (no risk)," & "IF occurrence IS almost none AND severity IS medium AND not detection IS very high then RPN IS low medium."

DEFUZZIFICATION

Mamdani min/max method of inference mechanism (input method: min; aggregate method: max) was used and the results were defuzzified by center of gravity method. As to the types of failure, the fuzzy RPN values provided in the model are given in a descending order in Table 3 in comparison with the RPN values of classical FMEA. The failure types containing the same RPN values were arranged according to the values of occurrence, severity and not detection (priority queues). The average number of RPN was found to be 4.733 (high low–low medium).

Table 3 Results of traditional& fuzzy FMEA

Nos	*Freuency*	*Consequence*	*Detection (not)*	*RPN*	*Rank*	*Fuzzy RPN*	*Fuzzy Rank*
1	2	6	2	24	**15**	5	**2**
2	2	9	2	36	**10**	7	**1**
3	2	9	2	36	**9**	7	**1**
4	4	8	2	64	**2**	5	**2**
5	2	9	2	36	**10**	7	**1**
6	2	8	3	48	**5**	5	**2**
7	4	6	2	48	**5**	5	**2**
8	5	5	2	50	**4**	5	**2**
9	5	5	2	50	**4**	5	**2**
10	2	6	2	24	**15**	5	**2**
11	5	4	2	40	**7**	5	**2**
12	2	8	2	32	**12**	5	**2**
13	5	8	2	80	**1**	5	**2**
14	2	8	2	32	**13**	5	**2**
15	4	8	2	64	**2**	5	**2**
16	5	4	2	40	**7**	5	**2**

CONCLUSION

The top ranking by traditional fmea results are totally revised by fuzzy fmea method. The top ranked failures of overfill storage tank, unloading hose connection leaks are reallocated in second priority level. The fuzzy method conveys the top priority failure to be considered as over pressure and failure of storage tank, pressure relief device failure and storage tank failure. The use of linguistic terms in the proposed approach allows for the experts to assign a more meaningful value for the factors considered. This ensures that identified events do not get overlooked (due to low a RPN) when considering the priority for attention. The proposed approach using fuzzy rule base could be suitable for use in formal safety assessment (FSA) process (at the hazard-screening phase). During the hazard-screening phase, only a relative ranking order is needed. This will distinguish the hazards with a high-risk level from those with a low-risk level. As the proposed method provides the analyst with the flexibility to decide which factor is more important to the analysis, the outcome of the analysis will provide valuable information for the decision making process.

The advantages of the proposed fuzzy rule base approach for application to FMEA of LPG refueling station can be summarized as follows:

- It provides an organized method to combine expert knowledge and experience for use in an FMEA study.
- The use of linguistic terms in the analysis enables the experts to express their judgements more realistically and hence improving the applicability of the FMEA.

REFERENCES:

Chin, K. S., Chan, A., & Yang, J. B. (2008), "Development of a fuzzy FMEA based product design system", International Journal of Advanced Manufacturing Technology, 36, 633–649.

Guimaraes & Lapa, 2004, "Fuzzy FMEA applied to PWR chemical and volume control system", Progress in Nuclear Energy, 44(3), 191–213

Pillay, A., & Wang, J. (2003), "Modified failure mode and effects analysis using approximate reasoning", Reliability Engineering and System Safety, 79, 69–85.Sharma et al., 2005

Wang, Y.-M., Chin, K.-S., Poon, G. K. K., & Yang, J.-B. (2009), "Risk evaluation in failure mode and effects analysis using fuzzy weighted geometric mean", Expert Systems with Applications, 36, 1195–1207.

Xu, K., Tang, L. C., Xie, M., Ho, S. L., & Zhu, M. L. (2002), "Fuzzy assessment of FMEA for engine systems", Reliability Engineering and System Safety, 75, 17–29.

ANALYSIS OF HUMAN RELIABILITY BY COGNITIVE RELIABILITY AND ERROR ANALYSIS METHOD (CREAM)

A. Maniram Kumar[1], S.Rajakarunakaran[2] and V. Arumuga Prabu[3]
[1]*Department of Mechanical Engineering, Dr. Sivanthi Aditanar College of Engineering, Tiruchendur 628215,*
[2]*Department of Mechanical Engineering, Ramco Institute of Technology, Rajapalayam 626117, Tamilnadu.,*
[3]*Department of Mechanical Engineering, Kalasalingam University, Anand Nagar,Krishnankoil 626126, Tamilnadu.*

Abstract: Human reliability analysis (HRA), related to various parameters such as the human factor, technology, and ergonomics, is always a critical consideration as regards to safety and environment in engineering industries. Human reliability (operation without failure) plays a crucial role in engineering industries where the execution of highly repetitive and standardized tasks occurs. Therefore, in this scenario, centrality and responsibility of the role entrusted to the human operators are exalted because it requires problem solving and decision making ability. Thus, human operator is the core of a cognitive process that leads to decisions, influencing the safety of the whole system in function of their reliability. The main focus of the research is to systematically predict human error potentials for designated tasks and to determine the required safety control levels during welding operations. The paper adopted CREAM (Cognitive reliability and error analysis method) basic and extended versions in order to assess human reliability and is demonstrated with an operational case study. Consequently, the research provides should contribute to safety at work and prevention of human injury and loss of life.

I. INTRODUCTION

Over the past years, technological developments have led to a decrease of accidents due to technical failures. The use of these advanced technologies, beside managerial advantages, has led to reliability issues specifically intended as the probability that a system fulfills the assigned mission. To the reliability concept are closely related risk and workers' safety that may be directly and indirectly affected by the processes on site. In this context one of the most "critical" components is "man", whose rate of error changes the rate of breakdowns of components with which it can interact. This has highlighted that the "human factor" contributes significantly in accident dynamics, both statistically and in terms of severity of consequences. It has been observed that system failures due to human intervention are not negligible [1]; in particular, some sources report that human error is the cause of failure systems which, in many cases, have disastrous consequences due to man - machine - environment interaction. In fact, estimates agree that the errors committed by man are causes over 60% of accidents and for the remaining part the causes are due to technical deficiencies.

Generally, in reliability systems studies [2], [3], assessment focuses on industry processes and technologies constituting it, disregarding aspects that depend on human factors and its contribution to the same reliability system; but it should be noted that human error is a major contributor to the risks and reliability of many systems: over 90% in nuclear industries [4], over 80% in chemical and petro-chemical industries [5], over 75% of marine casualties [6], and over 70% of aviation accidents [7], [8]. Thus, in order to ensure effective prevention of dangerous events, the role of humans in accident dynamics should be considered during risk assessment processes [9]. The researchers' great efforts to propose models of human behaviour [10] favouring numerical values of error probability in order to

predict and prevent unsafe conduct are clearly evident [11], [12]. Nowadays, the analysis of human factors constitute a highly interdisciplinary field of study not yet well defined, therefore, a complete and universally accepted taxonomy of different types of human errors and causes determining them, does not exist. We note that the objective difficulties of governing the human factor and human error have made many experts believe that the conduct of prevention and safety were related to a person's intrinsic characteristics, such as personality traits. [13], [14].

Fortunately, in recent years, technological advances have shifted human intervention from a direct commitment to the simple manual control of automatic machine processes. For this reason, starting from high risk industrial areas, such as nuclear, aerospace and petrochemical, up to individual SMEs, there was the need to analyze techniques of risk analysis with human factor evaluation methodologies, collected under the name Human Reliability Analysis (HRA). Human Reliability Analysis identifies errors and weaknesses in a system by examining methods of work including those who work in the system. HRA falls within the field of human factors and has been defined as the application of relevant information on human characteristics and behaviors to the design of objects, facilities and environments that people use [15]. HRA techniques may be used retrospectively, in accident analysis, or more likely prospectively to examine a system. Most approaches are firmly grounded in a systemic approach which sees the human contribution in wider technical and organizational contexts [16], [17]. The purpose is to examine task, process, system or organizational structure for where weakness may lie or create a vulnerability to errors, not to find fault or apportion blame. Any system in which human error can arise can be analyzed with HRA, which in practice, means almost any process in which humans are involved [18], [19]. These human reliability analysis methodologies are born first of all to be applied in the nuclear energy field, where it is greater than the risk of a relevant accident. Furthermore, the application of these methodologies is nontrivial and requires a high level of training.

II. CREAM APPROACH

CREAM methodology was developed by Eric Hollnagel in 1998 following an analysis of already in place HRA methods. It is the most widely utilized second generation HRA technique and is based on three primary areas of work; task analysis, opportunities for reducing errors and possibility to consider human performance with regards to overall safety of a system.

This methodology is a technique used in HRA for the purposes of evaluating probability of a human error occurring throughout completion of a specific task. From such analyses measures can then be taken to reduce likelihood of errors occurring within a system and therefore lead to an improvement in the overall levels of safety. HRA techniques have been utilized in a range of industries including healthcare, engineering, nuclear, transportation and business; each technique has varying uses within different disciplines. Compared to many other methods, it takes a very different approach to modelling human reliability.

There are two versions of this technique: basic version and extended version. Basic version provides an initial screening of human error, to understand the error probability range. Instead, extended version uses the results of basic version to obtain the detailed value of error probability. The application of the extended version is needed when the probability of action failures is acceptably low. These have in common two primary features: ability to

identify importance of human performance in a given context and a helpful cognitive model and associated framework, usable for both prospective and retrospective analysis.

CREAM methodology is based on a cognitive model which presents an error classification that integrates individual, technical and organizational factors and provides a step by step description of operator performance analysis. In particular, classification is based on two principles (Fig.1):

• human error may be related with its manifestations, called phenotypes, and its causes, called genotypes;

• phenotypes are result of interaction between genotypes and environment.

The identified cognitive model for CREAM methodology is called "CoCoM" (Contextual Control Model). In Fig.2 is shown Contextual Control Model.

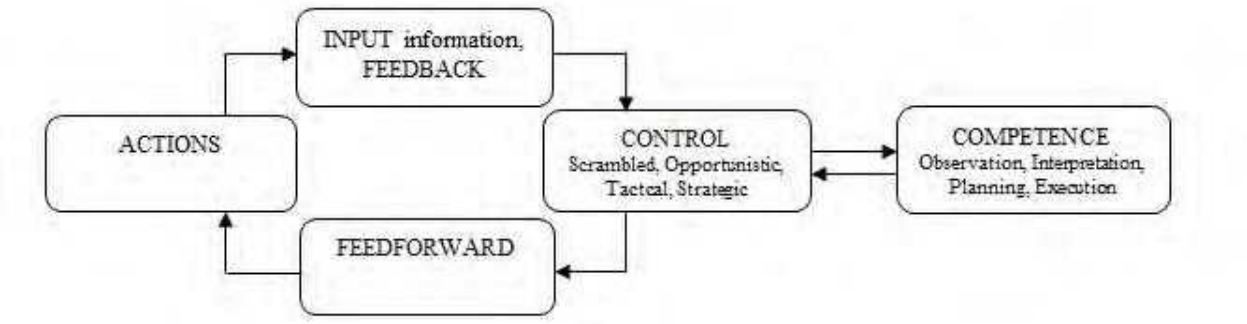

Figure. 1. Contextual Control Model "CoCoM"

Through this model it was possible to determine the requested cognitive functions level in order to implement the analysed performance. The cognitive model application takes place via the individuation of total occurrence of CoCoM functions in performance. Cognition concept is included in the CoCoM model through use of four basic "control modes" which identify differing levels of control that an operator has in a given context and characteristics which highlight occurrence of distinct conditions. The control modes which may occur are as follows (Fig.2):

- Scrambled control: The choice of next action is random or unpredictable. These modes indicates that the operator have minimum control over the system;

- Opportunistic control: The choice of next action is ascertained by careless characteristics of the situation which is due to lack of time, operator inexperience, etc. Situation is characterized by lack of planning and this may possibly be due to the lack of available time;

- Tactical control: performance typically follows planned procedures while some ad-hoc deviations are still possible;

- Strategic control: plentiful time is available to consider actions to be taken in light of wider objectives to be fulfilled and within the given context. This mode enables an operator to perform better and more efficient than the other modes.

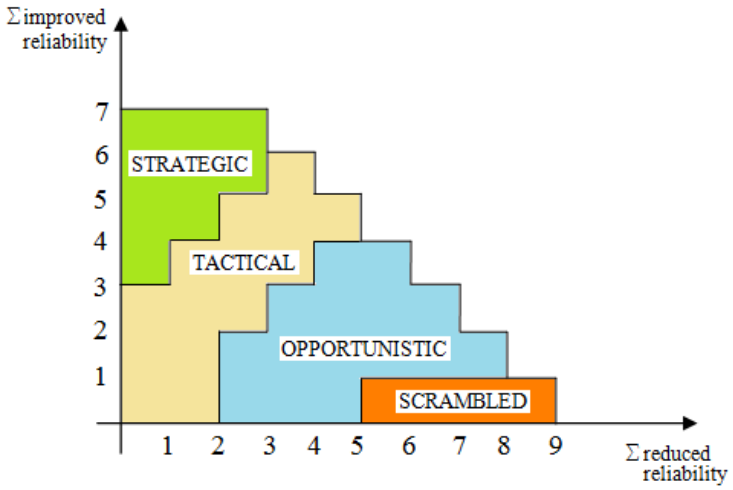

Figure. 2. Relations between Common Performance Conditions (CPCs) score and control modes

Error probability intervals classified on the basis of the various control modes are the following (Table I): The particular control mode determines level of reliability that can be expected in a particular setting and this is in turn determined by collective characteristics of relevant CPCs.

TABLE I
ERROR PROBABILITY INTERVALS

CONTROL MODES	ERROR PROBABILITY INTERVAL
STRATEGIC	0.5e-5 < p < 1e-2
TACTICAL	1e-3 < p < 1e-1
OPPORTUNISTIC	1e-2 < p < 0.5e0
SCRAMBLED	1e-1 < p < 1e0

CREAM methodology (basic and extended version) consists in the following steps:

BASIC VERSION

- Step 1. Hierarchical Tasks Analysis (HTA);
- Step 2. CPCs evaluation;
- Step 3. Control Mode/error interval determination;

EXTENDED VERSION (if needed)

- Step 4. Requested cognitive profile construction;
- Step 5. Possible failure modes of cognitive functions;
- Step 6. Error probability definition.

The main advantages of this methodology are: the technique uses the same principles for retrospective and predictive analyses; the approach is very concise, well-structured and follows a well laid out system of procedure; the technique allows for the direct quantification of HEP; it also allows evaluator using the CREAM method to specifically tailor the use of technique to contextual situation [20]; [21]. Instead, the main criticism are: this technique requires a high level of resource use, including lengthy time periods for completion; CREAM also requires an initial expertise in field of human factors in order to use technique successfully and may therefore appear rather complex for an inexperienced user; CREAM does not put forth potential means by which identified errors can be reduced; time required for application is very lengthy.

III. A CASE STUDY OF A HUMAN RELIABILITY ANALYSIS

In this paper the CREAM methodology applied in a real case study is presented. Here below the methodological approach is presented.

PHASE 1: MODEL DEFINITION

In the present phase the tool is defined. We applied the tool to a welding process.

ACTIVITY 1.1 - DEFINITION OF THE SCENARIO

The aim of the activity 1.1 is to define:

- the reference organizational scenario of mechanical sector(Welding Process) . It was outlined a description of the mechanical sector organization, through the analysis of main organizational and productive aspects including: time and processing methods; duty cycles; human aspects of work.

ACTIVITY 1.2 - ANALYSIS OF SAFETY AND RELIABILITY

The most critical activities are analyzed in the welding process. Check list and safety data sheets were defined according to risks associated for welding activity. In Figure. 3 is shown an extract of data analyzed.

Name	Welding
Description	• Arc welding is a liquid state welding process of joining two metals in which electrical energy produced by an arc between an electrode and a work piece is converted into heat and used for fusion welding.
Risks	• Source of ignition • Accidental contact
Prevention and Protection	• The machine must not be used in an explosive atmosphere • Suitable protective clothing • Hand held helmets with filter lens, Protective Clothing, and gloves

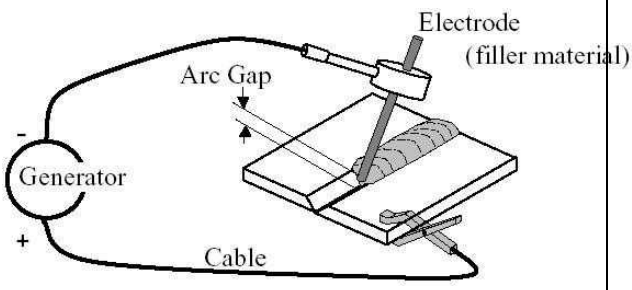

Figure. 3. Process descriptions

PHASE 2: CREAM METHODOLOGY APPLICATION

In the present phase CREAM methodology is applied. Basic Version and Extended version is analysed.

BASIC VERSION

ACTIVITY 2.1 - HIERARCHICAL TASKS ANALYSIS (HTA)

In a logical time sequence, specific operators' tasks are ordered. In this example is analysed the welding process of a manufacturing industry. (Table II).

TABLE II
TASK ANALYSIS OF WELDING PROCESS

ID	GOAL	ID	ACTIVITY
I	Work piece and electrode Positioning	I.1	Fix the work piece
		I.2	Open electrode holder
		I.3	Fix the electrode
		I.4	Close electrode holder
II	Welding process manual assistance	II.1	Make contact 45^0 between electrode and work piece with adequate gap
		II.2	Move to the weld length
III	Work piece removing	III.1	Remove weld electrode
		III.2	Space out the electrode holder
		III.3	Remove the work piece
IV	Cleaning (Slag removal)	IV.1	Take the hammer
		IV.2	Examine
		IV.3	Chipping
		IV.4	Re-examine

		IV.5	Remove & store the work piece

ACTIVITY 2.2 - CPCS EVALUATION

CPCs evaluation is made. The expected effect on the reliability of performance is shown in Table III.

TABLE III
CPCS TABLE REPRESENTATION AND EVALUATION

CPCs	Qualitative Level	Expected effect
Adequacy of organisation	Very efficient	Improved
	Efficient	Not significant
	Inefficient	Reduced
	Deficient	Reduced
Working conditions	Advantageous	Improved
	Compatible	Not significant
	Incompatible	Reduced
Adequacy of man-machine interaction and operational support	Supportive	Improved
	Adequate	Not significant
	Tolerable	Not significant
	Inappropriate	Reduced
Feasibility of procedures and plans	Appropriate	Improved
	Acceptable	Not significant
	Inappropriate	Reduced
Number of simultaneous goals	Fewer than capacity	Not significant
	Matching current capacity	Not significant
	More than capacity	Reduced
Available time	Adequate	Improved
	Temporarily inadequate	Not significant
	Continuously inadequate	Reduced
Time of day	Day time	Not significant
	Night time	Reduced
Adequacy of training and preparation	Adequate (high experience)	Improved
	Adequate (low experience)	Not significant
	Inadequate	Reduced
Crew collaboration quality	Very efficient	Improved
	Efficient	Not significant
	Inefficient	Not significant
	Deficient	Reduced

ACTIVITY 2.3 - CONTROL MODE/ERROR INTERVAL DETERMINATION

In the present activity CPCs characterization is made. Considering the relations between CPC score and control modes (Fig.3), it was possible determine the control mode. According to the previous results, the Control Mode is “Oppurtunistic/Tactical” and it is necessary to apply the extended version.

TABLE IV
CPCs Characterization

Common Performance Conditions	∑Improved	2
	∑Reduced	3

EXTENDED VERSION

ACTIVITY 2.4 - REQUESTED COGNITIVE PROFILE CONSTRUCTION

The purpose of this step is to define the Cognitive Profile considering dependencies between cognitive activities and CoCoM functions as shown in the following table (Table V):

TABLE V
Methodological Matrix of Cognitive Activities

COGNITIVE ACTIVITY	CoCoM Functions			
	Observation	Interpretation	Planning	Execution
Coordinate			X	X
Communicate				X
Compare		X		
Diagnose		X	X	
Assess		X	X	

Execute				X
Identify		X		
Maintain			X	X
Monitor	X	X		
Observe	X			
Plan			X	
Set		X		X
Adjust	X			X
Examine	X			
Verify	X	X		

In the specific case of welding it has (Table VI):

TABLE VI
Methodological Matrix of Cognitive Activities for Weldng

GOAL	ID	ACTIVITY	Cognitive activity	CoCoM Functions			
				Observation	Interpretation	Planning	Execution
Work piece and electrode Positioning	I.1	Fix the work piece	Set		X		X
	I.2	Open electrode holder	Execute				X
	I.3	Fix the electrode	Set		X		X
	I.4	Close electrode holder	Execute				X
Welding process manual assistance	II.1	Make contact 45^0 between electrode and work piece with adequate gap	Adjust	X			X
	II.2	Move to the weld length	Execute				X
Work piece removing	III.1	Remove weld electrode	Execute				X
	III.2	Space out the electrode holder	Execute				X
	III.3	Remove the work piece	Execute				X
Cleaning (Slag removal)	IV.1	Take chipping hammer	Execute				X
	IV.2	Examine	Examine	X			
	IV.3	Chipping	Execute				X
	IV.4	Re-examine	Observe	X			
	IV.5	Remove & store the work piece	Execute				X

ACTIVITY 2.5 - POSSIBLE FAILURE MODES OF COGNITIVE FUNCTIONS

In the present activity, the error of cognitive function is identified through the use of the following error modes, relating welding operations (Table VII; Table VIII):

TABLE VII
Cognitive Functions and Error Modes

Cognitive function	CoCoM functions	
	Error Modes	Mode Description
Observation	*O1*	Observation of wrong object
	O2	Wrong identification made
	O3	Observation not made
Interpretation	*I1*	Faulty (wrong or incomplete) diagnosis
	I2	Decision error (not making or wrong decision)
	I3	Delayed interpretation (not in time)
Planning	P1	Priority error
	P2	Inadequate plan formulated
Execution	*E1*	Execution of wrong type (force, distance, speed or direction)
	E2	Action at wrong time
	E3	Action at wrong object
	E4	Action out of sequence
	E5	Action missed (not performed)

TABLE VIII
Application on Welding Operations

ID	ACTIVITY	Cognitive activity	CoCoM Functions												
			Observation			Interpretation		Planning			Execution				
			O1	O2	O3	I1	I2	P1	P2	P3	E1	E2	E3	E4	E5
I.1	Fix the work piece	Set				X					X				
I.2	Open electrode holder	Execute										X			

I.3	Fix the electrode	Set					X							X	
I.4	Close electrode holder	Execute										X			
II.1	Make contact 450 between electrode and work piece with adequate gap	Adjust		X										X	
II.2	Move to the weld length	Execute										X			
III.1	Remove weld electrode	Execute										X			
III.2	Space out the electrode holder	Execute										X			
III.3	Remove the work piece	Execute												X	
IV.1	Take chipping hammer	Execute												X	
IV.2	Examine	Examine		X											
IV.3	Chipping	Execute												X	
IV.4	Re-examine	Observe		X											
IV.5	Remove & store the work piece	Execute												X	

ACTIVITY 2.6 – COGNITIVE FAILURE PROBABILITY (CFP) DEFINITION

Final values of Cognitive Error Probability (Table XI) are determined from nominal values of CFPs (Table IX), and the "weighting factors" (Table XI) to adjust nominal values of CFPs. The weighting factors are determined from the CFPs corrective factors described by Hollnagel.

TABLE IX
Nominal Value of CFPs

Cognitive function	CoCoM functions		
	Error Modes	Mode Description	Nominal value
Observation	O1	Observation of wrong object	1.0E-3
	O2	Wrong identification made	7.0E-3
	O3	Observation not made	3.0E-3
Interpretation	I1	Faulty (wrong or incomplete) diagnosis	2.0E-1
	I2	Decision error (not making or wrong decision)	1.0E-2
	I3	Delayed interpretation (not in time)	1.0E-2
Planning	P1	Priority error	1.0E-2
	P2	Inadequate plan formulated	1.0E-2
Execution	E1	Execution of wrong type (force, distance, speed or direction)	3.0E-3
	E2	Action at wrong time	3.0E-3
	E3	Action at wrong object	5.0E-4
	E4	Action out of sequence	3.0E-3
	E5	Action missed (not performed)	3.0E-2

TABLE X
CPCs Characterization

Common Performance Conditions	Associated Judgment	OBS	INT	PLAN	EXE
Appropriateness of organization	Not significant	1.0	1.0	1.0	1.0
Work place conditions	Improved	0.8	0.8	1.0	0.8
Appropriateness of man/machine interaction	Not significant	1.0	1.0	1.0	1.0
Feasibility of the procedures and planning	Reduced	2.0	1.0	5.0	2.0
Number of simultaneously tasks carried out by the operator	Reduced	2.0	2.0	5.0	2.0
Available time	Improved	0.5	0.5	0.5	0.5
Time of day in which the activity is carried out	Not significant	1.0	1.0	1.0	1.0
Adequacy of training and experience of worker	Not significant	1.0	1.0	1.0	1.0
Level of collaboration and interaction of department staff	Reduced	2.0	2.0	2.0	5.0
Total Influence of CPCs		3.2	1.6	25	8

TABLE XI

Adjusted CFPs for Cognitive Function Failures

ID	ACTIVITY	Error Modes	Nominal CFP	Weighting Factor	Adjusted CFP
I.1	Fix the work piece	I 1	2.0E-1	1.6	3.20E-01
		E 1	3.0E-3	8	2.40E-02
I.2	Open electrode holder	E 2	3.0E-3	8	2.40E-02
I.3	Fix the electrode	I 2	1.0E-2	1.6	1.60E-02
		E 4	3.0E-3	8	2.40E-02
I.4	Close electrode holder	E 2	3.0E-3	8	2.40E-02
II.1	Make contact 450 between electrode and work piece with adequate gap	O 2	7.0E-3	3.2	2.24E-02
		E 4	3.0E-3	8	2.40E-02
II.2	Move to the weld length	E 2	3.0E-3	8	2.40E-02
III.1	Remove weld electrode	E 2	3.0E-3	8	2.40E-02
III.2	Space out the electrode holder	E 2	3.0E-3	8	2.40E-02
III.3	Remove the work piece	E 4	3.0E-3	8	2.40E-02
IV.1	Take the hammer	E 4	3.0E-3	8	2.40E-02
IV.2	Examine	O 2	7.0E-3	3.2	2.24E-02
IV.3	Chipping	E 4	3.0E-3	8	2.40E-02
IV.4	Re-examine	O 2	7.0E-3	3.2	2.24E-02
IV.5	Remove & store the work piece	E 4	3.0E-3	8	2.40E-02

IV. RESULTS AND DISCUSSION

The welding process consists of 14 sub-tasks which h shall be conducted correctly in order to complete the whole sequential process in a manufacturing industry. From Table XI is possible determine the value of Cognitive Failure Probability. The probability value for most of the control modes are included in the “tactical” control mode range (1.0E-3 < p < 1E-1), as shown by the basic version of methodology. It means that if any of 14 sub-task operations fails, will lead to the failure of the welding operations which may lead to rework or replacement of the job. Since the subtasks have high dependency, overall human error probability value can be assigned as the maximum value of the sub-tasks which is 3.2 E-01. Further decrease in failure rate due to precautionary measures like, having a preset holder to the work piece or educating/training the operator futher reduces the failure probability in the ranges of tactical control mode.

V CONCLUSION

It is quite difficult to attain error data for most of HRA methods. Therefore, cognition method is an alternative solution to overcome scarcity of data. The CREAM extended version apparently gives satisfactory result since the methodology based on cause and effect classification scheme. Thus, the method should be utilised as guidance for data collection and assessment

REFERENCES

[1] B., Kirwan, Practical Guide to Human Reliability Assessment. Taylor and Francis (CRC Press), London, 1994.
[2] R. E., Barlow and F. Proschan, Statistical Theory of Reliability and Life Testing. Holt, Reinhart and Winston, New York, 1975.
[3] A. Høyland, M. Rausand, System Reliability Theory. John Wiley and Sons, New York, 1994.
[4] J. Reason, The contribution of latent human failures to the breakdown of complex systems. Philosophical Transactions of the Royal Society of London. B327(1241) 475-484, 1990.
[5] S. G. Kariuki and K. Lowe, Integrating human factors into process analysis. Reliability Engineering and System Safety. 92 1764-1773, 2007.
[6] J. Ren, I. Jenkinson, J. Wang, D. L. Xu and J. B. Yang, A methodology to model causal relationships in offshore safety assessment focusing on human and organisational factors. Journal of Safety Research. 39 87-100, 2008.
[7] R. L. Helmreich, On error management: lessons from aviation. British Medical Journal. 320(7237) 781–785, 2000.
[8] E. Hollnagel, Cognitive Reliability and Error Analysis Method – CREAM. Elsevier Science, Oxford, 1998.

[9] F. Longo, A.G. Bruzzone, Modelling and simulation applied to security systems Summer Computer Simulation Conference 2005, SCSC 2005, Part of the 2005 Summer Simulation Multiconference, SummerSim 2005, Pages 183-188.
[10] S. French, A. J. Maule and K. N. Papamichail, Decision Making: Behaviour, Analysis and Support. Cambridge University Press, Cambridge.
[11] A. Silvestri, F. De Felice, A. Petrillo. Multi-criteria risk analysis to improve safety in manufacturing systems. International Journal of Production Research 50 (17) , pp. 4806-4821, 2012
[12] G. Di Bona, V. Duraccio, A. Silvestri, A. Forcina. Validation and application of a safety allocation technique (integrated hazard method) to an aerospace prototype. 32nd IASTED International Conference on Modelling, Identification and Control, Innsbruck, 11-13 February 2013
[13] F. De Felice, A. Petrillo. Methodological Approach for Performing Human Reliability and Error Analysis in Railway Transportation System. International Journal of Engineering and Technology Vol.3 (5), 2011, 341-353.
[14] D. Falcone, G. Di Bona, V. Duraccio. A. Silvestri. Integrated hazards method (IHM): A new safety allocation technique. Proceedings of the IASTED International Conference on Modelling and Simulation , pp. 338-343, 2007.
[15] E. Grandjean, Fitting the Task to the Man. Taylor and Francis, London, 1980.
[16] D. E. Embrey, Data Collection Systems. Human Reliability Associates, Wigan, 2000.
[17] M. Lyons, A. Sally, M. Woloshynowych, C. Vincent, Human Reliability Analysis in healthcare: A review of technique. International Journal of Risk & Safety in medicine, 2004.
[18] O. Sträter, The use of incidents for human reliability management. Safety & Reliability, Vol. 26, No. 2 pp 26-47, 2006.
[19] P. C. Cacciabue, Human error risk management for engineering systems: a methodology for design, safety assessment, accident investigation and training. Reliability Eng System Safety RE & SS 83, 229–240., 2004.
[20] P. Salmon, N. A. Stanton and G. Walker, Humans Factors Design Methods Review. Defence Technology Centre, 2003.
[21] I.S. Kim Human reliability analysis in the man-machine interface design review. Annals of Nuclear Energy 28 (2001) 1069-1081.
[22] F. De Felice, A. Petrillo, Productivity analysis through simulation technique to optimize an automated assembly line. Proceedings of the IASTED International Conference, June 25 - 27, 2012 Napoli, Italy. Applied Simulation and Modelling (ASM 2012) DOI: 10.2316/P.2012.776-048 – pp 35-42.
[23] R. J. Vidmar. (1992, August). On the use of atmospheric plasmas as electromagnetic reflectors. *IEEE Trans. Plasma Sci.* [Online]. *21(3).* pp. 876–880. Available: http://www.halcyon.com/pub/journals/21ps03-vidmar

ICAMM 2015

INDO-BRAZIL Bilateral International Conference on
ADVANCED MATERIALS AND MANUFACTURING – ICAMM 2015
Tirunelveli-TN/INDIA, March 27-28, 2015

OPTIMIZATION OF BLIND SPOTS IN HEAVY TRANSPORT VEHICLES THROUGH THE OPTIMIZATION OF DRIVER SEAT DESIGN

Vincent. D.S[1], Pitchipoo. P[2#] , Rajini. N[3] and Rajakarunakaran. S[4]
[1]Tamil Nadu State Transport Corporation Ltd., Thiruvannamalai, India
[2]Department of Mechanical Engineering, P.S.R. Engineering College, Sivakasi, India
[3]Department of Mechanical Engineering, Kalasalingam University, Krishnankoil, India
[4]Department of Mechanical Engineering, Ramco Institute of Technology, Rajapalayam, India
Corresponding Author *Email: drpitchipoo@gmail.com*

Abstract: Statistics show that around 60% road accidents occur due to poor visibility of driver & fatigue. Reduction of blind spot area (Fig.1) improves the area of visibility of the driver which reduces the causes of the accidents. The driver seat design plays vital role in the driver's visibility while he is in the driver seat. This aim of this paper is to optimize the blind spot area by considering the design parameters used in the design of driver seat. To achieve this, a hybrid multi criteria decision making (MCDM) approach is proposed by integrating COPRAS (Complex Proportional Assessment of alternatives) technique and Fuzzy Analytical Hierarchy Process (FAHP). To prove the effectiveness of the developed model, a case study is conducted in a public transport corporation located in the southern part of India.

Keywords*: Driver seat design, Blind spots, COPRAS, FAHP*

1 Introduction

The driver seat is the only thing that the driver uses all the time while driving the vehicles. And so, the design of driver seat is very vital point to be considered in any automobile vehicle. The well – designed driver seat should assure the driver's satisfaction and less fatigue by way of its safety aspects, comfort and versatility. To design the seat the following criteria such as driver's anthropometric data, driver's visibility, driver reach to controls and size, shapes and deflection of the seat are considered (Mehdi and Christopher, 2005). Even though the design of driver seat by considering the above points will have the effect of reducing accident considerably, driver's fatigue is a major factor in commercial vehicle accidents (Shen and Vertiz, 1997). The fatigue and design of driver seat are having close relationships. Unlike sitting in a chair traditionally, a driver can't depend on his feet to assist with the support of the body because they are primarily devoted to the operation of pedals. Hence the design of seat should give assurance to the driver's body balance and control (Carrier, 1992). Seats that don't accommodate the size and shapes of the driver body will force the occupant into a poor sitting posture. Thus, lack of effective adjustable seats correlates with low back pain (LBP) in long – term drivers (Onawumi and Lucas, 2012). Hence it is evident that the poorly designed seats will cause fatigue to the drivers and in turn the fatigue will make the driver to drive without concentration ignoring completely all the blind spots which are the areas that the driver can't see with either side view or rear view mirrors or spots not within the area of driver's visibility (Park et al., 1998). Even if the driver drives with fatigue, he should be able to manage and control the blind spot and the design should support for this effect.

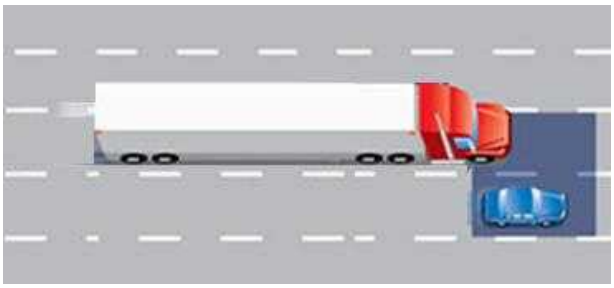

Fig. 1. Area of the blind spot in front of heavy vehicle

Wu et al. (2006) evaluated the safety of vehicles used in a coal mine by using TOPSIS. The criteria weights were computed based on grey entropy measurement. Qiong et al. (2012) proposed an intelligent decision support system (IDSS) to evaluate the road safety performance in European countries. To develop the IDSS, an improved hierarchical fuzzy TOPSIS model was used. The experts' knowledge was incorporated in the proposed model. To develop the IDSS, an improved hierarchical fuzzy TOPSIS model was used. The experts' knowledge was incorporated in the proposed model. Moataz and Julian (2013) evaluated the user's perception towards bus transit services by using a review. The gap in the perceptions held by current and potential users was also measured. First AHP model was developed to measure user preference. Then a weighted perception index (WPI) of both preference and satisfaction is developed through a multi criteria model. Finally, multivariate analysis of variance (MANOVA) is conducted to identify the level of variation in the perception of both current and potential users towards bus service quality.

In this paper an attempt is made to optimize the driver seat design to reduce the blind spots for heavy transport vehicles by conducting a case study.

2. Model Development

For the optimization of blind spot in heavy vehicle through the optimization of design parameters involved in driver's seat design, the tools such as COPRAS and FAHP are used. Fig.2 depicts the proposed framework followed in this paper.

2.1. COPRAS Method

The procedure consists of the following steps:

- *Identification and selection of influencing criteria (attributes) and the available alternatives*

First the attributes which are influencing the decision in the MCDM problem are identified and the available alternates are selected.

- *Preparation of decision matrix (Alternatives vs attributes) (X)*

The collected data (Alternatives and attributes) are shown in matrix form as shown in equation (1).

$$X = \begin{bmatrix} x_{11} & x_{12} & \dots . x_{1m} \\ x_{21} & x_{22} & \dots . x_{2m} \\ \vdots & \vdots & \vdots \\ x_{n1} & x_{n2} & x_{nm} \end{bmatrix} \quad (1)$$

where n= number of alternatives; m = number of attributes

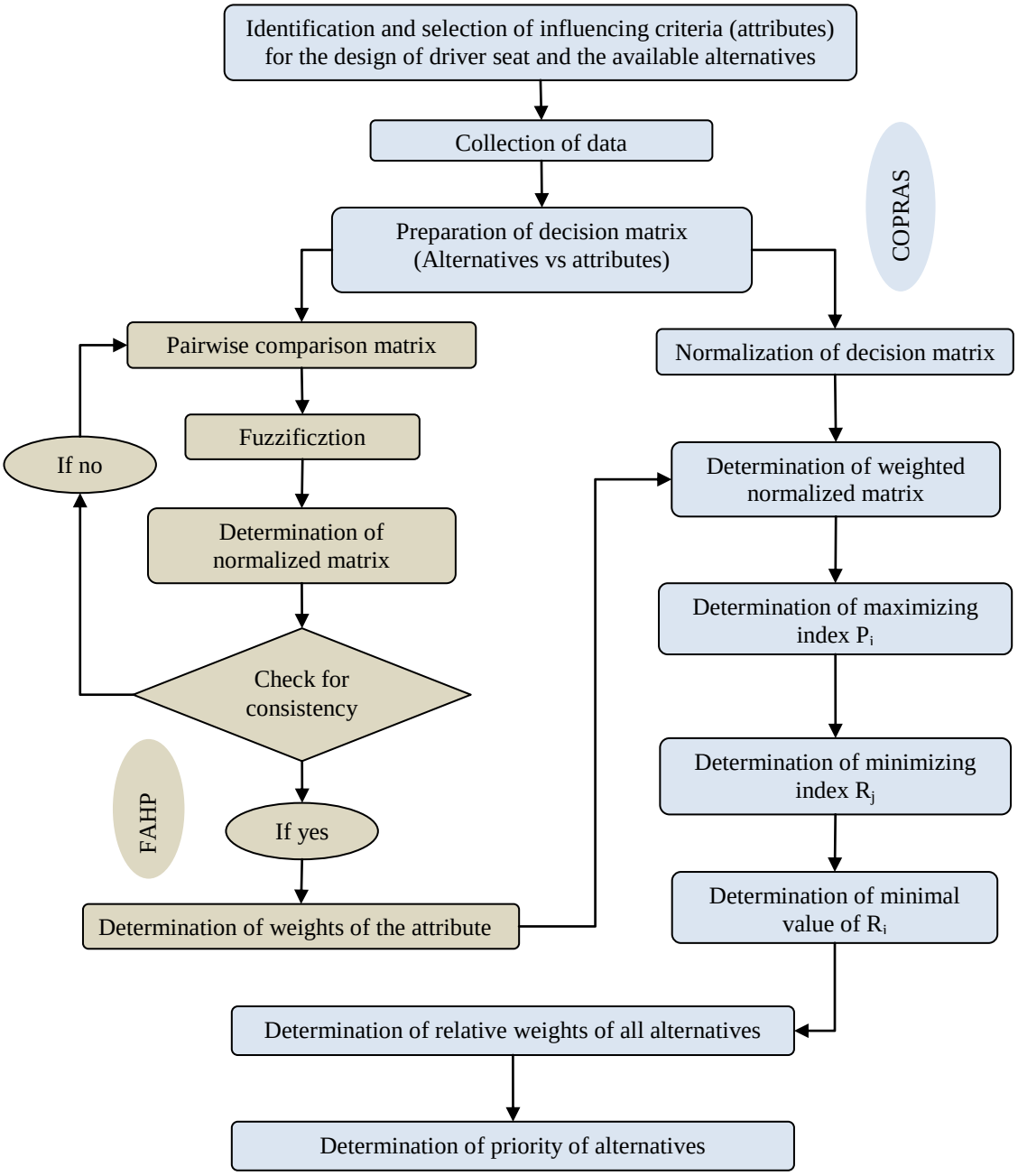

Fig. 2. Proposed frame work

- *Normalization of decision matrix ($\bar{X}$)*

The decision matrix is normalized as shown in equation (2).

$$\bar{X} = \begin{bmatrix} \bar{x}_{11} & \bar{x}_{12} & \ldots.\bar{x}_{1m} \\ \bar{x}_{21} & \bar{x}_{22} & \ldots.\bar{x}_{2m} \\ \vdots & \vdots & \vdots \\ \bar{x}_{n1} & \bar{x}_{n2} & \bar{x}_{nm} \end{bmatrix} \quad (2)$$

where $\bar{\boldsymbol{x}}_{\boldsymbol{ij}} = \frac{\boldsymbol{x_{ij}}}{\sum_{\boldsymbol{i=1}}^{\boldsymbol{n}} \boldsymbol{x_{ij}}}$; I = 1, 2, …..n; and j = 1, 2, … m

- *Determination of the weight of the attributes (W_j)*

The weights of the attributes are determined by using FAHP.

- *Determination of the weighted normalized matrix ($\hat{X}$)*

The determined weights are multiplied with the corresponding attribute value of all alternate to get the weighted normalized matrix.

$$(\hat{X}) = \begin{bmatrix} \hat{x}_{11} & \hat{x}_{12} & \ldots.\hat{x}_{1m} \\ \hat{x}_{21} & \hat{x}_{22} & \ldots.\hat{x}_{2m} \\ \vdots & \vdots & \vdots \\ \hat{x}_{n1} & \hat{x}_{n2} & \hat{x}_{nm} \end{bmatrix} \quad (3)$$

where $\hat{x}_{ij} = \bar{x}_{ij} * W_j$

- *Determination of maximizing index (P_j) and minimizing index (R_j)*

Based on the qualitative nature of the attribute, the maximizing index (P_j) and minimizing index (R_j) values are calculated. If the maximum value is optimum, for that attribute P_j is determined using equation (4). For others R_j will be calculated using equation (5).

$$P_{j=\sum_{i=1}^{k} \hat{x}_{ij}} \quad (4)$$

$$R_{j=\sum_{i=k+1}^{m} \hat{x}_{ij}} \quad (5)$$

where k = number of attributes which is to be maximized

- *Determination of relative weights of each alternative (Q_j)*

Finally, the relative weights of all the attributes will be calculated by using equation (6).

$$Q_j = P_j + \frac{\sum_{j=1}^{n} R_j}{R_j \sum_{j=1}^{n} \frac{1}{R_j}} \quad (6)$$

The alternative with the highest relative weights is considered as the best alternative**.**

2.2. FAHP

In FAHP, Saaty's (1990) analytical hierarchy process is combined with fuzzy concept. Based on the opinion of the decision maker, the evaluation criteria are compared. The ranking of the criteria used for evaluation was collected. Based on that first the criteria matrix was formed based on the Saaty's nine point scale which is shown in Table 1.

The pair wise comparison matrix is called original matrix or criteria matrix which is given by matrix X_{att} as shown below.

$$X_{att} = [a_{ij}]; 1 \le i, j \le m \quad (7)$$

where, a_{ij} = Pair wise comparison of i^{th} and j^{th} attribute. m = the number of alternatives

This was converted into fuzzy original matrix using TFN prescribed by Mohamad et al. (2009) which is also shown in Table 1. The fuzzy number in a fuzzy set can be represented by equation (8).

$$F = \{x, \mu F(x), x \in R\} \quad (8)$$

Table 1 Equivalent triangular fuzzy number for Saaty's nine point scale

Verbal judgment or preference	Saaty's scale of relative importance	Triangular fuzzy numbers
Extremely preferred	9	9,9,9
Very strongly to extremely preferred	8	7,8,9
Very strongly preferred	7	6,7,8
Strongly to very strongly preferred	6	5,6,7
Strongly preferred	5	4,5,6
Moderately to strongly preferred	4	3,4,5
Moderately preferred	3	2,3,4
Equally to moderately preferred	2	1,2,3
Equally preferred	1	1,1,1

where F is fuzzy set; x is fuzzy number; $R: -\infty \le x \le \infty$ and μF(x) is a continuous mapping from R in the interval [0, 1]. A TFN expresses the relative strength of each pair of elements in the same hierarchy and denoted as TFN (M) = (l, m, u) where $l \le m \le u$ in which l is the smallest possible value, m is the most promising value and u is the largest possible value in a fuzzy event. The triangular membership function of M fuzzy number can be described in equation (9). Then the fuzzy original matrix is normalized using equation (10).

$$\mu_A(x) = f(x) = \begin{cases} 0 & x < l \\ (x-l)/(m-l) & l \le x \le l \\ (u-x)/(u-m) & m \le x \le u \\ 0 & x > u \end{cases} \quad (9)$$

$$N_{ij} = \frac{a_{ij}}{T_j} \quad (10)$$

where a_{ij} is the cell value of i^{th} row and j^{th} column in the fuzzy original matrix; $1 \le i, j \le m$; and $T_j = \sum_{i=1}^{m} a_{ij}$

The weights were calculated by converting fuzzy numbers into crisp values by using defuzzification technique. The defuzzification has the capability to reduce a fuzzy to a crisp single-valued quantity. There are seven methods were used for defuzzification of the fuzzy output functions such as max-membership principle, centroid method, weighted average method,, mean–max membership, centre of sums, centre of largest area and first of maxima or last of maxima. In this study, centroid method was used for defuzzification which is given in equation (11).

Weights (Crisp value) $W_i = \frac{\sum_{i-1}^{k} D_p^i * O^i}{\sum_{i=1}^{k} D_p^i}$ (11)

where k is the number of rules, O^i is the class generated by rule i (from 0, 1, …. L-1); L is the number of classes and

$D_p^i = \prod_{i=1}^{n} m_{li}$ (12)

where n is the number of inputs and m_{li} is the membership grade of feature l in the fuzzy regions that occupies the i[th] rule.

Since the pairwise comparison matrix is formulated based on human judgment, it is must to ensure that the values collected are accepted values. To check the consistency, the Consistency Ratio (CR) is calculated using equation (13)

$CR = CI/RI$ (13)

where CI is Consistency Index which is determined using equation (14) and RI is random indices for criteria size 'm'.

$CI = \frac{\lambda_{max} - m}{m-1}$ (14)

where λ_{max} is the maximum eigen value and m is the number of criteria

RI was approximated by Saaty (1990) which is shown in table 2. If the CR is < 0.10 the decision maker's pairwise comparison matrix is acceptable.

Table 2. Random Indices

m	1	2	3	4	5	6	7	8	9	10	11	12
RI	0	0	0.58	0.90	1.12	1.24	1.32	1.41	1.45	1.49	1.51	1.58

3. Case Study

Tamil Nadu, one of the States in India, is having eight Transport Divisions satisfying, the transport need of people. Among the eight divisions, Madurai is having a fleet strength of 1235 vehicles covering nearly 4 Lakh Km/ day and nearly 9 lakh people are using these vehicles per day. Many of the vehicles run in the rural area and mainly through villages and stop at various stops which are in the residential area. The driver allows the passengers to alight and board the buses at these stops and again moves the bus to next stop. During this process, at bus stops, the driver is concentrating more on passenger activities and he is totally unaware of what is happening in front of the vehicle near the front bumper and in the blind area to the right and left side. Despite of consideration of all the factors for the design of driver seat, the current design are not concentrating on the blind spots.

Vincent et al. (2013) identified the following factors such as platform to seat height (A), total seat height (B), seat back rest to windscreen distance (C) and seat back rest to steering centre distance (D) are the influencing criteria for the design of driver seat to optimize the blind spot. In order to reduce the blind spot, maximum values are desirable in platform to seat height (A) and total seat height (B) while the minimal values are desirable in seat back rest to windscreen distance (C) and seat back rest to steering centre distance (D). The data of influencing criteria for the design of driver seat for four different body structures are given in Table 3.

TABLE 3 Data of influencing criteria for the design of driver seat

Types of Vehicle	A (cm)	B (cm)	C (cm)	D (cm)
In-House built vehicle (IS)	48.5	100	136	62
Outsourcing built vehicles (OS-1)	53	102	166	64
TATA Marocobolo built vehicles (OS-2)	49	99	134	63
Ashok Leyland Irizar built vehicles(OS-3)	49	99	144	66

3.1 COPRAS Based Ranking

The collected data are given in Table 3. These datasets are known as criteria matrix. These data are preprocessed (normalized) by using equation (2) and the values are given in Table 4. Then the absolute difference between the normalized cell value and the corresponding referential series value was determined by using equation (18). Then the weights are determined by using FAHP. It starts with the pairwise comparison matrix. Based on the ranking by Vincent et al. (2013) and from the experts, the criteria are compared with each other using Satty's nine point scale (Table 1). The crisp matrix is converted into fuzzy matrix using triangular fuzzy numbers recommended by Mohamad et al. (2009). The equivalent triangular fuzzy number for Saaty's nine point scale is shown in Table 1 was used. By

using this, the criteria matrix is converted into fuzzy criteria matrix which is shown in Table 5. The fuzzy criteria matrix was normalized and shown in the Table 6. The fuzzy numbers are defuzzified using equation (11) and the weights are obtained [Table 6]. The Consistency Ratio for this proposed FAHP model is calculated using equation (13) and is found as 0.0755 for the design of driver seat which is less than 0.1 and so the developed comparison is acceptable.

Table 4 Normalized Data

Types of Vehicle	Design of driver seat			
	A	B	C	D
IS	0.243	0.250	0.234	0.243
OS – 1	0.266	0.255	0.286	0.251
OS – 2	0.246	0.248	0.231	0.247
OS - 3	0.246	0.248	0.248	0.259

Table 5 Fuzzy Pairwise Comparison matrix

	A			B			C			D		
A	1.00	1.00	1.00	3.00	4.00	5.00	1.00	0.50	0.33	1.00	2.00	3.00
B	0.33	0.25	0.20	1.00	1.00	1.00	0.20	0.17	0.14	1.00	0.50	0.33
C	1.00	2.00	3.00	5.00	5.99	6.93	1.00	1.00	1.00	2.00	3.00	4.00
D	1.00	0.50	0.33	1.00	2.00	3.03	0.50	0.33	0.25	1.00	1.00	1.00
Total	3.33	3.75	4.54	10.0	12.99	15.96	2.70	2.00	1.72	5.00	6.50	8.33

Table 6 Fuzzy normalized matrix for the design of driver seat

	A			B			C			D			Weights
A	0.30	0.27	0.22	0.30	0.31	0.31	0.37	0.25	0.19	0.20	0.31	0.36	0.2834
B	0.10	0.07	0.04	0.10	0.087	0.06	0.07	0.08	0.08	0.20	0.08	0.04	0.0860
C	0.30	0.53	0.66	0.50	0.46	0.44	0.37	0.50	0.58	0.40	0.46	0.48	0.4745
D	0.30	0.13	0.07	0.10	0.15	0.19	0.19	0.17	0.15	0.20	0.15	0.12	0.1604

By using the weights, weighted normalized matrix is computed using equation (3) and shown in Table 7.

Table 7. Weighted Normalized Matrix

Types of Vehicle	A	B	C	D
IS	0.069	0.022	0.111	0.039
OS-1	0.075	0.022	0.136	0.040
OS-2	0.070	0.021	0.110	0.040
OS-3	0.070	0.021	0.118	0.042

Based on the qualitative nature of the criteria, the maximizing index (P_j) and minimizing index (R_j) values are calculated using equation (4) & (5). Finally, the COPRAS grades (Q_j) of all the alternatives will be calculated by using equation (6). Table 8 shows P_j, R_j *and* Q_j values.

From Table 15 and Figure 3, it is understood that OS - 2 vehicle has the higher GRG values followed by IS, OS-3 and OS-1 body built vehicles. Hence the vehicle body built by the second outsourced body building unit is having minimum blind spot.

Table 8 COPRAS Calculations

Types of Vehicle	P_i	R_i	$1/R_i$	Q_i	Rank
IS	0.090	0.150	6.655	0.257	2
OS-1	0.097	0.176	5.680	0.240	4
OS-2	0.091	0.149	6.700	0.259	1
OS-3	0.091	0.159	6.277	0.248	3

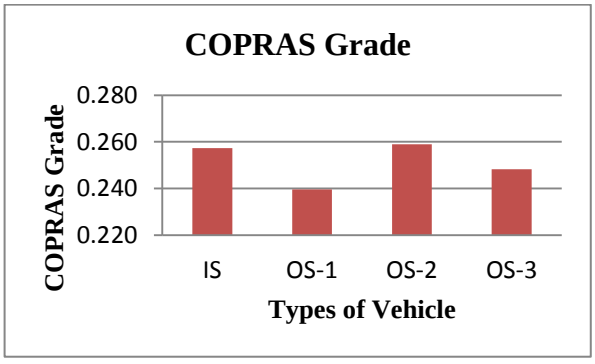

Fig.3. Ranking of vehicle

4. CONCLUSION

This paper discusses the optimization of blind spots in the front of the heavy vehicle which is an important aspect of road safety. A hybrid multi criteria optimization model by integrating COPRAS and FAHP was proposed in the reduction of blind spot. This model was tested by a case study and the effectiveness of the model was proved. Based on the suggestion of optimized design of driver's seat, there is a great chance for the reduction of area of blind spots in the front of the heavy vehicle.

REFERENCES

[1] R. Carrier "Ergonomic study of the Driver's work station in urban buses", *Canadian Urban Transit Association Publishers*, 1992.

[2] Mehdi Ahmadian and Christopher Boggs "Safety Effects of operator seat Design in large commercial vehicles", *Final Report Safety IDEA Project*, 2005.

[3] Onawumi A. Samuel and Lucas E. Babajide "Ergonomic Investigation of Occupational Drivers and Seat Design of Taxicabs in Nigeria", *ARPN Journal of Science and Technology*, Vol. 2, No.3, pp. 214-220, 2012.

[4] S. Park, Y. Lee, Y. Nahm, J. Lee and J. Kim "Seating Physical Characteristics and Subjective Comfort: Design Considerations", *SAE Technical Paper 980653*, doi: 10.4271/980653, 1998.

[5] W. Shen and A. Vertiz "Redefining Seat Comfort", *SAE Technical Paper 970597*, doi: 10.4271/970597, 1997.

[6] Wu Liyun, Yang Yuzhong and Jing Guoxun "Technique for order preference by similarity to ideal solution (TOPSIS) for safety synthetic evaluation on coal mine transportation system", *Progress in Safety Science and Technology* VI: 87-91, 2006.

[7] Qiong Bao, Da Ruan, Yongjun Shen, Elke Hermans and Davy Janssens "Improved hierarchical fuzzy TOPSIS for road safety performance evaluation", *Knowledge-Based Systems Archive*, Vol. 32, pp. 84-90, 2012.

[8] Moataz Mahmoud and Julian Hine "Using AHP to measure the perception gap between current and potential users of bus services", *Transportation Planning and Technology*, Vol. 36, No. 1, pp. 4-23, 2013.

[9] Thomas L. Saaty "How to make a decision: the analytic hierarchy process", *European Journal of Operations Research*, Vol. 48, No. 1, pp. 9-26, 1990.

[10] Mohamad Ashari Alias, Siti Zaiton Mohd Hashim and Supiah Samsudin "Using fuzzy analytic hierarchy process for southern Johor river ranking", International Journal of Advanced Soft Computing Applications, Vol. 1, No. 1, pp. 62-76, 2009.

[11] D.S. Vincent, P. Pitchipoo and S. Rajakarunakaran "Elimination of Blind Spots for Heavy Transport Vehicles by Driver Seat Design", *Proceedings of the second International Conference on Advanced Manufacturing and Automation*, Krishnankoil, India, 2013.

ICAMM 2015

INDO-BRAZIL Bilateral International Conference on
ADVANCED MATERIALS AND MANUFACTURING – ICAMM 2015
Tirunelveli-TN/INDIA, March 27-28, 2015

HYBRID INTELLIGENT DECISION MODEL FOR SUPPLIER EVALUATION AND SELECTION

Pitchipoo. P[1*], Ragavan. R[1], Rajakarunakaran. S[2]
[1]Department of Mechanical Engineering, P.S.R Engineering College Sivakasi-626 140.
[2] Department of Mechanical Engineering, Ramco Institute of Technology, Rajapalayam-626 117
*Corresponding Author *Email: drpitchipoo@gmail.com*

Abstract: Selecting the right suppliers significantly reduces the purchasing costs and improves corporate competitiveness. The importance on quality and timely delivery of raw materials plays a major role, since most of the industries have been spending around 60% of their revenues on purchasing. The supplier selection problem involves multiple conflicting tangible and intangible issues. The aim of this study is to develop an intelligent based hybrid decision model for supplier selection using Data Envelopment Analysis (DEA) and Fuzzy Analytic Hierarchy Process (FAHP). The DEA used to determine the relative efficiencies of multiple suppliers. FAHP is used to compute the weights of the evaluation criteria involved in supplier selection process. A case study is performed in a chemical processing industry and the effectiveness of the developed model is verified.

Keywords*: Supplier evaluation, Supplier selection, Data envelopment analysis, Fuzzy analytic hierarchy process*

1 Introduction

In the current global economy, organizations are forced to face variety of changes due to competitions. This situation increases pressures on organizations to adopt the concept of supply chain management (Tracey & Tan 2001). Supplier management comprises supplier evaluation, supplier selection and supplier development. The selection of supplier makes impact on the performance and competitive elements of the supply chain. The evaluation of supplier is an unstructured decision problem because of lack of adequate needed information and the availability of qualitative information in the form of intangible sense. In supplier evaluation decisions, the following fundamental questions such as "what criterion is used" and "what methods can be used" should be addressed. In today's competitive operating environment it is impossible to successfully produce low cost, high quality products without satisfactory vendors. Thus one of the important purchasing decisions is the selection and maintenance of a competent group of suppliers (Weber et al., 1991). The objective of this paper is to develop a hybrid model by combining DEA and FAHP for selecting the best supplier for a chemical processing industry. The remaining part of the paper is organized as follows: Section 2 illustrates the review of related literatures; Section 3 explains the development of model for supplier selection. In section 4, the case study is discussed. Finally, Section 5 concludes the study.

2 Literature Review

2.1 Review on supplier selection

Dickson (1966) carried out a study by the help of a survey which was conducted in 300 business organizations. The purchasing managers of those organizations were requested to identify the factors that were influencing the supplier selection. As an outcome of the survey, totally 23 factors were identified as important factors for the supplier selection decision problem. Supplier selection is complicated by the fact that various criteria must be considered in the decision making process. The analysis of criteria for selection and measuring the performance of the suppliers has been the focus of many research papers. Weber et al. (1991) reviewed a total of 74 research papers on supplier selection and identified net price (cost), delivery, quality, production capability, geographical location, technical capability, reputation, financial position, performance history and warranty are the most contributed criteria for supplier selection. Wilson (1994) reviewed the relative importance of supplier selection criteria and observed that quality, service, price and delivery are the most important selection criteria. Ho et al. (2010) made review about the literatures of the multi-criteria decision making approaches for supplier evaluation and selection. This research not only provided evidence that the multi-criteria decision making approaches are better than the traditional cost-based approach, but also aided the researchers and decision makers in applying the approaches effectively.

2.2 Review on DEA

Narasimhan et al. (2001) applied DEA model to evaluate alternative suppliers for a multinational corporation in the telecommunications industry. Eleven evaluating factors were considered in the model, in which there are six inputs related to the supplier capability, and five outputs related to the supplier performance. Talluri and Sarkis (2002) developed DEA based model for performance monitoring of suppliers. Wu and Blackhurst (2009) proposed a supplier evaluation and selection methodology based on an extension of DEA to evaluate suppliers. The weight constraints were introduced to reduce the possibility of having inappropriate input and output factor weights. Mishra and Patel (2010) will develop an application guideline for the assessment, improvement, and control of quality in SCM using DEA. Improvement in the quality of all supply chain processes lead to cost reductions as well as service enhancement. The data is collected from 25 suppliers of food and agro based industry. Amindoust et al. (2012) stated that the multiple attribute utility theory based on DEA applied to tackle this problem with consideration of some inputs and outputs. A real case study was implemented to show the application of DEA method and through this method the efficient and inefficient suppliers were identified to ranking them.

2.3 Review on FAHP

Chan et al (2008) applied FAHP to efficiently tackle both quantitative and qualitative decision factors involved in selection of global supplier. Kuo et al (2010) developed a performance evaluation method by integrating FAHP method and fuzzy DEA for supplier selection problem. FAHP method was first applied to find the indicators' weights through expert questionnaire survey and fuzzy DEA was applied for ranking. Pitchipoo et al (2013) used FAHP to determine the weights of the influencing

criteria while developing a decision model for supplier evaluation and selection. Ayhan (2013) used FAHP in a gear motor company to determine the best supplier. Do and Chen (2014) applied FAHP and DEA for measuring the efficiency scores of universities. FAHP was employed to get the weights of output indicators then. DEA approach measured the performance of Vietnamese universities.

3 Model Development

In this study the best supplier was selected by using Data Envelopment Analysis (Fig. 1). It can be used to evaluate the efficiency of a number of producers, generally referred as decision making unit (DMU).

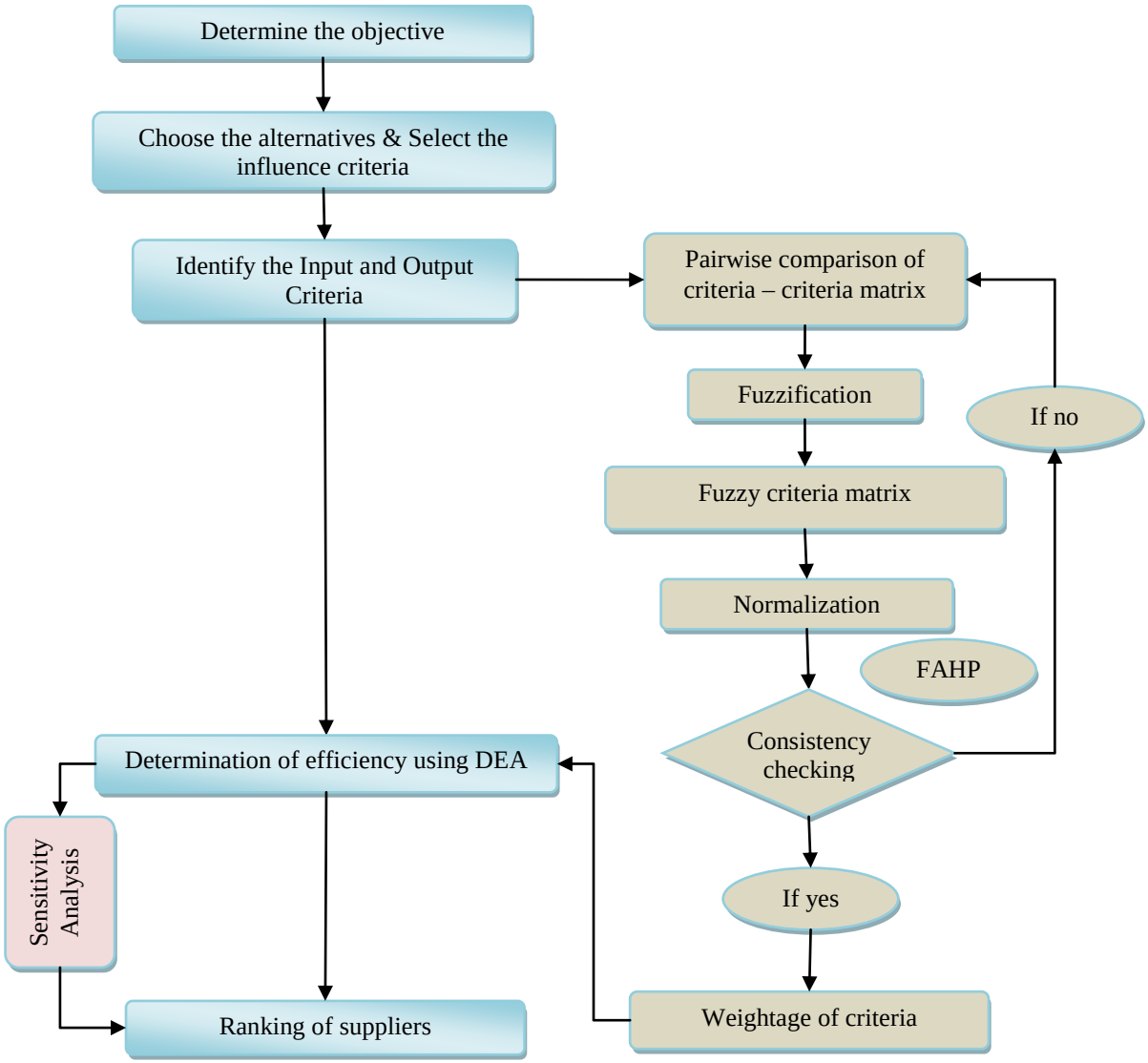

Fig.1. Proposed model

DEA compares each producer with only the "best" DMU in the group, which is better than the comparison with average of the group. In DEA, we can consider number of DMUs, each of them consuming similar inputs to varying level to produce. A fundamental assumption behind this method is that if a given DMU, is capable of producing units of output with inputs, then other DMUs shall also be able to do the same if they were to operate efficiently. Similarly, if DMU is capable of producing units of output with inputs, then other DMUs should also be capable of the same. DMUs and others can then be combined to form a composite producer i.e. virtual producer with composite inputs and composite outputs. The emphasis of DEA is on finding the "best" virtual producer for each real producer. Figure 1 explains the frame work for the supplier selection. DEA was used to evaluate the performance of hospitals, universities, cities, business firms etc.

A general mathematical formulation is needed to handle the case of multiple inputs and multiple outputs. This mathematical formulation was provided by Charnes et al. (1978). Let us use *x* and *y* to represent inputs and outputs, respectively. Let the subscripts *i* and *j* to represent particular inputs and outputs respectively. Thus x_i represents the i^{th} input, and y_j represent the j^{th} output of a decision-making unit. Let the total number of inputs and outputs be represented by *I* and *J* respectively, where *I, J* > 0. In DEA, multiple inputs and outputs are linearly aggregated using weights. Thus, the virtual input (eqn. 1) of a firm is obtained as the linear weighted sum of all its inputs.

$$Virtual\ Input = \sum_{i=1}^{I} u_i\, x_i \qquad (1)$$

Similarly, the virtual output (eqn. 2) of a firm is obtained as the linear weighted sum of all its outputs.

$$Virtual\ Output = \sum_{j=1}^{J} v_j\, y_j \qquad (2)$$

Given these virtual inputs and outputs, the *Efficiency* (eqn. 3) of the DMU in converting the inputs to outputs can be defined as the ratio of outputs to inputs.

$$Efficiency = \frac{Virtual\ Output}{Virtual\ Input} \qquad (3)$$

$$Efficiency = \frac{\sum_{j=1}^{J} v_j\, y_j}{\sum_{i=1}^{I} u_i\, x_i}$$

Where,

i = 1, 2, 3…..I are inputs
j = 1, 2, 3…..J are outputs
s = 1, 2, 3…..N are DMU_S
u_i = weight of i^{th} input
v_i = weight of j^{th} output
x_{is} = amount of the i^{th} input for s^{th} DMU
y_{js} = amount of the j^{th} output for s^{th} DMU

In this paper FAHP method is used to compute the weights of each criterion. In FAHP, Saaty's (1990) analytical hierarchy process is combined with fuzzy concept. Based on the opinion of the decision maker, the evaluation criteria are compared. The ranking of the criteria used for evaluation was collected and the criteria matrix was formed based on the Saaty's nine point scale which is shown in Table 1.

The pair wise comparison matrix is called original matrix or criteria matrix which is given by matrix X_{att} as shown below.

$$X_{att} = [a_{ij}]; 1 \le i, j \le m \qquad (4)$$

where, a_{ij} = Pair wise comparison of i^{th} and j^{th} attribute. m = the number of alternatives

Table 1 Equivalent triangular fuzzy number for Saaty's nine point scale

Verbal judgment or preference	Saaty's scale of relative importance	Triangular fuzzy numbers
Extremely preferred	9	9,9,9
Very strongly to extremely preferred	8	7,8,9
Very strongly preferred	7	6,7,8
Strongly to very strongly preferred	6	5,6,7
Strongly preferred	5	4,5,6
Moderately to strongly preferred	4	3,4,5
Moderately preferred	3	2,3,4
Equally to moderately preferred	2	1,2,3
Equally preferred	1	1,1,1

This was converted into fuzzy original matrix using TFN prescribed by Mohamad et al. (2009) which is also shown in Table 1. Then the fuzzy original matrix is normalized using equation (5).

$$N_{ij} = \frac{a_{ij}}{T_j} \qquad (5)$$

where a_{ij} is the cell value of i^{th} row and j^{th} column in the fuzzy original matrix; $1 \le i, j \le m$; and $T_j = \sum_{i=1}^{m} a_{ij}$

The weights were calculated by converting fuzzy numbers into crisp values by using defuzzification technique. In this study, centroid method was used for defuzzification which is given in equation (6).

$$\text{Weights } W_i = \frac{\sum_{i-1}^{k} D_p^i * O^i}{\sum_{i=1}^{k} D_p^i} \qquad (6)$$

where k is the number of rules, O^i is the class generated by rule i (from 0, 1, …. L-1); L is the number of classes and

$$D_p^i = \prod_{i=1}^{n} m_{li} \quad (7)$$

where n is the number of inputs and m_{li} is the membership grade of feature l in the fuzzy regions that occupies the i^{th} rule.

Since the pairwise comparison matrix is formulated based on human judgment, it is must to ensure that the values collected are accepted values. To check the consistency, the Consistency Ratio (CR) is calculated using equation (8)

$$CR = CI/RI \quad (8)$$

where CI is Consistency Index which is determined using equation (9) and RI is random indices for criteria size 'm'.

$$CI = \frac{\lambda_{max} - m}{m-1} \quad (9)$$

where λ_{max} is the maximum eigen value and m is the number of criteria

RI was approximated by Saaty (1990) which is shown in table 2. If the CR is < 0.10 the decision maker's pairwise comparison matrix is acceptable.

Table 2. Random indices

m	1	2	3	4	5	6	7	8	9	10	11	12
RI	0	0	0.58	0.90	1.12	1.24	1.32	1.41	1.45	1.49	1.51	1.58

4 Case Study

The case study was performed in a chemical industry which is located in the southern part of Tamilnadu. For this study, the supplier selection model was developed based on five suppliers (S1, S2, S3, S4 and S5) with five evaluating factors, that include three inputs and two outputs namely, delivery (D) in days, capacity (Ca) in units, warranty (W) in number of days, cost (C) in rupees and quality (Q) in percentage of acceptance respectively. The Table 3 shows the data of suppliers and the corresponding inputs and outputs.

Table 3 Datasets of inputs and outputs

Suppliers	Inputs			Outputs	
	D	Ca	W	C	Q
S1	12	170	28	2439	0.87
S2	12	260	21	2567	0.90
S3	14	280	21	2711	0.92
S4	10	260	24	2800	0.96
S5	13	290	18	2302	0.89

The weights of the attributes are calculated by using FAHP method using equations (4) to (6). The fuzzy original matrix is shown in Table 4. Then the fuzzy original matrix is normalized using equation (5) and shown in Table 5.

Table 4. Fuzzy original matrix

	C			Q			D			W			Ca		
C	1	1	1	1/3	1/4	1/5	1/5	1/6	1/7	4	5	6	4	5	6
Q	3	4	5	1	1	1	1	1/2	1/3	4	5	6	6	7	8
D	5	6	7	1	2	3	1	1	1	6	7	8	9	9	9
W	1/4	1/5	1/6	1/4	1/5	1/6	1/6	1/7	1/8	1	1	1	2	3	4
Ca	1/4	1/5	1/6	1/6	1/7	1/8	1/9	1/9	1/9	1/2	1/3	1/4	1	1	1
Total	9.5	11.4	13.3	2.75	3.59	4.5	2.48	1.92	1.71	15.5	18.33	21.25	22	25	28

Table 5. Fuzzy normalized matrix

	C			Q			D			W			Ca		
C	0.11	0.09	0.08	0.12	0.07	0.04	0.08	0.09	0.08	0.26	0.27	0.28	0.18	0.20	0.21
Q	0.32	0.35	0.38	0.36	0.28	0.22	0.40	0.26	0.19	0.26	0.27	0.28	0.27	0.28	0.29
D	0.53	0.53	0.52	0.36	0.56	0.67	0.40	0.52	0.58	0.39	0.38	0.38	0.41	0.36	0.32
W	0.03	0.02	0.01	0.09	0.06	0.04	0.07	0.07	0.07	0.06	0.05	0.05	0.09	0.12	0.14
Ca	0.03	0.02	0.01	0.06	0.04	0.03	0.04	0.06	0.06	0.03	0.02	0.01	0.05	0.04	0.04

Then the weights are calculated by using equation (6) and shown in Table 6. Then DEA efficiency for all suppliers is determined by using equation 3 and the values are tabulated in Table 7.

Table 6 Weights of the attributes

Criteria		Weights
Input	Delivery	0.442
	Capacity	0.050
	Warranty	0.078
Output	Quality	0.275
	Cost	0.165

Table 7 Efficiency of suppliers

Suppliers	Efficiency	
	Using FAHP	With Equal weights
S1	75.17	65.45
S2	79.71	67.24
S3	72.51	64.77
S4	96.7	73.34
S5	72.04	62.78

Fig.2 depicts the DEA Efficiency of the suppliers. From the table 7, the supplier with higher efficiency (ie. Supplier 4) is selected as best supplier.

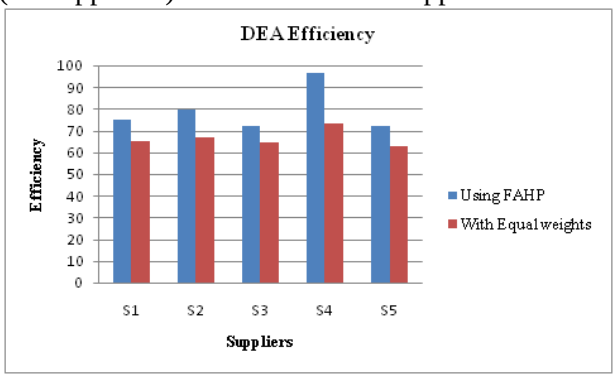

Fig. 2. DEA efficiency

Sensitivity analysis is used to determine how "sensitive" a model is during the changes in the value of the parameters of the model and in the structure of the model. It is performed to do a tradeoff study and to check the robustness of the model. In sensitivity analysis, the values of any one input parameter were changed and the changes in output performance indices were measured. In this study, equal weights were assumed for the criteria and the efficiency was observed. Fig. 3 shows the result of the sensitivity analysis. From the Fig. 3, it is observed that the ranking of the suppliers is not changing and hence the robustness of the proposed model is proved.

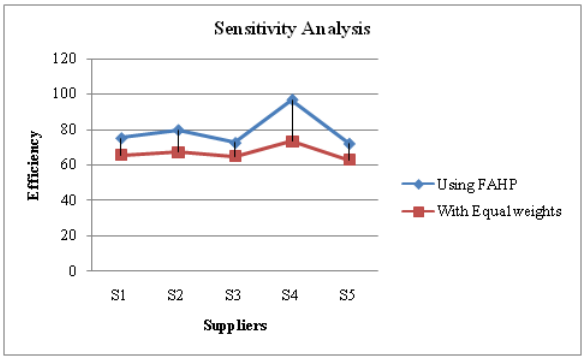

Fig. 3. Sensitivity of the DEA model

5 Conclusion

In this work a multi-criteria decision making model based on DEA for selecting the best supplier was developed. For the selection of supplier, multiple criteria which include quality, delivery, cost, capacity and warranty were considered. And the weights of the criteria were computed in FAHP technique. The results were compared and finally the robustness of the developed model was checked by the sensitivity analysis. This model gives a reliable result and it can be extended for the same kind of industries. This proposed model can be more flexible to accommodate the qualitative and quantitative criteria for supplier selection.

References

[1] A. Charnes, W.W. Cooper and E. Rhodes "Measuring the efficiency of decision making units", *European Journal of Operational research*, Vol. 2, No. 23, pp. 429-44, 1978.

[2] Atefeh Amindoust Shamsuddin Ahmed and Ali Saghafinia "Supplier selection and performance evaluation of telecommunication company", *American Journal of Engineering and Applied Sciences*, Vol. 5, No. 1, pp. 49-52, 2012.

[3] C.A. Weber, J.R. Current and W.C. Benton "Vendor selection criteria and methods", *European Journal of Operational Research*, Vol. 50, No. 1, pp. 2-18, 1991.

[4] E. Wilson "The relative importance of supplier selection criteria: A review and update," *International Journal of Purchasing and Material Management*, Vol. 30, No. 3, pp. 35–41, 1994.

[5] Felix T. S. Chan , N. Kumar , M. K. Tiwari , H. C. W. Lau and K. L. Choy "Global supplier selection: a fuzzy-AHP approach", *International*

Journal of Production Research, Vol. 46, No. 14, pp. 3825-3857, 2008./

[6] G.W. Dickson "An analysis of vendor selection systems and decisions", *Journal of Purchasing*, Vol. 2, No. 1, pp. 5-17, 1966.

[7] Michael Tracey and Chong Leng Tan "Empirical analysis of supplier selection and involvement, customer satisfaction, and firm performance", *Supply Chain Management: An International Journal*, Vol. 6, No. 4, pp.174 – 188, 2001.

[8] Mohamad Ashari Alias, Siti Zaiton Mohd Hashim and Supiah Samsudin "Using fuzzy analytic hierarchy process for southern Johor river ranking", *International Journal of Advanced Soft Computing Applications*, Vol. 1, No. 1, pp. 62-76, 2009.

[9] Mustafa Batuhan Ayhan "A fuzzy AHP approach for supplier selection problem: a case study in a gear motor company", *International Journal of Managing Value and Supply Chains*, Vol.4, No. 3, pp. 11-23, 2013

[10] P. Pitchipoo, P. Venkumar and S. Rajakarunakaran "Fuzzy hybrid decision model for supplier evaluation and selection", *International Journal of Production Research* Vol. 51, No. 13, pp. 3903-3919, 2013.

[11] Quang Hung Do and Jeng-Fung Chen "A Hybrid Fuzzy AHP-DEA Approach for Assessing University Performance", *WSEAS Transactions on Business and Economics*, Vol. 11, pp. 386-397, 2014.

[12] R. Narasimhan, S.Talluri and D. Mendez "Supplier evaluation and rationalization via data envelopment analysis: An empirical examination", *International Journal of Supply Chain Management*, Vol. 37, No. 3, pp. 28–37, 2001.

[13] R.J. Kuo, L.Y. Lee and Tung-Lai Hu "Developing a supplier selection system through integrating fuzzy AHP and fuzzy DEA: A case study on an auto lighting system company in Taiwan", *Production Planning & Control: The Management of Operations*, Vol. 21, No. 5, pp. 468-484, 2010.

[14] Rohita Kumar Mishra and Gokulananda Patel "Supplier development strategies: A data envelopment analysis approach, *Business Intelligence Journal*, Vol. 3, No. 1, pp. 84 – 95, 2010.

[15] S. Talluri and J. Sarkis "A model for performance monitoring of suppliers", *International Journal of Production Research*, Vol. 40, No. 16, pp. 4257–4269, 2002.

[16] Thomas L. Saaty "How to make a decision: the analytic hierarchy process", *European Journal of Operations Research*, Vol. 48, No. 1, pp. 9-26, 1990.

[17] William Ho, Xiaowei Xu and Prasanta K. Dey "Multi-criteria decision making approaches for supplier evaluation and selection: A literature review", *European Journal of Operational Research*, Vol. 202, No. 1, pp. 16–24, 2010.

[18] Wu and Jennifer Blackhurst "Supplier evaluation and selection: an augmented DEA approach", *International Journal of Production Research*, Vol. 47, No. 16, pp. 4593-4608, 2009.

INDO-BRAZIL Bilateral International Conference on
ADVANCED MATERIALS AND MANUFACTURING – ICAMM 2015
Tirunelveli-TN/INDIA, March 27-28, 2015

RISK PRIORITISATION OF FAILURE MODES FOR DISPENSING SYSTEM IN A LPG DISPENSING STATION

A. Maniram Kumar [1*], Sivaprakasam Rajakarunakaran [2], V. Arumuga Prabu [3]
[1] Department of Mechanical Engineering, Dr. Sivanthi Aditanar College of Engineering, Tiruchendur 628215, Tamilnadu, India,
[2] Department of Mechanical Engineering, Ramco Institute of Technology, Rajapalayam 626117, Tamilnadu, India,
[3]Department of Mechanical Engineering, Kalasalingam University, Anand Nagar,Krishnankoil 626126, Tamilnadu, India
* Corresponding author (maniramkumar.wings@gmail.com)

Abstract: A considerable interest nationwide is shown for using LPG as a vehicle fuel to address clean air goals and environmental issues. Safe practices in storage, handling, distribution, and end uses of LPG are essential for the successful promotion of LPG vehicles. Systematic risk control at each stage is required to minimize or eliminate failures. In this work, a risk analysis was performed using the FMEA technique, which helps to identify potential problems that may exist in a dispensing system of a LPG refuelling station before they occur. It was performed in a commercial LPG refueling outlet in Chennai (India). Possible failure modes contributing a risky hazardous situation or pose a disturbance to normal operation are identified, documented and analysed. Risk priority numbers were calculated to identify the risk level of each potential failure and ranked. A preventive maintenance schedule is suggested based on the FMEA results. The implemented FMEA study will aid, decreasing failures noticeably in all the processes and operations performed. The findings of this study can be used by the LPG refueling outlets located in different regions to ensure safe operation.

Keywords*:*
- Risk Assessment
- Failure mode effect analysis
- Risk prioritization
- Maintenance prioritization
- Failure mode

1 Introduction

Automotive Liquefied Petroleum Gas (LPG) is a mixture of light hydrocarbons primarily predominantly Propane or combinations of Propane : Butane 'mixes' derived from petroleum(BIS 14861), which is gaseous at ambient temperature and atmospheric pressure, is liquefied at ambient temperature with application of moderate pressure.

Increased public awareness for environmental protection and stricter pollution control norms propagating use of efficient fuels have steadily pulled to the trend for LPG conversion for auto fuel and diversion of domestic fuel to auto fuel at a steady growth of @ 8% p.a. in LPG consumption in India. [1]. LPG is a flammable, noncorrosive, nontoxic, odorless, liquid [2]. LPG, being heavier than air, having low boiling point and any leakage, will quickly vaporizes and accumulates, increasing the risk of explosion and fire [3]. Contact with LPG fire can cause the severe burns on skin and asphyxiation effects are possible [4]. Meticulous understanding of the failure of systems and its components, the causes, the consequences and the actions needed to avoid them is an important concern for stakeholders in the industry, highly recommended for loss prevention.

The FMEA is a proactive analysis tool, allowing engineers to define, identify, and eliminate known and/or potential failures, problems, errors, and so on from the system, design, process, and/or service [5,6]. Developed and implemented by the United States Army in the 1970s, its application field extended first to aerospace and automotive industry, then to general manufacturing [7]. Since then, it has become a powerful tool extensively used for risk and reliability analysis of systems in a wide range of industries, including automotive, construction, aerospace, nuclear, and electro-technical. FMEA is a structured, bottom-up approach that starts with potential/known failure modes at one level and investigates the effect on the next sub-system level [8]. Hence, a complete FMEA analysis of a system often spans all the levels in the hierarchy from bottom to top. In this case FMEA is applied to LPG dispensing in a refuelling station.

The organization of the paper is as follows: The paper begins with the introduction and motivation behind the work done on the paper. Discussion about the LPG dispensing outlet, technical details, the dispensing system and its operations are mentioned in Section 2. A brief introduction to FMEA is given in Section 3. The application of the FMEA for the risk analysis of the dispensing system is reported in Section 4. The concluding remarks and further research proposals are expressed in Section 5.

2 Liquefied petroleum gas dispensing station

Liquefied petroleum gas is delivered in LPG bullets to the sites via trucks. A Positive displacement sliding vane pump is used to transfer LPG from bullet to high pressure storage tank of 10,000 liters capacity. The storage tank is provided with a pump well for installing a submersible pump which fuels at 700 kPa with a flow rate of 65 L/min. A dispenser of flameproof type transfers LPG to vehicles from storage tank via nozzle. A return line leading to the vapor space of the LPG storage tank is provided for the dispenser.

Remote operated shut-off valve is provided for the return line of the dispenser. A pump control mechanism is provided in the dispenser such that the submersible pump of the filling system can be switched on/off automatically when the dispensing nozzle is in and out of its receptacle. A breakaway coupling is provided to protect against leakage of LPG liquid in the event of drive away with nozzle engaged to the vehicle. The LPG Fueling Station outlet studied has its common design bases as follows; Vehicles refueled=120 per day; Vehicles per hour= 5No's & Vehicle refueling time= 2 min/vehicle. The specifications for installation of an auto LPG Dispensing Station confirms with Oil Industry Safety Directorate Guidelines, SMPV Rules as amended in Feb 2000. The layout observes the separation distances of storage vessels between each other and from boundary line of the dispensing station stated in SMPV Rules. Figure 1 shows the process flow diagram.

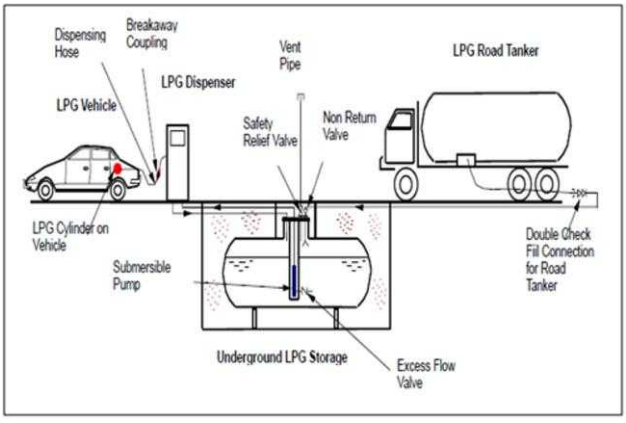

Fig.1. LPG dispensing station process flow diagram

.

3 FMEA

Applying FMEA follows a series of successive steps: analysis of the process, product or system in every single part, list of identified potential failures, evaluation of their frequency, severity (in terms of effects of the failure to the process/product/system and to its surroundings) and detection technique, global evaluation of the problem and identification of the corrective actions and control plans that could eliminate or reduce the chance of the potential failures [7, 9].

The Risk Priority Number (RPN) is calculated for each failure mode by multiplying the three determined values of occurrence, severity and not detection (O x S x D). The global value of the damages caused on the function or on the surroundings by every failure is indicated with the risk priority number (RPN) [7]. The RPN values of each failure mode are expressed on ordinal qualitative scales [10,11]. A number between 1 and 10 (with 1 being the best and 10 being the worst case) is given for each of the three factors to quantify them. The RPN calculated represents the seriousness of potential risks critical to reliability, safety of systems or productivity of process [12]. The RPN value helps the FMEA team to identify the components or subsystems that need the priority actions for improvement. Depending on the maintenance decisions, different criteria are used to trigger the improvement actions.

The process for carrying out an FMEA [13] using different standards are similar and simple. Table 1 show the qualitative scales commonly used for the occurrence, severity, and (not) detection indexes. This depicts the traditional use of five scales and scores of 1–10, to measure the probability of occurrence, severity and the probability of detection.

Table 1: FMEA scale for occurrence (O), severity (S), not detection (D)

Description	***Occurrence***	***Severity***	***Detection***	***Rank***
Very high	Persistent failures	Hazardous without warning	Absolute certain to not detect	10
Very high	Persistent failures	Hazardous with warning	Probably not detect	9
High	Frequent failures	Very high	Poor chance	8
High	Frequent failures	High	Poor chance	7
Medium	Occasional failures	Moderate	May detect	6
Medium	Occasional failures	Low	May detect	5
Medium	Occasional failures	Very low	Good chance	4
Low	Relatively few failures	Minor	Good chance	3
Low	Relatively few failures	Very minor	Almost certain	2
Almost none	Failure is unlikely	None	Certain to detect	1

4 FMEA applied to dispenser

The failure modes which are more possible to occur provided with higher ranking and other failure modes are ranked according to their percentage of occurrence. A single failure mode may be the result of a sequence of sub events each of which has an associated frequency of occurrence. In such cases, the relative risk rating that was assigned to the failure mode occurrence frequency was the sub-event frequency with the lowest risk rating. Typically this sub event would prevent other sub-events with higher risk-ratings from materializing. The failure modes which are related to safety and which has the potential to stop the process for more than two hours provided with higher severity rating. The severity ranking for the failure modes which have the tendency to stop the process for less than two hours are ranked according to their approximate repair time. Simple problems like rupture in hose are quite easy to detect. So these failure modes are categorized into low detection rating. Similarly complex problems like pump clearance checking, loose connections in electrical panel has higher detection rating and other failure modes were ranked according to the criticality of their detection. Based on the FMEA team's recommendation the scores for frequency, occurrence and detection were applied. The RPN scores allow for the overall identification of the prioritization of safety improvement efforts for the dispensing system.

5 Results and Discussion

The FMEA analysis shows the failure modes that are categorised as follows:

- LPG Dispenser - **II.1 to II.6** - (6 failure modes)
- LPG dispensing pump - V.1 to V.9 - (Submersible) (9 failure modes)
- Remote operated valve - VI.1 to VI.4 - (4 failure modes)

No	*Failure Mode*	*Cause*	*Effects (C)*	*Detection (D)*	*Frequency (F)*	*Controls*	*F*	*C*	*D*	*RPN*
LPG Dispenser										
1.	Piping failure	Vehicle impact to dispenser	Potential fire or explosion	Visual, Gas detection	Relatively few failures	Bollards around dispenser	2	8	3	48
2.	Drive away connected to dispenser	Human error	Rupture of hose & potential of fire	Visual indication	Occasional failures	Break away coupling	4	6	2	48
3.	Hose failure	Mechanical failure	Release of & potential of fire	Visual & Sensitive verification	Occasional failures	Odorized gas & LPG rated hose	5	5	2	50
4.	Leak in connection	O-ring damaged or nozzle damaged	Release of & potential of fire	Sensitive verification & Gas detectors	Occasional failures	Dispensers leak check before fill	5	5	2	50
5.	Vehicle pressure relief device leaks	Mechanical failure	Release of LPG & potential of fire or explosion	Visual & Sensitive verification	Relatively few failures	Relief valve on vehicle tank vents	2	6	2	24
6.	Nozzles leaks after disconnect	Mechanical failure	Release of LPG and potential of fire	Visual & Sensitive verification	Occasional failures	Dispenser valve closes	5	4	2	40
LPG Dispensing Pump (Submersible)										
7.	No Vehicle Fill	Dispenser malfunctioning or not authorizing	No delivery of fuel & fuel filling interrupted	Check the function of trigger	Occasional failures	Check function periodically	4	8	3	96
8.		Blocked filters	No delivery of fuel and fuel filling interrupted	Check the filter indicators	Occasional failures	Change filters periodically	4	8	3	96
9.		Insufficient LPG in tank	No delivery of fuel and fuel filling interrupted	Visual inspection	Occasional failures	Check fluid level periodically	4	8	3	96
10.	Low Fuel Flow	Restriction in nozzle	Fuel filling interrupted	Visual inspection	Occasional failures	Clean periodically	4	8	3	96
11.		Dirt/debris in pump	Heat generation and contamination	Visual inspection	Relatively few failures	Change filters periodically	2	5	4	40
12.		Faulty bypass valve	Pump system over pressure	Check the valve function	Relatively few failures	Provide good valve settings	3	5	5	75
13.	Pulsing Flow	Insufficient LPG in tank/excessive inlet restriction	Low pump output fuel supply interrupted	Visual inspection	Occasional failures	Check fluid level periodically	4	8	2	64
14.	No Fuel Output	No power supply to pump or pump contactor fault	No delivery of fuel and fuel filling interrupted	Check the voltage	Occasional failures	Provide correct fuse ratings	4	8	2	64
15.		Drive Motor fail	No delivery of fuel and fuel filling interrupted	Check Resistance of motor coils	Relatively few failures	Check & tight the terminals periodically	3	8	2	48

No	*Failure Mode*	*Cause*	*Effects (C)*	*Detection (D)*	*Frequency (F)*	*Controls*	*F*	*C*	*D*	*RPN*
Remote Operated Valve (ROV)										
16.	Valve Not Opening	No power supply	No fuel Delivery/Filling	Check the voltage	Relatively few failures	Provide correct fuse ratings	3	5	2	30
17.		Solenoid failure	No fuel Delivery/Filling	Check the coil resistance	Relatively few failures	Do thermography	3	7	5	105
18.		No adequate pneumatic pressure	No fuel Delivery/Filling	Check the air pressure	Occasional failures	Check compressor periodically	4	5	3	60
19.	Closing Very Slowly	Dirt in valve	Potential spreading of fire in case of any fire	Jerk in movement - valve spool	Relatively few failures	Change filters periodically	2	8	4	64

The results indicated that the ROV solenoid failure was source of major risks to safety and operation with the highest RPN followed by the dispenser malfunctioning and blocked filters in dispensing pump. The quantitative results derived from FMEA application are emphasized in this section. The average of the computed RPN number is found as "62.84'' that is recognized as the threshold value to decide whether the precautions are required. According to this assumption, a severe level of preventive action necessitates for especially for system components such as, ROV and dispensing pump, due to their high RPN values (i.e. RPN # 105, RPN # 96, RPN # 96, etc.). Dispenser failures were of RPN values less than the average computed RPN. Counting over the whole FMEA, the top 9 failure modes are depicted as histograms in Fig. 2. To express the utilization of the FMEA application results, one of the failure modes is discussed in detail. The results addresses that, solenoid failure on remote operated valve is the most significant failure mode with highest RPN value # 105. The aim is to remedy the gap between the process technology and operational practices by suggesting proactive maintenance regime and producing combined precautions. The number of times of open & close can be reconsidered in accordance life of the solenoid before maintenance/replacement. This operational control can be appreciated with technology integration into existing control systems. An additional unit that continuously monitors pumps performance (i.e. Opening/Closing, Inlet/Outlet flow rate, pressures, noise levels) can be integrated. The similar approach can be followed for the other components and their corresponding failure modes subsequently.

Consequently, the FMEA of the system aid us to produce precautions both in system design and operational levels to prevent the risks of failure mode. A preventive maintenance schedule is prepared, by which the reliability of the system enhances, is shown in Table4. The results from this study might help operators/manufacturers since the all LPG dispensing outlets share common operational stages.

6 Conclusion

FMEA approach, widely used for risk analysis, has been successfully applied to the dispensing system of a LPG refuelling station. The results from this study might help operators/manufacturers worldwide, since the all LPG dispensing outlets share common operational stages. A cost-benefit analysis for reducing failures could also be conducted based on a priority list of the most frequent failure modes. A similar analysis could also be considered based on failure modes severity. Further study proposals might include analyzing the major operating failures in other LPG systems and infrastructures such as; tankers, tanker transfers, vaporisers cylinder filling plant and stacks of cylinders and its transportation, storage yards, etc.

TABLE 3 : FMEA RESULTS *(*RANKING*)*

Rank	*FM No*	*Failure Mode*	*RPN*
1	**17**	Valve Not Opening	105
2	**7**	No Vehicle Fill	96
3	**8**	No Vehicle Fill	96
4	**9**	No Vehicle Fill	96
5	**10**	Low Fuel Flow	96
6	**12**	Low Fuel Flow	75
7	**13**	Pulsing Flow	64
8	**14**	No Fuel Output	64
9	**19**	Valve Closing Very Slowly	64
10	**18**	Valve Not Opening	60
11	**3**	Hose failure	50

12	**4**	Leak in connection	50
13	**1**	Piping failure	48
14	**2**	Drive away connected to dispenser	48
15	**15**	No Fuel Output	48
16	**6**	Nozzles leaks after disconnect	40
17	**11**	Low Fuel Flow	40
18	**16**	Valve Not Opening	30
19	**5**	Vehicle pressure relief leaks	24

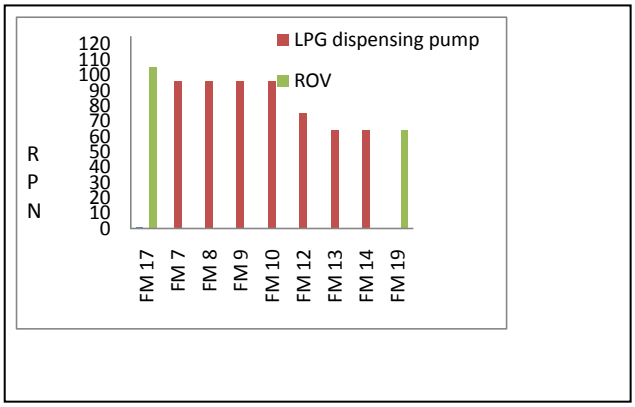

Fig. 2. Top Failure Modes and RPN scores

Table: 4 Preventive Maintenance Schedule

Maintenance procedures		PERIODICITY				
		Daily	**Weekly**	**Monthly**	**Quarterly**	**Half Yearly**
1	Check operation of emergency switch	▲				
2	Check function of Gas detectors			▲		
3	Check Mechanical seal / gland/pipe line leakage			▲		
4	Check Current ratings				▲	
5	Check vibration/Noise					▲
6	Check full closing/opening of valves		▲			
7	Check tightness of joints				▲	
8	Check suction strainers of Pumps			▲		
9	Check alignment pump/ motor					▲
10	Check Resistance value of earth connections					▲
11	Check lubrication Bearings			▲		
12	Check function of level Gauges/switches			▲		
13	Check function of pressure relief valve					▲
14	Check Hoses for damage/leak		▲			
15	Check Dispenser nozzle for damage/leak		▲			
16	Check breakaway couplings/excess flow valves			▲		
17	Check Fire fighting system			▲		

References

[1] Apurva Chandra, Indian LPG Market Prospects, World LPG Forum (2010)-Madrid. Retrived December 30, 2014 from petrofed.winwinhosting.net/upload/**Apurva_Chandra**.pdf

[2] Indian Oil Corporation Limited, LPG Specification, Retrieved December 20, 2014, from http://www.iocl.com/products/lpgspecifications.pdf

[3] R. Levine, and A.D. Little. Guidelines for Safe Storage and Handling of High Toxic Hazard Materials, Center for Chemical Process Safety (CCPS), American Institute of Chemical Engineers, 1988

[4] Centers for Disease Control and Prevention (1978), Occupational Health Guideline for LPG, retrieved December 28, 2014, from http://www.cdc.gov/niosh/docs/81-123/pdfs/0372.pdf

[5] Omdahl, T.P. Reliability, Availability and Maintainability Dictionary. American Society for Quality, Quality Press., 1988

[6] Stamatis, D.H., Failure Mode and Effect Analysis: FMEA from Theory to Execution, second ed. American Society for Quality, Quality Press, 2003

[7] Scipioni, A., Saccarola, G., Centazzo, A., Arena, F.," FMEA methodology design, implementation and integration with HACCP system in a food company", *Food Control*, 13, 495–501, 2002

[8] Sharma, R. K., Kumar, D. and Kumar, P. "Systematic failure mode effect analysis (FMEA) using fuzzy linguistic modelling". *Intl. J. Quality & Reliability Management*, 22(9), 986–1004, 2005.

[9] Ireson, G., Coombs, W., Clyde, F., Richard. Y.M., Handbook of Reliability Engineering and Management. (2nd ed.)New York: McGraw-Hill Professional, 1995.

[10] Fraser, N.M.,"Ordinal preference representations", *J. Theory and Decision* 36 (1), 45–67, 1994

[11] Franceschini, F., Rossetto, S," Design for quality: selecting product's technical features" *J. Quality Engineering*, 9 (4), 681–688, 1997

[12] Seung, NY., Kosuke J.R, Using cost based FMEA to enhance reliability and serviceability. *J. Advanced Engineering Informatics*, 17, 179–188, 2003

[13] Pillay, A., & Wang, J, "Modified failure mode and effects analysis using approximate reasoning", *Reliability Engineering & System Safety*, 79, 69-85, 2003.

ESTIMATION OF WEIGHTS IN MULTI CRITERIA DECISION MAKING PROBLEMS - A COMPARATIVE STUDY

Pitchipoo P[1], Vincent D.S[2], Rajini N[3], Rajakarunakaran S[4]
[1]*Department of Mechanical Engineering, P.S.R. Engineering College, Sivakasi.*
[2]*Tamil Nadu State Transport Corporation Ltd., Thiruvannamalai.*
[3]*Department of Mechanical Engineering, Kalasalingam University, Krishnankoil.*
[4]*Department of Mechanical Engineering, Ramco Institute of Technology, Rajapalayam.*
Email: [1]drpitchipoo@gmail.com

Abstract - Many decisions made in real world environment are depending on the evaluation of several influencing criteria called multi criteria decision making (MCDM) problems. The crucial part of MCDM problem is the determination of weights to the evaluation criteria. Improper weights lead poor decisions. Several methods are used to find the weights of the criteria. In this paper, a comparison of three human judgment based techniques such as Factor Relationship (FARE), Analytical Hierarchy Process (AHP) and Fuzzy Analytical Hierarchy Process (FAHP) is discussed using a case study.

Keywords - Multi criteria decision making; Weights; FARE; AHP; FAHP

I.INTRODUCTION

Evaluation of alternatives based on many criteria belongs to discrete MCDM models where all the alternatives and criteria are known. To solve this problem, it is must to know the preferences of the decision maker. These preferences can be described by the weights of the criteria. Lot of different methods ([1] & [2]) was used to determine the weights of the criteria. Entropy measurement, a mathematical method was used to determine the weightage of the criteria. Siva et al [3] used entropy measurement method to find the weights of the output responses while improving the mechanical properties of natural fiber composites. Pitchipoo et al [4] developed a decision model to select the optimal supplier for a chemical processing industry using grey relational analysis (GRA). Entropy measurement method was used to determine the weightage of the influencing criteria for supplier selection. Accommodation of qualitative criteria is the limitation of this method.

In real world many data are available in qualitative nature. To make accurate decisions all data should be used. In order to use the qualitative data, human judgment based techniques are used. Pitchipoo et al [5] used AHP and FARE methods to determine the weights of the design parameters used in the design of rear view mirror to reduce the blind spot area in heavy vehicles. The results are compared with the result obtained with the result obtained through entropy measurement method. As an outcome AHP and FARE outperform entropy measurement method. Ginevicius and Podvezko [6] applied FARE method for determining the criteria weights, to find the alternative solutions of wall insulation or winter proofing of buildings. Ginevicius [7] developed a new method of determining the criteria weights called FARE, based on the relationships between all the criteria describing the phenomenon considered.

Wang et al [8] developed an optimization model to address the modification of spare parts and evaluate the suppliers and distributes spare parts supplied by the suppliers. In this mathematical model, AHP was proposed for

the formulation of factor weights and particle swarm optimization (PSO) algorithm was used for solving the mathematical model. Lin and Hsu [9] developed a model for selecting Internet advertising networks. This model comprised of two parts in which AHP was used to determine the relative weights of evaluative criteria and in the second part GRA was used to rank the alternatives and select the best Internet advertising network for advertisers. Yang and Chen [10] proposed supplier evaluation model using combined AHP and GRA to select the optimal supplier for a notebook computer manufacturing industry. The AHP was used to determine the weightage of the criteria and GRA was used to rank the suppliers. Cao et al [11] developed an integrated decision making system using AHP and GRA for the selection of material for housing of an electronic device. AHP was used to determine the relative importance among the criteria and the GRA was used to select the material. Sevkli et al [12] developed data envelopment analytic hierarchy process for supplier selection Turkey. The weights of the criteria were determined using AHP and ranking was done by data envelopment analysis (DEA).For selecting optimum route of gas pipeline FAHP and GRA were integrated [13]. FAHP was used to find the weights and GRA was used for classification. Olson and Wu [14] presented the simulation of a multi attribute models for uncertain environment. The model was developed using fuzzy and GRA. This paper demonstrated how simulation can be used to reflect fuzzy inputs, which allows more complete probabilistic interpretation of model results.

Several researchers used different methods for the determination of weights of the criteria for MCDM problems. In this paper three different weight determination methods are compared using a MCDM problem.

II.METHODOLOGY

The weights of the criteria are calculated using FARE, AHP and FAHP methods. The algorithms of these methods are shown in Figure 1a, 1b and 1c.

A. FARE Method

Ginevicius [7] developed FARE method (Figure 1a) for determining the criteria weights in multi criteria decision making environment. First the potential impact of the criteria is determined using equation (1).

$$P = S\,(m - 1) \tag{1}$$

where P – Potential of the system's criterion impact; S – Maximum value of the scale of evaluation used (TableI);

m – Number of the system's criteria.

Next the criteria are ranked by the experts based on the importance. Then the relationship between the criteria is determined based on the rank using Table I. The procedure is as follows: the criterion of a lower rank has the smaller impact on the criteria having higher ranks and, therefore, it should transfer a larger part of its potential impact to them.

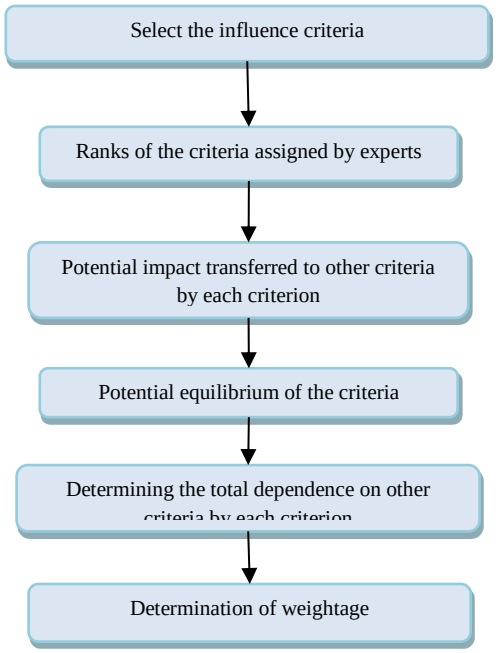

Figure 1a. FARE algorithm

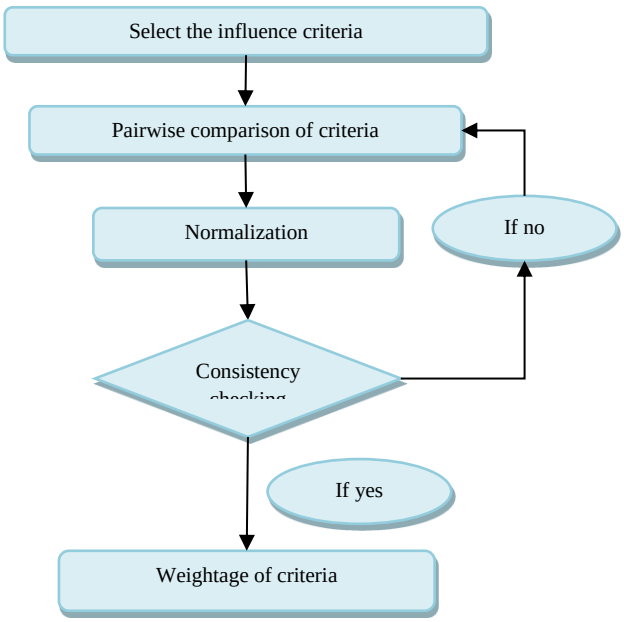

Figure 1b. AHP algorithm

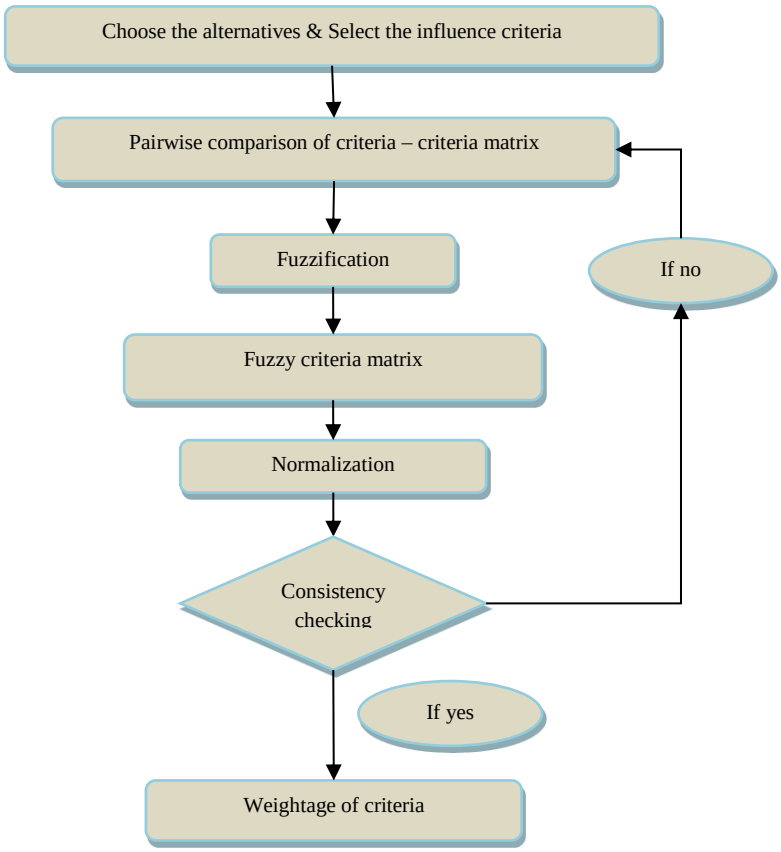

Figure 1c. FAHP algorithm

The impact of the criteria a_i on the main criterion is determined and then, this impact is transformed as follows:

$$a_{1i} = S - \tilde{a}_{1i} \quad (2)$$

where,

a_i – the impact of i^{th} criterion on the first main criterion;

$\tilde{a}_i$ – the part of i^{th} criterion's potential impact transferred to the main criterion

TABLE I

SCALE OF QUANTITATIVE EVALUATION OF INTERRELATIONSHIP BETWEEN THE SYSTEM'S CRITERIA

No.	Type of the Effect Produced	Rating of the Effect Produced by Interrelationship (in points)
1	Almost none	1
2	Very Weak	2
3	Weak	3
4	Lower than Average	4
5	Average	5
6	Higher than average	6
7	Strong	7
8	Very Strong	8
9	Almost absolute	9
10	Absolute	10

The total impact of any criterion, as well as the consistency level of a subset may be determined based on the data provided in the form of matrix. The subset considered in the matrix is consistent and stable if the total impact of its criteria with a positive sign is equal to their total impact with a negative sign, i.e. their sum is equal to zero [7]. Next the total impact P_i calculated using equation (3).

$$P_i = \sum_{i=1}^{m} a_{ij},\ j \neq i \quad (3)$$

After that, the total potential, required for determining the criteria weights, will be calculated based on the data presented in the first row of the matrix, thereby making the filling of all other rows of the matrix unnecessary. The following equation (4) is used for determining the total potential.

$$P_i = P_1 - m.\ a_{1i}, \quad (4)$$

where

P_i – the total impact (dependence) of the i^{th} criterion.

Finally, the criteria weights can be determined using equation (5).

$$\omega_i = \frac{P_i^f}{P_S} = \frac{P_1 - ma_{1i} + S(m-1)}{mS(m-1)} \quad (5)$$

where P_S = Total potential of a set of criteria which is found using equation (6) and

P_i^f = Actual total impact of the i^{th} criterion of the system which is calculated using equation (7)

$$P_S = m.\ P = mS\ (m - 1) \quad (6)$$

$$P_i^f = P_i + P \quad (7)$$

where P_i = Total impact produced by the i^{th} criterion of the system or its total dependence on other criteria.

B. AHP Method

AHP one of the human judgment based tool used to determine the weights of the criteria in the MCDM problems was introduced by Saaty [15], The weights of the criteria using AHP are determined by the following steps (Figure 1b):

- *Pairwise comparison of attributes*

Each attribute is compared with other attributes in a natural, pairwise mode. The fundamental scale that captures individual preferences with respect to quantitative and qualitative data [15] is shown in Table II. It converts individual preferences into a linear additive weight for each alternative. The pair wise comparison matrix is also called original matrix which is given by matrix X_{att} as shown in equation (8).

TABLE II

MEASUREMENT SCALE FOR PAIR WISE COMPARISON AND EQUIVALENT TRIANGULAR FUZZY NUMBER

Verbal judgment or preference	Numerical rating	Triangular fuzzy numbers
Extremely preferred	9	9,9,9
Very strongly to extremely preferred	8	7,8,9
Very strongly preferred	7	6,7,8
Strongly to very strongly preferred	6	5,6,7
Strongly preferred	5	4,5,6
Moderately to strongly preferred	4	3,4,5
Moderately preferred	3	2,3,4
Equally to moderately preferred	2	1,2,3
Equally preferred	1	1,1,1

All the cell values are assigned based on the importance of the attributes received from the experts.

$$X_{att} = [a_{ij}]; 1 \leq i, j \leq n \quad (8)$$

where, a_{ij} = Pair wise comparison of i^{th} and j^{th} attribute; n = the number of alternatives

$$X_{att} = \begin{bmatrix} a_{11} & a_{12} & \dots . a_{1n} \\ a_{21} & a_{22} & \dots . a_{2n} \\ \vdots & \vdots & \vdots \\ a_{n1} & a_{n2} & a_{nn} \end{bmatrix}$$

- *Normalization*

Then the pairwise comparison matrix is normalized using the equation (9) and the normalized matrix N_{att} is obtained.

$$N_{ij} = \frac{a_{ij}}{T_j} \quad (9)$$

where $T_j = \sum_{i=1}^{n} a_{ij}, 1 \leq j \leq n$

$$N_{att} = \begin{bmatrix} N_{11} & N_{12} & \dots . N_{1n} \\ N_{21} & N_{22} & \dots . N_{2n} \\ \vdots & \vdots & \vdots \\ N_{n1} & N_{n2} & N_{nn} \end{bmatrix}$$

- *Computation of weights*

After the normalization, the weights W_j are computed from the normalized matrix using equation (10).

$$w_j = \frac{\sum_{j=1}^{n} N_{ij}}{n} \quad (10)$$

From the weights of the attributes *Watt* matrix will be formulated as shown in equation (11)

$$W_{att} = \begin{bmatrix} w_1 \\ w_2 \\ w_3 \\ :: \\ :: \\ w_n \end{bmatrix} \tag{11}$$

- *Consistency checking*

The consistency of the proposed pairwise comparison was checked using the equation (12).

Consistency Ratio *CR = CI/RI* (12)

where *CI* = Consistency Index and *RI* = Random indices.

$$CI = \frac{\lambda_{max} - n}{n-1} \tag{13}$$

where $\lambda_{\max}$ = Max of B or n;

$$B = \left(\frac{\frac{A_1}{w_1} + \frac{A_2}{w_2} + \frac{A_3}{w_3} + \cdots + \frac{A_m}{w_m}}{m} \right) \tag{14}$$

where m=Number of criteria and A_1, A_2 ….. A_m are calculated using the equation (16).

$$[X_{att}] * [W_{att}] = [A] \tag{15}$$

$$\begin{bmatrix} a_{11} & a_{12} & \ldots . a_{1n} \\ a_{21} & a_{22} & \ldots . a_{2n} \\ : & : & : \\ a_{n1} & a_{n2} & a_{nn} \end{bmatrix} * \begin{bmatrix} W_1 \\ W_2 \\ : \\ W_n \end{bmatrix} = \begin{bmatrix} A_1 \\ A_2 \\ : \\ A_n \end{bmatrix} \tag{16}$$

Random indexes (*RI*) for various number of variables ‘n’ have been approximated by Saaty [15] as shown in Table III.

TABLE III

RANDOM INDICES

n	1	2	3	4	5	6	7	8	9	10
RI	0	0	0.58	0.90	1.12	1.24	1.32	1.41	1.45	1.49

If the CR < 0.10 the decision maker's pairwise comparison matrix is acceptable [15].

C. FAHP method

In FAHP (Figure 1c), Saaty’s [15] analytical hierarchy process is combined with fuzzy concept. Based on the opinion of the decision maker, the evaluation criteria are compared. The ranking of the criteria used for evaluation was collected and the criteria matrix was formed based on the Saaty’s nine point scale which is shown in Table II. This was converted into fuzzy original matrix using TFN prescribed by Mohamad et al. [16] which is also shown in Table II. Then the fuzzy original matrix is normalized using equation (9). The weights were calculated by converting fuzzy numbers into crisp values by using defuzzification technique. In this study, centroid method was used for defuzzification which is given in equation (17).

Weights $W_i = \frac{\sum_{i-1}^{k} D_p^i * O^i}{\sum_{i=1}^{k} D_p^i}$ (17)

where k is the number of rules, O^i is the class generated by rule i (from 0, 1, …. L-1); L is the number of classes and

$$D_p^i = \prod_{i=1}^{n} m_{li} \quad (18)$$

where n is the number of inputs and m_{li} is the membership grade of feature l in the fuzzy regions that occupies the i^{th} rule.

Since the pairwise comparison matrix is formulated based on human judgment, it is must to ensure that the values collected are accepted values. To check the consistency, the Consistency Ratio (CR) is calculated using equation (12).

III.RESULTS AND DISCUSSION

To test the developed models, a case study is conducted in a public transport division in Tamilnadu with four different types of vehicle bodies. One of the bodies of the vehicles is built in the same organization (IS) and other three are outsourced (OS -1, OS – 2 & OS – 3) bodies. The design and implementation of rear view mirror in heavy vehicle is a MCDM problem which is highly influenced by the following variables such as the distance between the driver and the right side of the body pillar or frame structure (A), the distance between the driver and the left side of the body pillar or frame structure (B), the distance of driver's eye right height from the platform (C) and the distance between the centre of the rear view mirror and the ground level (D). The data set collected through the case study is given in Table IV.

TABLE IV
DATA SET

Types of Vehicle	A (cm)	B (cm)	C (cm)	D (cm)
IS	36	178	122	242
OS – 1	34	181	123	240
OS – 2	34	182	123	224
OS - 3	34	177	119	204

A. Determination of Weights by FARE Method

- No. of criteria (m) = 4
- Max. value of scale (s) = 10
- Potential of the system (P) = 30
- total potential of individual criteria =PS = 120

The potential impact of the attributes for this work is 30. Next the attributes are ranked by the experts based on the importance. As per the experts opinion the order of attributes are A, B, D and C. The interrelationships between the system's attributes (Table V) based on their ranks are quantified by using Table I.

The potential impact transferred to the first main criterion is calculated by using equation (2) and shown in Table VI. Finally the weights of the attributes are determined by using the equations (3) to (7) and tabulated in the Table VI.

TABLE V

INTER RELATIONSHIP BETWEEN THE ATTRIBUTES

Attributes	A	B	C	D
A		2	6	4
B	-2		4	2
C	-6	-4		-2
D	-4	-2	2	

TABLE VI

POTENTIAL IMPACT, ACTUAL IMPACT (P_I^F) AND WEIGHTS OF THE CRITERIA

Attributes	A	B	C	D	Sum	P_i^f	Weight
A		8	4	6	18	48	0.4
B	-8		6	8	6	36	0.3
C	-4	-6		-8	-18	12	0.1
D	-6	-8	8		-6	24	0.2

B. Determination of Weights by AHP Method

The pair wise comparison matrix for this study is shown in Table VII. For the quantification, Table II is used.

TABLE VII

PAIR WISE COMPARISON MATRIX

	A	B	C	D
A	1	2	5	3
B	0.5	1	4	2
C	0.2	0.25	1	0.25
D	0.333	0.5	4	1
Total	2.033	3.75	14	6.25

Then the normalized matrix (Table VIII) is computed using equation (9). Next the consistency of the proposed pairwise comparison was checked using the equation (12) and found as 0.037 which is less than 0.1. Hence the used pairwise comparison is acceptable. The weights are computed from the normalized matrix using equation (10) and shown in Table VIII.

TABLE VIII

NORMALIZED MATRIX

	A	B	C	D	Weights
A	0.492	0.533	0.357	0.480	0.466
B	0.246	0.267	0.286	0.320	0.280
C	0.098	0.067	0.071	0.040	0.069
D	0.164	0.133	0.286	0.160	0.186

C. *Determination of Weights by FAHP Method*

First the pairwise comparison matrix shown in Table VII is fuzzified using triangular fuzzy numbers (Table II) and converted into fuzzy original matrix (Table IX). Then the fuzzy original matrix is normalized using equation (9) and given in Table X. The consistency of the proposed pairwise comparison was checked and found as 0.0907 which is less than 0.1. Hence the used pairwise comparison is acceptable. The weights are computed from the normalized matrix after defuzzification using equation (17) and shown in Table X.

TABLE IX

FUZZY ORIGINAL MATRIX

	A			B			C			D		
A	1.000	1.000	1.000	1.000	2.000	3.000	4.000	5.000	6.000	2.000	3.000	4.000
B	1.000	0.500	0.333	1.000	1.000	1.000	3.000	4.000	5.000	1.000	2.000	3.000
C	0.250	0.200	0.167	0.333	0.250	0.200	1.000	1.000	1.000	0.333	0.250	0.200
D	0.500	0.333	0.250	1.000	0.500	0.333	3.003	4.000	5.000	1.000	1.000	1.000
Total	2.750	2.033	1.750	3.333	3.750	4.533	11.003	14.000	17.000	4.333	6.250	8.200

TABLE X

FUZZY ADJUSTED MATRIX

	A			B			C			D			Weights
A	0.364	0.492	0.571	0.300	0.533	0.662	0.364	0.357	0.353	0.462	0.480	0.488	0.459
B	0.364	0.246	0.190	0.300	0.267	0.221	0.273	0.286	0.294	0.231	0.320	0.366	0.281
C	0.091	0.098	0.095	0.100	0.067	0.044	0.091	0.071	0.059	0.077	0.040	0.024	0.075
D	0.182	0.164	0.143	0.300	0.133	0.074	0.273	0.286	0.294	0.231	0.160	0.122	0.210

D. *Comparison of weights*

The weights computed by the three different techniques are shown in Table XI and Figure 2. All the three methods gave very closer weights for the criteria. Among these methods FAHP performs well because both tangible and intangible factors can be accommodated well than any other methods.

TABLE XI

COMPARISON OF WEIGHTS

	Weights of Criteria		
Criteria	FARE	AHP	FAHP
A	0.4	0.466	0.459
B	0.3	0.280	0.281
C	0.1	0.069	0.075
D	0.2	0.186	0.210

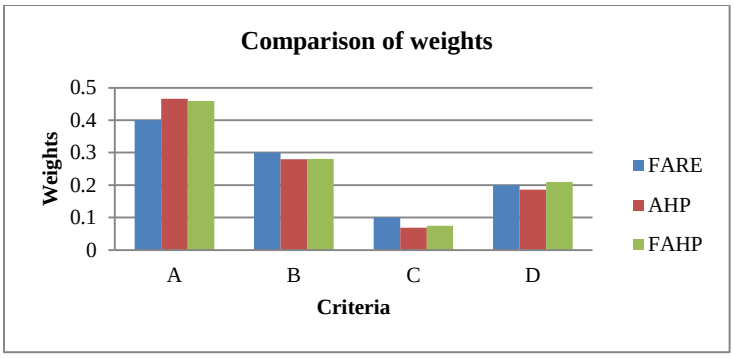

Figure 2 Comparison of weights

IV. CONCLUSION

This paper analyzes three human judgment based weight determination techniques and the results were compared. FARE method is basically simple method and the weights obtained are not accurate as AHP and FAHP. Conceptually both AHP and FAHP are same but FAHP gave accurate weights due to its ability to use vague and inaccurate data. AHP is a better method when the available data is in crisp form. FAHP can able to use continuous data and hence it produces accurate result than others.

REFERENCES

[1] G.W. Evans, "An Overview of Techniques for Solving Multiobjective Mathematical Programs", *Manage. Sci.,* Vol. 30, No. 11, 1984, pp.1268-1282.

[2] J. Figueira, S. Greco and M. Ehrgott, *Multiple criteria decision analysis - State of the art surveys.* New York: Springer, 2005.

[3] I. Siva, J.T. Winowlin Jappes, P. Pitchipoo, S.C. Amico, E.R. Nagarajan and N. Azhagesan, "Grey optimization of process parameters of surface modification of novel coconut sheath reinforced polymer composites" *J. Polym. Eng.*, Vol. 33, No. 7, 2013, pp. 665–672.

[4] P. Pitchipoo, P. Venkumar and S. Rajakarunakaran S, "Grey decision model for supplier evaluation and selection in process industry: A comparative perspective", *Int. J. Adv. Manuf.Technol.*, DOI 10.1007/s00170-014-6406-2, 2014.

[5] P. Pitchipoo, D.S. Vincent, N. Rajini and S. Rajakarunakaran S, "COPRAS decision model to optimize blind spot in heavy vehicles: A comparative perspective", *Procedia Eng.*, Vol. 97, pp. 1049 – 1059, 2014.

[6] Romualda Ginevicius and V. Podvezko, "The influence of complex evaluation methods on rating the alternative solutions of wall insulation", Presented at the 2007 Int. Conf. Mod. Build. Mat. Struct. Tech. Vilnius, Lithuani.

[7] Romualdas Ginevicius, "A new determining method for the criteria weights in multicriteria evaluation", *Int. J. Inf. Technol. Decis. Mak.*, Vol. 10, No. 6, 2011, pp. 1067–1095

[8] H.S. Wang , Z.H. Che and Chienwen Wu, "Using analytic hierarchy process and particle swarm optimization algorithm for evaluating product plans", *Expert Syst. Appl.* Vol. 37, 2010, pp.1023–1034

[9] Chin-Tasi Lin and Pi-Fang Hsu, "Selection of internet advertising networks using an analytic hierarchy process and grey relational analysis", *Inform. Manage.Sci.*, Vol. 14, No. 2, 2003, pp. 1-16.

[10] Ching-Chow Yang and Bai-Sheng Chen, "Supplier selection using combined analytical hierarchy process and grey relational analysis", *J. Manuf. Technol. Manage.*, Vol. 17, No. 7, 2006, pp. 926-941.

[11] Huajun Cao, Fei Liu, Congbo Li and Chun Liu, "An integrated method for product material selection considering environmental factors and a case study", *Mat. Sci.Forum*, Vol. 532-533, 2006, pp. 1032-1035.

[12] S.C. Mehmet Sevkli, Lenny Koh, Selim Zaim, Mehmet Demirbag and Ekrem Tatoglu, "An application of data envelopment analytic hierarchy process for supplier selection: a case study of BEKO in Turkey", *Int. J. Prod. Res.*, Vol. 45, No. 9, 2007, pp. 1973–2003.

[13] Ali Mohamadi and Payam shojaei, "Determining gas pipeline optimum route by using integrated FAHP/GRA model", *Australian J. Busi. Manage. Res.* Vol.1, No.3, 2011, pp. 75-88.

[14] David L. Olson and Desheng Wu, "Simulation of fuzzy multiattribute models for grey relationships", *Euro. J. Oper. Res.*, Vol. 175, 2006,

pp. 111–120.

[15] Thomas L. Saaty, *The analytic hierarchy process, planning, priority setting, resource allocation*. New York: McGraw-Hill, 1980.

[16] Mohamad Ashari Alias, Siti Zaiton Mohd Hashim and Supiah Samsudin, "Using fuzzy analytic hierarchy process for southern Johor river ranking", *Int. J. Adv. Soft Comput. Appl.*, Vol. 1, No. 1, 2009, pp. 62-76.

HYBRID DEA DECISION MODEL FOR SUPPLIER EVALUATION AND SELECTION

Pitchipoo. P[1*], Ragavan. R[1], Rajakarunakaran. S[2]

[1]Department of Mechanical Engineering, P.S.R Engineering College Sivakasi-626 140.

*Corresponding Author *Email: drpitchipoo@gmail.com*

[2] Department of Mechanical Engineering, Ramco Institute of Technology, Rajapalayam-626 117.

Abstract

Competitive international business environment has forced many firms to focus on supply chain management to cope with highly increasing competition. Selecting the right suppliers in the supply chain significantly reduces the purchasing costs and improves corporate price competitiveness. The emphasis on quality and timely delivery in today's globally competitive marketplace plays a major role, since most of the firms have been spending considerable amount of their revenues on purchasing. The supplier selection problem involves multiple conflicting issues that are tangible and intangible. Hence, the purpose of this study is to propose an integrated model for supplier selection based on Data Envelopment Analysis (DEA). It has been used to evaluate suppliers' performance when there are multiple inputs and outputs in the supplier selection problem. The DEA determines the relative efficiencies of multiple suppliers. In this paper, the Factor Relationship (FARE) is used to determine the weights of criteria involved in supplier selection process. A case study is made in chemical process industry based on the above model and its efficiency is verified.

Keywords: Supplier Evaluation, Supplier Selection, Data Envelopment Analysis, FARE

1 Introduction

Supply chain management (SCM) is the process of planning and monitoring the transformation of raw material into product in an organization. The concept of SCM was originally introduced by consultants in 1980s and has gained tremendous attention now. Several issues were identified and addressed by the researchers such as network planning, supplier management and physical distribution. Among those, supplier management is the key issue because more than 60% of the sales revenue is spent for the purchase of raw material. Supplier management comprises supplier evaluation, supplier selection and supplier development. Selecting a good set of suppliers to work with is crucial to a company's success. Over the years, the significance of supplier selection has been long recognized and emphasized. In today's competitive operating environment it is impossible to successfully produce low cost, high quality products without satisfactory vendors. Thus one of the important purchasing decisions is the selection and maintenance of a competent group of suppliers (Weber et al., 1991). More recently, with emergence of the concept of Supply Chain Management (SCM), more and more scholars and practitioners have realized that supplier selection and management was a vehicle that can be used to increase the competitiveness of the entire supply chain (Lee et al., 2001).

The evaluation of supplier is an unstructured decision problem because of lack of adequate needed information and the availability of qualitative information in the form of intangible sense. In supplier decisions, two fundamental questions must be addressed. Firstly, what criterion should be used and secondly, what methods can be used compare suppliers. The objective of this paper is to develop a hybrid model by combining AHP and for selecting the best supplier for a chemical processing industry. The remaining part of the paper is organized as follows: Section 2 illustrates the review of related literatures; Section 3 explains the development of model for supplier selection. In section 4, the case study is discussed. Finally, Section 5 concludes the study and outlines some future research directions.

2 Literature Review

Dickson (1966) carried out a study by the help of a survey which was conducted in 300 business organizations. The purchasing managers of those organizations were requested to identify the factors that were influencing the supplier selection. As an outcome of the survey, totally 23 factors were identified as important factors for the supplier

selection decision problem. Supplier selection is complicated by the fact that various criteria must be considered in the decision making process. The analysis of criteria for selection and measuring the performance of the suppliers has been the focus of many research papers. Weber et al. (1991) reviewed a total of 74 research papers on supplier selection and identified net price (cost), delivery, quality, production capability, geographical location, technical capability, reputation, financial position, performance history and warranty are the most contributed criteria for supplier selection. Wilson (1994) reviewed the relative importance of supplier selection criteria and observed that quality, service, price and delivery are the most important selection criteria. Ho et al. (2010) made review about the literatures of the multi-criteria decision making approaches for supplier evaluation and selection. This research not only provided evidence that the multi-criteria decision making approaches are better than the traditional cost-based approach, but also aided the researchers and decision makers in applying the approaches effectively.

Narasimhan et al. (2001) applied DEA model to evaluate alternative suppliers for a multinational corporation in the telecommunications industry. Eleven evaluating factors were considered in the model, in which there are six inputs related to the supplier capability, and five outputs related to the supplier performance. Talluri and Sarkis (2002) developed DEA based model for performance monitoring of suppliers. Wu et al. (2007) proposed an augmented DEA approach for selection of suppliers. The model was capable to handle imprecise data to rank the efficient suppliers and covered the discrimination among them based on discriminating efficient suppliers from relatively poor performers. Wu and Blackhurst (2009) proposed a supplier evaluation and selection methodology based on an extension of DEA to evaluate suppliers. The weight constraints were introduced to reduce the possibility of having inappropriate input and output factor weights. Mishra and Patel (2010) will develop an application guideline for the assessment, improvement, and control of quality in SCM using DEA. Improvement in the quality of all supply chain processes lead to cost reductions as well as service enhancement. The data is collected from 25 suppliers of food and agro based industry. Amindoust et al. (2012) stated that the multiple attribute utility theory based on DEA applied to tackle this problem with consideration of some inputs and outputs. A real case study was implemented to show the application of DEA method and through this method the efficient and inefficient suppliers were identified to ranking them.

3 Model Development

In this study the best supplier was selected by using Data Envelopment Analysis (Figure 1). It can be used to evaluate the efficiency of a number of producers, generally referred as decision making unit (DMU).

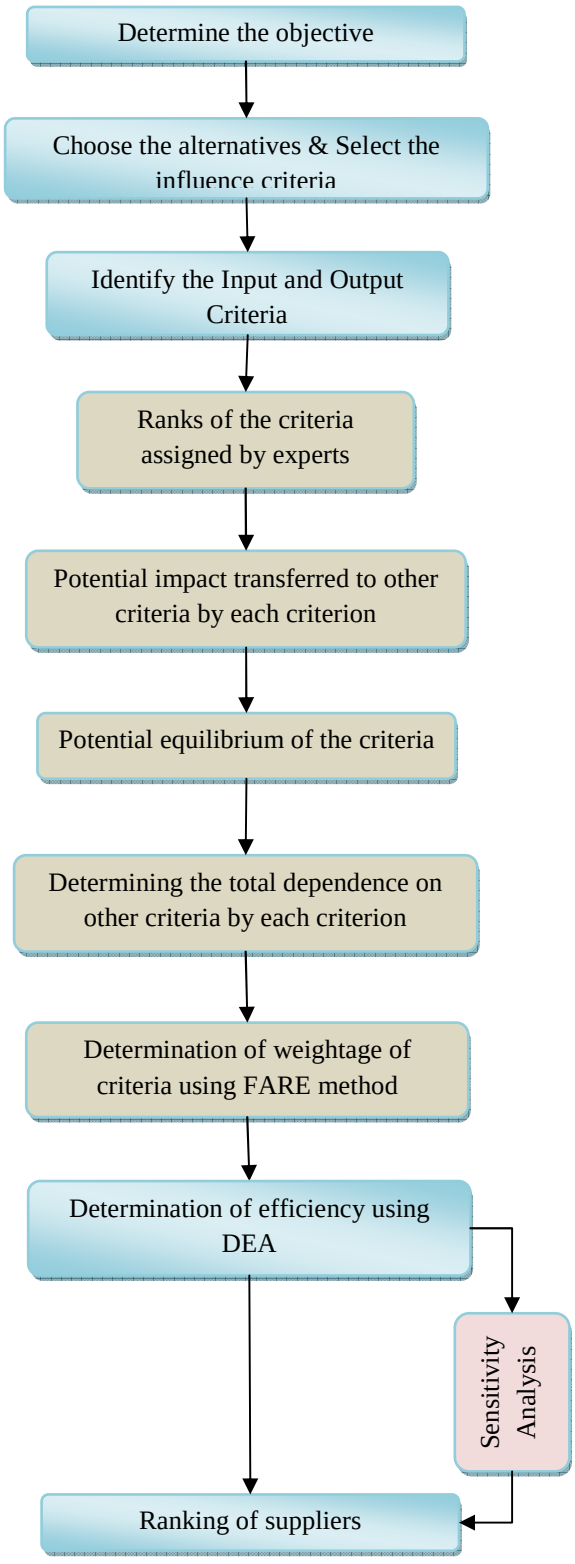

Figure 1 Proposed model

DEA compares each producer with only the "best" DMU in the group, which is better than the comparison with average of the group. In DEA, we

can consider number of DMUs, each of them consuming similar inputs to varying level to produce. A fundamental assumption behind this method is that if a given DMU, is capable of producing units of output with inputs, then other DMUs shall also be able to do the same if they were to operate efficiently. Similarly, if DMU is capable of producing units of output with inputs, then other DMUs should also be capable of the same. DMUs and others can then be combined to form a composite producer i.e. virtual producer with composite inputs and composite outputs. The emphasis of DEA is on finding the "best" virtual producer for each real producer. Figure 1 explains the frame work for the supplier selection. DEA was used to evaluate the performance of hospitals, universities, cities, business firms etc.

A general mathematical formulation is needed to handle the case of multiple inputs and multiple outputs. This mathematical formulation was provided by Charnes et al. (1978). Let us use *x* and *y* to represent inputs and outputs, respectively. Let the subscripts *i* and *j* to represent particular inputs and outputs respectively. Thus x_i represents the i^{th} input, and y_j represent the j^{th} output of a decision-making unit. Let the total number of inputs and outputs be represented by *I* and *J* respectively, where $I, J > 0$. In DEA, multiple inputs and outputs are linearly aggregated using weights. Thus, the virtual input (eqn. 1) of a firm is obtained as the linear weighted sum of all its inputs.

$$Virtual\ Input = \sum_{i=1}^{I} u_i\, x_i \qquad (1)$$

Similarly, the virtual output (eqn. 2) of a firm is obtained as the linear weighted sum of all its outputs.

$$Virtual\ Output = \sum_{j=1}^{J} v_j\, y_j \qquad (2)$$

Given these virtual inputs and outputs, the *Efficiency* (eqn. 3) of the DMU in converting the inputs to outputs can be defined as the ratio of outputs to inputs.

$$Efficiency = \frac{Virtual\ Output}{Virtual\ Input} \qquad (3)$$

$$Efficiency = \frac{\sum_{j=1}^{J} v_j\, y_j}{\sum_{i=1}^{I} u_i\, x_i}$$

Where,

i = 1, 2, 3…..I are inputs

j = 1, 2, 3…..J are outputs

s = 1, 2, 3…..N are DMU_S

u_i = weight of i^{th} input

v_i = weight of j^{th} output

x_{is} = amount of the i^{th} input for s^{th} DMU

y_{js} = amount of the j^{th} output for s^{th} DMU

In this paper Factor Relationship (FARE), a new weight determining method is used to compute the weights of each criterion. Romualdas (2011) developed FARE method for determining the criteria weights in multi criteria decision making environment. First the potential impact of the criteria is determined using equation (4).

$$P = S\,(m - 1) \qquad (4)$$

where

P – Potential of the system's criterion impact;

S – Maximum value of the scale of evaluation used (Table1);

m – Number of the system's criteria.

Next the criteria are ranked by the experts based on the importance. Then the relationship between the criteria is determined based on the rank using table 1. The procedure is as follows: the criterion of a lower rank has the smaller impact on the criteria having higher ranks and, therefore, it should transfer a larger part of its potential impact to them.

Table 1 Scale of quantitative evaluation of interrelationship between the system's criteria

No.	Type of the Effect Produced	Rating of the Effect Produced by interrelationship (in points)
1	Almost none	1
2	Very Weak	2
3	Weak	3
4	Lower than Average	4
5	Average	5
6	Higher than average	6
7	Strong	7
8	Very Strong	8
9	Almost absolute	9
10	Absolute	10

The impact of the criteria a_i on the main criterion is determined and then, this impact is transformed as follows:

$$a_{1i} = S - \tilde{a}_{1i} \qquad (5)$$

where,

a_i – the impact of i^{th} criterion on the first main criterion;

$\tilde{a}_i$ – the part of i^{th} criterion's potential impact transferred to the main criterion

The total impact of any criterion, as well as the consistency level of a subset may be determined based on the data provided in the form of matrix. The subset considered in the matrix is consistent and stable if the total impact of its criteria with a positive sign is equal to their total impact with a negative sign, i.e. their sum is equal to zero.

Next the total impact P_i calculated using equation (6).

$$P_i = \sum_{i=1}^{m} a_{ij},\ j \neq i \qquad (6)$$

After that, the total potential, required for determining the criteria weights, will be calculated based on the data presented in the first row of the matrix, thereby

making the filling of all other rows of the matrix unnecessary. The following equation (7) is used for determining the total potential.

$$P_i = P_1 - m.\ a_{1i}, \quad (7)$$

where

P_i – the total impact (dependence) of the i^{th} criterion.

Finally, the criteria weights can be determined using equation (8).

$$\omega_i = \frac{P_i^f}{P_S} = \frac{P_1 - ma_{1i} + S(m-1)}{mS(m-1)} \quad (8)$$

where P_S = Total potential of a set of criteria which is found using equation (9) and

P_i^f = Actual total impact of the i^{th} criterion of the system which is calculated using equation (10)

$$P_S = m.\ P = mS\ (m - 1) \quad (9)$$

$$P_i^f = P_i + P \quad (10)$$

Where

P_i = Total impact produced by the i^{th} criterion of the system or its total dependence on other criteria.

4 Case Study

The case study was performed in a chemical industry which is located in the southern part of Tamilnadu. For this study, the supplier selection model was developed based on five suppliers (S1, S2, S3, S4 and S5) with five evaluating factors, that include three inputs and two outputs namely, delivery (D) in days, capacity (Ca) in units, warranty (W) in number of days, cost (C) in rupees and quality (Q) in percentage of acceptance respectively. The Table 2 shows the data of suppliers and the corresponding inputs and outputs.

Table 2 Datasets of inputs and outputs

Suppliers	Inputs			Outputs	
	D	Ca	W	C	Q
S1	12	170	28	2439	0.87
S2	12	260	21	2567	0.90
S3	14	280	21	2711	0.92
S4	10	260	24	2800	0.96
S5	13	290	18	2302	0.89

The weights of the attributes are calculated by using FARE method using equations (4) to (10). The weights are shown in Table 3.

Table 3 Weights of the attributes

Criteria	Inputs			Outputs	
	Delivery	Capacity	Warranty	Quality	Cost
Weights	0.167	0.500	0.333	0.625	0.375

Then DEA efficiency for all suppliers is determined by using eqn. 3 and the values are tabulated in Table 4.

Table 4 Efficiency of suppliers

Suppliers	Efficiency	
	Using FARE	With Equal weights
S1	76.34	65.45
S2	83.39	67.24
S3	78.90	64.77
S4	92.09	73.34
S5	79.06	62.78

Figure 2 depicts the DEA Efficiency of the suppliers. From the table 4, the supplier with higher efficiency (ie. Supplier 4) is selected as best supplier. For this case study supplier 4 is selected as best supplier.

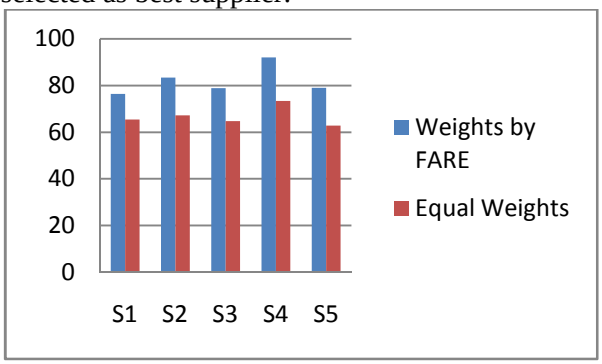

Figure 2 DEA efficiency

Sensitivity analysis is used to determine how "sensitive" a model is during the changes in the value of the parameters of the model and in the structure of the model.

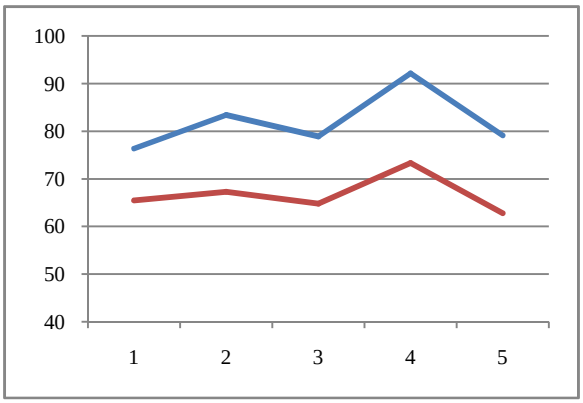

Figure 3 Sensitivity of the DEA model

It is performed to do a tradeoff study and to check the robustness of the model. In sensitivity analysis, the values of any one input parameter were changed and the changes in output performance indices were measured. In this study, equal weights were assumed for the criteria and the efficiency was observed. Figure 3

shows the result of the sensitivity analysis. From the Figure 2, it is observed that the ranking of the suppliers is not changing and hence the robustness of the proposed model is proved.

5 Conclusion

Decisions of evaluation and selection of a supplier is an important part of chain management. In today's intense competition, producing high quality products with minimum cost without satisfactory suppliers is not possible. In this work a multi-criteria decision making model based on DEA for selecting the best supplier was developed. For the selection of supplier, multiple criteria which include quality, delivery, cost, capacity and warranty were considered. And the weights of the criteria were computed in FARE technique. The results were compared and finally the robustness of the developed model was checked by the sensitivity analysis. This model gives a reliable result and it can be extended for the same kind of industries. This proposed model can be more flexible to accommodate the qualitative and quantitative criteria for supplier selection. DEA can help to evaluate and compare suppliers on different evaluation criteria which can offer a more robust tool to select and evaluate suppliers based on both qualitative and quantitative criteria. Future research can be possible by taking different factors relating to the supplier side by the help of soft computing multi criteria decision making approach like fuzzy set theory.

References

[1] Atefeh Amindoust Shamsuddin Ahmed and Ali Saghafinia. (2012), Supplier Selection and Performance Evaluation of Telecommunication Company, *American Journal of Engineering and Applied Sciences*, Vol. 5, No. 1, pp. 49-52.

[2] Charnes A., Cooper .W.W and Rhodes E. (1978), Measuring the efficiency of decision making units, *European Journal of Operational research*, Vol. 2, No. 23, pp. 429-44.

[3] Dickson, G.W. (1966), An analysis of vendor selection systems and decisions, *Journal of Purchasing*, Vol. 2, No. 1, pp. 5-17.

[4] Narasimhan, R Talluri, S. and Mendez, D. (2001), Supplier evaluation and rationalization via data envelopment analysis: An empirical examination, *International Journal of Supply Chain Management*, Vol. 37, No. 3, pp. 28–37.

[5] Rohita Kumar Mishra and Gokulananda Patel. (2010), Supplier Development Strategies: A Data Envelopment Analysis Approach, *Business Intelligence Journal*, Vol. 3, No. 1, pp. 84 – 95.

[6] Romualdas Ginevicius. (2011), A new determining method for the criteria weights in multicriteria evaluation, *International Journal of Information Technology and Decision Making*, Vol. 10, No. 6, pp. 1067–1095.

[7] Talluri, S and Sarkis, J. (2002), A model for performance monitoring of suppliers, *International Journal of Production Research*, Vol. 40, No. 16, pp. 4257–4269.

[8] Weber C.A Current J.R. and Benton W.C. (1991), Vendor selection criteria and methods, *European Journal of Operational Research*, Vol. 50, No. 1, pp. 2-18.

[9] William Ho, Xiaowei Xu and Prasanta K. Dey. (2010), Multi-criteria decision making approaches for supplier evaluation and selection: A literature review, *European Journal of Operational Research*, Vol. 202, No. 1, pp. 16–24.

[10] Wilson E. (1994), The relative importance of supplier selection criteria: a review and update, *International Journal of Purchasing and Material Management*, Vol. 30, No. 3, pp. 35–41.

[11] Wu and Jennifer Blackhurst. (2009), Supplier evaluation and selection: an augmented DEA approach, *International Journal of Production Research*, Vol. 47, No. 16, pp. 4593-4608.

Experimental Evaluation of Defect Identification In Composite Structures Using IR Thermography

J. Jerold John Britto[1*]
[1]Assistant Professor, Department of Mechanical Engineering,
Ramco Institute of Technology, Rajapalayam
jerold@ritrjpm.ac.in

A. Vasanthanathan[1]
[1]Assistant Professor (Sr. Gr) , Department of Mechanical Engineering,
Mepco Schlenk Engineering College, Sivakasi, India
vasanth@alumni.iitm.ac.in

***Abstract*– Composite materials are widely used in a number of industrial sectors from aviation, space, to boat building, automotive, and sports goods. The nondestructive testing and inspection of composite structures, both for manufacturing quality assurance and for in-service damage detection.. Characterization process is mandatory to carry out the NDT test for predicting the failure in the test coupons by using IR thermography method. IR thermography method is used to detect the internal defects. It is a powerful NDT method for the characterization of composite material. This technique involves heating of a specimen with short duration pulse of energy and monitoring the transient thermal response of the surface of the specimen with an infrared camera. It can detect internal voids, delamination and cracks.**

Keywords*: *NDT, IR Thermography, CFRP, Cracks, Thermogram.

I. INTRODUCTION

Composites are combinations of two materials in which one of the materials, called the reinforcing phase is in the form of fibres, sheets or particles, and is embedded in the other materials called the matrix phase. For instance, the term "FRP" (for Fiber Reinforced Plastic) usually indicates a thermosetting polyester matrix containing Fibers. Fiber – reinforced composites can be classified into broad categories according to the matrix used: polymer, metal ceramic, and carbon matrix composites.

FRPs are commonly used in the aerospace, automotive, marine, and construction industries [1]. Manufacturers of not only commercial airplanes but also military planes and helicopters have developed various usage of composite material. In every case, objectives of using composite material have been to reduce weight of planes and to have highly performing flying machines. Composite material also has contributed to those secondary objectives as saving of assembling manpower. Typical speeds for hypersonic aircraft are greater than 3000 mph and Mach number M > 5[1]. Thus, it will be experiencing the flight environment of an upper stage in launch vehicle during it's ascend phase and the flight conditions of an aircraft during its descend phase. Since lift and drag depend on the square of the velocity, hypersonic aircraft do not require a large wing area.

Carbon-fiber-reinforced polymers are composite materials. They have unique properties of relatively high strength at high temperatures coupled with low thermal expansion and low density. The physical properties of composite materials are generally not isotropic in nature, but rather are typically anisotropic (different depending on the direction of the applied force or load) [2]. For instance, the stiffness of a composite panel will often depends upon the orientation of the applied forces and/or moments.

II. MATERIALS AND METHODS

1. MATERIALS

a) Carbon Fibre

Carbon fibre is composed of carbon atoms bonded together to form a long chain. The fibres are extremely stiff, strong, and light, and are used in many processes to create excellent building materials. It has a good weight to strength ratio. Depending on the orientation of the fibre, the carbon fibre composite can be stronger in a certain direction or equally strong in all directions. A small piece can withstand an impact of many tons and still deform minimally.

b) Epoxy Resin & Hardener

Epoxy resins are the most used just after polyesters, their price being the only limit to their usage. They have better mechanical characteristics in tension, compression, impact and others when compared with polyester resins, and so they are preferred in the manufacturing of high performance parts like those used in aeronautics and others. Besides they present good heat resistance up to 15^0 to 190^0 C, have good chemical resistance, [6] low retraction, good reinforcement wetting and an excellent adhesion to metallic materials. As disadvantages, their cost is high, polymerization time is long there is the need to protect the workers that deal with it and they are sensible to cracks. The hardener will used to cure the matrix materials in fibre as faster than usual curing time. From that we can get excellent adhesive bonding together and normally the proportion of hardener, epoxy resin is equal amount and equal to weight of fibre.

2. Test Coupon Preparation

Hand lay-up is the conventional method for preparing composite materials. In Hand lay-up method Gel coat is first applied to the mold using a spray gun for a high-quality surface. When the gel coat has cured sufficiently, roll stock fiberglass reinforcement is manually placed on the mold. [7]The laminating resin is applied by pouring, brushing, spraying, or using a paint roller. FRP rollers, paint rollers, or squeegees are used to consolidate the laminate, thoroughly wetting the reinforcement, and removing entrapped air. Subsequent layers of fiberglass reinforcement are added to build laminate thickness. Low density core materials, such as end-grain balsa, foam, and honeycomb, are commonly used to stiffen the laminate to produce sandwich construction. Fig. (a – d) shows the ASTM D30309 of tensile test specimen.

(a)

(b)

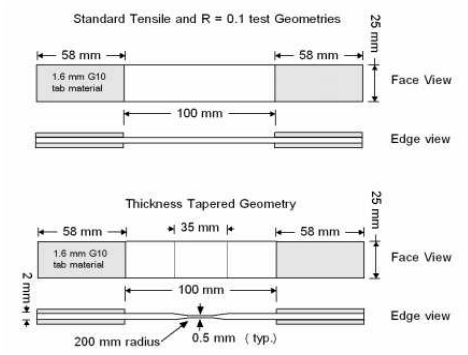

(c)

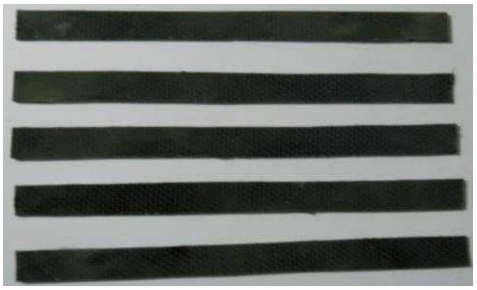

(d)

Fig. 1 (a-d) Test coupon preparation & configuration

III. EXPERIMENTATION

1. Experimental Setup

IR is a powerful NDT method for the characterization of composite material. Generally, this technique involves the heating of a specimen with a short duration pulse of energy and monitoring the transient thermal response of the surface of the specimen with an infrared camera. It can detect internal voids, delamination, and cracks [3].

Principal components in IR Thermography :

1. Halogen lamp
2. Infrared Camera
3. Sample holder
4. Personal computer

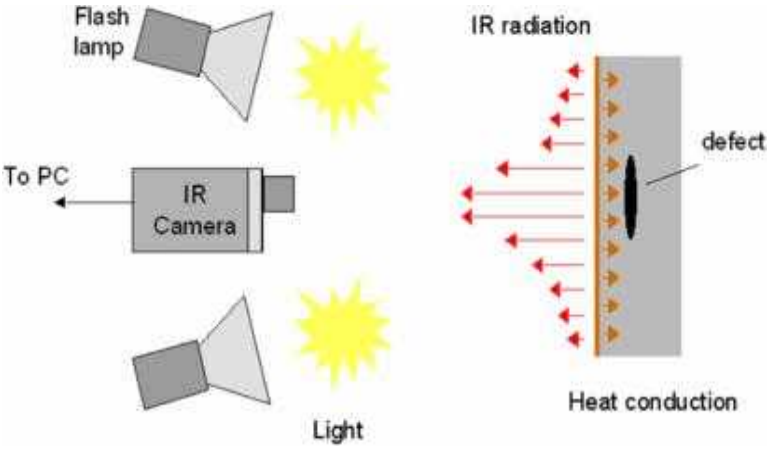

Fig. 2 Experimental setup for IR THERMOGRAPHY

Fig. 3 NDT testing on CFRPtest Coupon

Table I

Test conditions

Name	Avg	Min	Max	Emissivity	Background	St. Dev.
L0	86.4°C	45.1°C	97.0°C	0.98	20.0°C	9.63

1.1 Information About the Image

Background temperature	33°C
Emissivity	0.98
Image Range	34.0°C to 97.3°C
Camera Model	Fluke Ti32
IR sensor Size	320 × 240
Camera Serial Number	Ti32-10060564 (9 Hz)
Camera Manufacturer	Fluke Thermography
Calibration Range	-10.0°C to 600.0°C

Table II

IR Thermography – consolidated Test Results

Sample No.	T_{Avg}	T_{Min}	T_{Max}	Emissivity	Background Temp	Standard Deviation
CFRP1 F	86.4°C	45.1°C	97.0°C	0.98	33.3°C	9.63
CFRP1 B	75.5°C	58.2°C	83.0°C	0.98	33.3°C	6.17
CFRP2 F	110.8°C	45.6°C	118.4°C	0.98	33.3°C	8.85
CFRP2 B	83.8°C	61.7°C	88.2°C	0.98	33.3°C	5.15

❖ Highlighting Indicates the maximum defective materials that can be rejected for material characterization purpose.

IV. RESULTS AND DISCUSSIONS

1. IR THERMOGRAPHY RESULTS

From the table II the IR thermography result shows the white color indicates maximum defects, the red indicates next level of white, the yellow color indicates intermediate level of defect, and finally the blue color indicates low level of defect, [4] finally CFRP1, CFRP4, CFRP5 test coupon selected for material characterization. The following thermogram and graph results shows the NDT method for CFRP Test Coupons

CFRP 01 (FRONT) THERMOGRAM

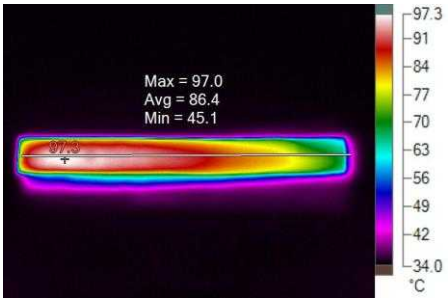

CFRP 01 (FRONT) GRAPH

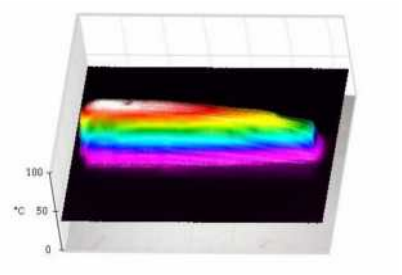

CFRP 01 (BACK) THERMOGRAM

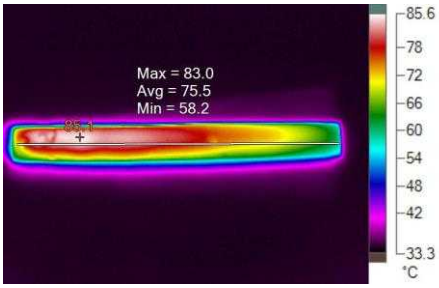

CFRP 01 (BACK) GRAPH

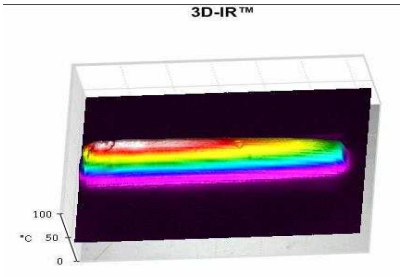

CFRP 02 (FRONT) THERMOGRAM

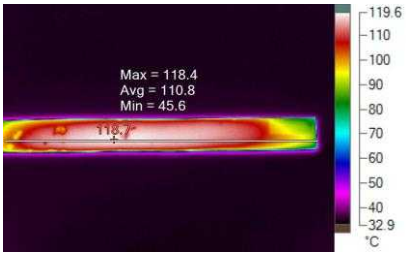

CFRP 02 (FRONT) GRAPH

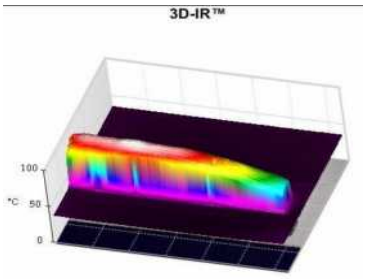

CFRP 02 (BACK) THERMOGRAM

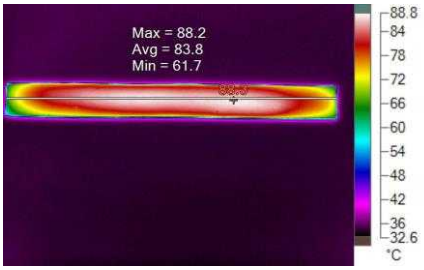

CFRP 02 (BACK) GRAPH

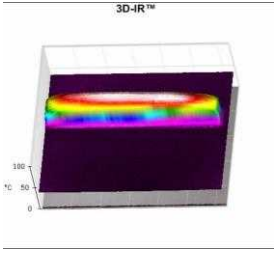

Fig. 4 IR Thermography Image with graph

V. CONCLUDING REMARKS

The following conclusions were drawn from the present experimental investigations:

1. The test coupon preparation method is a conventional one, so the defect will occur due to the hand operation. (Fig. 1).
2. To identify these defects by IR Thermography method with HOT and Cold conditions
3. The test results shows the rejection and selection rate of test coupon for further use..
4. The Thermogram and Graph gives the damage identification with specified location of the specimen and we can avoid the damage during the test coupon preparation.
5. This paper would give an ample suggestion to carry out experiments for the estimation of defect in composite material with the help of NDT method..

ACKNOWLEDGEMENT

All the praise goes to Almighty God for his source of all inspirations, for showering his divine and merciful blessings on us. We express our heartiest gratitude and the authors would like to thank The Principal/RAMCO Institute of Technology, Rajapalayam and The Principal/MEPCO SCHLENK Engineering College, Sivakasi for providing facilities to carry out this research work.

REFERENCES

[1] Deborah D.L. Chung, "Composite Materials Functions and modern Technologies" composite materials laboratory, University of Buffalo, New York, 2009..

[2] M.M. Shokrieh, A.R. Ghanei Mohammadi, "Non-destructive testing (NDT) techniques in the measurement of residual stresses in composite materials: an overview", Residual stresses in Composite Materials, 2014.

[3] R.H. Bossi[1], V. Giurgiutiu[2], "Nondestructive testing of damage in aerospace composites", Polimer composites in the Aerospace Industry.

[4] Xingwang Guo, , Yuxin Mao, "Defect identification based on parameter estimation of histogram in ultrasonic IR thermography", Mechanical Systems and Signal Processing, 58-59.

[5] N.P. Avdelidis , T.-H. Gan, "Non-destructive evaluation (NDE) of Composites: infrared (IR) thermography of wind turbine blades", Non – Destructive Evaluation (NDE) of Polymer Matrix Composites, 2013.

[6] P. K. Mallick, "Fiber-Reinforced Composites: Materials, Manufacturing and Design" – Taylor & Francis Group, LLC.

[7] G. C. Sih and S. E. Hsu, "Advanced Composite Materials and Structures" – Publisher VNU Science Press BV.

[8] A. Miravete, "Composites Properties and Applications", Publisher-UNIVERSITY OF ZARAGOZA.

5th International Congress on
Computational Mechanics and Simulation,
10-13 December 2014, India

FINITE ELEMENT MODELING AND SIMULATION OF CFRP SHELLS UNDER AXIAL IMPACT USING LS-DYNA®

A.VASANTHANATHAN[1,*], P.NAGARAJ[2], J.JEROLD JOHN BRITTO[3]

[1,*] *Asst. Professor (Sr.Grade), Dept. of Mechanical Engg, MEPCO SCHLENK Engg College, Sivakasi, Tamilnadu, India.*
E-mail: vasanthan@mepcoeng.ac.in Mobile: +91-9894781354
[2] *Sr.Professor & Head, Dept. of Mechanical Engg, MEPCO SCHLENK Engg College, Sivakasi, Tamilnadu, India.*
E-mail: pnagaraj@mepcoeng.ac.in
[3] *Asst. Professor, Dept. of Mechanical Engg, RAMCO Institute of Technology, Rajapalayam, Tamilnadu, India.*
E-mail: jerold@ritrjpm.ac.in

ABSTRACT

The principal objective of this paper is to describe the finite element modelling studies that are performed for the development of carbon fabric reinforced epoxy composite shell structures. Analysis of composite structures using FEA certainly needs the assistance of commercial software packages to predict the behaviour of composite structures under impact loading by the numerical simulation of the actual composite structure. The scope of the present paper is to study the dynamic response of the thin-walled carbon fabric epoxy composite shell under axial compression using Finite Element investigations. The finite element analysis for the present study is employed with the explicit finite element software LSDYNA® wherein the experimentally determined material properties of carbon fabric/epoxy composite are incorporated into the FEModel. The history of deformation for carbon fabric/epoxy composite shells under impact loading is generated using LS-PrePost®. In every impact analysis, the maximum vertical displacement at the mid node of the top shell structure and element stresses are recorded and plotted. Low velocity axial impact experiments using drop mass setup are also conducted for the validation of finite element model made with LSDYNA®.

Keywords: Thin-walled shell; CFRP; fabric; axial impact; Finite Element Analysis & LS-DYNA®.

Introduction

Structures composed of carbon fibre (Mitra, 1992) reinforced epoxy composite laminates are mainly applied in the aircraft and spacecraft industries because of the weight saving of the principal structural components. Researchers have indicated that woven fabric reinforced or Textile composites (Murphy, 1998) become more applicable to many engineering applications like aircraft and spacecraft structures due to their low processing cost, superior impact resistance and high process ability. The spacecraft industry predominantly uses carbon fabric composites (Mazumdar,

ISBN:978-981-09-1139-3 || doi:10.3850/978-981-09-1139-3_115

2010) impregnated with epoxy matrix system due to their high performance characteristics at elevated temperatures. The rocket motor cases, space platforms, supporting structures, antenna and solar panels have been constructed using carbon fabrics (Brent, 2008).

Materials

The fiber used in this study was plain weave carbon fabrics (Bhardwaj, 1992). The carbon fabrics (Fig.1b) were 3k count along warp and 3k count along weft directions. The matrix material used was AW106 type epoxy resin with hardener HV 953 U. The warp and weft directions of the carbon fabric are clearly indicated in Fig.1(a). Fig.1(c) shows the surface morphology of carbon fiber using a SEM photograph.

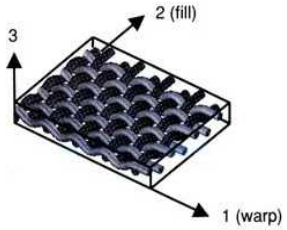

(a) Principal Direction


(b) Photograph

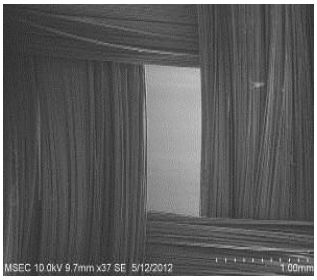

(c) SEM Photograph

Fig. 1. Carbon Fabric structure

The unidirectional mechanical properties of Carbon fabric reinforced epoxy have been considered for the present analysis work.

Thin-walled Composite Shell Structures

Advanced composite structures widely used in aerospace and spacecraft structures include thin-walled laminated shell structures which are composed of layers of Carbon Fabric Reinforced Plastic (CFRP) material. Thin-walled composite shells are widely used in launch vehicles and satellite structures because of its high energy absorbing capabilities.

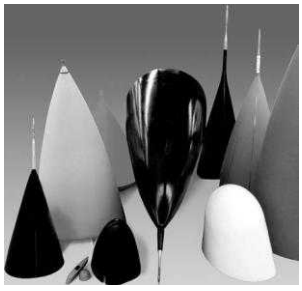

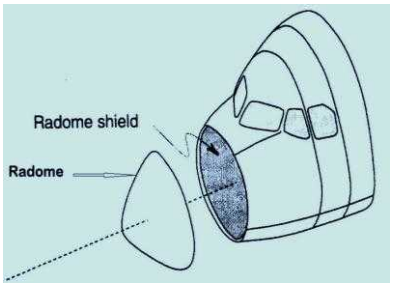

Fig. 2. Applications of Thin-walled Composite shell structures

Thin-walled composite shells are used as space capsules (Narasaiaha et al., 2009) in launch vehicle (ISRO, 2007) and re-entry vehicle applications which accommodate expensive electronic packages. Thin-walled composite shells (Mazumdar, 2010) are widely used in commercial aircrafts for making components like radome, rudders, centre fuselage, rear fuselage, nacelle, air conditioning ducts, outboard and inboard aircraft flaps, aileron, engine nose cone and rotor blades which are represented in Fig.2.

Structural Geometry

The present research is aimed at making a composite shell structural model subjected to impact loading which would be useful in space applications. The structural shell model selected in this paper is a thin-walled structure with a combined geometry of frustum of conical shell and a shallow spherical shell at the top.

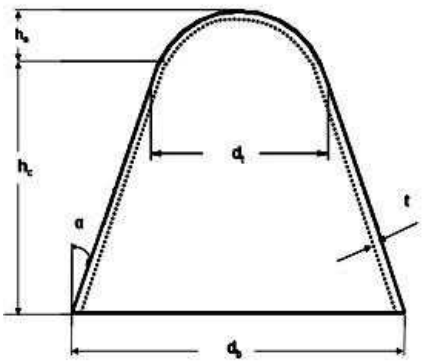

Fig. 3. Shell Structural Configuration

Fig. 4. Shell Modeling using PROE ®

In this paper, the specimen configuration (h_c = 95; h_s= 45; d_b =147; d_t= 90; $\alpha = 22^0$; t = 3; All dimensions are given in mm) shown in Fig.3 is considered as a structural module. The geometry of the shell specimen is modeled by using PROE® software package as shown in Fig.4.

Finite Element Modeling & Simulation using LSDYNA®

The finite element modeling and simulations of the thin-walled CFRP shell structures under low velocity (Shiuh, 2004) axial impact (Gupta, 2007) is carried out using LS-Dyna® (Vasanthanathan, 2013a) finite element software. Fig.5 describes the Finite Element Model of the axial impact setup. The unidirectional mechanical properties (Vasanthanathan, 2013b) of Carbon fabric reinforced epoxy composite obtained from the material characterization as per ASTM standards (Hodgkinson, 2000; Daniel, 2007) are incorporated into the FEModel. The modes of collapse of carbon fabric/epoxy composite shells under impact are numerically investigated using LS-Dyna®. The impact time duration and output time step are specified in LS-DYNA® for controlling the computational run and to get the results at desired time interval. The output file is stored in the form of d3plot which can be analysed using LS-Prepost®.

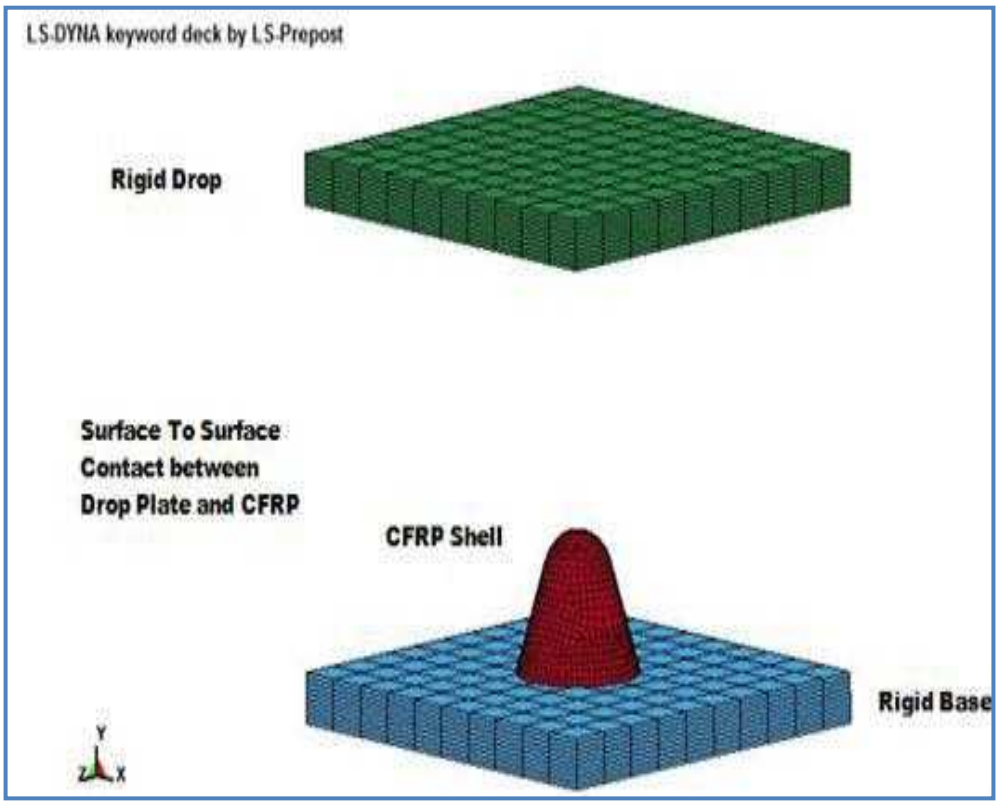

Fig. 5. FEModel of CFRP shell structure under axial impact

Table 1 illustrates the Finite Element Analysis descriptions which are given as input into the FEModel using LS-DYNA®.

Table 1. FEA Description-CFRP shells under axial impact

Parts	Material	Material Model	Element Type	Boundary Conditions	Material Property
For Drop plate	Mild Steel	Rigid	Solid	x = 1, y = 0, z = 1, θx = 1, θy = 1, θz = 1	ρ = 7.83e-9T/mm^3 E = 210 GPa υ = 0.3
For Base plate	Mild Steel	Rigid	Solid	x = 1, y = 1, z = 1, θx = 1, θy = 1, θz = 1	ρ = 7.83e-9T/mm^3 E = 210 GPa υ = 0.3
For CFRP Shell	Carbon fabric/epoxy Composite	Composite Damage (Thatte, 2008)	Shell	x = 1, y = 1, z = 1, θx = 1, θy = 0, θz = 1 (applied for shell bottom nodes)	ρ = 2.16e-9T/mm^3 E_1 = 5985 MPa E_2 = 5985 MPa υ_{12} = 0.297 G_{12} = 3770 GPa

FEA Results

(a) Deformation Plot for impact velocity 3m/s

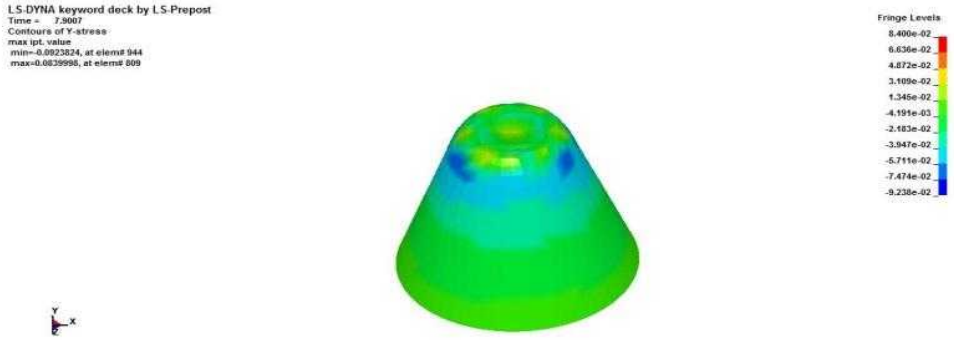

(b) Y-Stress Plot for impact velocity 3m/s

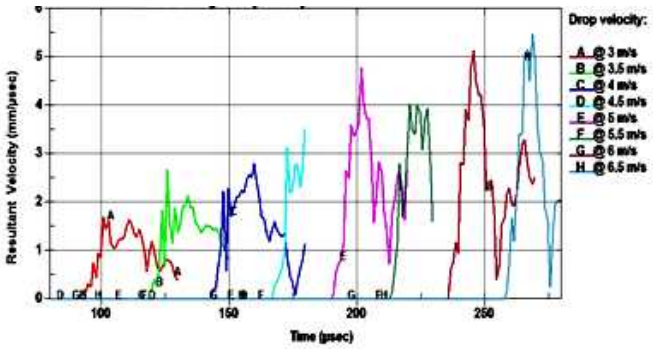

(c) Resultant Velocity Plot

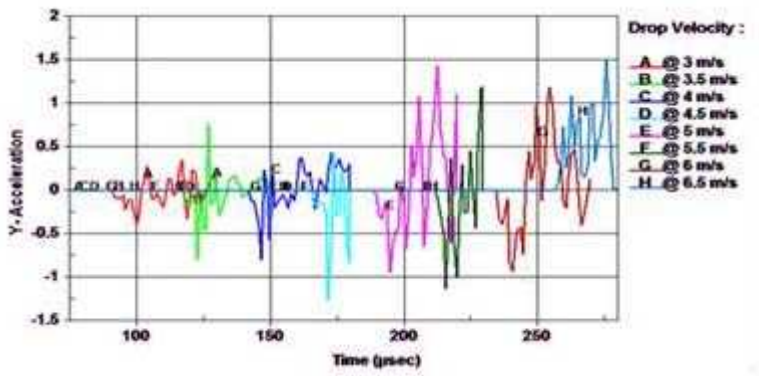

(d) Resultant Acceleration Plot

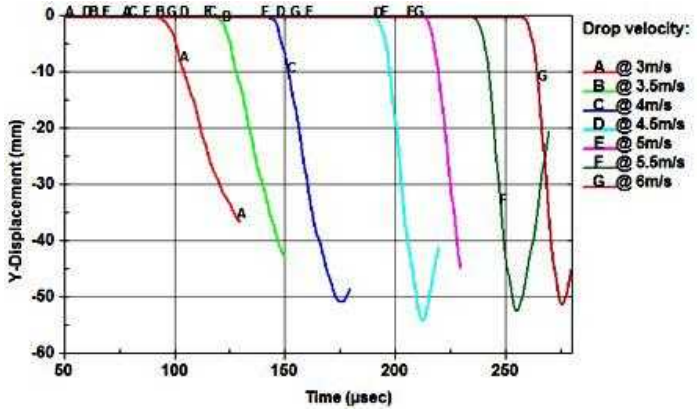

(e) Deflection Plot

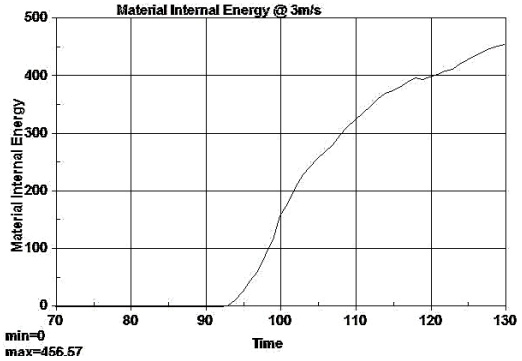

(f) Energy Plot for impact velocity 3m/s

Fig. 6. History of Deformation

Fig 6 illustrates the history of deformations for the finite element studies performed using LS-DYNA® with reference to time for every impact analysis between 3 m/s to 6 m/s. A sample for the deformation plot and stress plot are included in this paper an impact velocity of 3m/s.

Experimental Validation

The validation of the finite element model is done by conducting experiments using drop mass set up which is schematically shown in Fig.7. The low velocity impact experiments (Fig.8a, 8b) were conducted on carbon/fabric epoxy composite shell specimens and visual inspection were carried out for the sake of comparing the experimental deformed shape with the finite element counterpart. The dynamic axial compression tests (Vasanthanathan, 2012) are performed by using the drop mass setup at a low-velocity impact range of 3m/s to 6m/s. For impact experiments, the top plate is freely dropped from a height so as to ensure a low-velocity impact. The experiments were carried out using the same drop height and impact velocity as that of Finite Element Analysis (Vasanthanathan, 2011). Visual inspections were carried out for the observation of the experimental and numerical damage pattern of the carbon/fabric epoxy composite shells. The experimental deformed shape of the carbon/fabric epoxy composite shell (Fig.9a) matches with the numerical deformed shape (Fig. 9b).

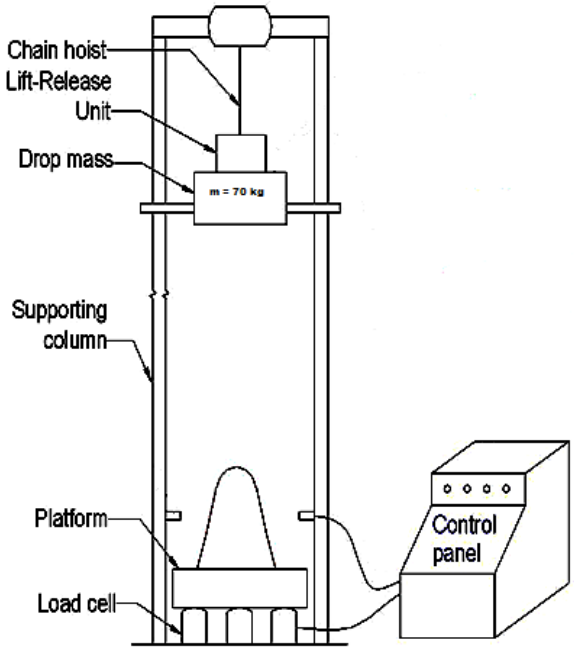

Fig. 7. Schematic Sketch of Drop Mass setup

For all the impact tests, the centroid of the drop hammer and the carbon fabric shell specimen were to be aligned collinear. Different loads could be applied by varying the respective drop height in the drop mass setup. The drop heights are changed by the chain hoist movement and the top plate is dropped by an electromagnet.

(a) At the time of Impact (b) After Impact

Fig. 8. Impact Testing of CFRP Shells

(a) Experimental (b) FE Analysis

Fig. 9. Deformed shape of CFRP Shells

Fig.9 represents the experimental and numerical deformed shape of the carbon/fabric epoxy composite shell under axial impact under 3m/s impact velocity. All the deformed shapes between impact velocity 3m/s to 6 m/s were not included in this paper just for the sake of brevity.

Conclusion

The impact responses of the carbon fabric reinforced epoxy composite shells are evaluated in the present study by finite element predictions. Finite Element Simulation is implemented by creating Finite Element Model using LSDYNA® under axial impact loads and the results are compared with the experimental drop test results. Using LS-Prepost the history of deformation for every low velocity impact analysis between 3 m/s to 6 m/s are generated. It has been numerically found that a

maximum of 54 mm CFRP shell compression are recorded using the FEA software. The qualitative deformed shapes of the thin-walled carbon/fabric epoxy composite shells under impact loading conditions are found in good agreement with the experimental counterparts.

References

Bhardwaj, IS. (1992), "Carbon Fibre Composites-An Overview" in Composites Science and Technology: proceedings of the National Conference on Composites: Science & Technology, ed. RC. Prasad & P. Ramakrishnan, New Delhi, pp.49-56.

Brent Strong, A. (2008), "Fundamentals of Composites Manufacturing Materials, Methods and Applications", Society of Manufacturing Engineers, Dearborn, Michigan.

Daniel M Isaac. (2007), "Engineering Mechanics of Composite Materials", Oxford University Press, New York.

Gupta, N.K.., Mohamed Sheriff, N., Velmurugan, R. (2007), "Experimental and numerical investigations into collapse behavior of thin spherical shells under drop hammer impact". International Journal of Solids and Structures 44(10), 3136-3155.

Hodgkinson, JM. (2000), "Mechanical Testing of Advanced Fibre Composites", CRC Press, USA.

ISRO Countdown. (2007), "Space Capsule Recovery: A Success Story", The House Journal of Vikram Sarabhai Space Centre, no.321, pp.1-12.

Mazumdar K Sanjay. (2010), "Composites Manufacturing-Materials, Product and Process Engineering", CRC Press, Florida.

Mitra, P. (1992), "Advanced Polymer Composites with special reference to Carbon Fibre Reinforced Polymer (CFRP)", in Composites Science and Technology: proceedings of the National Conference on Composites: Science & Technology, ed. RC. Prasad & P. Ramakrishnan, New Delhi, pp.31-48.

Murphy John. (1998), "The Reinforced Plastics Handbook", Elsevier Advanced Technology, New York.

Narasaiaha, N., Varaprasad, R., Seshagiri Raob, V., Krishnamurty, V & Sanyald, MK. (2009), "Space capsule recovery - Evaluation of risk factors, safety plans and procedures and design of experiments for systems qualification", Acta Astronautica 65(9-10), 1224-1230.

Shiuh Chuan Her & Yu Cheng Liang. (2004), "The finite element analysis of composite laminates and shell structures subjected to low velocity impact", Composite Structures, vol.66, pp.277-285.

Thatte S Bhushan, Chandekar S Gautham, Kelkar D Ajith, Pramod Chaphalkar. (2008), "Studies on behaviour of carbon and fiber glass epoxy composite laminates under low velocity impact loading using LSDYNA®".Proceedings of the tenth International LS-DYNA® Users Conference, Dearborn, USA, pp.9-54.

Vasanthanathan, A & Nagaraj, P. (2011), "Experimental and FEAnalysis of axial compression of thin-walled Carbon/Epoxy Composite shells", Proceedings of the ANSYS Academic Users Conference, Bangalore.

Vasanthanathan, A & Nagaraj, P. (2012), “Experimental and FE Analysis of Thin-walled CFRP Composite shells under axial impact loading”, in Mechanics of Functional Materials and Structures: proceedings of the third ACMFMS conference, ed. Santhosh Kapuria, S.Pradyumna, ACMFMS, IIT Delhi, pp.779-782.

Vasanthanathan, A., Nagaraj, P. (2013b), “Correlation Study of IR TNDT Analysis with Structural failure modes of carbon-fabric-reinforced epoxy Composites”, Journal of Engineered Fibres and Fabrics, USA, Accepted for publication in vol. 10, Issue 2 on June 1, 2015.

Vasanthanathan, A., Nagaraj, P., Nivas, S.S. (2013a), “Significance of Material Characterization in FEModeling of glass fabric/epoxy composite shell structure using LSDYNA®”, Journal of Structural Engineering 40(2), 185-195.

Strategies and Methodologies to Improve the Vocabulary Knowledge of the Students

M.Anand M.A., M, PHIL., (PH.D)

Assistant Professor, Deparment of English,

Ramco Institute of Technology, North Venganallur Village, Rajapalayam.

Introduction:

People have become prodigious for the knowledge they possess. Intelligence is what people are known for; our physical struggle for existence had been worn and replaced by intellectual struggle, and knowledge of words has become a most treasured tool. The more vocabulary we possess, the more resourceful are the tools of thought. With a good vocabulary, which indicates scope of knowledge, we grasp the thoughts of others and are able to communicate our own thoughts. Although a large, exact vocabulary is of first importance if we want to make the most of our talents and get the most from life, we also need a specialized vocabulary for our particular work. Almost every field has its own jargon which we need to speak to be successful. This is especially crucial in the technical fields. In science and engineering, for example, changes are taking place so rapidly that knowledge up-to-date is essential to compete with recent graduates. But students of the present find great difficulty to cope up with this drastic change inVocabulary building which requires both patience and effort.Vocabulary for students is the first and foremost important step in language acquisition. The more we know not only helps to insure greater inner success, but the knowledge gives us greater inner resources and self-confidence, as well as a deeper understanding of the world in which we live. This paper is an attempt to study and explore the various strategies and methodologies that can be incorporated to improve the vocabulary of the students.

Patterns of Difficulty in Vocabulary

In early days much was talked about the patterns of difficulty in vocabulary learning. Key issues were highlighted related to words, the native language factor and about patterns. Even Spanish, French and Mexican patterns of difficulty in their respective vocabulary items were analyzed. It was stated that while dealing with vocabulary one should take into account three important aspects of words - their form, their meaning and their distribution - and one should consider various kinds of classes of words in the function of the language. It is said that the forms, meaning distribution and classification of words are different in different languages and revealed that these differences might lead to the planning of vocabulary problems.

Vocabulary and Anatomy

Methods to improve students' abilities to explore, store and to use vocabulary items started to build. The role of vocabulary learning and how a teacher could help their learners were

ANNA UNIVERSITY : CHENNAI
BHARATHIDASAN INSTITUTE OF TECHNOLOGY
TIRUCHIRAPPALLI - 620 024

6274

DEPARTMENT OF ENGLISH

TEQIP II Sponsored International Conference on

ENLIGHTENING THE PEOPLE ABOUT THE RICHNESS OF ENGLISH LANGUAGE AND LITERATURE

Certificate

This is to certify that Dr./Prof./Mr./Ms. M. ANAND
AP (ENGLISH) RAMCO INSTITUTE OF TECH _ RAJAPALAYAM.
chaired a session / participated / presented a paper on Strategies and Methoddogies to Improve the Vocabulary Knowledge of the students.
in the TEQIP II sponsored International Conference on *"Enlightening the people about the richness of English Language and Literature"* from 9th to 10th August, 2014 organized by the Department of English, Anna University: Chennai, BIT Campus-Tiruchirappalli, Tamilnadu, India.

Dr.R.KRISHNAVENI	Dr.N.CHITRA	Dr.P.SURESHKUMAR	Dr.T.SENTHILKUMAR
Coordinator	HOD (i/c)	Coordinator (TEQIP)	Dean

New York Times article titled "The Value of Mom and Dad," "The most powerful antidote to this violence would be to ensure that more black children were raised by both their father and their mother." (nytimes.com) However, in "The Seventh Son," the boy escapes the clutches of the devil and returns home with a lot of wealth. The tale ends with the son driving his father away from the house with the following words,

"You didn't love your children enough to work for them and keep them, but you took them out in the woods where the wild animals could eat them, and you left them there all by themselves ...Now we don't need you. Let all fathers be aware how they treat their children."(112) This sure is suggestive of saying irresponsible fathers who shy away from their commitments deserve no mercy. The abandoned son abandons the escapist father.

Whatever tale the African Americans told, reference to fleeing white domination and escaping the tyranny of the slave owners always found a place. The tale 'Mary Bell' talks of a woman (Mary Bell) escaping from her demonic husband. Here, marriage imagery is used to highlight the slavery system in the new land: Mary Bell is given in marriage to a demon who feigns to be a handsome bridegroom. Tales such as "Courted by the Devil," "Married to a Boar Hog," "The Devil's Bride Escapes" etc. talk of brides given in marriage to demonic husbands and the attempts made by such enslaved wives to escape their husbands' clutches. In "Mary Bell," the demonic husband takes his wife to his house which is a typical haunted house. Being displaced from her house (homeland), she feels trapped in her husband's house (foreign land). She sees heads of women up and a cast of blood in her husband's house ("Mary Bell" 65). The demonic husband is also addressed as "Massa by the rooster in the house. These characters typify certain people. The demonic husband typifies the white slave owners who are often referred to as a "devil" or a "massa". The displaced Mary Bell reminds of the displaced blacks who were enslaved in bizarre circumstances in a foreign land. The corpses in the husband's house are images of brutality that remind the readers of the sufferings of blacks in the white man's land and Mary Bell's desire to escape back to her house signifies the longing of the Blacks to escape the cruelties of the Whites and may be get back to their own homeland, i.e., Africa. While escaping to the industrial north seemed a good solution for many of the enslaved African Americans, going back to their own homeland too was considered. As early as 1787, Prince Hall, a noted and tireless African American abolitionist supported and strove for African emigration. Wilson Jeremiah Moses, an African American historian mentions of Prince Hall's efforts as such:

"In fact, he represented a group of seventy-three "African Blacks" who in 1787 presented the General Court of Massachusetts with a plan for resettlement in Africa due to the "disagreeable and dis advantageous circumstances" that attended life in the United States."(Moses, xv)

Mary Bell too, one day, decides to escape back to her home. She mounts a horse named 60 miles (it covers 60 miles in every leap) and heads back home. The demonic husband makes her escape tough by chasing her on a horse named 50 miles. Though he catches on her thrice, she drops a magical needle each time to create a barrier between her and him and thereby slows him down. Finally, the tale ends saying, "He catch at her. She step into her father's house." (65) Though this is a tale that talks of an escape of a woman from a demonic husband, it highlights the anxieties and the living condition of the blacks in the foreign land. The institution of marriage is used as an image of confinement. The wife who, supposedly, is weaker than the husband and is expected to obey him decides to break free. Mary Bell, easily identified with blacks either had to be confined by this bond of marriage or take the chance of breaking free from it. She does not feel obliged to stay under him because he had cheated her by feigning to be a good groom. Finally, to realize her freedom and escape her demonic husband, she flees back home. Home is where, some blacks felt they belonged. For them, Africa was the place where they felt at ease. Africa was their homeland and therefore would like to get back there to escape torture.

Conclusion: On analyzing these four tales, it is evident that the marriage imagery has been used to talk of power struggle at home. The tales "De ways of de Wimmens" and "Sis 'Coon Shows Brother 'Coon Who's the Boss," ascertain that, at home, it is the wife who enjoys supremacy. These tales give voice to black wives and also earn them an identity. Wives are said to have solutions to domestic problems. They hold the keys to the kitchen and the bedroom and husbands have to go out into the world to assert his supremacy. The institution of marriage is also used to highlight the abandoning and escaping attitude of black men. They often desert their families leaving women helpless. The tale "Seventh Son" through the act of discarding the father who could not take care of his two sons ends up pronouncing judgment on such fathers. Moreover the image of marriage is used to talk of escaping slavery too. The story of "Mary Bell" talks of a woman being married by a devil. It metaphorically implies the system of slavery in America in which blacks are bound to their white masters like a wife being wedded to a demonic

NATIONAL CONFERENCE ON INNOVATIONS IN ENGINEERING, SCIENCE AND TECHNOLOGY

(NCIEST)
6-7 March 2015

CHIEF PATRON
Shri . P. R. Ramasubrahmaneya Rajha
Chairman, Ramco Institute of Technology

PATRON
Shri. P.R.Venketrama Raja
Vice-Chairman, Ramco Institute of Technology

ORGANISING HEAD
Dr. R.V. Mahendra Gowda
Principal, Ramco Institute of Technology

RAMCO INSTITUTE OF TECHNOLOGY
RAJAPALAYAM, TAMIL NADU

NUCLEAR ICE BREAKER SHIP

M.B.Vyas Narayana, Thyvilagathu Abin Baby,
Ramco Institute of Technology, Rajapalyam.
Email : vyasmechanical@gmail.com

A nuclear-powered icebreaker is a nuclear-powered ship purpose-built for use in waters covered with ice. The only country constructing nuclear-powered icebreakers is Russia. Nuclear-powered icebreakers have been constructed by the USSR and later Russia primarily to aid shipping along the Northern Sea Route in the frozen Arctic waterways north of Siberia.

Nuclear-powered icebreakers are much more powerful than their diesel-powered counterparts, and although nuclear propulsion is expensive to install and maintain, very heavy fuel demands and limitations on range can make diesel vessels less practical and economical overall for these ice-breaking duties.

MATHS / 2014-15 / 01

ENCLAVELESS SET IN FUZZY GRAPHS

L.Sathikala, Ramco Institute of Technology, Rajapalayam- 626117
Email: sk1998@gmail.com

In this paper the concept of fuzzy enclave less set and fuzzy co irredundant sets are introduced and the relation between the lower and upper parameters are obtained.

MATHS / 2014-15 / 02

ON $s^{*}g$ – CLOSED MAPS ON IDEAL TOPOLOGICAL SPACES

K. Basari Kodi and K. Subramanian
Department of Mathematics, Ramco Institute of Technology, Rajapalayam, Tamil Nadu, India

In this paper, authors introduce and study the notion of $s^{*}g-$closed maps in ideal topological spaces.

CHE / 2014-15 / 02

EFFICIENT SYNTHESIS OF NANO IRON OXIDE Fe_3O_4 (SNIO) BY ACID –BASE HYDROLYSIS

G. Kanthimathi, Department of Chemistry, Ramco Institute of Technology, Rajapalayam-626117
M. Kottaisamy, Department of Chemistry, Thiagarajar College of Engineering, Madurai – 625 015,
Email: kanthi_somu@rediffmail.com

Nanoparticles represent a new generation of environmental remediation technologies that could provide cost-effective solutions to some of the most challenging environmental clean-up problems; pollution monitoring, ground water and soil remediation.

ZnO NANOPARTICLES ENCAPSULATED BY CHITOSAN MICRO GELS

O. Senthilkumar, Department of Chemistry,
Ramco Institute of Technology, Rajapalayam, Tamilnadu – 626 117.
K. Senthilkumar, Centre for Material Science and Engineering,
National Institute of Technology, Hamirpur – 177005
Y. Fujita, Department of Electronics and Control Systems Engineering,
Shimane University, Matsue, Japan – 6908504.

ZnO nanoparticle-Chitosan composites are prepared from the aqueous phase at neutral pH. The change in properties of the nanoparticles is explained in detail. The potential applications of the composites are discussed.

BARIUM CHLORIDE TRANSPARENT CERAMICS FOR RADIATION DETECTORS

P. Samuel, Ramco Institute of Technology, Rajapalayam, Tamilnadu – 626 117.
W. T. Shoulders, R. Gaume, College of Optics and Photonics, University of Central Florida, USA.

Scintillator ceramics are finding interest in the areas of radiation detectors as an alternative to single crystals. In this current paper, recent work on the development of barium chloride transparent ceramics are studied.

SECURITY PROBLEMS OF STORING BIG DATA IN CLOUD

M.Swarna Sudha, B.Vijayalakshmi, and P.M.G.Jegathambal
Department of Computer Science and Engineering
Ramco Institute of Technology, Rajapalayam.

With the advancement in technology, industry, e-commerce and research a large amount of complex and pervasive digital data is being generated which is increasing at an exponential rate and often termed as big data. Big Data concern large-volume, complex, growing data sets with multiple, autonomous sources. Traditional Data Storage systems are not able to handle Big Data and also analysing the Big Data becomes a challenge and thus it cannot be handled by traditional analytic tools. Cloud computing plays a very vital role in protecting data, applications and the related infrastructure with the help of policies, technologies, controls, and big data tools. Cloud Computing can resolve the problem of handling, storage and analysing the Big Data as it distributes the big data within the cloudlets. Currently, storing the data safely and efficiently on Cloud is one of the biggest challenges in Cloud computing. There is always a potential risk to the security of Big Data storage in Cloud Computing. These security and privacy issues have been addressed in this paper.